Detection and characterization of lipopeptide-specific T cells in guinea pigs sensitized with bacteria of the *Mycobacterium tuberculosis* complex

EVA KAUFMANN

Inaugural-Dissertation zur Erlangung des Grades eines
Dr. med. vet.
beim Fachbereich Veterinärmedizin der Justus-Liebig-Universität Gießen

édition scientifique
VVB LAUFERSWEILER VERLAG

1. Auflage 2016

1st Edition 2016

© 2016 by VVB LAUFERSWEILER VERLAG, Giessen
Printed in Germany

édition scientifique
VVB LAUFERSWEILER VERLAG

STAUFENBERGRING 15, D-35396 GIESSEN
Tel: 0641-5599888 Fax: 0641-5599890
email: redaktion@doktorverlag.de

www.doktorverlag.de

Aus dem Institut für Hygiene und Infektionskrankheiten der Tiere
der Justus-Liebig-Universität Gießen
Betreuer: Prof. Dr. Rolf Bauerfeind
und
aus dem Paul-Ehrlich-Institut Langen
Betreuer: Dr. Max Bastian

Detection and characterization of lipopeptide-specific T cells in guinea pigs sensitized with bacteria of the *Mycobacterium tuberculosis* complex

INAUGURAL-DISSERTATION
zur Erlangung des Grades eines
Dr. med. vet.
beim Fachbereich Veterinärmedizin
der Justus-Liebig-Universität Gießen

eingereicht von

Eva Kaufmann

Tierärztin aus Heppenheim/Bergstraße

Gießen 2016

Mit Genehmigung des Fachbereichs Veterinärmedizin
der Justus-Liebig-Universität Gießen

Dekan: Prof. Dr. Dr. h.c. Martin Kramer

1. Gutachter: Prof. Dr. Rolf Bauerfeind
2. Gutachter: Prof. Dr. Jens Peter Teifke
Prüfer: Prof. Dr. Christian Menge

Tag der Disputation: 11. Mai 2016

Für Alexander und meine Eltern

Publications

Parts of this project are published in:

Kaufmann E, Spohr C, Battenfeld S, De Paepe D, Holzhauser T, Balks E, Homolka S, Reiling N, Gilleron M, Bastian M. (2016) BCG vaccination induces robust $CD4^+$ T cell responses to *Mycobacterium tuberculosis* complex-specific lipopeptides in guinea pigs. J Immunol. 196:2723–2732.

Spohr C, **Kaufmann E**, Battenfeld S, Duchow K, Cussler K, Balks E, Bastian M. (2015) A new lymphocyte proliferation assay for potency determination of bovine tuberculin PPDs. ALTEX 32:201–210.

Presentations

Kaufmann E, Spohr C, Gilleron M, Bauerfeind R, Balks E, Cussler K, Bastian M. (03/2013) The role of immunogenic mycobacterial lipopeptides – investigations in the guinea pig model. 17th Symposium „Infection and Immune Defense“ of the German Society for Hygiene and Microbiology (DGHM) and the German Society for Immunology (DGfI), Rothenfels, Germany, oral presentation.

Kaufmann E, Spohr C, Gilleron M, Bauerfeind R, Balks E, Cussler K, Bastian M. (09/2013) Lipopeptide specific T cells in the early immune response against mycobacteria – investigations in the guinea pig model. 43rd Annual Meeting of the German Society for Immunology (DGfI), Mainz, Germany, poster presentation.

Kaufmann E, Spohr C, Gilleron M, Bauerfeind R, Balks E, Cussler K, Bastian M. (03/2014) Lipopeptides in the early immune response against mycobacteria. 18th Symposium „Infection and Immune defense“ of the German Society for Hygiene and Microbiology (DGHM) and the German Society for Immunology (DGfI), Rothenfels, Germany, oral presentation.

Kaufmann E, Spohr C, Gilleron M, Bauerfeind R, Balks E, Cussler K, Bastian M. (10/2014) Antigenic mycobacterial lipopeptides – investigations in the guinea pig model. 43rd Joint Conference of the German Society for Hygiene and Microbiology (DGHM) and the Association for General and Applied Microbiology (VAAM), Dresden, Germany, oral presentation.

Kaufmann E, Spohr C, Gilleron M, Bauerfeind R, Balks E, Cussler K, Bastian M. (10/2014) Investigations on the Antigenicity of mycobacterial lipopeptides. Joint Conference: German Symposium on Zoonoses Research 2014 and 7th International Conference on Emerging Zoonoses, Berlin, Germany, poster presentation.

Kaufmann E, Spohr C, Balks E, Cussler K, Bauerfeind R, Gilleron M, Bastian M. (03/2015) The antigenic potential of lipopeptides from bacteria of the *M. tuberculosis* complex. 19th Symposium „Infection and Immune defense“ of the German Society for Hygiene and Microbiology (DGHM) and the German Society for Immunology (DGfI), Rothenfels, Germany, oral presentation.

Table of Contents

1 Introduction and Objective

Mycobacterium tuberculosis is an ancient primate pathogen and has coevolved with its human host for thousands of years (Gutierrez *et al.* 2005; Comas *et al.* 2013). All modern mycobacteria which constitute the *Mycobacterium tuberculosis* complex developed from a common early ancestor. While the *M. bovis* lineage broadened its host repertoire and in addition to primates now efficiently infects ruminants and several other mammal species, *M. tuberculosis* has little zoonotic potential and under natural conditions almost exclusively infects humans and other non-human primates *(Brosch et al.* 2002; Hunter 2011). *M. tuberculosis* is the most successful bacterial human pathogen. In 2014 approximately 9.6 million new TB cases occurred worldwide (World Health Organization 2015a). More than 90 % of these people develop latent tuberculosis (Shaler *et al.* 2012). Latent infections can reactivate decades later leading to effective transmission of the disease to other subjects (Hunter 2011). It is estimated that 1.5 million people die due to primary or reactivated disease per year (World Health Organization 2015a).

Efficient and cost-effective strategies are urgently required to curtail the global tuberculosis pandemic. However, the ability of *M. tuberculosis* to override the defense mechanisms of the human immune system has so far foiled all efforts to develop an effective vaccine (Comas *et al.* 2010). An attenuated *M. bovis* strain, Bacille Calmette-Guérin, that was first used in 1921 (Behr and Small 1999), is still the only licensed TB vaccine (Moliva *et al.* 2015). It offers protection against severe manifestations of childhood tuberculosis (Rodrigues *et al.* 1993), but it does not reliably protect against the epidemiologically most important pulmonary manifestation in adults (Colditz *et al.* 1994; Fine 2001). Most of the approaches for the development of a new TB vaccine focus on eliciting inflammatory and cytolytic T cells specific for immunogenic mycobacterial proteins (Moliva *et al.* 2015). However, it becomes apparent that it is not sufficient just to provoke more inflammation. New approaches are required to counteract the subtle mechanisms the pathogen employs to manipulate the host immune system. For this, a deeper understanding of highly immunogenic antigens of *M. tuberculosis* as well as *M. bovis* BCG is an essential prerequisite.

In 2008, Bastian *et al.* described a highly immunogenic class of mycobacterial lipopeptides as potent activators of adaptive immune responses in *Mycobacterium tuberculosis*-infected humans (Bastian *et al.* 2008). Five years later the findings were independently confirmed by another group (Seshadri *et al.* 2013). The responding T cells were found to express high amounts of pro-inflammatory cytokines and *in vitro* lysed infected macrophages by granule exocytosis-mediated cytotoxicity which indicates that these cells may contribute to the elimination of mycobacteria. However, similar frequencies of specific T cells were found in

latently infected donors and in TB patients. So, the mere presence of these T cells did not correlate with protection.

Instead, we hypothesize that the exceptional immunogenicity of this novel class of lipopeptides is part of the elaborate strategy of mycobacteria to deceive the host immune system (Comas *et al.* 2010). We set up an animal model to study the functional role of these lipopeptides in detail and, in particular, in the context of BCG sensitization.

The aims of the current study were:

- to prove whether guinea pigs are suited as a small animal model to study adaptive, cellular immune responses upon sensitization with bacteria of the *Mycobacterium tuberculosis* complex,
- to test whether BCG sensitization induces adaptive immune responses to lipid preparations of *M. bovis* BCG and *M. tuberculosis*,
- to investigate whether lipopeptides are the relevant stimulatory antigens in the mycobacterial lipid preparations,
- to investigate the expression of the lipopeptide antigens across different mycobacterial strains, clades and species,
- to identify – if possible – the molecular nature of the lipopeptide antigens.

2 Literature review

2.1 *Mycobacterium tuberculosis* complex

Mycobacterium is the only genus in the family *Mycobacteriaceae*, which belongs to the order *Corynebacteriales* in the class of *Actinobacteria* within the phylum *Actinobacteria*. *Actinobacteria* stain gram-positive whereas mycobacteria often express gram-lability but can be characterized by their acid-fastness in Ziehl-Neelsen-staining. *Mycobacterium* is defined by its lipid-rich cell wall and the high guanine and cytosine content in the DNA (57 – 73 mol%). The genus is subdivided into two taxonomic groups: the slow-growing species with a cultivation time of seven or more days under optimal conditions and the rapid-growing species with a cultivation time of less than seven days (Wayne and Kubica 1986). The rapid-growing group comprises more apathogenic than (facultative) pathogenic bacteria (Goodfellow and Magee 1998). Some of the most fatal human bacterial pathogens are found within the slow-growing group, such as *Mycobacterium tuberculosis* and *Mycobacterium leprae*. Bacteria of the *Mycobacterium tuberculosis* complex (MTC) are the causative agents of tuberculosis in mammals. The MTC comprises *M. tuberculosis, M. africanum, M. bovis, M. caprae, M. microti, and M. pinnipedii* (Cousins *et al.* 2003; Whitman *et al.* 2012). Recently, a novel pathogen named *M. mungi*, probably also forming part of the MTC, was described (Alexander *et al.* 2010).

2.1.1 Taxonomy and general characteristics of *M. tuberculosis* and *M. bovis*

M. tuberculosis was discovered by Robert Koch in 1882 (Koch 1882), first designated as “bacterium tuberculosis Koch” by Zopf in 1883 (Zopf 1883) and assigned to the genus “*Mycobacterium*” by Lehmann and Neumann in 1896 (Lehmann and Neumann 1896). A “typus humanus” and a “typus bovinus” was officially described by Lehmann and Neumann in 1907 (Lehmann and Neumann 1907). *M. tuberculosis* are acid-alcohol-fast, nonmotile rods with a size of 0.3 – 0.6 x 1 – 4 µm. The generation time is 14 – 15 h under optimal conditions (temperature 37 °C, pH 6.4 – 7.0, aerobic conditions with 5 – 10 % CO_2 and 0.5 % glycerol in the culture medium) (Whitman *et al.* 2012). The entire genome of the best-characterized *M. tuberculosis* strain H37Rv was sequenced in 1998 by Cole *et al.* (Cole *et al.* 1998). *M. tuberculosis* is highly adapted to its human host, but can also infect other primates as well as some companion and laboratory animals. It is pathogenic but of minor virulence for bovine animals (Whitman *et al.* 2012). *M. tuberculosis* is a facultative intracellular pathogen, which mainly resides within host macrophages.

M. bovis is the main causative agent of bovine tuberculosis. For many years it was assumed that a different pathogen was responsible for bovine tuberculosis (Smith 1898), yet it was only described as its own species in 1970 by Karlson and Lessel (Karlson and Lessel 1970). *M. bovis* is acid-fast, non-motile, slow-growing, short to moderately long and rod-shaped (Whitman *et al.* 2012). In primary cultures *M. bovis* often presents as microaerophilic, but adapts to aerobic culture conditions upon subcultivation (Schmiedel and Gerloff 1965). Garnier *et al.* (Garnier *et al.* 2003) sequenced its genome in 2003. *M. bovis* has a very broad host repertoire ranging from domesticated and wild ungulates as well as carnivores to primates, including man (Francis 1958; Lepper and Corner 1983). It is generally more virulent for animals than *M. tuberculosis* (Whitman *et al.* 2012). As the name suggests, cattle are the main host. At present, the most relevant wildlife reservoirs are the brush-tailed possum (*Trichosurus vulpecula*) in New Zealand (Ekdahl *et al.* 1970; Nugent *et al.* 2015), and the badger (*Meles meles*) mainly in the UK (Murhead and Burns 1974; King *et al.* 2015). However, there are many more recognized wildlife reservoirs which are capable of maintaining and transmitting the pathogen (Palmer *et al.* 2014): e.g., wild boars (*Sus scrofa*) in Spain (Naranjo *et al.* 2008), African buffalos (*Syncerus caffer*) in South Africa (Rodwell *et al.* 2001; le Roex *et al.* 2015), and white-tailed deer (*Odocoileus virginianus*) in the USA (Schmitt *et al.* 1997; O'Brien *et al.* 2001).

2.1.2 Tuberculosis as zoonosis

At the British Congress on Tuberculosis in 1901, Dr. Robert Koch denied the high zoonotic potential of *M. bovis* (Grange and Collins 1997). However, the zoonotic character of the disease was proven to be true shortly afterwards (Eastwood *et al.* 1911; Francis 1959) as already assumed by Klencke in 1846 (Klencke 1846; Moore 1913). *M. bovis* does not only constitute a zooanthroponosis: human-to-human transmission is rare yet also possible, as first described by Griffith (1937). At the end of the 19th century, around 30 % of the cattle in Europe were infected with *M. bovis* (Francis 1947; Grange and Collins 1987), while it also accounted for up to 33 % of human tuberculosis cases (Griffith 1937). The risk for bovine TB infection could be drastically reduced by control and preventive measures such as pasteurizing milk and strict test-and-culling procedures which led to the eradication of bovine tuberculosis in most of the industrialized countries (la Rua-Domenech 2006). However, there are other risk factors which have evolved, in particular the HIV/AIDS epidemic with its associated immunosuppression (Grange 2001). Today, *M. bovis* is the causative agent of a median of 0.3 % of all specifically tested human TB cases in the Americas (with a range of 0 to 33.9 %) and 2.8 % in Africa (with a range of 0 to 37.7 %) (Müller *et al.* 2013). It must be considered that these data rely on surveys and statistics which often lack integrity due to

diverging data presented in national epidemiological reports and low rates of strain characterization in tuberculosis diagnostics.

In particular, no differentiation between *M. tuberculosis* and *M. bovis* infections is possible by tuberculin skin reaction (Whitman *et al.* 2012) nor by clinical or radiological findings (Griffith 1937). The differentiation by bacteriological methods alone is complex and not always distinct due to variant strains (Collins and Grange 1983). Furthermore, among all members of the MTC, the 16S rRNA and ITS sequences are identical (Frothingham *et al.* 1994). The determination of the *gryB* sequence can be useful for the differentiation of some MTC members (Kasai *et al.* 2000). However, today's molecular typing methods permit not only the differentiation of distinct mycobacterial species, but also the assignment to diverging genetic strains. In particular, spoligotyping is a PCR-based approach identifying the strain-specific polymorphisms of the nonrepetitive spacer sequences in the chromosomal direct repeat locus (DR) (Kamerbeek *et al.* 1997). This first-line, clade-defining screening test is in the next instance complemented by methods with an even higher discriminatory potential, such as *IS6110*-RFLP or MIRU-VNTR analysis. *IS6110*-RFLP analysis is performed by extraction of the DNA and restriction endonuclease digestion, followed by Southern Blotting (van Embden *et al.* 1993). Today's gold standard in MTC-genotyping is MIRU-VNTR, a multiplex PCR followed by amplicons' size determination and an automated calculation of the variable numbers tandem repeats (VNTR) of mycobacterial interspersed repetitive units (MIRUs) (Supply *et al.* 2001; Supply *et al.* 2006).

2.1.3 Genetic evolution of the *Mycobacterium tuberculosis* complex

M. tuberculosis and *M. bovis* are the two most important members of the MTC, which currently includes five other species as well (see above). Brosch *et al.* presented a pioneering theory about the evolution of the MTC in 2002 (Brosch *et al.* 2002). According to this theory, all strains of the MTC, as well as *M. canetti,* derive from a common ancestor which was most likely a human and not a zoonotic pathogen. While *M. canetti* separated from this common ancestor quite early, an "ancestral" *M. tuberculosis* strain remained. From this ancestral strain, the "ancient" lineages (clade II), namely *M. africanum*, *M. microti* and *M. bovis*, separated by loss of region of difference 9 (RD9). RD9 contains the genes Rv2072c (*cobL*), involved in cobalamin biosynthesis, Rv2073c, a probable shortchain dehydrogenase, and Rv2074 which might be involved in the biosynthesis of pyridoxine and pyridoxal phosphate. Further divergences occurred, mainly due to deletions, continuing the separation of these strains. The "modern" *M. tuberculosis* lineages (clade I) separated from the ancestral strain by the "tuberculosis specific deletion 1" (TbD1). The corresponding

sequence in *M. bovis* (AF2122/97, genes *mmpS6* and *mmpL6*) encodes for membrane proteins. Reiling *et al.* investigated whether the strains within these distinct clades evolved specific traits influencing their virulence and creating clade-specific virulence patterns (Reiling *et al.* 2013). They could delineate three profiles with two of them characterizing high-virulence phenotypes within clade I and one low-virulence phenotype in clade II. The Beijing virulence profile of clade I consists of low uptake by macrophages, low cytokine induction and high growth rates, whereas Haarlem strains are characterized by high rates in uptake, cytokine induction and growth. The low-virulence phenotype of East-African Indian strains of clade II displays low rates in all categories (Reiling *et al.* 2013).

2.1.4 Beyond the *Mycobacterium tuberculosis* complex: Non-tuberculous mycobacteria

Within the genus *Mycobacterium*, the MTC only represents a very small, although highly important group. Its uniformity was demonstrated early on by DNA-DNA hybridization (Baess 1979) and could be confirmed by other methods such as the identical 16S rRNA sequences later on (Böddinghaus *et al.* 1990; Frothingham *et al.* 1994). Even if a much more detailed analysis and resolution are possible today through molecular analyses (see above), the highly conserved 16S rRNA sequence in addition to the internal transcribed spacer (ITS) sequence remains, due to its very low mutation rate, a valuable possibility to detect phylogenies. As revealed by Harmsen *et al.* (2003), the MTC is a distinct group within the slow-growing mycobacteria.

All mycobacteria which do not belong to the MTC are classified as “non-tuberculous mycobacteria” (NTM). This diverse group consists of slow- and rapid-growing mycobacteria accounting for a wide range of both opportunistic and obligatory pathogenic bacteria as well as apathogenic bacteria. Some of the most important ones are briefly described below in the order of their nearest relatedness to the MTC based on the 16S rRNA analysis (Harmsen *et al.* 2003).

M. marinum (Aronson 1926) is the causative agent of the so-called “swimming pool granuloma”: cutaneous granulomas resulting from wound infections acquired in swimming pools or fish tanks. *M. marinum* infection in zebrafish is a recognized model for aspects of human tuberculosis, e.g., the pathogenesis of granuloma (Cronan and Tobin 2014).

M. avium ssp. *avium* (Chester 1901; Thorel *et al.* 1990) together with *M. intracellulare* forms the *M. avium-intracellulare*-complex. *M. avium* ssp. *avium* (MAA) is the causative agent of tuberculosis in birds and is a facultative pathogen in immunocompromised humans.

M. avium ssp. *paratuberculosis* (MAP) (Thorel *et al.* 1990) causes paratuberculosis (Johne's Disease), a chronic diarrhea in cattle and other ruminants. It is suspected to be involved in the pathogenesis of *Morbus Crohn* in humans (Chiodini 1989; Corman 1989; Naser *et al.* 2014).

M. leprae (Hansen 1880; Lehmann and Neumann 1896) is one of the oldest known pathogens. It is an obligate intracellular bacterium and *in vitro* cultivation has not been possible so far. *M. leprae* is the causative agent of leprosy in humans which is a chronic granulomatous skin disease and peripheral neuropathy.

M. fortuitum (Cruz 1938) is a rapid-growing species mainly found in water-associated environments and hospitals. It causes nosocomial wound, soft tissue, and pulmonary infections (Kothavade *et al.* 2013).

2.2 The mycobacterial cell envelope

The hallmark of mycobacteria is their unique lipid-rich cell envelope. It consists of a plasma membrane, the cell wall, and an outer layer.

The plasma membrane is made up of a phospholipid bilayer, generally as in a typical bacterium. In mycobacteria, it mainly consists of phosphatidyl-*myo*-inositol and phosphatidyl-*myo*-inositol mannosides (PIM) as well as of phosphatidylglycerol, diphosphatidylglycerol (cardiolipin), and phospatidylethanolamine (Brennan and Nikaido 1995). PIMs are unique to *actinomycetes* (Brennan and Nikaido 1995) and exist in *di*- to *hexa*-mannosylated forms. Within the plasma membrane, PIMs are the anchors of the important mycobacterial virulence factors lipomannan (LM) and lipoarabinomannan (LAM) (Gilleron *et al.* 2003). A periplasmic space surrounding the plasma membrane, comparable to that of gram-negative bacteria, was proposed by Daffé and Draper (1998). It was substantiated by recent findings by Zuber *et al.* (2008) and Hoffmann *et al.* (2008).

The basic structure of the cell wall is a covalently bound skeleton which consists of heavily cross-linked peptidoglycan, the heteropolysaccharide arabinogalactan, and long-chain mycolic acids (Daffé and Draper 1998). Proteins, lipids and glycans are bound noncovalently to the cell wall skeleton (Kotani *et al.* 1959). The three main components are arranged in a layered manner. The inner layer is formed by peptidoglycan (also called mucopeptide, murein) which consists of a glycan backbone of disaccharides coupled to a cross-linking peptide moiety (Lederer *et al.* 1975). The following arabinogalactan layer is attached to the peptidoglycan by an actinomycete-specific diglycosylphosphoryl-bridge (McNeil *et al.* 1990).

Arabinogalactan consists of alternating 5- and 6-linked *β*-D-galactofuranosyl residues with arabinan chains being attached to the C-5 of some 6-linked galactofuranosyl residues (Daffé *et al.* 1990). It constitutes approximately 35 % of the cell wall mass (Besra *et al.* 1995). Mycolic acids are coupled by an ester linkage to the 5-hydroxy groups of the arabinofuranosyl (Azuma *et al.* 1968; McNeil *et al.* 1991). Mycobacteria-specific mycolic acids are α-alkyl, β-hydroxy fatty acids containing 70 to 90 carbons. They can be separated into a meromycolate backbone and a saturated, approximately C_{24}-long α-branch (Brennan and Nikaido 1995).

Recent investigations of the mycobacterial cell envelope model originally proposed by Minnikin in 1982 (Minnikin 1982) confirmed the existence of an outer membrane which is comparable with that of gram-negative bacteria (Hoffmann *et al.* 2008; Zuber *et al.* 2008). The mycolic acids constitute the innermost leaflet of this outer membrane, whereas the outermost leaflet consists of extractable lipids which are intercalated with the mycolic acids. These lipids are mainly derivatives of mycolic acids, such as glycolipids [e.g., trehalose monomycolate (TMM), trehalose dimycolate (TDM, cord factor), glucose monomycolate (GMM)], but also phospholipids (PIMs), and species-specific lipids (e.g., sulfolipids of *M. tuberculosis*; glycopeptidolipids such as GPL and C-mycosides of e.g., the *M. avium-intracellulare* complex; phtiocerol dimycocerosate such as DIM, and phenolic glycolipids such as PGL and mycosides) (Brennan and Nikaido 1995; Zuber *et al.* 2008). Hydrophilic molecules gain access to the bacterial cell through porins comparable to those in gram-negative bacteria (Senaratne *et al.* 1998).

A capsule that, controversial to the first assumptions, is not only present in pathogenic mycobacteria, but in non-pathogenic species as well, covers the cell-wall structure. It is mainly composed of arabinomannan, α-glucan, and oligomannosyl-capped glycolipids (Sani *et al.* 2010). A maximum of 6 % of the surface-exposed components are lipids – the ubiquitous phosphatidylethanolamine (PE) and phosphatidylinositolmannoside (PIM), as well as species- and type-specific lipids (Ortalo-Magné *et al.* 1996). Proteins associated with the capsule are the 19 kDa and the 38 kDa lipoproteins, the 30/31 kDa fibronectin-binding protein (Antigen 85B/C), the 40 kDa L-alanine dehydrogenase (Ortalo-Magné *et al.* 1995), and the 45/47 kDa protein (apa) (Dobos *et al.* 1996; Ragas *et al.* 2007). The majority of cell surface-associated proteins are also shed into the culture filtrate. However, there are still some proteins that can only be found within one compartment, e.g., the secreted 24 kDa protein MPB/T 64.

2.3 Mycobacterial antigens

2.3.1 Tuberculins

2.3.1.1 Koch's Old Tuberculin and Purified Protein Derivatives

Tuberculin was developed by Robert Koch in 1890 as a potential therapeutic agent for tuberculosis (Koch 1890; Koch 1891a; Koch 1891b; Koch 1897), but was not effective for this purpose. It was introduced as a diagnostic agent in 1907 by Clemens Freiherr von Pirquet (Pirquet 1907a; Pirquet 1907b). The application procedure was modified by Charles Mantoux in 1908 using a cannulated needle and syringe instead of a lancet for intracutaneous injection (Daniel 2006). Koch's "Old tuberculin" (OT) is described in the current European pharmacopoeia as a live mycobacteria-free filtrate of a mycobacterial culture of "one or more strains of *M. bovis* and/or *M. tuberculosis*", grown in glycerolated broth or a synthetic medium, inactivated in an autoclave or in flowing steam, and concentrated by evaporation (European Directorate for the Quality of Medicine and Health Care 2013).

In 1934, Florence Seibert developed the significantly more consistent Purified Protein Derivative of tuberculin (PPD) (Seibert 1934). Since then, PPD has been used in the tuberculin skin test (TST) which is one of the most important methods for diagnosing tuberculosis in humans and animals until today. According to the European Pharmacopoeia (European Directorate for the Quality of Medicine and Health Care 2013), PPD for human use (*M. tuberculosis* and/or *M. bovis*), as well as bovine (*M. bovis*) and avian (*M. avium*) PPDs, derive from mycobacterial cultures grown in a liquid synthetic medium and inactivated in an autoclave (not for avian PPD) or in flowing steam. The active fraction is isolated from the inactivated culture by precipitation. After washing and redissolving, the final reagent is obtained and may be stabilized or freeze-dried if necessary. The standard PPD of Florence Seibert contained 92.9 % protein, 5.9 % polysaccharide and 1.2 % nucleic acid (Seibert and Glenn 1941; Yang *et al.* 2012). Her preparation procedure therefore led to a drastically reduced amount of polysaccharides and nucleic acids as well as lipids, compared to OT. The standard preparation protocol is still employed today apart from the addition of Tween 80. Tween 80 reduces the adsorption of the reagent to the container and acts only as a technical component (Magnus *et al.* 1956).

Tuberculin, including both OT and PPD, induces a delayed-type hypersensitivity reaction to mycobacterial antigens in MTC-sensitized humans and animals. Nevertheless, up to 25 % of TST-tested, MTC-sensitized persons can be non-responders (Nash and Douglass 1980). The reaction might be significantly reduced to nonexistent in cases of severely depressed T cell responses, which might occur for example, in immunocompromised individuals

infected with HIV or anergic patients with active pulmonary tuberculosis (Nash and Douglass 1980; Huebner *et al.* 1993; Converse *et al.* 1997). These conditions reduce the sensitivity of the test. Many mycobacterial antigens exhibit conserved epitopes and hence cause cross-reactivity to tuberculins generated from mycobacterial species other than those having caused the infection. This has a significant impact on the specificity of diagnostic tests. However, the reaction is usually strongest if the tested tuberculin species is the same as the infecting species (Chaparas *et al.* 1970). For example, to differentiate between *M. bovis* and *M. avium* ssp. *paratuberculosis* infections in cattle, a simultaneous test with bovine and avian PPD is used. In humans, the test result might be false-positive in BCG-vaccinated or NTM-infected individuals (Farhat *et al.* 2006). Despite these disadvantages, tuberculin skin testing with PPD is still a reliable and cost-effective diagnostic tool which is used worldwide.

2.3.1.2 The proteome of Purified Protein Derivatives

The entire composition of PPD and all relevant antigens have not yet been clearly defined. Therefore, the potency of each PPD batch still needs to be determined in a guinea pig *in vivo* assay. In this assay, the delayed-type hypersensitivity skin reaction following the intradermal injection of the test batch PPD is compared with the skin reaction following the simultaneous administration of a standard PPD in MTC-sensitized guinea pigs (European Directorate for the Quality of Medicine and Health Care 2013). Despite official preparation protocols and standardization, substantial potency variation was even found among PPD preparations which should be equivalent, but have been produced in different countries (Rangel-Frausto *et al.* 2001). Furthermore, there is inter-standard variation in the proportions of constituents, e.g., the US standard PPD-S2 is composed of 93 % proteins, 1 % nucleic acids, and 6 % carbohydrates whereas the Danish PPD-RT23 is composed of only 80 % proteins, but 20 % nucleic acids, and less than 1 % carbohydrates (Cho *et al.* 2012).

Until now, investigations concentrated on detecting the presence of specific proteins within PPD (Kitaura *et al.* 1999; Coler *et al.* 2000). Already technical in nature, the procedure of defining protein antigens in PPD is very difficult due to its preparation procedure including filtration and autoclaving. As a more general approach, Borsuk *et al.* (2009) performed LC-MS/MS analysis after in-gel trypsin digestion of bovine and avian PPDs. They found a total of 171 unique proteins. From these 171 proteins, 37 were present in two distinct bovine PPD samples with 21 of them being found in bovine PPD only but not in avian PPD, with 10 of those not being encoded in the *M. avium* genome. Cho *et al.* (2012) investigated the proteins present in trypsin- or chymotrypsin-digested US standard PPD-S2 after separation by two-dimensional liquid chromatography. By this approach, 208 and 149 fractions were obtained,

respectively, and subjected to LC-MS/MS which yielded 240 proteins, 50 of which had been previously identified as T cell antigens. The relative quantities were explored by spectral counting. Prasad *et al.* (2013) analyzed trypsin-digested Connaught Tuberculin 68 (PPD-CT68) by high resolution LC-MS/MS and found 142 proteins shared between PPD-CT68 and PPD-S2 among a detected total of 265 proteins in PPD-CT68.

Despite the degradation of the proteins by heat inactivation of the culture filtrate, the fragments still demonstrate antigenic potential. Fragments of most of the previously described immunodominant antigens of the MTC have been found in PPD: MPT53, MPT64, MPT70, MPT83, GroEL, GroES, HspX, ESAT-6, CFP10, and CFP21. Four of them (MPT64, CFP21, CFP10, and ESAT-6) are suited to discriminate between infection and BCG vaccination (Borsuk *et al.* 2009). Of the 116 proteins found to be present in *M. bovis* PPD, 80 were identified in *M. tuberculosis* PPD as well. Seven highly abundant *M. bovis* PPD proteins were located within the range of the ten most abundant proteins in *M. tuberculosis* PPD. Thus, the dominant fractions seem to be conserved throughout different PPDs (Cho *et al.* 2012). The overlap with NTM proteins needs to be studied. The most promising proteins deriving from the three described investigations are displayed in **Table A1** of Annex 1. The table shows proteins found in two human PPDs and indicates whether they were additionally found in a bovine PPD. The proteins displayed were not detected in avian PPD, however, they might be coded for in the genome of *M. avium*. These proteins could be suited for distinguishing MTC from other mycobacterial infections. Altogether, though more purified than Koch's Old Tuberculin, PPDs are still very heterogeneous antigen preparations with high, but also strongly diverging potencies.

2.3.2 Protein antigens

The bacteria of the MTC possess a very thick, lipid-rich cell wall. However, the antigens that are most frequently studied are proteins due to the various techniques available to characterize, express or synthesize them. In the following text passage, some of the most important and best-characterized protein antigens of the MTC are described.

These are, first of all, those proteins whose gene sequences are deleted with the Region of Difference 1 (RD1) in the mycobacterial vaccine strain BCG (see section 2.5.1) (Mahairas *et al.* 1996). These proteins, namely ESAT-6 and CFP10, have been extensively studied for their potential to discriminate between MTC infection and BCG vaccination and are implemented in diagnostic tests (Harboe *et al.* 1996; Buddle *et al.* 1999; Johnson *et al.* 1999; Brock *et al.* 2001; Chapman *et al.* 2002; Mori *et al.* 2004; Ravn *et al.* 2005; Moradi *et al.*

2015). In addition to their potential to discriminate between MTC and BCG sensitization, these proteins are only found in a minority of NTM strains, e.g., *M. marinum*, and, most importantly, not in strains of the *Mycobacterium avium* complex (Pollock and Andersen 1997b; Arend *et al.* 2000; Andersen *et al.* 2000; Mori *et al.* 2004).

ESAT-6 (Rv3875, gene *esxA*): The 6 kDa early secretory antigenic target is present in the cytosol, the cell wall, and the short-term culture filtrate of *M. tuberculosis* (Sørensen *et al.* 1995). Orthologs are present in *M. bovis*, *M. leprae*, *M. marinum*, and *M. smegmatis* (Lew *et al.* 2011). ESAT-6 induces a strong IFN-γ secreting T cell response in *M. tuberculosis* or *M. bovis*-sensitized humans and experimental animals (Sørensen *et al.* 1995; Brandt *et al.* 1996; Pollock and Andersen 1997a; Elhay *et al.* 1998; Ravn *et al.* 1999). Evidence for the function of ESAT-6 as a virulence factor mainly comes from comparisons of ESAT-6/CFP10-bearing strains and strains devoid of ESAT-6/CFP10. ESAT-6 has been assumed to be involved in virulence due to the demonstration that the loss of RD1 is associated with attenuation of *M. bovis* BCG (Pym *et al.* 2002). ESAT-6 could be shown to influence at least the innate immune response and to shift the cytokine response towards a more restrictive pattern (Pathak *et al.* 2007). Further impact as a virulence factor through modulation of the macrophage cell death is suggested (Guo *et al.* 2012).

CFP10 (Rv3874, gene *esxB*): The 10 kDa culture filtrate protein (Berthet *et al.* 1998) forms a heterodimeric complex with ESAT-6 (Renshaw *et al.* 2002). It is found within the same mycobacterial species as ESAT-6 and they are often jointly investigated (see above). It is also considered a virulence factor (Renshaw *et al.* 2002).

ESAT-6 and CFP10 together with the less dominant protein TB7.7 (Rv2654c) (Lindestam Arlehamn *et al.* 2015) are used in the QuantiFERON®-TB Gold In-Tube test (Diel *et al.* 2006). According to the manufacturer (Qiagen), this ELISA detects IFN-γ secretion of whole blood cells after incubation with the antigens if the blood donor is infected with MTC. Another test, the ELISpot T-Spot.TB only uses ESAT-6 and CFP10 as antigens to induce IFN-γ secretion in enriched PBMCs from humans (manufacturer based information, Oxford Immunotec).

The immunogenic proteins of the MTC which are listed in the following are currently under investigation for use as vaccine antigens (see section 2.5.2.).

Antigen 85 complex: This important complex was initially described by Yoneda *et al.* (Yoneda and Fukui 1965). The secreted and transiently cell wall associated antigen 85 complex possesses major culture filtrate proteins of *M. tuberculosis* strain H37Rv (Nagai *et al.* 1991; Wiker and Harboe 1992; Målen *et al.* 2007). However, it is not MTC-specific. In detail, the complex consists of the 35.7 kDa AG85A (Rv3804c, MPT44, gene *fbpA*) (Wiker *et*

al. 1986; Borremans *et al.* 1989), the 34.6 kDa AG85B (Rv1886c, MPT59, gene *fbpB*) (Wiker *et al.* 1986; Matsuo *et al.* 1988), the 36.7 kDa AG85C (Rv0129c, MPT45, gene *fbpC*) (Wiker *et al.* 1990; Content *et al.* 1991), and the 31 kDa AG85D (Rv3803c, MPT51, gene *fbpD*) (Nagai *et al.* 1991; Ohara *et al.* 1995; Cole *et al.* 1998). Orthologs of all these proteins are found within *M. bovis*, *M. leprae*, *M. marinum,* and *M. smegmatis* (Lew *et al.* 2011). The AG85 (A-C) proteins each have a carboxylesterase domain and function as mycolyl-transferases which are required for the generation of trehalose di-mycolate (TDM, cord factor) (Belisle *et al.* 1997). In particular, inactivation of AG85C results in a 40 % decrease of the amount of cell wall-linked mycolic acids (Jackson *et al.* 1999). Furthermore, these proteins bind fibronectin (Abou-Zeid *et al.* 1988), a large glycoprotein in the blood plasma and other body fluids, connective tissue and basement membranes which facilitates binding of mycobacteria to epithelial and other cells (Ratliff *et al.* 1987). Fibronectin-binding may also contribute to modulation of the T cell responses involved in delayed type hypersensitivity reactions to PPD (Godfrey *et al.* 1992; Pais *et al.* 1998). In contrast, AG85D does not seem to express any mycolyltransferase-activity due to a devastating mutation in the carboxypeptidase catalytic site, but might also be involved in interacting with extracellular ligands such as fibronectin (Puech *et al.* 2002; Wilson *et al.* 2004).

Mtb32A (Rv0125, gene *pepA*): This 35 kDa protein found in *M. tuberculosis*, with orthologs in *M. leprae*, *M. bovis,* and *M. avium* ssp. *paratuberculosis* (Lew *et al.* 2011) is probably a serine protease (Skeiky *et al.* 1999) and is one of the most abundant proteins in culture filtrates of *M. tuberculosis* strain H37Rv (Målen *et al.* 2007).

Mtb39A (Rv1196, gene *PPE18*): This PPE family protein of 39 kDa is present in *M. tuberculosis* lysates, but is not a secreted antigen. It induces strong T cell IFN-γ responses and has been demonstrated to induce protection if administered in mice (Dillon *et al.* 1999). Orthologs of this protein were found in *M. bovis*, *M. leprae,* and *M. marinum* (Lew *et al.* 2011).

TB10.4 (Rv0288, CFP7, gene *esxH*): A core mycobacterial gene (Marmiesse *et al.* 2004) encodes this 10 kDa protein belonging to the ESAT-6 protein family (Rindi *et al.* 1999). It was found in *M. tuberculosis* and as orthologs in *M. bovis*, *M. leprae*, *M. marinum*, and *M. smegmatis* (Lew *et al.* 2011). Interestingly, this protein displays more antigenic variation among different *M. tuberculosis* strains than most of the other T cell antigens (Comas *et al.* 2010).

Rv2660c (gene *Rv2660c*): This 7.6 kDa protein is highly upregulated during nutrient starvation of *M. tuberculosis* in culture (Betts *et al.* 2002). An ortholog was only found in *M. bovis* (Lew *et al.* 2011).

PPE42 (gene *Rv2608*): This PPE family protein of 60 kDa is present in *M. tuberculosis* and has an ortholog in *M. bovis* (Lew *et al.* 2011). It is a secreted factor (Beaulieu *et al.* 2010) and is known to be a dominant B cell antigen (Chakhaiyar *et al.* 2004).

Rv3619c (mtb9.9D, gene *esxV*): Rv3619c encodes for a 9.9 kDa putative ESAT-6-like protein without an ortholog in *M. bovis* (Lew *et al.* 2011).

Rv3620c (gene *esxW*): This 11 kDa putative ESAT-6-like protein secreted by *M. tuberculosis* is coded in RD9 and is therefore missing in *M. bovis* and *M. bovis* BCG (Mattow *et al.* 2003) (see section 2.5.1). Five orthologs were found in *M. marinum* (Lew *et al.* 2011).

Rv1813c (gene *Rv1813c*): This 15 kDa protein is induced by hypoxia (Sherman *et al.* 2001). Orthologs are found in *M. bovis* and *M. marinum* (Lew *et al.* 2011).

2.3.3 Lipid antigens

Genome analysis revealed that 5.7 % of all *M. tuberculosis* genes are involved in the lipid metabolism of this bacterium presenting a high range of unusual or even unique lipids (Cole 1999). Lipids play important and distinct roles in the physiology and the parasitic lifestyle of this pathogen. According to their structures, the lipids can be distinguished in trehalose-containing glycolipids, phosphatidylinositol-derived lipoglycans, and mycoserosate-containing lipids (Neyrolles and Guilhot 2011).

The most important members of the trehalose-containing glycolipids are trehalosemonomycolate (TMM) and trehalosedimycolate (6,6'-dimycoloyl-a-D-trehalose, TDM, cord-factor). Mycolic acids consist of an α-branch (the fatty acid) and a meroaldehyde (Barry *et al.* 1998). Mycobacteria-specific mycolic acids have very long fatty acid chains with 60 to 90 carbons and vary by species in their functional groups (Neyrolles and Guilhot 2011). Further lipids in this category are the *M. tuberculosis*-specific di-acyltrehaloses (DAT), tri-acyltrehaloses (TAT) and poly-acyltrehaloses (PAT), as well as sulfatides (SL) found in *M. tuberculosis* and *M. canetti,* and lipooligosaccharides (LOS).

Phosphatidylinositol-derived lipoglycans are synthesized by all mycobacterial species. This category is composed of phosphatidyl-*myo*-inositol mannosides (PIM), lipomannan (LM), and lipoarabinomannan (LAM). PIM is a phosphatidyl-*myo*-inositol with 2 to 6 mannosides (PIM_2, PIM_3, PIM_4, PIM_5, and PIM_6). PIM_2 and PIM_6 are the most abundant forms in *M. tuberculosis*, *M. bovis* BCG, and *M. smegmatis* (Gilleron *et al.* 2003). LM is a polymannosylated PIM_4 while LAM is constituted of LM with an additional D-arabinan. LAM is always strain-specific

(Gilleron *et al.* 2008). However, three general groups can be defined based on the capping motifs on the nonreducing ends of the arabinosyl side chains, as firstly described by Chatterjee *et al.* (1992). Motifs identified so far are mannose-capped LAM (ManLAM) in slow-growing species, phospho-inositol-capped LAM (PILAM) in fast-growing species, and non-capped arabinan termini (AraLAM) in *M. chelonae* (Guerardel *et al.* 2002).

Mycoserosate-containing lipids are phenolic glycolipids (PGL) and phthiocerol dimycocerosates (DIM), both of which are produced by the important pathogens *M. tuberculosis*, *M. leprae,* and *M. ulcerans* among others, but not by all mycobacterial species (Daffé and Lanéelle 1988).

The biological functions of the most important ones of these lipids are described below.

The mycolate composition of glycolipids proved to be important to ensure the cell wall permeability (Yuan *et al.* 1998; Dubnau *et al.* 2000). Furthermore, TDM in particular, induces a Th1/Th17 immune response and granuloma formation *in vivo* through Mincle-FcγR signaling (Ishikawa *et al.* 2009; Schoenen *et al.* 2010). In this line, the strong adjuvant effect of TDM to induce a cell-mediated as well as humoral immune response needs to be highlighted (Davidsen *et al.* 2005; Agger *et al.* 2008). The Mincle signaling seems to be supplemented by signaling through the scavenger receptor MARCO in conjunction with TLR2 and CD14 (Bowdish *et al.* 2009).

PIM, or rather the phosphatidyl-*myo*-inositol mannosyltransferase PimA has been shown to be essential for the growth of the bacterium *in vitro* and *in vivo* (Korduláková *et al.* 2002; Morita *et al.* 2004; Haites *et al.* 2005; Boldrin *et al.* 2014). The PIM progeny LAM is specifically recognized by the mannose receptor (MR) and dendritic cell-specific intercellular adhesion molecule-3 grabbing non-integrin (DC-SIGN) mediating uptake of the pathogen into macrophages and dendritic cells (Schlesinger 1993; Tailleux *et al.* 2003; Pitarque *et al.* 2005; Appelmelk *et al.* 2008). It was assumed for a long time that the interaction of ManLAM with these receptors would constitute an immune escape mechanism of the bacterium through inhibition of pro-inflammatory immune mechanisms and stimulation of anti-inflammatory cytokines (Johansson *et al.* 2001; Nigou *et al.* 2001; Geijtenbeek *et al.* 2003). This view was recently challenged with evidence that DC-SIGN signaling resulted in host protection through inhibition of tissue damage or, together with TLR-signaling, in production of protective inflammatory cytokines (Schaefer *et al.* 2008; Tanne *et al.* 2009; Ehlers 2010; Neyrolles and Guilhot 2011). ManLAM was further shown to induce the phagosomal maturation block, e.g., by specifically inhibiting the recruitment of the Rab5 effector early endosome autoantigen (EEA1) to the phagosome (Fratti *et al.* 2001; Fratti *et al.* 2003; Vergne *et al.* 2003) or generally by invading the membrane rafts of the macrophage (Welin *et al.* 2008).

In addition to inducing innate immune responses, lipid antigens also stimulate adaptive immune reactions after presentation through CD1 molecules (Cluster of Differentiation 1) (Porcelli *et al.* 1992; Beckman *et al.* 1994; Ulrichs *et al.* 2003).

2.3.4 Lipoprotein antigens

2.3.4.1 Biosynthesis of mycobacterial lipoproteins

Structurally, a lipoprotein consists of a lipid moiety which is covalently linked to an N-terminal cysteine residue of a protein (Sutcliffe and Russell 1995). Lipoproteins have various functions in bacterial physiology but also virulence in gram-negative as well as gram-positive bacteria (Nakayama *et al.* 2012).

In *M. tuberculosis*, 99 putative lipoproteins have been described, which equals 2.5 % of the predicted proteome (Sutcliffe and Harrington 2004). Post-translational modification as described by Sutcliffe *et al.* (2004) and Nakayama *et al.* (2012) is crucial in the biosynthesis pathway of lipoproteins: The signal peptide directs the translocation of the preprolipoprotein across the plasma membrane using either the general secretory (Sec) pathway for unfolded proteins or the twin arginine protein transport (Tat) system for folded proteins (Hutchings *et al.* 2009). After this translocation a diacylglycerol moiety from membrane phospholipids (mainly phosphatidylglycerols) is coupled to the N-terminal cysteine residue by thioether linkage. This transfer is catalyzed by the prolipoprotein diacylglyceryl transferase (Lgt) (Tschumi *et al.* 2012) which recognizes a conserved sequence in the N-terminal type II signal peptide (the "lipobox", [LVI][ASTVI][GAS][C]) (Babu *et al.* 2006). The diacylglycerol is associated with $C_{16:0}$ (palmitic acid) and $C_{19:0}$ (probably the mycobacteria-specific tuberculostearic acid) fatty acids (Tschumi *et al.* 2009). The described reaction results in the prolipoprotein. Next, the signal peptide is cleaved from the N-terminus by a type II signal peptidase (LspA) (Sander *et al.* 2004). This reaction yields the apolipoprotein (diacyl lipoprotein). The resulting amino group is coupled with a C_{16} ($C_{16:0}$ or $C_{16:1}$ palmitoleic acid) acyl chain of phospholipids, catalyzed by lipoprotein N-acyl transferase (Lnt) (Tschumi *et al.* 2009). This produces the final hololipoprotein (triacyl lipoprotein). All three required enzymes are integral plasma membrane proteins (Robichon *et al.* 2005; Sutcliffe *et al.* 2012; Pailler *et al.* 2012; Zueckert 2014). Next, the lipoprotein is transported to the outer membrane using the lipoprotein outer membrane localization (Lol) pathway machinery (Zueckert 2014). The lipid moiety anchors the lipoprotein in the inner leaflet of the outer membrane of the bacterium, but lipoproteins can be secreted as well (Zueckert 2014).

2.3.4.2 Overview of *Mycobacterium tuberculosis* lipoproteins

Functionally, lipoproteins can be categorized into solute binding proteins (SBP) of ABC transport systems, lipoprotein enzymes, adhesins and members of the mammalian cell entry (mce) gene family, lipoproteins with signaling or sensory functions, and lipoproteins of unknown function (Sutcliffe and Harrington 2004). Those putative lipoproteins of *M. tuberculosis* which have been addressed in the present study (n = 78) including their presumed functions are displayed in Annex 5.

A brief description of the best-known lipoproteins is provided below.

LpqH (Rv3763, the 19 kDa lipoprotein, gene *lpqH*): The membrane-associated as well as released 19 kDa lipoprotein (de Souza *et al.* 2011) is probably the best-studied lipoprotein in *M. tuberculosis*. It is glycosylated to regulate proteolytic cleavage (Herrmann *et al.* 1996). The 19 kDa lipoprotein was shown to play an important role in the development of pathogenic host responses mediated through inducing stimulating as well as depressing processes (see below for details). However, to date there is no consensus regarding a conclusive role of this important antigen. LpqH-mediated effects *in vivo* are probably a multifactorial result of pathogen properties and host environment. Lower virulence of an *M. tuberculosis* strain lacking an intact Rv3763 was demonstrated, as well as the restoration of virulence by transformation of the bacterium with the wild-type LpqH gene (Lathigra *et al.* 1996). Orthologs are found in *M. bovis*, *M. leprae*, *M. marinum*, and *M. smegmatis* (Lew *et al.* 2011).

LppX (Rv2945c, gene *lppX*): Rv2945c belongs to the mycobacteria-specific “core” genes (Marmiesse *et al.* 2004). The probable conserved 24 kDa LppX is assumed to transport phtiocerol dimycocerosate (DIM) from the plasma membrane to the outer membrane of the bacterial cell envelope which is important for the virulence of *M. tuberculosis* (Sulzenbacher *et al.* 2006). Orthologs are found in *M. bovis*, *M. leprae,* and *M. marinum* (Marmiesse *et al.* 2004; Lew *et al.* 2011). Despite the location in the cell envelope, the ortholog in *M. bovis* BCG was additionally found in the culture filtrate (Lefèvre *et al.* 2000).

LprA (Rv1270c, gene *lprA*): The possible 25 kDa lipoprotein LprA has a strong sequence conservation (Sinha *et al.* 2002) and was found in the membrane protein fraction as well as in the culture filtrate (de Souza *et al.* 2011). Orthologs exist in *M. bovis* and *M. marinum* (Lew *et al.* 2011). It was found to be an antigen present during early stages of infection in the lungs of guinea pigs (Kruh *et al.* 2010). LprA acts as a TLR2 agonist inducing the expression of TNF-α, IL-10 and IL-12 genes as well as the maturation of dendritic cells. In contrast, after 24 h it decreases the IFN-γ-induced MHC II function and expression in macrophages, which might be important for immune evasion of the bacterium (Pecora *et al.* 2006).

LprF (Rv1368, gene *lprF*): The probable conserved LprF has a molecular mass of 27 kDa (Lew *et al.* 2011). As for LprA (see above), it also demonstrates strong sequence conservation (Sinha *et al.* 2002), and was found in a cell membrane-associated as well as in a secreted fraction of *M. tuberculosis* (de Souza *et al.* 2011). Orthologs were found in *M. bovis* and *M. marinum* (Lew *et al.* 2011). LprF together with LprJ (Rv1690) play a role as accessory or ligand-binding proteins in the histidine kinase Kdp signaling pathway which is upregulated upon osmotic stress affecting the bacterial cell (Steyn *et al.* 2003).

LprG (Rv1411c, P27, the 27 kDa lipoprotein, gene *lprG*): The conserved lipoprotein LprG has a true molecular mass of 24.5 kDa (Bigi *et al.* 1997; Lew *et al.* 2011). It is a core mycobacterial gene that is sustained in different strains (Marmiesse *et al.* 2004). Orthologs are described for *M. bovis*, *M. leprae*, *M. marinum*, and *M. smegmatis* (Lew *et al.* 2011). LprG is localized in the cell membrane and is also secreted (de Souza *et al.* 2011). The gene sequence encoding LprG (P27) forms an operon with the gene encoding the P55 multidrug efflux pump (Bigi *et al.* 2000; Silva *et al.* 2001). A ΔP27 mutant strain of *M. tuberculosis* H37Rv neither demonstrated expression of P27 nor of P55. ΔP27 was attenuated in an immunocompetent mouse model. This phenotype was reversed by a complemented strain (Bigi *et al.* 2004). LprG has recently been demonstrated to associate with LM, LAM as well as PIM, which on the one hand enhances recognition by TLR2 receptors, while on the other hand might provide a transport function for those triacylated glycolipids (Drage *et al.* 2010).

MPT83 (Rv2873, gene *mpt83*): MPT83 constitutes a 22 kDa cell surface protein which can also be secreted (de Souza *et al.* 2011). Orthologs are found in *M. bovis*, *M. marinum*, *M. smegmatis* (Lew *et al.* 2011), and with varying extents in different *M. bovis* BCG strains (Harboe *et al.* 2002). A distinct function of this lipoprotein could not yet be delineated, but it is assumed to be an adhesin (Hewinson *et al.* 1996).

A mycobacterial gene cluster encodes three phosphate-binding lipoproteins, namely **PstS1** (Rv0934, gene *pstS1*) (Andersen and Hansen 1989; Braibant *et al.* 1996a; Braibant *et al.* 1996b; Lefèvre *et al.* 1997), **PstS2** (Rv0932c, gene *pstS2*) (Braibant *et al.* 1996a; Braibant *et al.* 1996b; Lefèvre *et al.* 1997), and **PstS3** (Rv0928, gene *pstS3*) (Braibant *et al.* 1996a; Braibant *et al.* 1996b; Lefèvre *et al.* 1997). All three 38 kDa lipoproteins were found within the cell envelope as well as in secreted form (de Souza *et al.* 2011). They actively transport anorganic phosphate into the bacterial cell, which was first described for PstS1 (Torres *et al.* 2001). The most probable purpose of this function is to ensure the phosphate supply of the bacterium. PstS1 and PstS3 were identified 90 days, but not 30 days after *M. tuberculosis* H37Rv-infection in the lungs of guinea pigs (Kruh *et al.* 2010). Orthologs of PstS2 and PstS3 are encoded by *M. bovis*, *M. leprae,* and *M. marinum*, while orthologs of PstS1 are found in the first two species only (Lew *et al.* 2011).

2.3.4.3 Mycobacterial lipoprotein mutant strains

Different lipopeptide deficient or overexpressing mutant strains were investigated to obtain insights into the relative contribution of lipoproteins to the immunogenicity and virulence of *M. tuberculosis*. For instance, a recombinant 19 kDa-deficient strain proved attenuation in human monocytes, whereas overexpression increased the innate immune mechanisms triggering immunactivation (IL-12, IL-1β, and TNF-α) (Stewart *et al.* 2005). Attenuation of *M. tuberculosis* virulence in BALB/c mice was observed after deletion of the 27 kDa lipoprotein (Bigi *et al.* 2004). Another knockout mutant (Δ*lpqS*) showed reduced growth in medium and attenuation upon infection of a human monocyte line (Sakthi and Narayanan 2013).

Differing from those mutants only deficient in one lipoprotein, Sander *et al.* (2004) developed an *M. tuberculosis* strain deficient in *lspA*. No efficient processing, in particular cleavage of the signal peptide from the immature prolipoprotein could be achieved due to the lack of the prolipoprotein signal peptidase. This critical intervention affects all lipoproteins. The *in vitro* growth of this strain was not affected by the deletion, but the virulence of the Δ*lspA* mutant was severely compromised. Using a similar mutant also lacking *lspA*, Banaiee *et al.* (2006) could demonstrate that lipoproteins are not the only inhibitors of macrophage responses to IFN-γ as a late effect of innate immune stimulation. This finding of a lipopeptide independent pathway contributed to the prevention of overestimation of the potency of mature lipopeptides relative to other constituents of the mycobacterial cell wall (e.g., PIM). Recently, Tschumi *et al.* (2012) investigated mycobacterial *Δlgt* mutants lacking the prolipoprotein diacylglycerol transferase and thus the initial lipidation of the prolipoproteins. It was not possible to generate an *M. tuberculosis Δlgt* mutant strain without concurrent *lgt* complementing. They could thereby demonstrate that *lgt* is essential for the growth of *M. tuberculosis*. *M. smegmatis* has two Lgt homologues. Deletion of the major *lgt* in *M. smegmatis* resulted in growth retardation, which could be restored by introduction of the *M. tuberculosis lgt* (Tschumi *et al.* 2012).

2.4 Human and bovine tuberculosis

2.4.1 The immune responses in primary tuberculosis

2.4.1.1 Initial recognition and replication of *Mycobacterium tuberculosis*

Human tuberculosis is usually the consequence of an airborne infection: *M. tuberculosis* is inhaled and directly reaches its main target location - the alveoli of the lungs. Alveolar

macrophages (AM), a distinct subset of macrophages equipped for initial particle and pathogen contact, express a plethora of immune receptors: Fcγ receptors, complement receptors (CR), Toll-like receptors (TLR), mannose receptors (MR), dectin-1, Mincle, and scavenger receptors (SR) (Dey and Bishai 2014) which bind to mycobacterial structures and trigger different signaling pathways. These AM as well as lung-resident dendritic cells (DC) with their receptor DC-SIGN are among the first cells to encounter the bacterium. The dendritic cell-specific intracellular adhesion molecule-3-grabbing non-integrin (DC-SIGN) binds to the mycobacterial ManLAM, PIM (Ehlers 2010), LM and α-glucan (Geurtsen *et al.* 2009).

Inside the cell, mycobacteria actively inhibit phago-lysosomal fusion. This important mechanism for the intracellular survival of *M. tuberculosis* occurs through inhibition of the Rab conversion. The early endosomes incorporating the pathogen upon receptor-mediated uptake into the cell express the small GTPase Rab5 on their surface. This GTPase mediates the fusion of endosomes and endocytosed vesicles (Hutagalung and Novick 2011) and supports mycobacterial survival (Vergne *et al.* 2004), e.g., through the acquisition of iron-loaded transferrin and other nutrients (Clemens and Horwitz 1996). The early Rab5-positive endosome usually matures into a late Rab7-positive endosome (Hutagalung and Novick 2011). Late endosomes fuse with lysosomes and degradation of pathogens occurs through acidification and hydrolases (Luzio *et al.* 2007). In detail, the maturation block by *M. tuberculosis* is initiated through the following cascade: *M. tuberculosis* alters the usual Ca^{2+} signaling in macrophages which occurs upon endocytosis of pathogens (Malik *et al.* 2000; Malik *et al.* 2003). The low Ca^{2+} levels lead to decreased levels of the Ca^{2+}-dependent CaM (calmodulin) and the CaM-dependent protein kinase II (CaMKII) on phagosomes containing live *M. tuberculosis* (Malik *et al.* 2001; Vergne *et al.* 2003). Ca^{2+}/CaM usually recruits EEA1 and Hrs through a PI3P-kinase-dependent pathway, which is thereby also blocked (Fratti *et al.* 2001; Vergne *et al.* 2003; Vieira *et al.* 2004). EEA1 and Hrs are both important for endosomal sorting and the actual fusion with lysosomes (Philips 2008). The PI3P-kinase hVPS34/p150 would directly interact with Rab7 (Stein *et al.* 2003). This maturation block is further supported by the active recruitment of Rab22a by *M. tuberculosis* (Roberts *et al.* 2006). For the long-term maintenance of the characteristics of the mycobacterial phagosome, Rab5 is supported by Rab14 (Kyei *et al.* 2006). It is evident that this phagosomal vacuole is the predominant location of viable *M. tuberculosis* in the host cell. Nevertheless, vacuole-escape mechanisms have been described for mycobacteria (Stamm *et al.* 2003) and may possibly be dependent on ESAT-6 (van der Wel *et al.* 2007; Smith *et al.* 2008). Cytosolic escape could facilitate direct cell-to-cell spread of the bacteria. However, this intracytoplasmic residence is still being discussed for *M. tuberculosis* (DiGiuseppe Champion and Cox 2007; Welin and Lerm 2012). ESX-1, a secretion system deleted in BCG,

was also described to support apoptosis of infected macrophages which could play a role in antigen presentation and spreading of the disease (Schaible *et al.* 2003; Aguiló *et al.* 2013).

2.4.1.2 Innate immune responses with particular focus on mycobacterial lipoprotein antigens

M. tuberculosis activates various innate immune cells such as macrophages, DCs, neutrophils, and natural killer cells. Their functions and effects strongly affect the initial phase of the infection and also influence the adaptive immune response (Sia *et al.* 2015). In the following, the focus is on those innate immune pathways which are triggered by mycobacterial lipoproteins.

Mycobacterial lipoproteins are potent activators of innate immune responses mainly through TLR signaling (Philips and Ernst 2012). Diacylated and triacylated lipoproteins are recognized by TLR2 in association with the functional co-receptors TLR6 and TLR1, respectively (Takeda *et al.* 2002). Toll-like receptors are conserved pattern recognition receptors (Muzio *et al.* 1998; Yang *et al.* 1998; Kirschning *et al.* 1998). Similar to LPS-stimulation, co-expression of the CD14-receptor enhances the recognition of triacylated lipoproteins by the TLR2/TLR1 complex (Brightbill *et al.* 1999; Nakata *et al.* 2006).

TLR2 binding of mycobacterial lipoprotein initiates a MyD88-dependent signaling pathway which recruits and activates IL-1 receptor-associated kinase 4 (IRAK4). IRAK4 phosphorylates IRAK1. The association of the activated IRAK1 with the TNF receptor-associated factor 6 (TRAF6) pursues the signaling cascade through the formation of a complex with TGF-β-activated kinase 1 (TAK1), its binding proteins (TAB1 and TAB2) and the proteins Ubc13 and Uev1A, leading to the activation of TAK1. This TAK1 degrades “IκB kinase kinase” (IKK) which itself leads to release of NF-κB from the sequestration by IKK in the cytoplasm (Underhill *et al.* 1999; Akira 2003; Takeda and Akira 2004).

NF-κB translocates into the nucleus to induce the transcription of genes of pro-inflammatory cytokines (Kleinnijenhuis *et al.* 2009; Murphy 2011). Some of the most prominent representatives of these cytokines are (Zhang *et al.* 2015):

- Tumor necrosis factor α: TNF-α, together with Interferon-γ (IFN-γ), initiates the synthesis of nitric oxide synthetase 2 (NOS2) in murine macrophages (Ding *et al.* 1988; Flesch *et al.* 1994). This direct microbicidal immune mechanism occurring upon TLR2 signaling was only found in mice (Brightbill *et al.* 1999), but not in humans (Thoma-Uszynski *et al.* 2001). However, TNF-α must also play an important role in protection against human tuberculosis as treatment with TNF-α blockers can trigger active disease (Harris and Keane 2010).
- Interleukin-1β: IL-1β mainly acts through IL-1-receptor type I and provides a positive feedback mechanism for the further production of various pro-inflammatory cytokines (Berrington and Hawn 2007), such as TNF as well as its TNF-receptor (Jayaraman *et al.* 2013).
- Interleukin-6: IL-6 promotes early IFN-γ secretion (Saunders *et al.* 2000).

Furthermore, lipoprotein TLR2 signaling promotes innate immune mechanisms such as DC maturation (Hertz *et al.* 2001) and induction of apoptosis (Lopez *et al.* 2003; Ciaramella *et al.* 2004; Sanchez *et al.* 2009; Sánchez *et al.* 2012).

Apart from these “classical” innate immune responses, TLR2 signaling of mycobacterial lipoproteins also influences the adaptive immunity. NF-κB-mediated transcription of IL-12 (Murphy *et al.* 1995) activates NK T cells to produce IFN-γ (Murphy 2011). This IFN-γ triggers activation of STAT1 and thereby activation of naïve CD4-positive T cells. The then initiated expression of the transcription factor T-bet upregulates IFN-γ and the IL-12-receptor in the T cells. Next, IL-12 acts directly through STAT4, leading to expansion of these Th1 cells. Th1 cells predominantly secrete IFN-γ which again acts as a positive stimulus for the expansion of further Th1 cells (Murphy 2011).

In contrast to these “activating” mechanisms, mediating the down-regulation of the IFN-γ secretion (Pai *et al.* 2003) as well as the MHC II expression and thus the antigen presentation (Noss *et al.* 2001; Fulton *et al.* 2004; Gehring *et al.* 2004; Stewart *et al.* 2005) have also been described as some of the various effects and potencies of mycobacterial lipoprotein TLR2 signaling.

2.4.1.3 Adaptive immune responses to mycobacterial lipoprotein antigens

Apart from innate immune responses, mycobacterial lipoproteins trigger cellular and humoral adaptive immune responses. Innate mechanisms can occur in conjunction with adaptive responses. For example, Hovav *et al.* (2003) observed the induction of NO as well as a Th1 profile and high IgG titers upon immunization of BALB/c mice with the recombinant 27 kDa lipoprotein of *M. tuberculosis*.

T cell-mediated immunity is determined as the requirement for efficient tuberculosis control (Jasenosky *et al.* 2015). In this line, upon stimulation with mycobacterial lipoprotein antigens, a classical Th1 profile is observed in most studies, e.g., in immunization of BALB/c mice with recombinant 27 kDa lipoprotein (Hovav *et al.* 2003; Hovav *et al.* 2004). However, CD8-positive T cells were also shown to recognize mycobacterial lipoprotein, e.g., the *M. tuberculosis* 19 kDa antigen (Mohagheghpour *et al.* 1998), but this lipoprotein derived from rapid-growing species seemed to induce a much more efficient MHC I presentation (Neyrolles *et al.* 2001). Epitopes for the MHC-restricted induction of T cells were found, for example, on the 19 kDa lipoprotein (Mohagheghpour *et al.* 1998), the 27 kDa lipoprotein (Bigi *et al.* 1997), the 38 kDa lipoprotein (Vordermeier *et al.* 1991; da Fonseca *et al.* 1998), and MPT83 (Kao *et al.* 2012). Lipopeptides can further be presented by CD1 molecules (Moody *et al.* 2004; van Rhijn *et al.* 2005).

Though it is not the main mechanism of tuberculosis control, mycobacterial lipoproteins also stimulate B cells: The *M. tuberculosis* recombinant 27 kDa lipoprotein induced B cell proliferation in a TLR2-dependant manner (Hovav *et al.* 2004) and initiated a strong antibody response in BALB/c mice with particularly high IgG2a titers (Hovav *et al.* 2003). This isotype specifically indicates a Th1 immune response, despite BALB/c mice usually showing a Th2 IgG1 phenotype (Natsuume-Sakai *et al.* 1977).

In the following, the focus is on the adaptive immune responses to a broad range of lipopeptides contained in hydrophobic antigen preparations of *M. tuberculosis*.

Bastian *et al.* (2008) demonstrated that a chloroform-methanol extract (CME) of *M. tuberculosis* induces cytokine and chemokine release, cytotoxicity, and direct antimicrobial activity in the stimulated lymphocytes from BCG-vaccinated or latently infected donors or patients with active TB. High proportions of activated, IFN-γ and TNF-α secreting, MHC II-restricted Th1 effector memory T cells were revealed. These T cells were not observed in naïve donors indicating a requirement of prior sensitization. The T cell responses were highest in latently infected individuals, reduced in TB patients, and weak in BCG vaccinated donors. The expanded T cells did not respond to tetanus toxoid, LPS or the synthetic lipopetide Pam_3Cys. This finding indicates antigen specificity. Interestingly, Bastian

et al. (2008) could demonstrate that an exceptional T cell subset – antigen-specific CD4-positive MHC II-restricted T cells with cytolytic activity (secretion of granulysin and in particular perforin and granzyme B) and the potential to kill intracellular bacteria – responds to the CME stimulus. An altered, mature phenotype of the APCs could not be observed upon CME stimulation, suggesting that those cells were not involved in this immune response, apart from antigen presentation through MHC II (Bastian *et al.* 2008). Altogether the findings of the required sensitization, the anti-specificity and the immature APCs indicate an adaptive immune response.

Confirmation that lipopeptides were the relevant antigens in CME was obtained by the observation that both proteinase K treatment and delipidation abolished the antigenicity of CME (Bastian *et al.* 2008). Seshadri *et al.* (2013) confirmed that lipopeptides are important antigens for CD4-positive MHC II-restricted T cells in *M. tuberculosis* infection and that stimulation is not dependent on TLR2 signaling. They determined that the lipopeptides require cell-to-cell contact between the CD4-positive T cells and APCs or endosomal processing by APCs for loading onto MHC II molecules. Significantly reduced T cell activation was observed in response to a lipid preparation obtained from the Δ*lspA* mutant, which lacks prolipoprotein signal peptidase. It was concluded from this finding that the strong T cell response to the mycobacterial lipid preparations is preferentially induced by mature triacylated lipopeptides (Seshadri *et al.* 2013).

Using MHC II blocking antibodies, Bastian *et al.* (2008) demonstrated an 80 % reduction of IFN-γ production in human T cell-enriched PBMCs co-incubated with autologous APCs. Using CD1 antibodies, they could additionally detect antigen presentation through CD1 in two of nine donors, both of whom demonstrated MHC II presentation as well. The MHC II blocking experiment of Seshadri *et al.* (2013) reduced the IFN-γ production significantly as well, but a very weak proportion remained in accordance with the findings of Bastian *et al*. (2008). These findings suggest that in addition to the clearly predominant MHC II presentation, another way of presenting lipoprotein antigens must exist, probably by CD1. Such a population of lipopeptide-specific, IFN-γ and TNF-α secreting T cells restricted for CD1a was recently identified (Kasmar *et al.* 2013). Nevertheless, as clearly demonstrated by Bastian *et al.* (2008) and Seshadri *et al.* (2013), mycobacterial lipoproteins are in the majority presented by MHC II in humans.

Both of those studies did not investigate the T cell response to lipid antigens after vaccination with BCG in a defined setting. Bastian *et al.* (2008) considered BCG-vaccinated individuals as a distinct group from naïve and latently infected individuals, and observed significantly lower T cell responses in the group of BCG vaccinees compared with individuals latently infected with *M. tuberculosis*. Interestingly, the T cell response of the vaccinees was,

however, stronger than the naïve immune reaction. For those analyses, PBMCs were obtained from adults who had received BCG vaccination many years ago and it is well known that BCG immunity wanes over time (Fine 2001). Seshadri *et al.* (2013) did not specify whether the donors in their experiments had been BCG-vaccinated. For these reasons, the stimulation of those potent T cells by BCG required re-investigation in a defined experimental setting.

2.4.1.4 The protective effect of immune responses elicited by mycobacterial lipoproteins

The strong Th1 immune responses following stimulation with lipopeptides suggest protection against MTC infection. The expression of the 19 and 38 kDa lipoproteins in recombinant vaccinia virus-infected cells yielded promising results (Zhu *et al.* 1997) and a subunit vaccine with recombinant MPT83 induced protection in C57BL/6 mice resulting in significantly reduced bacterial loads in the lungs and the spleen upon *M. tuberculosis* H37Rv challenge (Kao *et al.* 2012).

Yet the opposite was observed in most other *in vivo* protection studies. Neither deletion nor overexpression of the 19 kDa lipoprotein had an effect on the protective efficacy of BCG upon *M. tuberculosis* infection in C57BL/6JCit mice as described by Yeremeev *et al.* (2000). Rao *et al.* (2005) determined that 19 kDa lipoprotein overexpression in BCG resulted in abolishment of the protective BCG efficacy upon *M. tuberculosis* challenge in guinea pigs. Using BALB/c mice, they could further show that immunization with 19 kDa lipoprotein overexpressing BCG initially elicited a Th1 immune response which, however, shifted towards Th2 upon *ex vivo* contact of splenocytes with total BCG sonicate (Rao *et al.* 2005). Accordingly, in BALB/c mice vaccinated with the recombinant 27 kDa lipoprotein, significantly increased numbers of CFU were observed in the spleen upon *M. tuberculosis* and *M. bovis* BCG challenge compared with control groups, despite a previously demonstrated Th1 immune response (Hovav *et al.* 2003). The same findings were observed upon *M. tuberculosis* H37Rv challenge of BALB/c mice immunized with recombinant LprN – LprN sensitization even increased the tissue damage in the lungs and the spleen upon infection (Pasricha *et al.* 2014). Furthermore, upon co-administration, the 27 kDa lipoprotein abolished any protection deriving from other mycobacterial vaccines (Hovav *et al.* 2003). Similar findings upon *M. tuberculosis* challenge were achieved by Abou-Zeid *et al.* (1997) when analyzing immunity and protection of C57BL/6 mice sensitized with *M. vaccae* expressing a recombinant 19 kDa lipoprotein. In this line, a DNA vaccine encoding the *M. bovis* LppX did not provide protection in mouse experiments either (Lefèvre *et al.* 2000).

Altogether, these results suggest that mycobacterial lipopeptides own a rather low to non-existent potential to stimulate protection in vaccinated subjects though they mount strong immune responses. Furthermore, the assessment of vaccine candidates which reliably convey protection is particularly difficult in tuberculosis research as no correlates of protection could be defined yet (Nunes-Alves *et al.* 2014; Fletcher 2015).

2.4.2 Granulomas and caseation in human and bovine tuberculosis

2.4.2.1 The immunology of tuberculosis granulomas

Granulomas in tuberculosis have long been thought of as protective measures of the host immune system. However, there is increasing evidence that they constitute at least additional pathogen-protective structures which promote bacterial spread in early stages and extracellular existence in late stages, which is strongly growth-permissive (Pagán and Ramakrishnan 2015). Additionally, many human T cell epitopes of *M. tuberculosis* antigens have been found to be hyperconserved suggesting that *M. tuberculosis* benefits from recognition through the host immune system (Comas *et al.* 2010).

The formation of granulomas in tuberculosis can be divided into different stages: the innate granuloma, the immune granuloma and the chronic granuloma (Shaler *et al.* 2013).

Using zebrafish infected with *M. marinum* as a model for mammalian pulmonary *M. tuberculosis* infection, important mechanisms of early granuloma formation could be identified. Upon infection, the mycobacteria are first encountered by macrophages which transport the pathogen from the lung epithelium into the parenchyma (Clay *et al.* 2007). A permissive phenotype of the host cell is therefore initiated by the pathogen through masking of the bacterial PAMPs and thus evasion from TLR2 signaling (Cambier *et al.* 2014). Through a host chemokine receptor 2-mediated pathway, which was induced through bacterial phenolic glycolipids (PGL), further permissive macrophages are attracted (Cambier *et al.* 2014) forming the early granuloma composed of innate immune cells. Aggregation of the macrophages as well as bacterial dissemination is dependent on the secretion system ESX-1 which is absent in the attenuated vaccine strain BCG (Volkman *et al.* 2004; Parasa *et al.* 2014). Macrophage chemotaxis is further initiated through matrix metalloproteinase-9 (MMP-9) secretion of epithelial cells near the granuloma. This MMP-9 release is induced by the ESX-1-secreted antigen ESAT-6 (Pagán and Ramakrishnan 2015).

Infected macrophages and DC not only reside in the innate granuloma, but also migrate to the mediastinal lymph nodes. During this process mycobacterial antigens are processed and

loaded onto antigen-presenting molecules for the efficient presentation to lymphocytes. As described above, the presentation of protein/lipoprotein antigens occurs mainly through MHC II and elicits a predominantly Th1 immune response which is characterized in particular by IFN-γ secretion (Mogues *et al.* 2001). Subsequently, the effector T cells are directed by chemokine sensing to migrate back to the lung. At the infection site T cells provide a positive feed-back mechanism to sustain microbicidal mechanisms of the infected macrophages (Shaler *et al.* 2013). Though Th1 cells constitute the most prominent population, other cells are activated as well: Th17 cells (Torrado and Cooper 2010), γ:δ T cells (Meraviglia *et al.* 2011), and CD8-positive T cells (Winau *et al.* 2006). Together with the activated macrophages these lymphocytes induce a pro-inflammatory environment, mainly mediated through IL-1β, IL-6, IL-12, IL-23, TNFα, IL-21, IL-22, and IL-17. For instance, the activation of Th17 cells with its cytokine repertoire of IL-17, IL-21, and IL-22 predominantly induces strong microbicidal effects of neutrophils which at the same time result in tissue damage (Torrado and Cooper 2010). It is counter-regulated by Th1 and T_{reg} responses (Marin *et al.* 2010). These cell-mediated mechanisms constitute the crucial steps to form the "immune granuloma" which is tightly regulated by host factors such as TNFα and IFN-γ (Cavalcanti *et al.* 2012).

In most cases, containment of *M. tuberculosis* does not lead to the elimination of the bacteria but to the establishment of latent infection (LTBI) – possibly due to the slow onset of adaptive immune responses compared with other diseases (Shaler *et al.* 2012). According to the WHO (World Health Organization 2015b), approximately one third of the world's human population is latently infected with *M. tuberculosis*. Latency is reflected in an altered gene expression profile of the bacterium (Schuck *et al.* 2009; Rohde *et al.* 2012). Within the granuloma, the mycobacteria now influence the functions of the infected macrophages towards an anti-inflammatory response with low NO but high IL-10 production (Higgins *et al.* 2009; Shaler *et al.* 2011; O'Leary *et al.* 2011). However, it must be considered that mechanisms suppressing excessive immune responses might be beneficial for the host as well (Shaler *et al.* 2013). Interestingly, macrophage functions are very selectively suppressed as APCs are continuously attracted to the granuloma through chemokine secretion (Shaler *et al.* 2011).

Although organized in a virtually layered manner in humans, the mycobacterial granuloma is a dynamic structure. Fluctuation of the cells is common and could be a source of early dissemination of the pathogen from the primary site to other host tissues and organs (Schreiber *et al.* 2011).

The immune granuloma and the chronic granuloma, unless calcified, consist of a core surrounded by CD4- and CD8-positive lymphocytes with follicular aggregates of APCs and

B cells (Ulrichs and Kaufmann 2005; Tsai *et al.* 2006). In the core, infected macrophages obtain an epithelioid phenotype and assemble to form multinucleated Langhans giant cells (Ulrichs and Kaufmann 2005; Tsai *et al.* 2006). The development of foamy macrophages occurs through phagocytosis of infected apoptotic macrophages and accumulation of lipids. The bacteria in these cells reside in a dormant stage (Peyron *et al.* 2008). Hypoxia is another important feature of human tuberculosis granulomas, as it further alters the pathogen's gene expression and reduces its susceptibility to drugs (Wayne and Hayes 1996; Cho *et al.* 2007; Galagan *et al.* 2013).

In the long term, known as the „chronic" stage, a fibrotic capsule can form around the granuloma and the center can calcify. The rare occurrence of a healed granuloma is characterized by complete central calcification (Shaler *et al.* 2013). It is, however, more common for caseation of the granuloma to occur than calcification.

Caseation evolves due to necrosis of the hypoxic granuloma center (Kim *et al.* 2010) or due to the onset of caseous pneumonia as post-primary tuberculosis manifestation (Hunter 2011). Caseation is supported by the extended synthesis of the potentially cytotoxic trehalose 6, 6'-dimycolate (TDM) by the bacterium, leading to enhanced synthesis and sequestration of host lipids (Geisel *et al.* 2005; Guidry *et al.* 2007; Kim *et al.* 2010). The differences in caseation between *M. tuberculosis* and *M. bovis* infection are described in detail in section 2.4.2.2. Caseation in its species-specific form is an essential step towards cavitation of the host tissue and accessing the airways (Hunter *et al.* 2007) which allows for aerogenic host-to-host transmission of the pathogen. Such reactivation of LTBI to active disease occurs in 5 − 15 % of latently *M. tuberculosis*-infected individuals (World Health Organization 2015a; Getahun *et al.* 2015).

2.4.2.2 Caseation and pathomorphological differences between *M. tuberculosis* and *M. bovis* infections

The pathology of human tuberculosis, mainly caused by *M. tuberculosis*, is often described as being indistinguishable from *M. bovis* infections in humans (Grange 2001). This may be partially correct regarding the later phenotypes when both infections present with the hallmark of the disease – the granuloma – and cavities in the lung tissue which permit the aerogenic transmission of the pathogen to another host, but it did not prove true during primary and initial post-primary infection in immunocompetent individuals (Hunter 2011).

The major recent insights into immunology and pathology of human tuberculosis are obtained from animal models, e.g., rabbits forming caseous granulomas upon infection with

M. bovis (Dannenberg 2001). These granulomas are considered „human-like“, but little validation through the comparison with cases of untreated, non-disseminated tuberculosis in non-immunocompromised persons has been possible in the last decades. Thus, the contemporary model of “human tuberculosis” is based on granulomas undergoing caseation leading to subsequent erosion into the airways and actually describes the phenotype of pulmonary *M. bovis*, but not *M. tuberculosis* infection (Collins and Grange 1983).

When comparing descriptions of the pathology of pulmonary tuberculosis in the pre-antibiotic era with the contemporary model of human tuberculosis it was revealed that immense differences between infections of immunocompetent humans with *M. tuberculosis* and *M. bovis* exist in terms of granuloma formation and latency (Hunter 2011). *M. bovis* infection itself manifests alike in humans and cattle (Hunter 2011). Significant differences between the manifestations of MTC infections in untreated, immunocompetent humans and treated or immunocompromised patients were additionally found. The main characteristics of *M. tuberculosis* infection in humans are summarized in **Table 2.1**, and the phenotype of *M. bovis* infection in humans as well as in cattle is depicted in **Table 2.2**.

A possible explanation for these differences could be the typical life span of the main host organism of the bacteria. Humans live much longer than cattle and the pathogen can remain latent for decades. This would also explain why most animals cannot host a complete life cycle of *M. tuberculosis* which is required for cavity formation and subsequent efficient spreading (Waters *et al.* 2010; Hunter 2011), although the pathogen can be transmitted to animals in close contact with infected humans (Michel *et al.* 2010).

Table 2.1 Phenotypes and characteristics of *M. tuberculosis* infection in humans.

Subject	Description	Reference
Principle of manifestation in an untreated, immuno-competent host	– Three phases: primary infection, latency, and post-primary tuberculosis.	Hunter 2011
Area of manifestation in the lungs	– The initial infection can occur anywhere in the lungs. – Cavitation manifests in the apex.	Balasubramanian *et al.* 1994 Hunter 2011
Characteristics of the granulomas in primary infection	– Caseating granulomas with necrosis and layers of epithelioid macrophages and lymphocytes. – Moderate size of approximately 2.5 cm in diameter. – Healing of the lesions through calcification and fibrosis is possible, but most often a latent TB infection arises.	Hunter 2011
Latency	– Can remain latent for decades.	Bandera *et al.* 2001
Post-primary tuberculosis:	– Development of post-primary tuberculosis occurs endogenously by reactivation or exogenously through reinfection. – An initial transient immunosuppression in an otherwise immunocompetent person is often the trigger for post-primary infection development. – Three phases: lipid pneumonia phase, caseous pneumonia phase, cavity formation.	Bandera *et al.* 2001 Hunter 2011
– Lipid pneumonia phase	– An initially exudative pneumonia in the upper lobes of the lung. – Initiated by mycolic acid-mediated accumulation of foamy macrophages in alveoli which contain mycobacteria. – Further accumulation of fibrin, cell debris, erythrocytes, leukocytes, and more lipid through the alveolar macrophages over a period of months to years until the affected alveolus is obstructed. – These lesions can heal, which occurs in 90 % of cases and leaves small scars in the lung apices. – Bacterial numbers are relatively low at this stage.	Korf *et al.* 2005 Hunter 2011

The table continues on the next page.

Table 2.1 (continued)

Subject	Description	Reference
– Caseous pneumonia phase	– The 10 % non-healing lipid pneumonia lesions progress to the caseous pneumonia phase. – Increase in bacterial numbers, probably associated with extensive production of TDM, initiates necrotic caseation of the lesions. – Necrotic caseation is an exudative process leading to complete homogeneity of the tissue with elastic fibers being the only remaining structures which keep the mass together now.	Hunter 2011.
– Cavitation	– Softening and fragmentation of the necrotic mass can occur, which produces cavities and openings into the airways through expectoration. – Only a few bacteria are present during early cavitation. – An acute and fatal break-down of the disease is possible. – After acute illness, the remnants of this infection are cavities with a thin fibrotic wall which now strongly enhance extracellular bacterial growth. – Cavity formation was never observed in association with caseous granulomas, which often were not even present in the lungs.	Hunter 2011 Welsh *et al.* 2011
Chronic stage tuberculosis („open tuberculosis“)	– Accounts for nearly 100 % of transmission because the patients are in principle in good health. – The lesions of post-primary tuberculosis can become surrounded by caseating granulomas which may progress to chronic fibrocaseous tuberculosis. – Different stage granulomas can then exist within one host.	Hunter 2011
Characteristics of the disease in an immuno–compromised host	– High bacterial numbers. – Poorly formed cavities which do not allow efficient transmission. – Early generalized disease or tuberculoid meningitis is particularly frequent. – Granuloma stages are homogeneous.	Aaron *et al.* 2004 Hunter 2011

Table 2.2 Phenotypes and characteristics of *M. bovis* infection in humans and cattle.

Subject	Description	Reference
Principle of manifestation in an untreated, immuno-competent host	– Aggressive primary tuberculosis with access to the airways. – No real latency. – Occurrence of different stages of lesions including chronic ones is possible in one individual.	Collins and Grange 1983 Hunter 2011 Menin *et al.* 2013
Area of manifestation in the lung	– TB in cattle mainly manifests in the dorso-caudal lobes of the lungs. – TB granulomas in humans are mainly found in the apex (see above). There is evidence for this localization in *M. tuberculosis* as well as in *M. bovis* infections of humans. – The area of manifestation in the lungs seems to rather be influenced by the anatomical factors of the host than by a localization preference of the pathogen.	Francis 1947 McIlroy *et al.* 1986 Cassidy 2006 Shrikrishna *et al.* 2009 Waters and Palmer 2015
Characteristics of the granulomas	– Small, up to 2 cm in diameter, „Pearl Disease“. – Caseous center. – Multiple granulomas can form clusters in the shape of bunches of grapes, or coalesce. – Softening of the central tissue leads to erosion into the airways as small cavities.	Hunter 2011

2.5 Bacille Calmette-Guérin

2.5.1 Origin and characteristics

The live attenuated *M. bovis* strain Bacille Calmette-Guérin is one of the most abundant vaccine strains worldwide, but gives rise to many controversies. The BCG vaccine has several disadvantages. However, despite many attempts no improved alternative TB vaccine has been fully licensed so far. In the following, the development and characteristics of BCG since its introduction by Albert Calmette and Camille Guérin is described, with special attention on its genetic evolution.

BCG development started in 1908 and continued through 230 *in vitro* passages of a virulent *M. bovis* strain, until the attenuated strain was first used as a vaccine in humans in 1921. From that time it was administered to a rising number of children (Sakula 1983) and in 1928 the Health Committee of the League of Nations declared it to be highly effective (Calmette 1931; Smith and Starke 2004). The original BCG Pasteur strain was continuously cultivated and passaged *in vitro* at the Institut Pasteur Paris until 1961, when it was lyophilized after

1173 passages which explains its current name: “BCG Pasteur 1173”. However, along with its expanding clinical use, the BCG strain has also been distributed throughout the world from 1924 (Behr and Small 1999) and a total number of 49 production substrains has been reported (Corbel *et al.* 2004). The original BCG strain was cultivated on glycerinated bile potato (Calmette 1931), but worldwide distribution and propagation of derivatives was often accompanied by changes in culture medium (Osborn 1983; Oettinger *et al.* 1999).

The separation of the most important early and late BCG daughter strains is displayed in **Figure 2.1** (Behr and Small 1999).

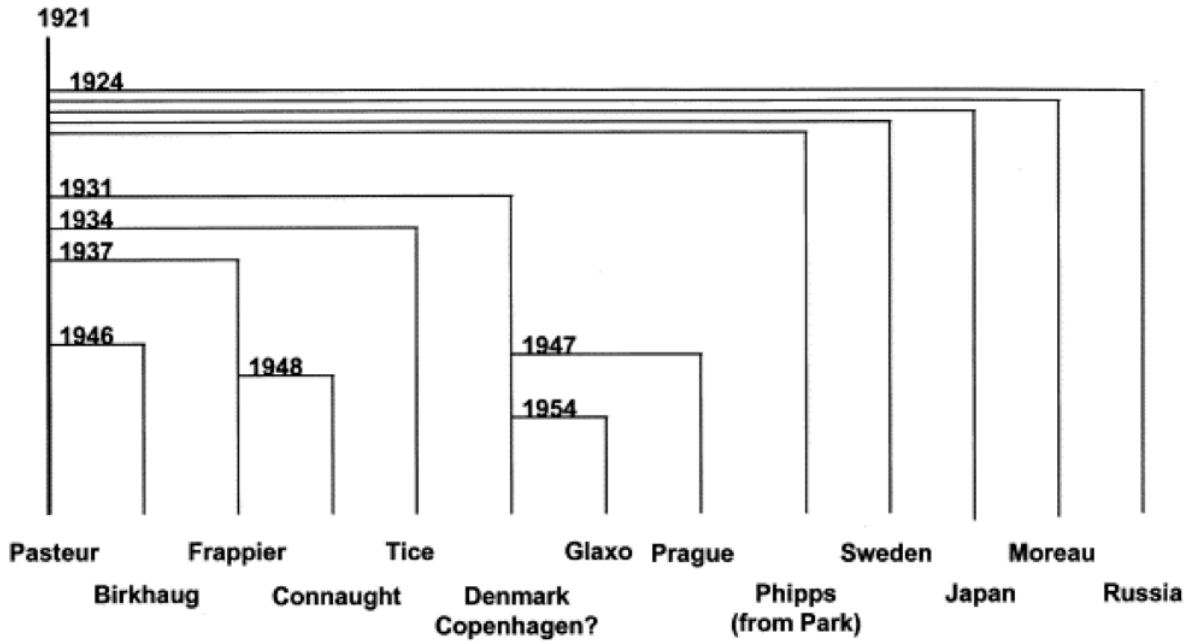

Figure 2.1 Genealogy of BCG strain dissemination.

The vertical axis scales to time. The horizontal dimension does not scale to genetic difference. Reproduced from “A historical and molecular phylogeny of BCG strains”, M. A. Behr, P. M. Small, Vaccine, 1999, volume 17, issues 7-8, pages 915-922, with permission from Elsevier.

Comparative genomics enabled the in-depth description of distinctions on the gene level that were obtained during these subcultivations (Brosch *et al.* 2007; Leung *et al.* 2008). The loss of the region of difference 1 (RD1) is the common deletion in all BCG strains, accounting for its initial attenuation. RD1 encodes, among others, for the important protein antigens ESAT-6 and CFP10 as well as for their secretion system ESX-1 (Mahairas *et al.* 1996; Lewis *et al.* 2003; Guinn *et al.* 2004) (**Figure 2.2**). However, re-introduction of RD1 led to only partial reversal of the attenuation (Pym *et al.* 2002). Therefore, the genetic variations that occurred subsequently in addition to the loss of RD1 must be important for the attenuation as well. For

instance, BCG strains obtained after 1927 are deleted in RD2 which encodes for the immunogenic protein MPT64 (Mahairas *et al.* 1996; Behr and Small 1999; Leung *et al.* 2008). Daughter strains which derived from the original strain later than 1933 show additional deletion in N-RD18 which encodes the regulatory gene *sigI* and conserved hypothetical proteins (Brosch *et al.* 2001; Brosch *et al.* 2007; Leung *et al.* 2008).

Further alterations mainly affected either a single BCG vaccine strain, or only some of the strains. For example, BCG Moreau shows two deletions affecting the genes *fadD26* and *ppsA* which are necessary for the biosynthesis of the virulence-associated cell wall lipids phtiocerol dimycocerosates (PDIMs) and phenolic glycolipids (PGLs) (Cox *et al.* 1999; Reed *et al.* 2004; Hotter *et al.* 2005; Leung *et al.* 2008). Numerous polymorphisms within the BCG substrains are also found for the *phoP-phoR* locus (Leung *et al.* 2008). This locus encodes for an *M. tuberculosis* two-component system (Cole *et al.* 1998) consisting of a transmembrane histidine kinase (PhoR) and a response regulator (PhoP) essential for *M. tuberculosis* virulence (Walters *et al.* 2006; Martin *et al.* 2006; Frigui *et al.* 2008; Lee *et al.* 2008).

Apart from deletions, up to two independent tandem duplications, DU1 and DU2, are found within the genome of different BCG strains (Brosch *et al.* 2000; Brosch *et al.* 2007) rendering the BCG genome larger than the one of *M. bovis* (Garnier *et al.* 2003). DU1 is limited to BCG Pasteur, whereas DU2 occurs in all BCG strains, assigning them to four different groups (DU2-I to DU2-IV) (Brosch *et al.* 2007). Brosch *et al.* (2000) could show that the overlapping regions of DU2-I to IV comprise genes whose enhanced expression could be advantageous for the cultivation in glycerol-containing medium. Furthermore, different duplication sequences are described that only occur in one BCG substrain, e.g., DU-Tice or DU-Birkhaug (Leung *et al.* 2008).

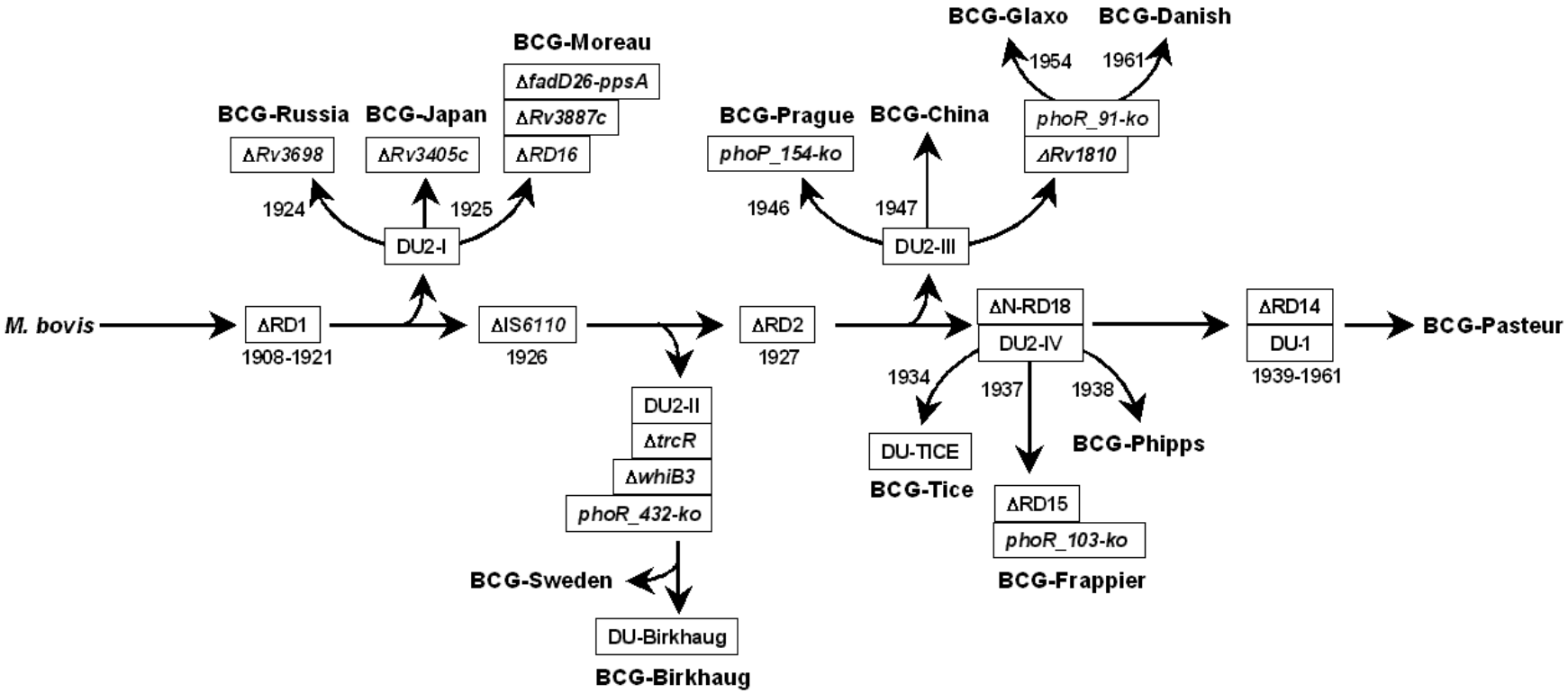

Figure 2.2 Genealogy of BCG vaccine strains.

This work has been adapted from the original article "Novel genome polymorphisms in BCG vaccine strains and impact on efficacy" by A. S. Leung, V. Tran, Z. Wu, X. Yu, D. C. Alexander, G. F. Gao, B. Zhu, J. Liu with minor modifications. BMC Genomics 2008, 9:413. doi: 10.1186/1471-2164-9-413.

In view of all these differences, Behr (2001a) introduced the term of a “vaccine family” of BCG, instead of “one vaccine”.

BCG induces a cellular immune response which can be analyzed in *ex vivo* studies and which involves mainly CD4-, but also CD8-positive T cells (Turner and Dockrell 1996; Esin *et al.* 1996; Smith *et al.* 1999). Likewise, a preferentially Th1/IL-12/IFN-γ-driven immune response is also observed after infection with *M. tuberculosis*. This immune response seems to be essential to combat mycobacterial infections (Newport *et al.* 1996; Altare *et al.* 1998), but IFN-γ quantification in different experimental settings could not yet been shown to constitute a good correlate of protection (Leal *et al.* 2001; Kagina *et al.* 2010). Whether the BCG-induced immune responses provide the maximum possible protection remains to be determined. This question is currently under investigation, e.g., by using a genetically modified BCG strain which favors the induction of CD8-positive T cells (Grode *et al.* 2005). Furthermore, there is an urgent need for investigation of the potential of BCG to elicit immune responses to unconventional antigens, e.g., mycobacterial lipopeptides.

2.5.2 Utilization as live vaccine and current modifications

Highly variable efficacies of 0 to 80 % are reported for BCG vaccination of humans (Fine 1995) with an approximate 50 % TB risk reduction (Colditz *et al.* 1994; Brewer 2000). This may in part be caused by strain specificities, but the effect of heterogeneous study conditions, e.g., in terms of host factors and delivery of the vaccine, cannot be quantified (Lagranderie *et al.* 1996; Behr 2001b).

Despite this varying and rather low efficacy, the WHO recommends the intradermal BCG vaccination as soon as possible after birth to all children living in high-disease burden countries, except if HIV-positive (World Health Organization 2015c). Revaccination is not recommended (World Health Organization 2004). To date, BCG is the only safe and at least partially protective vaccine available against TB. It reliably prevents severe disease outcomes in young infants, namely tuberculoid meningitis and miliary TB (Rodrigues *et al.* 1993). In adults, particularly in areas near the equator, the protective efficacy of BCG vaccination against pulmonary TB is low (Wilson *et al.* 1995; Tuberculosis Research Centre ICMR 1999; Fine 2001). It does not protect against reactivation of latent TB infection (LTBI) nor from transmission of the disease. However, there are reports on cross-reactivity of the immune responses induced by BCG vaccination. These immune responses could in part protect against non-tuberculous mycobacterial (NTM) diseases, e.g., leprosy and Buruli ulcer (Karonga Prevention Trial Group 1996; Portaels *et al.* 2004). The lack of specific vaccines

against those diseases further endorses the recommendation of BCG vaccination. Controversy remains whether BCG vaccination provides additional advantages against other infections, e.g., with nematodes (Elliott *et al.* 1999; Barreto *et al.* 2000; Randall *et al.* 2002; Cooper *et al.* 2003; Lipner *et al.* 2006).

A limitation in the use of this live attenuated vaccine is HIV infection. HIV-positive children receiving the BCG vaccine have an increased risk of severe side effects. However, these side effects, namely BCGitis and BCGosis as forms of lymphadenitis and osteitis/osteomyelitis may occur in healthy individuals as well. The risk for fatal outcomes is estimated to be 0.19 – 1.56/1,000,000 vaccinees and it almost exclusively affects immunocompromised individuals (World Health Organization 2004; Ladeira *et al.* 2014). However, non-generalized adverse effects, such as erythema, induration, abscesses, ulceration, and local lymphadenitis, are much more frequent, occurring in approximately 17.8 % of all vaccinees (Dommergues *et al.* 2009). The occurrence of adverse events seems to be strain-specific (Milstien and Gibson 1990). Today, BCG vaccination is no longer recommended in many Western countries because of a negative risk-benefit-assessment in low-endemic areas.

BCG vaccination can induce a positive TST result (Wang *et al.* 2002; Tissot *et al.* 2005). Due to this limitation that BCG puts on an important diagnostic option, the vaccination was never introduced in some countries such as the USA and the Netherlands (Luca and Mihaescu 2013). However, it does not alter the results in the IFN-γ release or ELISpot assay as they use antigens which are deleted in BCG (Ewer *et al.* 2003; Kang *et al.* 2005; Diel *et al.* 2006).

Despite its disadvantages, BCG is still one of the most frequently used vaccines worldwide with more than 80 % of the annual birth cohort being vaccinated (100 million infants) (Trunz *et al.* 2006; WHO-UNICEF 2014). By reliably protecting against tuberculoid meningitis and disseminated disease, it prevents approximately 41,500 infant TB cases per year (Trunz *et al.* 2006). Every new vaccine would first need to prove at least the same efficacy in children to be considered as a replacement. Another strategy is the development of a prime-boost vaccine to complement BCG vaccination. The general aims of the current TB vaccine development are the induction of protection against reactivation of latent TB infection (LTBI), which is mainly relevant in adulthood, and the possibility of administration to immunocompromised persons. The main strategies investigated in these purposes are viral vector vaccines and recombinant BCG, as well as subunit approaches using adjuvanted proteins. The vaccine candidates currently in clinical trials are depicted in **Table 2.3.**

To date, no vaccine candidate could demonstrate efficacy superior to BCG (Moliva *et al.* 2015). Despite the urge to keep searching for new vaccine candidates and best supporting

adjuvants, it will also be crucial to define correlates of protection in TB to better understand and predict vaccine efficacies (Nunes-Alves *et al.* 2014; Fletcher 2015).

Table 2.3 Current vaccine candidates in clinical trials (World Health Organization 2015a).

Designation	Type	Institution	Description	Clinical phase	Reference
Ad5Ag85A	Viral vector	CanSino; McMaster University, Canada	Adenovirus serotype 5 vector expressing AG85A; booster vaccine to BCG	Phase I trial, safety and immunogenicity, completed	Wang *et al.* 2004 Santosuosso *et al.* 2006 Smaill *et al.* 2013
ChAdOx1.85A	Viral vector	Oxford University, UK	Simian adenovirus expressing AG85A; booster vaccine to BCG; intramuscular or aerosol administration	Phase I trial alone and in a prime-boost strategy with MVA85A, ongoing	Stylianou *et al.* 2015
Crucell Ad35/AERAS-402, together with MVA85A	Viral vector	Aeras; Crucell; Oxford University, UK	Crucell Ad35/AERAS-402: adenovirus vector expressing AG85A, AG85B and TB10.4; MVA85A: vaccinia virus vector expressing AG85A	Phase I/II trial with one or two doses of Crucell Ad85/AERAS-402 and one dose of MVA85A or three doses of Crucell Ad85/AERAS-402, ongoing	Abel *et al.* 2010 Tameris *et al.* 2015
DAR-901	Whole cell	Aeras; Dartmouth University, NH	Heat-inactivated *M. obuense*; booster vaccine to BCG	Phase I trial, safety and immunogenicity, ongoing	Reyn *et al.* 2010 (proof-of-concept with *M. vaccae*) Bazzi *et al.* 2015

The table continues on the next page.

Table 2.3 (continued)

Designation	Type	Institution	Description	Clinical phase	Reference
H1:IC31	Adjuvanted subunit vaccine	Aeras; EDCTP; Staten Serum Institute, Denmark; TBVI	AG85B and ESAT-6; adjuvant: IC31	Three Phase I trials, safety and immunogenicity, completed; phase II trial, safety and immunogenicity, completed; phase II trial, immunogenicity, completed; advancement to H56:IC31; no further clinical trials planned	Weinrich Olsen *et al.* 2001 Reither *et al.* 2014
H4:IC31	Adjuvanted subunit vaccine	Aeras; Sanofi-Pasteur; Staten Serum Institute, Denmark	Fusion protein of AG85B and TB10.4; booster vaccine to BCG; adjuvant: IC31	Phase II trial, ongoing; phase II trial, proof-of-concept to prevent *de novo M. tuberculosis* infection, ongoing; immunogenicity study planned	Dietrich *et al.* 2005 Geldenhuys *et al.* 2015
H56:IC31	Adjuvanted subunit vaccine	Aeras; Staten Serum Institute, Denmark	AG85B, ESAT-6 and the „latency antigen“ Rv2660c; adjuvant: IC31	Phase I trial, safety and immunogenicity, completed; two Phase I trials, safety and immunogenicity, ongoing; efficacy trial planned	Aagaard *et al.* 2011 Lin *et al.* 2012 Luabeya *et al.* 2015
ID93+GLA-SE	Adjuvanted subunit vaccine	Aeras; Infectious Disease Research Institute	Fusion protein expressing three immunodominant *M. tuberculosis* antigens (Rv2608, Rv3619, Rv3620) and one *M. tuberculosis* latency antigen (Rv1813); adjuvant: GLA-SE	Phase I trial, safety and immunogenicity, completed; phase I trial, safety and immunogenicity, ongoing; phase IIa trial, safety and immunogenicity, ongoing; phase IIb, efficacy, planned	Baldwin *et al.* 2012

The table continues on the next page.

Table 2.3 (continued)

Designation	Type	Institution	Description	Clinical phase	Reference
M. Vaccae™	Lysate	AnHui Zhifei Longcom Biologic Pharmacy Co., Ltd.	*M. vaccae* lysate; immunotherapeutic agent for shortening TB treatment (licensed by China FDA)	Phase III trial, safety and efficacy, ongoing	Stanford *et al.* 2004 Yang *et al.* 2010
M72 + $AS01_E$	Adjuvanted protein subunit vaccine	Aeras; GSK	Recombinant fusion protein of *M. tuberculosis* antigens mtb32A and mtb39A; adjuvant: $AS01_E$; booster vaccine to BCG	Phase IIb trial, primary endpoint: protective efficacy of two doses against pulmonary TB; secondary endpoints: safety and immunogenicity, ongoing	Skeiky *et al.* 2004 Penn-Nicholson *et al.* 2015
MTBVAC	Attenuated *M. tuberculosis*	BIOFABRI; Institute Pasteur; TBVI; University of Zaragosa, Spain	Live attenuated *M. tuberculosis* with deletion of the *phoP* and *fadD26* genes; booster vaccine to or replacement of BCG	Phase I trial, completed; phase I/II trial, planned	Arbues *et al.* 2013
MVA-85A (Aerosol)	Viral vector	Aeras; Oxford University, UK	Vaccinia virus vector expressing AG85A; booster vaccine to BCG	Phase I trial, safety and immunogenicity, aerosol *versus* intradermal administration, completed	McShane *et al.* 2004 Tameris *et al.* 2013 Ndiaye *et al.* 2015 Satti *et al.* 2014
RUTI	Liposomes	Archivel Pharma, S.L.	Non-live vaccine; fragmented and detoxified *M. tuberculosis* encapsulated in liposomes	Phase II trial, completed; further trials planned	Vilaplana *et al.* 2011 Nell *et al.* 2014

The table continues on the next page.

Table 2.3 (continued)

Designation	Type	Institution	Description	Clinical phase	Reference
TB/FLU-04L	Viral vector	Research Institute for Biological Safety Problems, Kazhachstan; Research Institute on Influenza, Russia	Attenuated replication-deficient influenza vector (H1N1) with recombinant expression of *M. tuberculosis* AG85A and ESAT-6; mucosal booster vaccine to BCG	Phase I trial, intranasal administration, completed; phase IIa trial, planned	Stukova *et al.* 2006 Kuznetsova *et al.* 2014
VPM1002	Live recombinant vaccine	Max Planck Institute, Germany; Serum Institute of India; TBVI; Vakzine Projekt Management	BCG Prague strain expressing the listeriolysin gene (*Listeria mono-cytogenes*) and deleted in the urease gene	Phase IIa trial, completed; phase II trial, safety and immunogenicity, planned	Grode *et al.* 2005 Grode *et al.* 2013 Vogelzang *et al.* 2014

Abbreviations: **AG85** = Antigen 85; **BCG** = Bacille Calmette-Guérin; **EDCTP** = European and Developing Countries Clinical Trials; **ESAT-6** = 6 kDa Early secretory antigenic target; **FDA** = Food and Drug Administration; **GSK** = GlaxoSmithKline; **TB** = Tuberculosis; **TBVI** = Tuberculosis Vaccine Initiative; **UK** = United Kingdom

2.6 The guinea pig as a small animal model of tuberculosis

Since the very beginning, guinea pigs (*Cavia porcellus*) have been used as a small animal model in TB research (Fox 1868). It permits valuable insights into the course and immunology of tuberculosis (Clark *et al.* 2014). Furthermore, it has great implications in the development of vaccines and is still essential for tuberculin batch testing. The greatest advantages of this animal species are its susceptibility to MTC infection, the development of granulomas, and the natural expression of CD1 molecules relevant for lipid antigen presentation. One disadvantage is the limited availability of biologicals and diagnostic tools, such as recombinant cytokines and antibodies, for this species.

2.6.1 Tuberculosis of the guinea pig

Guinea pigs are highly susceptible to *M. tuberculosis* infection. As in humans, only very small numbers (5 or even 2 – 3 viable bacilli only) are required for infection and the macrophages efficiently support the intracellular growth of the mycobacteria (Wiegeshaus *et al.* 1970; Smith *et al.* 1970; Smith and Harding 1977; Chanwong *et al.* 2007; Clark *et al.* 2014).

Tuberculosis in guinea pigs is a chronic progressive disease (Smith *et al.* 1970; Turner *et al.* 2003; Sakamoto 2012). Subsequent to the aerogenic entry, replicating bacteria cause lung lesions and then spread and cause progressive granulomatous and necrotizing lesions in the mediastinal lymph nodes which are obvious from week three post infection (Basaraba *et al.* 2006a). This is known as primary complex formation in humans. In general, pulmonary lymphatics are heavily infected in guinea pigs (Basaraba *et al.* 2006b) with severe lymph node affection resembling lymphadenitis in childhood TB (Basaraba *et al.* 2006a). Furthermore, mycobacteria are hematogenously disseminated, e.g., into the spleen, but also back to the lungs where they establish a secondary infection (Fok *et al.* 1976; Harding and Smith 1977; Ho *et al.* 1978; Balasubramanian *et al.* 1994). Secondary granulomas close to the pleura can also develop upon lymphogenic dissemination (Orme and Basaraba 2014).

The development of primary lesions in the lung can be divided into four stages (Turner *et al.* 2003): Stage 1, at day 11, is represented by discrete lesions in the parenchyma formed by epithelioid macrophages, rodent-specific pseudoeosinophilic granulocytes and few lymphocytes. The lesions enlarge until day 21, or stage 2. First signs of granulomatous lymphadenitis appear at this stage (Turner *et al.* 2003). Granulocytes and lymphocytes are observed in the lesions, but not in the necrotic center. The development of necrosis is preceded by iron accumulation (Basaraba *et al.* 2008). The release of hydrolytic enzymes by the granulocytes is suspected to induce the guinea pig-characteristic necrosis with

eosinophilic debris (Orme and Basaraba 2014). Rodent-characteristic pseudoeosinophilic granulocytes are present throughout the whole disease process (Ordway *et al.* 2007). These granulocytes contain cationic proteins with microbicidal activity and do not have correlates in human granulocytes (Zeya and Spitznagel 1966; Lehrer *et al.* 1975). Bacteria are found intracellularly in macrophages but also extracellularly in an acellular rim around the actual necrosis (Lenaerts *et al.* 2007). The classical granuloma is formed at day 31, or stage 3, consisting of a necrotic core surrounded by a layered structure of epithelioid macrophages, granulocytes, lymphocytes, and fibrin. CD4-positive T cells are especially abundant, but CD8-positive T cells are also present, mainly in the periphery (Ordway *et al.* 2007; Orme and Basaraba 2014). Interestingly, CD4-positive T cell numbers decline in the lesions from day 30 (Ordway *et al.* 2007).

If the guinea pig had been BCG-vaccinated, levels of activated CD4- and CD8-positive T cells in the lesions as well as levels of MHC II-expressing macrophages are increased. Interestingly, the number of granulocytes in the lesions is reduced. An early influx of B cells in the lungs can be observed. These altered cellular responses lead to reduced pathology of vaccinated animals upon aerosol challenge compared with unvaccinated ones (Ordway *et al.* 2008). The cytokine response upon initial infection is pro-inflammatory while anti-inflammatory responses are observed after vaccination or reinfection (Ly *et al.* 2008).

All observations after day 31 account for stage 4 with confluence of multiple granulomas and possible calcification, collagen deposition and extensive inflammation (Turner *et al.* 2003). Granulomas in guinea pigs induce hypoxia through compression of blood vessels (Lenaerts *et al.* 2007; Via *et al.* 2008). The number of bacilli remains static from day 21, but starts increasing again during stage 4, accounting for clinical disease which ultimately leads to death at day 100 to 140 (Turner *et al.* 2003). Healing of granulomas can occur, e.g., if the animal had been vaccinated (Shanley *et al.* 2014), but coalescence of lesions is also possible and is mostly dependent on the virulence of the strain (Palanisamy *et al.* 2009).

Similar to humans, guinea pigs develop small-airway inflammation with larger numbers of bacteria in association with secondary lesions (Saunders *et al.* 2008). The rare cavity formation in guinea pigs is, in accordance with findings in humans (Hunter 2011), not adjacent to primary lesions, but embedded in inflammatory tissue (Orme and Basaraba 2014). Secondary and post-primary lesions contribute to the fatal outcome of the disease in stage 4 due to their large size and inflammation, resulting in restriction of the lung functions (Williams *et al.* 2009).

Taken together, the most prominent feature of guinea pig tuberculosis, which resembles human tuberculosis, is the development of granulomas with distinction between primary and

secondary or post-primary lesions, though the latter two are not yet well delineated in the literature (Fok *et al.* 1976; Harding and Smith 1977; Ho *et al.* 1978; Balasubramanian *et al.* 1994; Saunders *et al.* 2008; Orme and Basaraba 2014). A further similarity of the infection in both host species is the ability of the granulomas to undergo necrosis and calcification, which is dependent upon iron acquisition and associated with hypoxia (Basaraba *et al.* 2008) (Turner *et al.* 2003; Lenaerts *et al.* 2007; Via *et al.* 2008; Orme and Basaraba 2014). The cellular immune responses are similar, apart from the finding of pseudoeosinophilic granulocytes in guinea pigs and a possible decline of CD4-positive T cells in the lesions from day 30, of which the relevance is currently unknown (Turner *et al.* 2003; Ordway *et al.* 2007). Further advantages of the guinea pig model are the occurrence of bacterial dissemination as well as lymphadenitis resembling a form of childhood TB (Fok *et al.* 1976; Harding and Smith 1977; Ho *et al.* 1978; Balasubramanian *et al.* 1994; Basaraba *et al.* 2006a; Basaraba *et al.* 2006b; Orme and Basaraba 2014). Though tuberculosis is a chronic disease in guinea pigs, one important feature of human tuberculosis is lacking in this model: a phase of real latency (Smith *et al.* 1970; Turner *et al.* 2003; Sakamoto 2012). However, the guinea pig still remains one of the best and most feasible animals to model human TB infection with many of its facets (Clark *et al.* 2014).

2.6.2 Use of the guinea pig as a small animal model for tuberculosis research

Guinea pigs have been used in tuberculosis research for more than a century. They contributed to Robert Koch identifying the causative agent of the disease (Koch 1891c) and remain important for understanding fundamental pathomechanisms of tuberculosis until today (Clark *et al.* 2014). A main advantage of the guinea pig in this respect is that the appearance of *M. tuberculosis* infection in this host species closely resembles the human disease with the formation of the hallmark – the granuloma – and many of its associated features. The similarity of the pathology clearly surpasses the mouse model (Gupta and Katoch 2005) and the guinea pig is not as restricted by regulations and is also not as expensive as larger animal models such as non-human primates. However, the mouse model has two strategic advantages over the guinea pig: the existence of many immunological reagents to characterize the immune response and the availability of knock-out strains, which enable specifically targeted investigations of the pathogenesis and immunology of the disease.

The most widely used guinea pig strain is the outbred Dunkin-Hartley strain, but inbred strains exist as well. Today, inbred strains 2 and 13 remain from 23 strains developed by

brother-sister-mating from 1906 (Wright and Eaton 1929). They were thoroughly investigated for their characteristics (Loeb and Wright 1927; Bauer 1958; Shevach and Schwartz 1977) and due to their MHC compatibility they were preferentially used for investigations on antigen presentation (Clark and Shevach 1982). However, the described use of the guinea pigs mainly in infection studies seemed to render these strains redundant. Additionally, their poor reproducibility limited their availability (personal communication, E. Shevach). Nonetheless, these strains remain valuable tools for the generation of cell clones (see 3.10).

As in humans, guinea pigs can easily acquire the infection via the airborne route with only a few bacilli (Wiegeshaus *et al.* 1970; Smith *et al.* 1970; Smith and Harding 1977; Clark *et al.* 2014). Today, they are therefore mainly used for the evaluation of vaccine efficacies determined by CFU scores, survival or pathology upon mycobacterial challenge (Clark *et al.* 2014). The guinea pig is thus a valuable model to test vaccine candidates before clinical trials. Besides vaccination efficacy testing, the virulence of different mycobacterial strains can be characterized by their potential to induce intra- and extrapulmonary lesions in infection studies (Palanisamy *et al.* 2008; Palanisamy *et al.* 2009). As guinea pigs express hypoxic regions in their granulomas, they are exceptionally well-suited to screen drugs for their efficacy to reach bacteria in these shielded locations (Lenaerts *et al.* 2007). Furthermore, the guinea pig is used to model particular clinical conditions, such as malnutrition (Cegielski and McMurray 2004) and diabetes (Podell *et al.* 2012). The current development of immunological tools and techniques will further improve the assignment of guinea pigs to immunological studies (Tree *et al.* 2006; Ordway *et al.* 2007; Padilla-Carlin *et al.* 2008). Interestingly, the guinea pig expresses several proteins of the CD1 multigene family which were demonstrated to be involved in lipid antigen presentation in humans (Dascher *et al.* 1999; Hiromatsu *et al.* 2002).

The guinea pig is completely indispensable for batch potency testing of tuberculins as determined in the European Pharmacopoeia (European Directorate for the Quality of Medicine and Health Care 2013). The ability of sensitized guinea pigs to exhibit a delayed-type hypersensitivity reaction is thereby used to evaluate the potency of a test batch in comparison with a standard tuberculin preparation in the tuberculin skin test (Gupta and Katoch 2005; European Directorate for the Quality of Medicine and Health Care 2013). No *in vitro* assay capable of determining the potency of the complex and currently in large parts undefined mixtures is licensed to date. An alternative *ex vivo* method has recently been developed (Spohr *et al.* 2015), but implementation in the European Pharmacopoeia is a long procedure. For these reasons, the guinea pig is still the only suitable animal model for batch potency testing of tuberculins with regard to legislation, manageability, and costs.

3 Material and Methods

3.1 Bacterial strains

The following bacterial strains were used in this study:

- Live attenuated *M. bovis* Bacille Calmette-Guérin (BCG) strain Pasteur 1173, kindly provided by Dr. Walter Matheis, Paul-Ehrlich-Institut (PEI), Germany
- Heat-inactivated (100 °C, 60 min) wet mass of *M. bovis* strain AN5, kindly provided by Dr. Peter Schaufuss, Serumwerke Memsen, Germany
- Heat-inactivated (100 °C, 60 min) wet mass of *M. avium* ssp. *avium* D4, kindly provided by Dr. Peter Schaufuss, Serumwerke Memsen, Germany
- Live *M. paratuberculosis* ssp. *paratuberculosis*, ATCC-BAA968, kindly provided by Prof. Dr. Rolf Bauerfeind, JLU Giessen, Germany
- Chloroform-methanol (1:1, v/v) inactivated *M. tuberculosis* East African-Indian strain 1797, kindly provided by Prof. Dr. Stefan Niemann and PD Dr. Norbert Reiling, Research Center Borstel (RCB), Germany
- Chloroform-methanol (1:1, v/v) inactivated *M. tuberculosis* Beijing strain 1934, kindly provided by Prof. Dr. Stefan Niemann and PD Dr. Norbert Reiling, Research Center Borstel (RCB), Germany
- Chloroform-methanol (1:1, v/v) inactivated *M. tuberculosis* Haarlem strain 2336, kindly provided by Prof. Dr. Stefan Niemann and PD Dr. Norbert Reiling, Research Center Borstel (RCB), Germany
- *Escherichia coli* Top10 (Life Technologies) (*E. coli*), kindly provided by Dr. Holger Loessner, PEI, Germany
- *Salmonella enterica* ssp. *enterica* serovar Typhi strain Ty21a (*S.* Typhi) (Germanier and Fürer 1975), kindly provided by Dr. Holger Loessner

The following strains were grown in the laboratory of the veterinary immunobiology group, PEI.

M. bovis BCG Pasteur 1173 was obtained in lyophilized form. It was resuspended in PBS and seeded in Middlebrook 7H9 medium with OADC-enrichment and glycine (see Annex 3) in a roller bottle with continuous rotation at 37 °C for 14 days (exponential phase, standard cultivation) or 5 months (static phase). For harvesting, bacteria in medium were collected in plastic tubes with screw caps, centrifuged (1,500 x *g*, 10 min, 20 °C), poured off and either

stored at –80 °C until needed for chloroform-methanol extraction, or resuspended in Middlebrook 7H9 medium containing 10 % glycine and stored at –80 °C for use in sensitization procedures.

M. avium ssp. *paratuberculosis* (MAP) ATCC-BAA968 was grown on BBL™ Herrold's Egg Yolk Agar Slant with mycobactin J and ANV (amphotericin B, nalidixic acid, vancomycin) (Becton, Dickinson and Company) at the Institute for Hygiene and Infectious Diseases of Animals, JLU Giessen, Germany. At PEI, bacteria were first transferred to 7H11 agar plates with mycobactin J and incubated at 37 °C for 7 weeks. Subsequently, they were expanded in modified Watson-Reid medium with mycobactin J (see Annex 3) in 500 ml Erlenmeyer flasks with foam plugs at 37 °C for 3 months. For harvesting, the culture medium was removed and bacteria were inactivated in chloroform-methanol (1:2, v/v). The bacteria in chloroform-methanol were stored at –80 °C until further processing.

3.2 Media and Buffers

Media and buffers are listed in Annex 3. All non-commercial media as well as Laemmli buffer, PBS and sodium chloride were produced in the solvent and media supply unit of the PEI.

3.3 Antigens

3.3.1 Bacterial culture supernatant

Bacterial culture supernatant was obtained from a BCG culture in the exponential growth phase (see section 3.1). It was sterile-filtered (0.2 µm, Sartorius) and stored at 4 °C.

3.3.2 Tuberculins

Tuberculins were either purchased or kindly provided by the manufacturer. All tuberculins used in this study are listed in **Table 3.1**.

Table 3.1 Tuberculins used in this study.

Name	Origin	Concentration	Storage
Koch's Old Tuberculin Tub12	PEI, Langen, Germany	$3x10^5$ IU/ml	4 °C
WHO International Standards for Purified Protein Derivatives *M. tuberculosis* (WHO_{hum})	NIBSC, South Mimms, UK	5,000 IU/ml	Lyophilized at –20 °C until use Reconstituted in PBS and stored at 4 °C
WHO International Standards for Purified Protein Derivatives *M. bovis* (WHO_{bov})	NIBSC, South Mimms, UK	11,700 IU/ml	Lyophilized at –20 °C until use Reconstituted in PBS and stored at 4 °C
WHO International Standards for Purified Protein Derivatives *M. avium* ssp. *avium* (WHO_{av})	NIBSC, South Mimms, UK	100,000 IU/ml	Lyophilized at –20 °C until use Reconstituted in PBS and stored at 4 °C
Test PPD *M. bovis* 1	Manufacturer 1	50,000 IU/ml	Obtained refrigerated and stored at 4 °C until use
Test PPD *M. bovis* 2	Manufacturer 2	67,900 IU/ml	Obtained refrigerated and stored at 4 °C until use
Test PPD *M. bovis* 3	Manufacturer 3	30,000 IU/ml	Obtained refrigerated and stored at 4 °C until use

Koch's Old Tuberculin Tub12 was used for decades as reference for human tuberculins by the manufacturer Behring, as well as by the Paul-Ehrlich-Institut, Langen, Germany. The stock solution was nationally certified in 1958 by the Paul-Ehrlich-Institut. Though the mycobacterial strain used for its preparation was not indicated, there is significant evidence that it was an *M. tuberculosis* strain. By 1958, the existence of both human and bovine strains of the tuberculosis-causing mycobacterium was well known. However, it was only in 1975 that *M. bovis* PPDs were described (Lesslie *et al.* 1975). The Tub12 tuberculin had been calibrated against the WHO standard tuberculin (personal communication Dr. Elisabeth Balks and Dr. Walter Matheis).

Based on the results depicted in section 4.1.1, Tub12 was used as the positive control in this study because it provided a wider range of mycobacterial antigens compared with PPD. In addition, it is more standardized than a BCG lysate.

3.3.3 Chloroform-methanol extracts (CMEs)

The aim of chloroform-methanol extraction is to separate the lipids of a bacterial cell from its other constituents. Folch extraction is used to further increase enrichment of hydrophobic molecules (Folch *et al.* 1957; Bligh and Dyer 1959; Cala-De Paepe 2011).

Chloroform-methanol extracts (CMEs) of *M. tuberculosis* H37Rv, *M. bovis* BCG, *M. marinum* and *M. fortuitum* were kindly provided by Dr. Martine Gilleron, IPBS Toulouse, France. CMEs of *M. tuberculosis* CDC 1551, *M. tuberculosis* HN 878, *M. canetti* and *M. leprae* were obtained from Mycobacterial Research Laboratory (MRL), Fort Collins, CO, USA, through Biodefence and Emerging Infectious Research Resources Repository (BEI Resources, NIAID, NIH). CMEs of the bacterial strains listed in section 3.1 were generated in the laboratory of the veterinary immunobiology group at PEI, Langen, Germany, and are part of this doctoral thesis work (see **Table 3.2**).

CME protocols of these three manufacturers differ slightly. For comparison purposes all protocols are listed below.

Chloroform-methanol extraction by Dr. Martine Gilleron, IPBS Toulouse, France (Cala-De Paepe 2011)**:**

The bacteria were inactivated and lipids were extracted with chloroform-methanol (1:2, v/v) at RT. This extraction step was repeated twice with chloroform-methanol (1:1, v/v) to obtain the total lipid extract. The polar components were eliminated by a partition with chloroform-water (1:1, v/v).

A modification of this protocol was used to extract lipids from *M. bovis* BCG and *M. tuberculosis* H37Rv for chromatographic purification purposes (see section 3.3.10): The chloroform-methanol extraction was carried out as described above. Subsequently, the dried CME material was assimilated with 3 ml chloroform, 3 ml methanol and 1.5 ml milliQ water and dissolved by turning in the sonication bath. For undissolved residuals, 1 ml milliQ water was added. These CME preparations were then subjected to phenol partitioning (see section 3.3.8).

Chloroform-methanol extraction by MRL, Fort Collins, CO, USA (Dobos 2015)**:**

Bacterial strains were grown to late-log phase (day 14) in glycerol-alanine-salts (GAS) medium. The culture was washed with PBS, inactivated by gamma-irradiation (2.5

megarads) and lyophilized. The pellet was suspended in chloroform-methanol (2:1, v/v) with 30 ml/g (v/w) to extract cellular lipids while stirring at 55 °C for 18 h. Insoluble material was separated by filtration and contaminating hydrophilic molecules were removed from the eluent by biphasic partitioning with water (Folch wash with a final ratio chloroform-methanol-water of 4:2:1, v/v/v). The lower organic phase of the Folch wash was collected and dried. Resuspension in chloroform-methanol (2:1, v/v) was performed, if necessary, for quality control or use in cell assays.

Chloroform-methanol extraction at veterinary immunobiology group, PEI, Langen, Germany (protocols "PEI 2014" and "PEI 2015"):

For these extractions, bacterial strains described in section 3.1 were processed. Protocols were adapted to the MRL protocol as most CMEs of different strains were obtained from MRL.

Bacteria were resuspended in chloroform-methanol (2:1, v/v) with 30 ml/g (v/w) and extracted by stirring at 55 °C for 18 h. If the bacteria were initially inactivated in chloroform-methanol (1:1, v/v), the supernatant as well as the remaining pellet were dried by evaporation in a water bath (50 °C) and then resuspended in chloroform-methanol (2:1, v/v). This procedure was applied to the samples obtained from the Research Center Borstel. A centrifugation step (950 x *g*, 15 min, 20 °C) followed to separate the insoluble material. The pellet was discarded, the supernatant was collected and ultrapure water was added (1:5 of the chloroform-methanol volume) for Folch extraction (Folch *et al.* 1957; Bligh and Dyer 1959). The mixture was vortexed for 5 min and then centrifuged (950 x *g*, 15 min, 20 °C). It separated into an upper water-phase as well as an inter- and the lower chloroform-phase (**Figure 3.1**). All fractions were collected separately, dried in a rotavap (Heidolph Instruments) (2014) or evaporated in a SpeedVac® (Thermo Fisher Scientific) (2015). They were weighed before dissolving in appropriate solvent mixtures (chloroform, methanol, ultrapure water) in defined concentrations. These mixtures were stored at –80 °C as stock solutions.

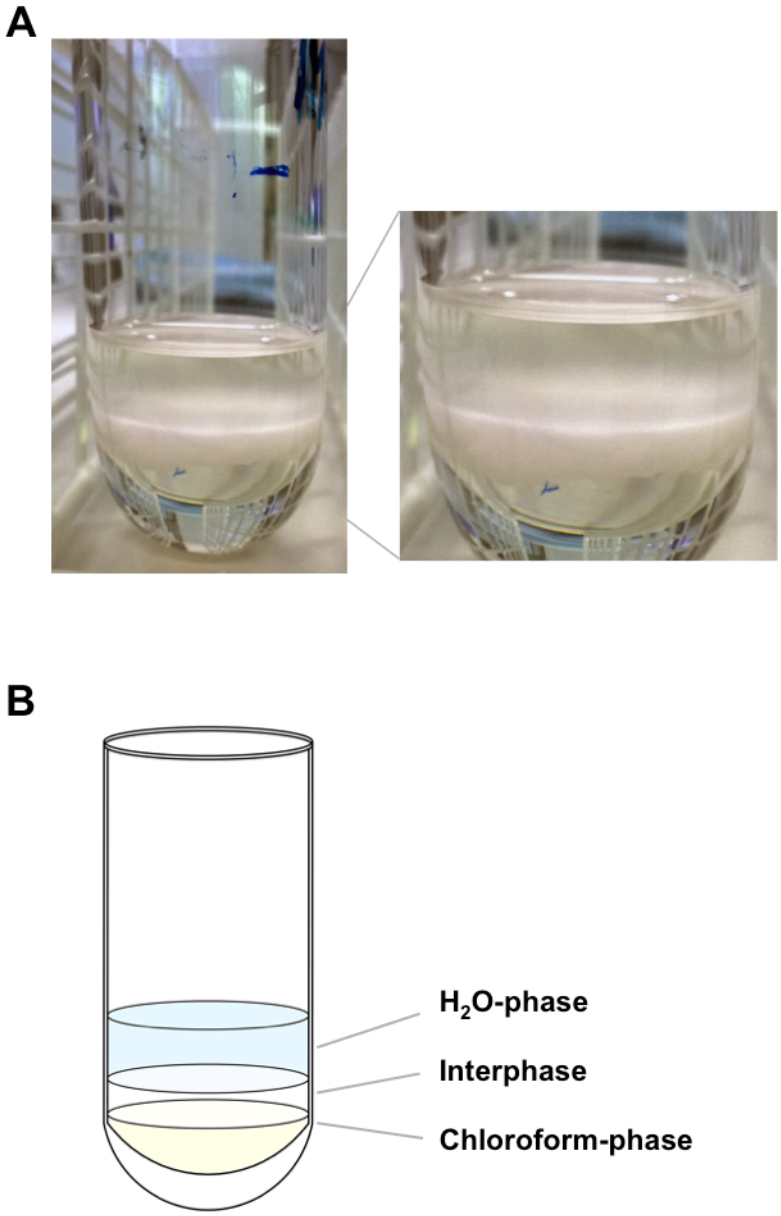

Figure 3.1 Chloroform-methanol extraction, Folch extraction step.

A. and **B.** A picture and a scheme of the Folch extraction step of the chloroform-methanol extraction showing the upper water-, the inter- and the lower chloroform-phase.

The CMEs used in this study are listed in **Table 3.2**.

Table 3.2 CME preparations used in this study.

Designation	Source (species, strain)	Origin	Preparation procedure
CME_{H37Rv}	*M. tuberculosis* H37Rv	IPBS Toulouse, France	IPBS Toulouse
CME_{BCG}	*M. bovis* BCG	IPBS Toulouse, France	IPBS Toulouse
CME *M. marinum*, CME *Mar.*	*M. marinum*	IPBS Toulouse, France	IPBS Toulouse
CME *M. fortuitum*, CME *Fort.*	*M. fortuitum*	IPBS Toulouse, France	IPBS Toulouse
CME AN5	*M. bovis* AN5 wet mass	Serumwerke Memsen, Germany	PEI 2014
CME MAA	*M. avium* ssp. *avium* D4 wet mass	Serumwerke Memsen, Germany	PEI 2014
CME EAI 1797	*M. tuberculosis* East African-Indian strain 1797	Research Center Borstel (RCB), Germany	PEI 2015
CME Beijing 1934, CME B 1934	*M. tuberculosis* Beijing strain 1934	Research Center Borstel (RCB), Germany	PEI 2015
CME Haarlem 2336, CME H 2336	*M. tuberculosis* Haarlem strain 2336	Research Center Borstel (RCB), Germany	PEI 2015
CME MAP	*M. avium* ssp. *paratuberculosis*	JLU Giessen, Germany / PEI Langen, Germany	PEI 2015
CME *M. leprae*	*M. leprae*	MRL, Fort Collins, CO, USA	Fort Collins
CME CDC 1551	*M. tuberculosis* CDC 1551	MRL, Fort Collins, CO, USA	Fort Collins
CME HN 878	*M. tuberculosis* HN 878	MRL, Fort Collins, CO, USA	Fort Collins
CME EAI 91/0079	*M. tuberculosis* East African-Indian strain 91/0079	MRL, Fort Collins, CO, USA	Fort Collins
CME *M. canetti*	*M. canetti*	MRL, Fort Collins, CO, USA	Fort Collins

3.3.4 Lipopeptide-enriched subfraction (LppEL)

The lipopeptide-enriched subfraction (LppEL, French: lipopeptides de l'extrait lipidique) was kindly provided by Dr. Martine Gilleron from IPBS Toulouse, France. It was produced by Dr. Diane Cala-de Paepe (Cala-De Paepe 2011). The different manufacturing steps (see below) have been described for the purification of lipoproteins (Bordier 1981; Lee *et al.* 2002; Gehring *et al.* 2004; Målen *et al.* 2010).

After chloroform-water partitioning (1:1, v/v), CME *M. tuberculosis* H37Rv was incubated in a buffer containing 50 mm Tris, 150 mm NaCl pH 7.4, and 4 % Triton X-114 at 4 °C for 16 h with gentle agitation. It was subsequently placed in 37 °C for 15 min to obtain a detergent and a water phase. The detergent phase was washed three times with the Tris-NaCl-buffer. Protein precipitation was obtained by addition of acetone at 4 °C and incubation at –20 °C for 16 h. After centrifugation (500 x *g*, 20 min, 4 °C) the acetone-insoluble fraction was dried. The protein amount was measured using the Bradford assay and the fraction was resuspended in PBS to obtain a protein concentration of 2 mg/ml (w/v). An equivalent volume of PBS saturated with phenol was added and the mixture was incubated at 25 °C for 4 h, with gentle agitation. After centrifugation (500 x *g*, 30 min, 25 °C) and replacement of the water phase with PBS twice for washing of the phenol phase, the phenol phase was recovered. It was dialyzed against water for 48 h (threshold of 6,000-8,000 Da) for elimination of the phenol. The lipopeptide-enriched subfraction LppEL was obtained by subsequent drying.

3.3.5 Ultrasonication of bacterial pellets

Ultrasonication serves to disrupt cells through lysis, to form the so-called lysate. Many molecules of the cells become accessible through this disruption, which facilitates antigen presentation.

A frozen pellet of *M. bovis* BCG (see section 3.1) was weighed, resuspended in PBS and subjected to ultrasonication (3 x 2 min, 60 cycles each, on ice) (Bandelin). The sample was centrifuged (3,000 x *g*, 8 min, 4 °C) and the supernatant was collected. The procedure was repeated once with the remaining pellet. The whole supernatant was centrifuged again (6,000 x *g*, 10 min, 4 °C and 70,000 x *g*, 45 min, 4 °C). The supernatant of this centrifugation step was collected with a syringe (B. Braun) and sterile filtered (Sartorius). Protein concentrations were determined in the nanodrop photometer (Implen) at OD 280 nm and protein concentrations of 10 mg/ml (w/v) were adjusted with PBS. Samples were stored at –80 °C until use.

The same procedure was performed with pellets of *E. coli* and *S.* Typhi (see section 3.1). Following ultrasonication, protein concentrations were adjusted to 100 µg/ml (*E. coli*) or 160 µg/ml (*S.* Typhi).

3.3.6 Heat inactivation of bacteria

Heat inactivation of bacteria enables the comparison of presentation by antigen presenting cells (APCs) brought into contact with live or dead bacteria *in vitro*.

Heat inactivation of *M. bovis* BCG (see section 3.1) was achieved by heating to 80 °C in the thermomixer (Eppendorf) for 90 min.

3.3.7 Dissolving of CME antigens in different solvents

Dissolving CME antigens in different solvents aimed at obtaining the soluble and insoluble portions for this particular solvent and concentration. Therefore, a defined amount of CME was dried in the SpeedVac® (Thermo Fisher Scientific) and resuspended in a solvent, e.g. 40 % AcN/H_2O. The resolution was enhanced during 15 minutes in the ultrasound bath at 50 °C. Next, the mixture was centrifuged at 50,000 x *g* for 15 min. The supernatant was collected as the soluble and the pellet as the insoluble portion. The solvent was dried again in the SpeedVac® to recover the extracted antigens for use in the *ex vivo* lymphocyte proliferation assay (see section 3.8.1).

3.3.8 Phenol-water partitioning of CMEs

The aim of phenol-water partitioning was to further select for lipopeptide-containing portions of the chloroform-methanol extract.

To this end, the chloroform-methanol extracted material of *M. bovis* BCG and *M. tuberculosis* H37Rv, dissolved in chloroform-methanol-water (see section 3.3.3) was dried with nitrogen on a bioblock heater (Fisher Scientific) at 35 °C. The dried material was weighed to determine the initial mass.

Phenol saturated with water was produced by boiling (50–100 °C) crystallized phenol with an open cap in a waterbath for 2 h. Following this step, 25 ml milliQ water was mixed with 12 ml liquefied phenol and vortexed for 1 min. After 5 min of settling, two phases appeared. To enhance this partition, a centrifugation step followed (950 x *g*, 15 min, 15 °C) and the yellow phenol phase was collected.

Six millilitres of milliQ water and 6 ml phenol saturated with water were added to the initial material and agitated for 2 h at 60 °C. The mixture was centrifuged (950 x *g*, 15 min, 15 °C),

in order to collect the lower, yellow phenol phase while discarding the upper water- and interphase.

A dialysis membrane (Spectra Por, MWCO 1,000) was rinsed with milliQ water and the phenol phase was filled in. The phenol phase was dialyzed in 1 L of milliQ water with frequent water exchange and with gentle agitation overnight at RT. The resulting yellowish to brown stones and film were resolved and collected with milliQ water in a 15 ml tube.

The phenol-partitioned CME preparations were analyzed using the TLR2 assay (see section 3.8.4) and the *ex vivo* lymphocyte proliferation assay (see section 3.8.1) and they were subjected to chromatographic purification (see section 3.3.10).

3.3.9 Biochemical degradation of antigens

Protocols by Bastian *et al.* (2008) were adapted for biochemical degradation of lipid antigens. CME_{BCG} at a concentration of 10 mg/ml (w/v) as well as Tub12 at a concentration of 3×10^4 IU/ml were subjected to this biochemical degradation. Concentrations of CME and Tub12 were equivalent according to their stimulatory capacity in the immunological *ex vivo* lymphocyte proliferation assays (see section 3.8.1).

3.3.9.1 Mild sodium hydroxide treatment of antigens

Mild sodium hydroxide treatment of lipid preparations was used to achieve delipidation of the antigens (Bastian *et al.* 2008). Compared to usual sodium hydroxide treatment it does not induce total degradation of antigens regardless of their type.

CME_{BCG} (100 µg, 10 µl) or Tub12 (300 IU, 10 µl) respectively (see above) were diluted with 90 µl 1 N NaOH and incubated for 30 min at 50 °C in the thermocycler (Eppendorf). The pH was subsequently neutralized by addition of 8.5 µl 10 N HCl. SF-IMDM was added to the sample to reach a total volume of 1 ml. The pH was measured using pH-Fix test strips (Roth) and adjusted to 7.0. Antigens were used in the lymphocyte proliferation assay in the same concentration as the untreated antigens (10 µg/ml or 30 IU/ml, respectively) (see section 3.8.1).

For control purposes, 90 µl 1 N NaOH were neutralized by adding 8.5 µl 10 N HCl and adjusting the pH to 7.0. The antigen preparation (100 µg CME_{BCG} or 300 IU Tub12, respectively) was added to this solution and the mixture was incubated for 30 min at 50 °C in

the thermocycler. After incubation, SF-IMDM was added and the antigens were used in the *ex vivo* lymphocyte proliferation assay in concentrations as previously described.

As a control for any changes due to high temperatures, antigen samples were diluted in 90 µl PBS and subjected to 30 min 50 °C in the thermocycler. SF-IMDM was added and the antigens were used as described above.

3.3.9.2 Proteinase K treatment of antigens

Proteinase K from *Engyodontium album* (former *Tritirachium album*) is an endo- and serine protease with broad specificity. It specifically splits peptides C-terminal of hydrophobic, aliphatic and aromatic amino acids (Lottspeich and Engels 2012).

Proteinase K (Sigma-Aldrich) was purchased as a lyophilized powder and reconstituted with PBS to achieve a concentration of 10 mg/ml (w/v). Stock and working solutions were stored at –20 °C until use.

The above-mentioned antigen preparations CME_{BCG} (100 µg, 10 µl) or Tub12 (300 IU, 10 µl) respectively (see section 3.3.9.1), were diluted with 80 µl PBS in a 0.2 ml PCR reaction tube (Roth) and 100 µg (10 µl) proteinase K were added. The samples were gently mixed and incubated for 30 min at 50 °C in the thermocycler (Eppendorf) to allow the enzyme to function efficiently. Afterwards, the temperature in the thermocycler was increased to 90 °C for 10 min for inactivation of the enzyme. Following this incubation, 900 µl SF-IMDM were added to each sample and they were used in the *ex vivo* lymphocyte proliferation assays at the same concentrations as the original antigens (10 µg/ml or 30 IU/ml) (see section 3.8.1).

For control purposes, one sample of each antigen preparation was treated with inactivated proteinase K. To this end, 100 µg proteinase K were diluted with 80 µl PBS and inactivated at 90 °C in the thermocycler for 10 min. Inactivated proteinase K was added to both 100 µg and 300 IU antigen, respectively, after which these mixtures were then incubated with the other samples for 30 min at 50 °C in the thermocycler. Subsequently, 900 µl SF-IMDM were added and the antigen preparations were used in the same concentrations as previously described.

To exclude side effects of the temperature treatment, additional samples of each antigen preparation were prepared. CME_{BCG} (100 µg, 10 µl) or Tub12 (300 IU, 10 µl), respectively, were diluted with 90 µl PBS and subjected to incubations at 50 °C for 30 min and at 90 °C for 10 min in the same cycle as the antigen preparations containing the active enzyme.

Likewise, 900 µl SF-IMDM were added and the antigen preparations were used in the lymphocyte proliferation assay at the same concentrations.

3.3.9.3 Pronase E treatment of antigens

Pronase E derives from *Streptomyces griseus* and has broad substrate specificity due to many different proteolytic activities. According to the manufacturer, there are at least three caseinolytic enzymes present – *Streptomyces griseus* protease A, B and the serine protease trypsin, which hydrolyzes peptide bonds on the carboxyl side of glutamic or aspartic acids – as well as an aminopeptidase.

Pronase E (Sigma-Aldrich) was obtained as a powder and reconstituted with PBS at a concentration of 10 mg/ml. Stock and working solutions were stored at –20 °C until use.

For pronase E degradation of CME_{BCG} and Tub12, the same protocol and controls as for proteinase K degradation were applied (see section 3.3.9.2).

3.3.10 Chromatographic purification of antigens

Preparative chromatography is separated into normal (NPC) and reversed phase chromatography (RPC) (Schmidt-Traub *et al.* 2012). In NPC, a polar stationary phase adsorbs the likewise hydrophilic molecules, which are eluted using a mobile phase directed from apolar to polar solvents. The “reverse” takes place in RPC: Hydrophobic molecules are bound by a stationary phase, which expresses a different degree of hydrophobicity due to the lengths of its covalently bound alkyl chains (C4, C8, C18 with C18 being the most hydrophobic). The hydrophobic molecules are then eluted with a mobile phase ranging from polar to apolar (Schmidt-Traub *et al.* 2012).

3.3.10.1 Chromatographic purification of phenol-partitioned CME

This chromatographic purification attempt was made possible by Dr. Martine Gilleron, who kindly assisted with a one-month scientific stay and supervision at the Institute of Pharmacology and Structural Biology (IPBS) Toulouse, France.

All tubes and bottles were heated to 180 °C for at least 2 h to obtain LPS-free glassware. A defined amount of phenol-partitioned CME was dried in the rotavap (Buechi Labortechnik),

thoroughly resuspended in 2 to 3 ml milliQ water and loaded onto a C4 reversed phase silica column (Interchim Puriflash). 0.1 % trifluoroacetic acid (TFA, 13N) was added to all solvents for better solubility of proteins.

The gradient for the first chromatographic fractionation (sample: phenol-partitioned CME_{BCG}) was: 100 % H_2O to 100 % acetonitrile (AcN) in 15 min with a plateau for 3 min at 100 % H_2O and 100 % AcN respectively. The flow rate was 2 ml/min and a total of 24 fractions were collected.

After that first chromatography, the column was washed with 100 % AcN, 100 % Cyclohexan, 100 % AcN and 100 % H_2O to remove any remaining material.

The gradient for the second (sample: phenol-partitioned CME_{BCG}) and third chromatography (sample: phenol-partitioned CME_{H37Rv}) was: 100 % H_2O to 100 % AcN and manual wash with 100% Cyclohexan, 100 % AcN, 100 % H_2O. The flow rate was 1 ml/min for normal gradient chromatography, which took 39 min. The flow rate for washing was 2 ml/min. A total of 44 fractions were collected in each chromatography. The flow was monitored at 200 and 280 nm.

3.3.10.2 Chromatographic approach with preselection of lipophilic peptides

A defined amount of CME_{BCG} was dried and resuspended in 300 µl 40 % AcN in the ultrasonication bath (Bender & Hobein) for 10-20 min. A centrifugation step followed (8,000 x *g*, 10 min, 15 °C) to separate insoluble material. The supernatant was filled into an in-house packed C18 column. 0.1 % trifluoroacetic acid (TFA, 13N) was added to all solvents for better solubility of proteins. The first gradient was 40 % AcN to 97 % AcN with plateaus at the beginning as well as at the end, and the second gradient decreased from 97 % to 40 % AcN with another plateau at the end. The flow rate was 1 ml/min and 55 fractions of 1 ml each were collected. The flow was monitored at 280 nm.

3.3.10.3 Further processing of the collected fractions

Fractions were harvested in pre-weighed glass tubes and dried in the Heto vacuum centrifuge (Oy Halton) or in the SpeedVac® (Thermo Fisher Scientific), respectively. The weight of each sample was determined. Subsequently, fractions were subjected to TLR2 assays, Bradford assays, and/or *ex vivo* lymphocyte proliferation assays (see sections 3.8.4, 3.4.3, and 3.8.1).

3.3.11 Synthetic peptides of *M. tuberculosis* lipoproteins

The TB Database from the Stanford Microarray Database and the Broad Institute provides amino acid sequences of *M. tuberculosis* proteins (http://genome.tbdb.org/-annotation/genome/tbdb/FeatureSearch.html) (Reddy *et al.* 2009; Galagan *et al.* 2010). Further information on these proteins can be found in the tubercuList from the Global Health Institute at the Ecole Polytechnique Fédérale de Lausanne and the Swiss Institute of Bioinformatics (http://tuberculist.epfl.ch) (Lew *et al.* 2011). These sources were used to identify amino acid sequences of putative *M. tuberculosis* lipoproteins. The sequences are listed in Annex 5.

Signal peptides and unlipidated N-terminal peptides of the mature lipoproteins were synthesized with a length of 15 amino acids based on these sequences. The Merrifield-type synthesis of soluble peptides with 9-fluorenylmethoxycarbonyl (Fmoc)-protected amino acids was done using an automated multi-peptide synthesizer as described by Albrecht *et al.* (2009). Briefly, 15-mer peptides were synthesized as C-terminal amids on the ends of Fmoc-Rink-Amide (aminomethyl)-resin according to the manufacturer´s instructions (Intavis Bioanalytical Instruments, Cologne, Germany). After deprotection and cleavage from the linkers, peptides were precipitated with tert-butylmethyl-ether, dissolved in water (with up to 30 % acetonitrile), and lyophilized before storage. According to the instrument's manufacturer, synthesis yields of 50 – 80 % and peptide purity of 70 % or more should be obtained. No further purification or identity proof was performed. Peptides were kindly provided by Dr. Thomas Holzhauser and Stefanie Randow, Division of Allergology, Paul-Ehrlich-Institut, Langen.

3.3.12 The recombinant protein AG85A of *M. tuberculosis*

The recombinant *M. tuberculosis* protein antigen 85A, expressed in *E. coli*, was purchased from Lionex GmbH in lyophilized form and stored at –20 °C. Following to the manufacturer's instructions, it was reconstituted at a concentration of 200 µg/ml with PBS.

3.4 Antigen characterization

3.4.1 SDS-PAGE analysis

Sodium dodecyl sulfate polyacrylamide gel electrophoresis (SDS-PAGE) was used to separate the antigen preparations according to the molecular weight of their proteins

(Laemmli 1970). Fresh Gels were prepared with the Mini-Protean® Tetra Cell system of BioRad on the day of use. For a 10 % SDS separation mini gel (5 x 8.3 x 0.075 cm), a 3.1 ml volume of H_2O was mixed with 1.875 ml 4x lower buffer and 2.5 ml 30 % acrylamide-bis solution. For polymerization, 75 µl of 10 % APS and 10 µl TEMED were added. After polymerization, the stacking gel for concentration of the samples and a comb with 10 chambers were inserted. One stacking gel contained 1.5 ml H_2O, 0.625 ml upper buffer and 0.313 ml 30 % acrylamide-bis solution. It further contained 75 µl 10 % APS and 10 µl TEMED for polymerization. Antigen samples were diluted or resuspended in 2x loading buffer. Chloroform-methanol extracts and large volume antigen preparations were dried in the SpeedVac® (Thermo Fisher Scientific) prior to resolution to remove chloroform-methanol or to reduce the total volume. In most analyses, the used antigen content correlated with the concentration in the *ex vivo* lymphocyte proliferation assay (see section 3.8.1). The content per slot is always indicated in the results section. Quantities of 5 µl were used per slot. Molecular weight marker (2 µl, Thermo Fisher Scientific) was used to determine the size of the proteins.

The gels were run in BioRad Mini Protean N™ chambers containing 1x Laemmli buffer for approximately 2 h at 115 Volts. The run was stopped when the buffer front reached approximately 1 cm from the lower edge of the gel.

Following electrophoresis, the gels were subjected either to staining or blotting on nitrocellulose membranes.

3.4.1.1 Coomassie Blue staining

Proteins in the gel can be detected through the nonspecific binding of the organic triphenylmethan-dye Coomassie Blue to protonated basic or aromatic amino acids under acidic conditions (Steinberg 2009; Lottspeich and Engels 2012).

Coomassie Blue stain was prepared following the manufacturer's instructions by adding 2.5 ml well-shaken Roti-Blue® (Roth) to 10 ml, 30 % methanol. For staining, the gel was placed in a covered tray containing 12.5 ml of the staining solution and it was left on a shaker at RT overnight. It was destained using 30 % methanol for several changes over a period of 1-2 h. The gel was recorded using the table top scanner CanoScan (Canon).

3.4.1.2 Silver staining

Silver staining is a highly sensitive method to detect proteins in the gel. Ions of a silver nitrate solution bind to proteins in the gel through interaction with functional groups and peptide bonds. By adding strong reduction catalysts, these silver ions are reduced to metallic silver, which appear dark in color (Lottspeich and Engels 2012).

Silver staining of SDS gels was performed with the Invitrogen Silver Quest Silver Staining Kit, which contained required reagents and instructions. All solutions were prepared immediately prior to staining. For one mini-gel, 100 ml of each solution were used and incubation took place on a shaker (Biometra).

The gel was removed from the cassette directly after electrophoresis, placed in a clean staining tray and rinsed briefly with ultrapure water. It was fixed in fixing solution for 20 min, then washed with 30 % ethanol for 10 min. It was incubated for 10 min in sensitizing solution and washed again with 30 % ethanol for 10 min, and then in ultrapure water for 10 min. The gel was subsequently incubated in staining solution for 15 min. After staining was completed, it was washed with ultrapure water for 60 sec. Next, the gel was incubated in developing solution for 4 − 8 min until the dark bands appeared. Once the required staining intensity was achieved, the pH was lowered immediately through addition of 10 ml stopper solution to avoid high background staining by unbound silver ions in the gel. The stopper solution was gently agitated for 10 min. Finally, the gel was washed with ultrapure water for 10 min and archived using the table top scanner CanoScan (Canon).

3.4.1.3 Western blotting

Western blotting is a highly specific method to detect antigens. Proteins in the gel are subjected to electrophoretic transfer onto a nitrocellulose membrane and to immobilization for subsequent immunoreaction (Renart *et al.* 1979; Towbin *et al.* 1979). Assuming that proteins generate antibody responses upon MTC infection or sensitization and that these antibodies are available in serum of sensitized guinea pigs, the serum can be used for specific detection of such antigenic proteins (see section 3.7).

Protran nitrocellulose and filter paper (both GE Healthcare), cut in the size of the SDS-gel, were assembled to the blotting sandwich according to the following scheme:

- 2 filter sheets soaked with anode solution 1
- 1 filter sheet soaked with anode solution 2
- Nitrocellulose soaked with anode solution 2

- SDS gel
- 3 filter sheets soaked with cathode solution

Air bubbles were squeezed out and the sandwich was placed in the blotting device (Hoefer Scientific Instruments). A current of 0.8 mA/cm^2 was applied for 2 h.

The blotted nitrocellulose membrane was transferred into a tray and blocked in blocking buffer at 4 °C overnight to prevent non-specific binding. The membrane was then washed three times with PBS + 0.05 % Tween 20. A volume of 10 ml of the first antibody solution (1:10 diluted pool sera of 10 BCG-sensitized guinea pigs in 1 % Skim Milk in PBS + 0.05 % Tween 20) was added and incubated on a shaker for 1 h at RT. The membrane was then washed three times with PBS + 0.05 % Tween 20 for 5 min each at RT. Afterwards, the membrane was incubated with the second antibody (goat anti-guinea pig IgG, horseradish peroxidase (HRP) conjugated, 1:5,000 diluted in 1 % skim milk in PBS + 0.05% Tween 20) on the shaker at RT for 2 h. After incubation, the membrane was washed 5 times with PBS + 0.05 % Tween 20 for 5 min each and once with PBS for 10 min at RT. The membrane was subsequently washed with substrate buffer once for 5 min at RT and incubated in AEC buffer until the specific bands appeared. Adding H_2O stopped the reaction and pictures were taken immediately with the table top scanner CanoScan (Canon).

3.4.2 Thin layer chromatography

Thin layer chromatography (TLC) is a well-suited method to fractionize lipid preparations (Christie and Han 2010).

A 0.2 mm silica gel with fluorescence indicator on a glass plate (Sigma-Aldrich) was used as the stationary phase. The mobile phase was chloroform-methanol-H_2O (65:25:4). The solvent mixture was poured into a glass beaker lined with filter paper and covered with aluminium. The chamber was left to equilibrate for approximately 1 h at RT to achieve a saturated atmosphere. The antigen preparation samples were dried on the thin layer plate in quantities of 1 µl before adding the next quantity. The used antigen contents are indicated in the results section. After thorough drying, the thin layer plate was placed in the chamber so that the solvent did not reach the samples directly. The cover was replaced immediately and the samples migrated by solvent drag for nearly 30 min until the front reached approximately 1 cm below the upper rim of the plate. During migration, the solvent moved upwards directed by the capillary force of the silica gel, taking along the different components of the antigen preparations to a varying extent. The plate was removed, left to dry and analyzed with the GeneSnap program using UV short wave for 800 ms in a G-box (SynGene).

3.4.3 Bradford assay

The Bradford assay is a sensitive method to quantify proteins through photometry (Bradford 1976). The acid dye Coomassie brilliant blue G250 forms complexes with cationic and non-polar, hydrophobic side chains of proteins, thereby shifting the absorption maximum from 465 nm to 595 nm (Lottspeich and Engels 2012).

For the Bradford assay in cuvettes, serial dilutions of the sample (5, 10, 20, 50 µl per 800 µl total volume) as well as bovine serum albumin (BSA, 0.1 mg/ml, w/v) (0, 10, 50, 100, 150 µl per 800 µl total volume) were used by diluting with milliQ water to the total volume. 200 µl Bradford reagent with phosphoric acid and methanol were added. The mixture was covered with parafilm and mixed by inverting. The read-out was performed at 595 nm in the photometer (BMG labtech).

For the Bradford assay in 96-well microtiter plates, serial dilutions of both the sample (1, 15, 20 µl) and BSA (1 mg/ml, w/v) (0, 2, 4, 6, 10, 15, 20 µl) were mixed with 40 µl Bradford reagent, with milliQ water added to reach a total volume of 0.2 ml. The read-out was performed at 595 nm in the photometer.

3.5 Animals

According to the German Animal Welfare legislation, this study was approved by the competent authority (Veterinary Department, Regierungspraesidium Darmstadt, Germany, ref.: V 54 – 19 c 20/15 – F 107/110 with extension from 8 January 2013/6 March 2013 and V 54 – 19 c 20/15 – F 107/125).

3.5.1 Dunkin-Hartley guinea pigs

Female Dunkin-Hartley guinea pigs were originally purchased from Charles River Laboratories, Sulzfeld, Germany. At a body weight of around 500 g, they had been used in safety and challenge studies for human vaccines such as diphtheria toxin and tetanus toxoid, or batch potency testing of veterinary vaccines such as equine influenza and tetanus toxoid. The tests with human vaccines were considered non-burdensome. At the end of the trial a veterinarian examined the animals. Guinea pigs with low or no burden were approved by the animal trial protocol for further experiments following the concept of 3R: reducing the number of animals in experiments by repeated use. In batch potency testing of veterinary vaccines,

animals were vaccinated with different vaccine doses. Four weeks later, the guinea pigs were anesthetized and blood was taken to assess the antibody levels.

After a resting period of at least one week, often without the need to change the housing room, the guinea pigs were used in the present study. They were sensitized (see section 3.6.2) and rested for another four weeks before blood was taken.

All guinea pigs were housed in accordance with Appendix A of the European Convention for the Protection of Vertebrate Animals used for Experimental and other Scientific Purposes as adopted by the German Animal Welfare Legislation (Federal Ministry of Food and Agriculture, 2007). They had sufficient space (79 x 58 x 49 cm) in stainless steel cages for groups of 2 to 5 animals, depending on their weight. The cages were equipped with dust-free wooden bedding and had two houses (30 x 20.5 x 18.5 cm), which provided additional space due to flat roofs. Access to pellets and water was *ad libitum*. Generous amounts of hay and vegetables were provided daily. The animal rooms were air-conditioned and large windows allowed the animals to experience natural day and night cycles.

3.5.2 Inbred strain 2 guinea pigs

Inbred strain 2 guinea pigs were kindly offered by Dr. Hubert Schaefer from the Robert Koch Institute (RKI) and Dr. Mechthild Ladwig from the German Federal Institute for Risk Assessment, both Berlin, Germany. Strain 2 guinea pigs are histocompatible (Loeb and Wright 1927; Bauer 1958), making them favorable for use in immunological studies. However, breeding facilities are rare, probably due to their poor reproduction performance (E. Shevach, NIAID, USA, personal communication). After initially testing whether these guinea pigs were suited for our studies to the same extent as outbred Dunkin-Hartley guinea pigs, 10 guinea pigs were used to start a breeding colony. The offspring was used either for breeding or experimentation.

Guinea pigs which were used in experiments were housed as stated above (see section 3.5.1). Female breeding animals were housed in large, ground-based group-housings (170 x 100 x 45 cm or 112 x 100 x 45 cm) with around 5 guinea pigs. Male breeding guinea pigs were housed in individual cages (73 x 53 x 25 cm) with one plastic refuge as described above and joined the group housings during the breeding period. All housings were in accordance with Appendix A of the European Convention for the Protection of Vertebrate Animals used for Experimental and other Scientific Purposes as adopted by the German Animal Welfare Legislation (Federal Ministry of Food and Agriculture, 2007). According to § 11, section 1, number 1 of the German animal protection law as of 2006 May 18, the Paul-

Ehrlich-Institut has been granted permission to keep and breed laboratory animals (ref.: F 107; V 54 – 19 c 20/21 I – F 107).

Blood collection from non-sensitized strain 2 guinea pigs was reported according to the German legislation (ref.: F 107/Anz. 1006).

3.5.3 Numbers of guinea pigs used in the present study

At day 30, blood was obtained from a total of 73 BCG-sensitized Dunkin-Hartley guinea pigs, with the datasets of the *ex vivo* lymphocyte proliferation assay of 51 of these animals being included in the analyses presented in this thesis. At day 60, blood was obtained from a total of 51 iAN5-sensitized Dunkin-Hartley guinea pigs, with the datasets of the *ex vivo* lymphocyte proliferation assay of 40 of these animals being included in the analyses presented in this thesis. Please refer to Annex 6 for details.

A total of 15 strain 2 guinea pigs was used for *ex vivo* lymphocyte proliferation assays and the generation of guinea pig T cell lines. A total of 9 strain 2 guinea pigs was used for the generation of syngenic PBMCs for antigen presentation.

3.6 Animal experiments

3.6.1 Anesthesia

All animals were clinically checked and weighed before each anesthesia. The animals involved in the 6-month pilot study were checked before, one day after, and one week after each anesthesia and/or cardiocentesis by a veterinarian using a strict scoring plan (see Annex 2).

Sensitization with iAN5 (see section 3.6.2.2), blood sample collection by cardiocentesis (see section 3.6.3) and euthanasia (see section 3.6.4) were only performed on animals under general anesthesia. An anesthetic, a mixture of 10 mg Ketamine (WDT) and 0.5 mg Xylazin (Bayer) was therefore administered per 100 g body weight by subcutaneous injection with 26 G needles in the skin fold of the neck. During anesthesia, the eyes were protected with Thilo-Tears® Gel (Alcon Pharma).

3.6.2 Sensitization procedures

Guinea pigs were sensitized at an approximate body weight of 700 g (Dunkin-Hartley) or 350 g (inbred strain 2 guinea pigs). After sensitization they had a resting period of four weeks to develop immune responses.

The guinea pigs were sensitized either by subcutaneous vaccination with live BCG, or by deep intramuscular administration of wet mass of the heat-inactivated virulent *M. bovis* strain AN5 (iAN5).

3.6.2.1 BCG

The live attenuated *M. bovis* Bacille Calmette-Guérin (BCG) strain Pasteur 1173 (see section 3.1) was used for sensitization as well as for chloroform-methanol extraction (see section 3.3.3). A dose of 2 x 10^6 bacteria was thoroughly resuspended in 0.5 ml PBS and injected subcutaneously behind the left forelimb of the guinea pig. For injection, 23 G needles were used.

3.6.2.2 iAN5

Heat-inactivated wet mass of the virulent *M. bovis* strain AN5 (see section 3.1) was used for sensitization of guinea pigs and for chloroform-methanol extraction (see section 3.3.3). For sensitization, 2 mg wet mass was thoroughly resuspended in 0.5 ml light mineral oil (Merck) at 38 °C and equally distributed into the *Mm. gastrocnemius* of both hind limbs of the anesthetized guinea pig, using 23 G needles.

3.6.3 Blood sample collection by cardiocentesis

For cardiocentesis, anesthetized guinea pigs were placed on their back and the injection site was cleaned with skin disinfectant (Henry Schein®). The first syringe was pre-filled with 1.5 ml sodium citrate to avoid coagulation. A 22 G needle (Terumo, 0.7 x 40 mm) with the mounted 10 ml syringe (B. Braun) was vertically inserted between the *processus xiphoideus* and the left costal arch. It was advanced in cranio-dorsal direction towards the right clavicle of the animal with light aspiration. As soon as blood entered the needle, advancement was stopped and blood was carefully aspirated. Next, another 5 ml syringe (B. Braun) was mounted to obtain blood for extraction of autologous serum (see section 3.7.1). After this

blood sample collection, aspiration was stopped and the needle with mounted syringe was removed from the animal. Directly after cardiocentesis, the guinea pigs were placed on their right side to facilitate cardiac work and they were monitored during the wake-up phase.

Given a reconvalescence time of four weeks and a minimum body weight of 400 g, a maximum of 5 ml blood could be obtained per cardiocentesis, according to the veterinary license of the competent authority. We were allowed to collect blood from the guinea pigs either three, or for a small pilot study 6 times, in 4-week intervals. For the final cardiocentesis, the maximum blood volume was permitted for collection.

Whenever possible throughout this study, antigens were tested in BCG-sensitized animals at day 30. Following the principle of 3R (Refinement, Reduction, Replacement of animal experiments (Russell and Burch 1959)), if possible, the animals were re-used for pilot experiments at other time points to reduce the total number of animals required for this project. The blood of the iAN5-sensitized animals was used at days 0 and 30 in the partner project. In most of the animals we were only allowed to take blood a total number of three times. For this reason and because iAN5-sensitized animals constituted only comparison groups to BCG sensitization in this study, if possible, their PBMCs were analyzed at day 60. Strong immune responses were already mounted until this day. The day of blood collection is always indicated in the captions.

Prior to sensitization, blood samples were collected from a number of guinea pigs to test whether their immune responses were naive for mycobacterial antigens. Guinea pigs with multiple cardiocenteses were used for blood sample collection every four weeks.

3.6.4 Euthanasia

Immediately after the final cardiocentesis, while still under anesthesia, animals were euthanized by carbon dioxide inhalation. Only the animals in the 6-month pilot study were euthanized with carbon-dioxide in deep anesthesia one week after the last cardiocentesis and clinical follow-up. The results of the 6-month pilot study are described in Annex 2.

3.7 Serum processing and cytological techniques

3.7.1 Serum processing

Directly after collection (see section 3.6.3), the blood in the second syringe was transferred into a serum container (Greiner bio-one) and centrifuged (5600 x *g*, 5 min, 20 °C).

Autologous serum was stored at 4 °C for use in the *ex vivo* lymphocyte proliferation assay which was performed on the same day as the blood collection took place. Autologous serum samples were stored in Eppendorf tubes or cryogenic vials (Nalgene) at –20 °C for usage in subsequent assays. Equal portions of serum samples of 10 BCG-sensitized guinea pigs were pooled for Western blot analysis (see section 3.4.1.3).

3.7.2 PBMC purification

For PBMC purification, whole citrate blood (see section 3.6.3) was diluted with PBS to a total volume of 20 ml. The blood-PBS mixture was carefully layered on 15 ml Ficoll-Paque (1.047 g/ml density; GE Healthcare) in a 50 ml plastic tube (Greiner), using 25 ml plastic pipettes (Greiner bio-one) to avoid adhesion of blood cells to the pipette. A gradient centrifugation was performed with the layered mixture (600 x *g*, 45 min, 20 °C, without acceleration and brake), separating peripheral blood mononuclear cells (PBMCs) not only from plasma, but also from erythro- and granulocytes. The intermediate phase containing the lymphocytes was carefully transferred to a new 50 ml tube and washed twice with PBS + 1 % FCS (900 x *g*, 5 min, 15 °C). Next, it was transferred in a 15 ml tube (Greiner) and washed again with PBS + 1 % FCS to remove thrombocytes (150 x *g*, 7 min, 15 °C). Where erythrocytes remained in the PBMC fraction, erythrolysis was performed using 500 µl erythrolysis buffer per sample, for 5 minutes. Subsequently, the cells were washed twice with PBS + 1 % FCS (900 x *g*, 5 min, 15 °C).

Finally, the pellet was resuspended in 1 ml PBS and the cell number was determined in a Neubauer Improved Cell counter using trypan blue staining. Trypan blue is a diazo dye that penetrates the cell walls of dead cells, but not of living ones. The dye creates distinction between the viable and dead cells, allowing only living cells to be counted (Lam *et al.* 2015). Cells in one to four large squares, depending on the number of cells, were counted and if necessary, divided through 4. This total number per large square was multiplied with 1 for the volume the cells were resuspended in, and multiplied with 6 for the ratio when mixing cells with trypan blue (50 µl trypan blue and 10 µl cell suspension, 10 µl of this mixture was

inserted into the cell counter). This number was divided through 100 to obtain the total number of cells in millions.

3.7.3 Freezing of PBMCs and cell lines

Portions of PBMCs were frozen on the day of blood collection for future use, for example, in the lymphocyte restimulation assay (see section 3.8.2). T cell lines (see section 3.10) were frozen regularly as backups and for future experiments.

For freezing, cells were washed with PBS + 1 % FCS (900 x *g*, 5 min, 15 °C), resuspended in 90 % FCS + 10 % DMSO at a concentration of up to 20 x 10^6 cells/ml and filled in pre-cooled cryo vials. The cryo vials were immediately frozen at –80 °C.

3.7.4 Irradiation of PBMCs

Irradiation of PBMCs should restrict their function to antigen presentation for a couple of days (Collison and Vignali 2011) and should prevent their proliferation. PBMCs were washed with PBS + 1 % FCS (900 x *g*, 5 min, 15 °C), resuspended in 1 ml PBS + 1 % FCS and irradiated with 40 Gray in a gamma-irradiation facility (STS Steuertechnik). Subsequently, the cells were washed three times with PBS + 1 % FCS (900 x *g*, 5 min, 15 °C) to remove toxic substances.

3.8 Cytological analyses

3.8.1 *Ex vivo* lymphocyte proliferation assay (CFSE assay)

The basis of the *ex vivo* lymphocyte proliferation assay used in this study was described before (Bastian *et al.* 2008).

PBMCs were labeled with the green fluorescent dye carboxy-fluorescein-succinimidyl-ester (CFSE, Enzo Life Sciences). CFSE penetrates the cells and the acetate groups are subsequently cleaved by intracellular esterases to yield the carboxyfluorescein molecule, while the succinimidyl group crosslinks to amino groups of intracellular proteins (Quah *et al.* 2007). In flow cytometry, cell proliferation can be measured as successive halving of the fluorescence intensity per cell (Lyons and Parish 1994; Quah *et al.* 2007). CFSE stock was manufactured by mixing 3 µl CFSE with 300 µl DMSO (v/v) and stored as 10 µl-aliquots with

a concentration of 0.5 mM at –20 °C. Directly prior to use, this stock was diluted 1:10 with PBS for a concentration of 0.05 mM.

After counting, PBMCs were adjusted to 1 x 10^7/ml in PBS. PBS + 1 % FCS would inhibit CFSE staining. A volume of 20 µl CFSE working solution was added per 1 ml of cell suspension and the mixture was incubated at 37 °C in a water bath, for exactly 12 min. Next, the PBMCs were washed twice with cold PBS + 1 % FCS (900 x *g*, 5 min, 15 °C) and then resuspended in serum-free Iscove's modified Dulbecco's medium (SF-IMDM) at a cell concentration of 2 x 10^6/ml. 10 % autologous serum was added (see section 3.7.1).

96-well round bottom microtiter plates (Thermo Fisher Scientific) were filled with 50 µl/well of antigens in duplicates. Medium-only wells served as a negative control. Positive controls consisted of phytohemagglutinin (PHA, Thermo Fisher Scientific) at a concentration of 0.05 µg/ml (w/v) or tuberculin Tub12 at a concentration of 30 IU/ml, unless otherwise stated. All other tuberculins were used at the same concentration. CMEs and LppEL were employed at a concentration of 10 µg/ml (w/v), unless otherwise stated. Further antigen preparations and their concentrations used in the assay are described in section 3.3 and are indicated in the results section.

To 50 µl prefilled antigens, 50 µl PBMC suspension were added, resulting in a total PBMC content of 1 x 10^6 cells/ml with 5 % autologous serum.

Plates were incubated for 5 days at 37 °C and 5 % CO_2. They were subsequently analyzed by flow cytometry (see section 3.8.4).

3.8.2 Lymphocyte restimulation assay

In line with this project, a new lymphocyte restimulation assay was developed and approved to investigate antigen specificity of the cells. It consists of three single steps: the antigen-specific expansion of sensitized lymphocytes *ex vivo*, the sorting for the expanded lymphocytes and the restimulation and testing of the antigen specificity of these lymphocytes.

For this restimulation assay, irradiated autologous PBMCs (see section 3.7.4) were needed to act as antigen-presenting cells (APCs). Therefore, a portion of the PBMCs was frozen in 90 % FCS + 10 % DMSO at –80 °C after purification on the day of blood collection (see section 3.7.3).

3.8.2.1 Antigen-specific expansion of lymphocytes

On the day of blood collection, after determination of cell numbers, PBMCs selected for the lymphocyte restimulation assay were incubated with 10 µl 2 mM biotin in DMSO (EZ-Link® Sulfo-NHS-LC-Biotin, Thermo Fisher Scientific) for 30 min at 4 °C. This allowed the biotin molecules to bind to the cell. Afterwards, cells were washed with PBS + 1 % FCS and with PBS only (900 x *g*, 5 min, 15 °C) to remove unbound biotin. CFSE labeling was performed as described above (section 3.8.1).

2 x 10^6 PBMCs in 1 ml SF-IMDM containing 5 % autologous serum were seeded per well in a 24-well flat bottom plate (Becton Dickinson) and 30 IU/ml Tub12 or 10 µg/ml (w/v) CME were added for antigen-specific expansion of the cells. Plates were incubated for 6 days at 37 °C and 5 % CO_2.

3.8.2.2 Sorting of expanded lymphocytes

After incubation, cells were harvested and resuspended in MACS buffer. Cells were washed once with this buffer (900 x *g*, 5 min, 15 °C) and the buffer was poured off, not aspirated. Cells were resuspended in the remaining buffer (approximately 80 µl). 10 µl streptavidin MACS beads were thoroughly vortexed and added to the cell suspension. Incubation for at least 30 minutes took place on a rolling wheel at 4 °C. After incubation, cells were washed once with 10 ml MACS buffer (900 x *g*, 5 min, 15 °C) to remove unbound streptavidin beads and then resuspended in 1 ml MACS buffer. MACS midi magnetic columns (Miltenyi Biotec) were placed on the magnetic holder and equilibrated with 500 µl MACS buffer. Next, the cells were carefully placed on the column and the draining solution was collected as "$biotin_{negative}$ cells" in a 15 ml tube. Once all the fluid passed the column, it was washed once with 500 µl MACS buffer and the draining solution was collected as "flow-through" in another 15 ml tube. After all fluid having passed again, the column was removed from the magnet and washed twice with 1 ml and 0.5 ml MACS buffer respectively, with pressure generated by the provided plunger. Non-proliferated cells adhering to the magnetic column due to remaining biotin and thus streptavidin binding were forced out. This sorting fraction was collected as "biotin-positive cells".

Samples of the cells were collected directly after harvesting, as well as of all fractions, for flow cytometric analysis of the sorting effectiveness (see section 4.3.1). To ensure the purity of the expanded cells, samples with less than 80 % $CFSE_{low}$ cells in the $biotin_{negative}$ population were not further analyzed in the restimulation assay.

Furthermore, a cell sample collected directly after harvesting was incubated with streptavidin$^{PE\text{-}Cy5.5}$ (Life Technologies) for 0.5 h at 4 °C. It was washed once with PBS + 1 % FCS (900 x *g*, 5 min, 15 °C) and was also analyzed by flow cytometry (see section 3.8.3). It served as a control for remaining biotinylation of the cells.

3.8.2.3 Restimulation of sorted lymphocytes

$Biotin_{negative}$ cells were counted as described above (see section 3.7.2).

Frozen autologous PBMCs (see section 3.7.3) were thawed, washed with PBS + 1 % FCS and irradiated with 40 Gray (see section 3.7.4). Afterwards, they were washed with PBS + 1 % FCS three times to remove toxic substances, resuspended in PBS and counted.

$Biotin_{negative}$ cells and irradiated PBMCs were mixed at a ratio of 1:1 and the mixed cells were washed once with PBS (900 x *g*, 5 min, 15 °C). Subsequently, they were resuspended in PBS at a concentration of 1 x 10^7 $biotin_{negative}$ cells/ml, but at least in 500 µl. They were labeled with 10 µl CFSE working solution (0.05 mM, see section 3.8.1) per 500 µl PBS in the 37 °C water bath for 12 minutes. Afterwards, they were washed with PBS + 1 % FCS twice and resuspended in SF-IMDM at a concentration of 4 x 10^5 $biotin_{negative}$ cells per ml. 10 % autologous serum was added. Control cells - irradiated PBMCs only or $biotin_{negative}$ cells only - were resuspended at a concentration of 8 x 10^5 cells/ml in order to achieve the same total cell numbers per well as in the mixed suspensions.

50 µl of these cell suspensions were added per well, in 96-well round bottom microtiter plates, prefilled with 50 µl antigen suspension in duplicate as described above (see section 3.8.1). Plates were incubated for 5 days at 37 °C and 5 % CO_2.

Flow cytometry for the detection of proliferated cells was performed as described in section 3.8.4. Assays with > 20 % $CFSE_{low}$ lymphocytes in the medium-only control were excluded from further analysis.

3.8.3 Phenotypical characterization of lymphocytes

For phenotypical characterization, antibodies to pan T cell marker (Bio-Rad AbD Serotec), guinea pig CD4 (Bio-Rad AbD Serotec) and guinea pig CD8 (kindly provided by Dr. Hubert Schaefer, RKI Berlin, Germany) were used on PBMCs directly *ex vivo,* as well as after 5 days of incubation in the lymphocyte proliferation assay (see section 3.8.1).

Non-CFSE-labeled and unbiotinilated cells *ex vivo,* or unbiotinilated cells after 5 days of incubation, were washed once with PBS + 1 % FCS (900 x *g*, 5 min, 15 °C). Approximately 3 x 10^4 cells were resuspended with the first antibody mixture containing 0.5 µl anti-guinea pig pan T cell^{APC} antibody, 0.5 µl anti-guinea pig CD4^{PE} antibody and 1 µl biotinilated anti-guinea pig CD8 antibody in 20 µl total volume PBS + 1 % FCS.

After incubating for 35 min at 4 °C, cells were washed with PBS + 1 % FCS (900 x *g*, 5 min, 15 °C). Next, they were incubated with 0.02 µl Strepavidin$^{PE\text{-}Cy5.5}$ (Life Technologies) in 20 µl total volume PBS + 1 % FCS, for another 35 minutes at 4 °C. After washing with PBS + 1 % FCS (900 x *g*, 5 min, 15 °C) the cells were resuspended in 100 µl PBS + 1 % FCS and analyzed by flow cytometry as described in section 3.8.4.

Cell suspensions with unstained PBMCs, 2nd only, pan T cell only, CD4 only and CD8 + 2nd only staining in 20 µl total volume PBS + 1 % FCS served as controls. Additionally, isotype controls were performed.

3.8.4 Flow cytometry

Fluorescence-activated cell sorting (FACS) is used to analyze cell populations for their specific characteristics. Therefore, cells are separated to single cell suspensions and beamed with lasers. Fluorescence emission is detected and recorded. For standard characterization, one laser beam of 488 nm (blue) serves to detect the size, also called forward scatter (FSC), as well as the granularity of the cells (side scatter, SSC, measured in 90 °C angle to the FSC). General fluorescence of the cells (e.g. by CFSE labeling) or fluorescence-marked antibodies bound to certain markers of the cell, can be detected using lasers of different colors (Brown and Wittwer 2000; Bakke 2001).

Flow cytometry was performed using an LSR II and a C6 Accuri flow cytometer (both Becton Dickinson). FACSDiva (Becton Dickinson) and FlowJo (FlowJo, LLC) or CFlow Plus Analysis software (Becton Dickinson) were used, respectively, for identification of cell populations. Run settings of the flow cytometer were 30 seconds at medium flow with a threshold of 1,000,000 on FSC.

Flowcytometric analysis of the *ex vivo* lymphocyte proliferation assay (CFSE assay)

Lymphocytes were gated by their characteristic localization in the FSC versus SSC plot. The lymphocyte gate was further analyzed in the green fluorescence channel (FL-1, CFSE)

versus FSC. In this plot, the percentage of $CFSE_{low}$ cells compared to the total lymphocyte population was determined by gating (**Figure 3.2**). Next, the percentage was averaged over each antigen's duplicate. Unless otherwise stated, assays which did not meet the validity criteria of ≤ 20 % $CFSE_{low}$ lymphocytes in the medium-only control and ≥ 20 % $CFSE_{low}$ lymphocytes in Tub12-positive control were excluded from further analysis.

Flowcytometric investigation of the count of living lymphocytes

The count of living lymphocytes was determined as one parameter for lymphocyte stimulation in investigations of cell stimulation when the cells could not be labeled with CFSE (e.g., if only a few cells of guinea pig T cell lines (see section 3.10) were available). The count of living lymphocytes was determined by gating for the lymphocyte population in FSC versus SSC plot. The total counts of lymphocytes were investigated in defined volumes (e.g., 20 µl) and they were compared between the differentially stimulated wells.

Flowcytometric analysis of blasting lymphocytes

To further analyze whether an antigen preparation stimulated lymphocytes which could not be labeled with CFSE (see above), the number of blasting lymphocytes was determined through gating the cells which were, among the lymphocytes, located furthest right on the FSC axis (FSC_{high}) in the FSC versus SSC plot.

Flowcytometric investigation of cytotoxicity

To investigate whether an antigenic stimulus had a cytotoxic effect, total counts of lymphocytes were determined by gating for the lymphocyte population in FSC versus SSC plot as described for the flowcytometric analysis of the count of living lymphocytes (see above). Cytotoxicity was characterized by nearly abolished lymphocyte counts in the respectively stimulated wells and significantly lower counts than in the medium-only control wells (ratio *t* test).

Flowcytometric analysis of the sorting procedure of expanded lymphocytes and of the lymphocyte restimulation assay

The actual sorting procedure of expanded lymphocytes is delineated in section 4.3.1. In flow cytometry, sorted cell populations were analyzed in the same manner as the CFSE-labeled cells in the *ex vivo* lymphocyte proliferation assay (see above).

The control incubations of biotinylated lymphocytes with streptavidin$^{PE\text{-}Cy5.5}$ were gated in FSC versus SSC plot according to the description above. Subsequently, the lymphocytes were gated in FL-1 (CFSE) versus FSC plot for the $CFSE_{low}$ cells and these were next analyzed in FL-3 (PE-Cy5.5) versus FSC for their percentages of $SAv^{PE\text{-}Cy5.5}{}_{positive}$ and $SAv^{PE\text{-}Cy5.5}{}_{negative}$ cells.

Cells in the restimulation assay were analyzed by flow cytometry according to the analysis of the lymphocytes in the *ex vivo* lymphocyte proliferation assay (see above).

Flowcytometric analysis of the phenotypical characterization

In flowcytometric analysis of the FACS staining for phenotypical characterization (see section 3.8.3), cells were first gated for the lymphocyte population in FSC versus SSC plot (see above). The lymphocyte population was further examined in an FL-1 (green fluorescence, CFSE) versus FL-4 (purple fluorescence, pan T cell marker^{APC}) plot. In this plot, cells were detected as T cells and, if cells were analyzed post-stimulation, they were additionally distinguished into $CFSE_{low}$ and $CFSE_{high}$, thus in proliferated and non-proliferated ones, respectively. Each of these populations was further processed separately in FL-3 (red fluorescence, CD8 marker$^{PE\text{-}Cy5.5}$) versus FL-2 (yellow fluorescence, CD4 marker^{PE}) plots for their percentages in each marker (**Figure 3.3**). If signs of spectral spillover occurred, fluorescence compensation was applied.

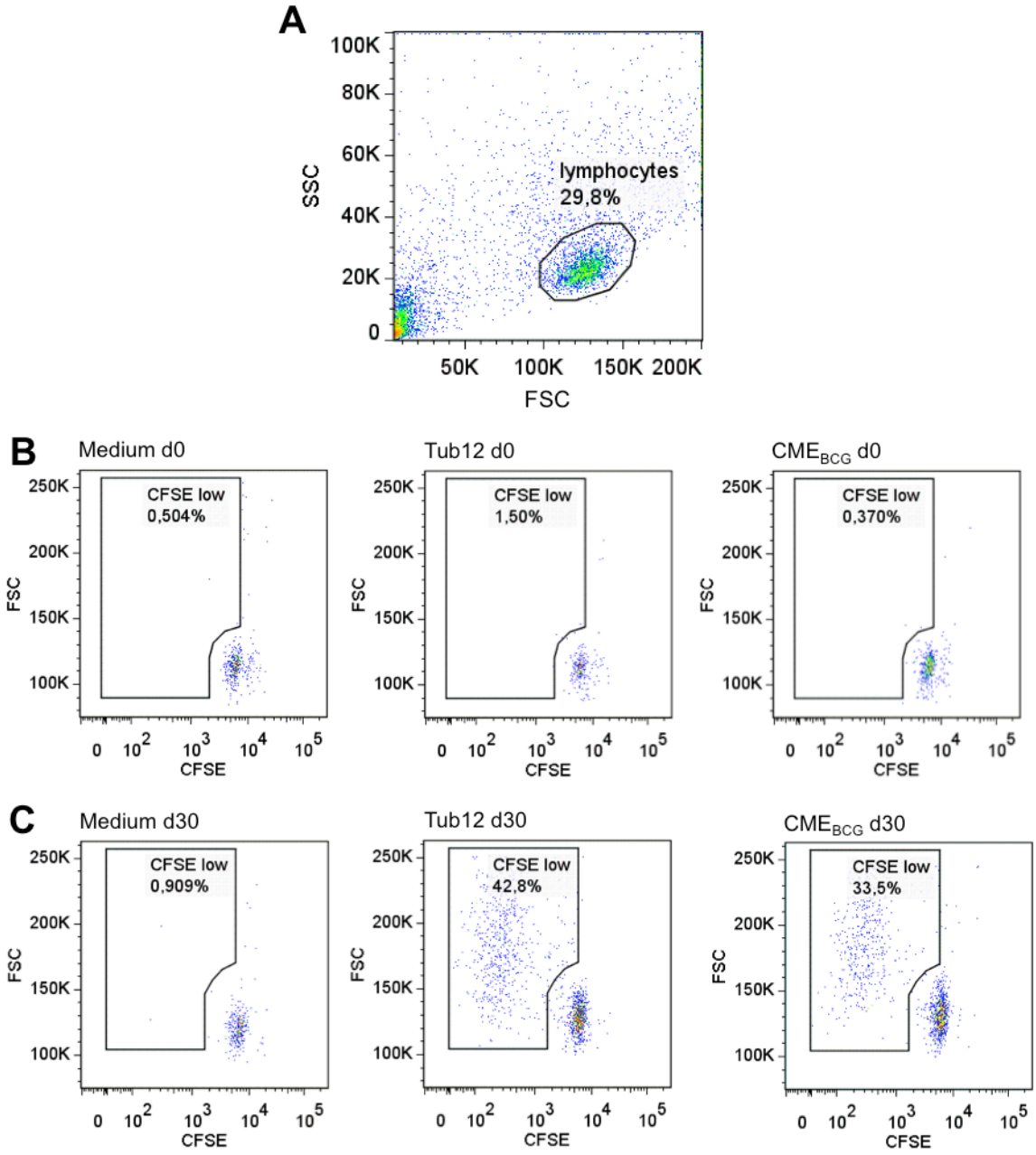

Figure 3.2 Gating strategies for CFSE-labeled lymphocytes in flow cytometry.

A. Gating of the lymphocyte population in the forward (FSC) versus side scatter (SSC) plot. **B** and **C.** Further processing of these gated lymphocytes in green fluorescence (FL-1, CFSE) versus FSC plot. Antigens used for stimulation in the *ex vivo* lymphocyte proliferation assay are indicated. The gates mark the $CFSE_{low}$ population within the lymphocytes. Numbers indicate the percentages of $CFSE_{low}$ cells in relation to the whole lymphocyte population in the respective test well of a 96-well microtiter plate. PBMCs for these experiments were obtained from guinea pigs before (day 0, B) or after MTC sensitization (day 30, C). The plots have been illustrated using FlowJo Single Cell Analysis Software.

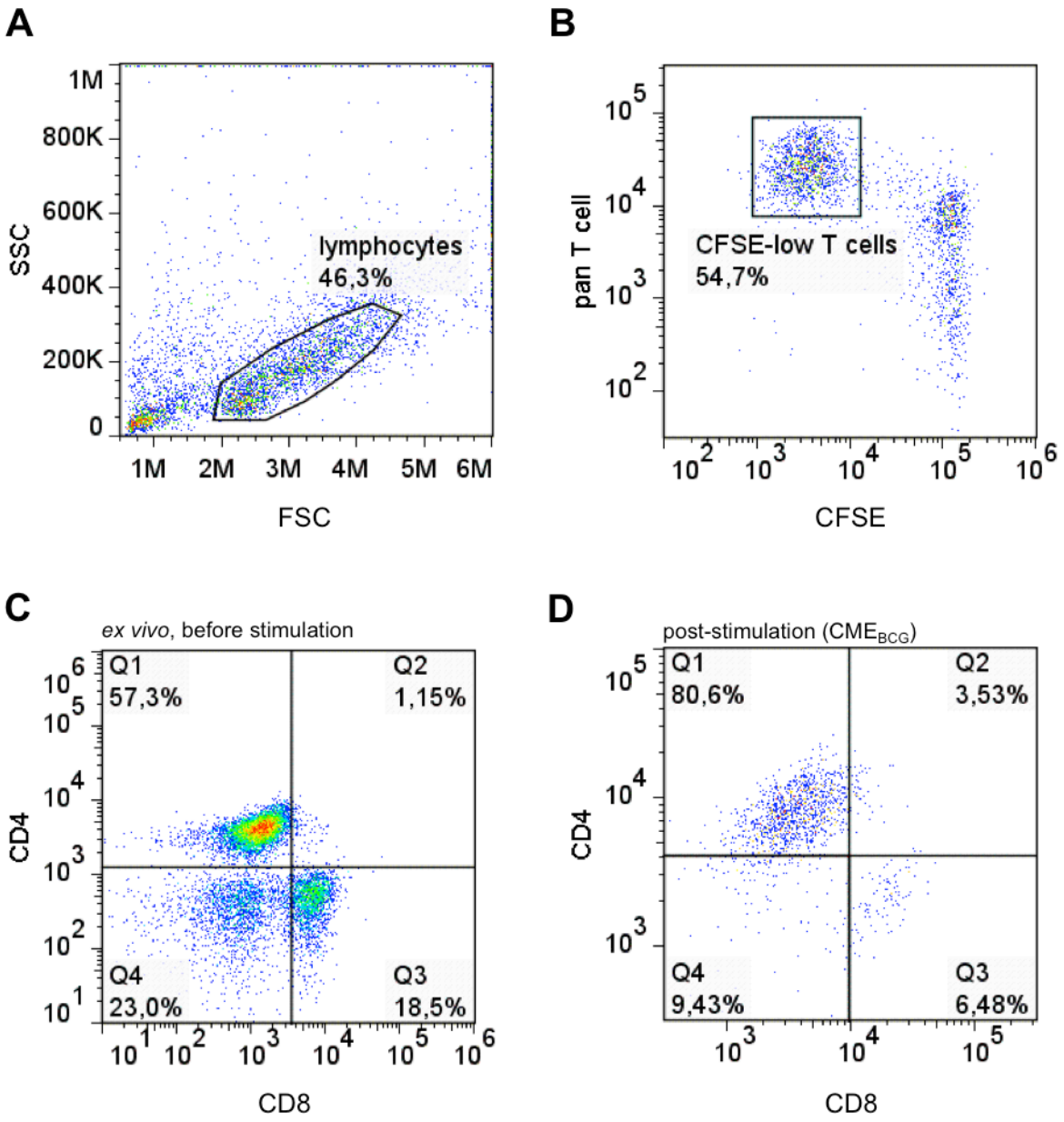

Figure 3.3 Gating strategies for phenotypical characterization of guinea pig PBMCs in flow cytometry.

A. Gating of the lymphocytes in FSC versus SSC plot after 5 days of incubation with CME_{BCG}. The guinea pig was sensitized for mycobacteria 30 days prior blood collection. **B.** Presentation of the lymphocyte population post-stimulation in CFSE versus pan T cell marker plot. The gate marks the $CFSE_{low}$, proliferated T cells. If lymphocytes were analyzed before *in vitro* stimulation, only T cells in general would be gated in this plot. **C.** Further analysis of the T cells obtained before *in vitro* stimulation in CD8 versus CD4 marker plot. **D.** Further analysis of the T cells after 5 days of incubation with CME_{BCG} in CD8 versus CD4 marker plot.
The plots have been illustrated using FlowJo Single Cell Analysis Software.

3.8.5 TLR2 assay

The HEK 293 hTLR2-CD14 cell line is stably co-transfected with the human TLR2 receptor and CD14, as described in the product information by the manufacturer (InvivoGen). It was used to test for TLR2 ligands in antigen preparations. For example, lipoproteins can constitute such TLR2 ligands (Ozinsky *et al.* 2000; Girard *et al.* 2003; Thakran *et al.* 2008). The cell line was expanded in Dulbecco's modified Eagle medium (DMEM, Lonza Biosciences) with L-glutamine, 10 ml/l (v/v) premixed penicillin-streptomycin solution (Lonza Biosciences) and 10 % FCS.

For the TLR2 assay, ten-fold serial dilutions of the phenol-partitioned CME (see section 3.3.8) (10 µg/ml to 0.0000001 ng/ml), as well as of the control lipopeptide Pam3CSK4 (Cayla-InvivoGen) (1 µg/ml to 0.1 ng/ml), and a medium control were added to 50,000 cells per well, in a 96-well flat bottom microtiter plate. The plate was incubated overnight at 37 °C and 5 % CO_2. After incubation, 20 µl/well supernatant were transferred into the wells of a new 96-well flat bottom microtiter plate and 180 µl/well Quanti-Blue^{TM} (Invivogen) was added. Quanti-Blue is a dye used to detect NF-κB, a transcription factor that is secreted by HEK TLR2 CD14 293 cells upon stimulation with TLR2 ligands. The mixture was incubated at 37 °C for 2 h and again subjected to laser detection. Laser detection of an increase in blue color took place in a Bio-Trek µQuant Instrument at 620 nm.

3.9 TNFα ELISA

TNFα is an important cytokine secreted by immune cells after MTC infection (Cavalcanti *et al.* 2012). An ELISA for guinea pig TNFα is commercially available (Kingfisher Biotech) and was utilized to further analyze *ex vivo* lymphocyte responses, as well as to characterize T cell lines. For this purpose, supernatant of the cell culture was collected mainly after overnight incubation or as indicated. Then, 96-well MaxiSorb plates (Thermo Fisher Scientific) were coated with 50 µl/well anti-gp TNFα in PBS (concentration 1 µg/ml, w/v) overnight at RT. The next day, after tapping out the antibody solution, non-specific binding sites were blocked with 200 µl/well PBS + 0.05 % Tween 20 + 4 % bovine serum albumin (BSA) for 1 h at RT. After tapping out the blocking buffer, samples were added and incubated for 2 h at RT. Subsequently, the content of the plates was discarded and the plates were washed three times with 100 µl/well PBS + 0.05 % Tween 20. The plates were then tapped out until dry and 50 µl/well anti-guinea pig TNFα$_{biotin}$ in PBS + 0.05 % Tween 20 (concentration of 0.1 µg/ml, w/v) were added and incubated for 1 h at RT. After repetition of the washing steps, 50 µl/well streptavidin^{HRP} in PBS + 0.05 % Tween 20 (Dianova,

concentration of 0.1 µg/ml, w/v) was added and incubated for 30 min at RT. The washing step was repeated 5 times and the ELISA was then developed with 50 µl/well TMB substrate. After color development, which took around 10 minutes, the reaction was stopped with 50 µl/well 1 M H_2SO_4. The read-out took place at 450 nm and 620 nm for correction of optical imperfections of the microplate. If indicated, the values were normalized by background subtraction.

3.10 Establishment and characterization of guinea pig T cell lines

Characterized oligo- or monoclonal cell lines are valuable tools to identify as yet undefined antigen preparations. To our knowledge, there are no monoclonal guinea pig T cell lines established at present.

The here described methods are in parts based on the techniques for generation of monoclonal human T cell lines as published by Mariotti and Nisini (2009).

For generation of T cell lines, PBMCs of inbred strain 2 guinea pigs were used as this guinea pig strain is histocompatible (Loeb and Wright 1927; Bauer 1958). It is thereby possible to use PBMCs of another strain 2 animal for syngenic restimulation of the cells. This is particularly important because animals can only be used in experiments for a very short period of time. The establishment of a cell line often takes longer than this period and thereafter the cell line should usually be maintained over years (Stacey 2004; Nair 2007). Guinea pig strain 2 animals were sensitized with either BCG or iAN5 as described above (see section 3.6.2).

3.10.1 Production of recombinant guinea pig Interleukin-2

Interleukin-2 (IL-2) is an important growth factor for CD4-positive T cells (Oppenheim 2007). Recombinant guinea pig IL-2 (gpIL-2) was generated by Christina Spohr from the veterinary immunobiology group, PEI, using the protocol described in her thesis (Spohr 2015) and the following primers (ThermoFisher, Ulm):

Gp IL-2 forward: ggatccgccaccatgtacaagacgctactc, 479 base pairs, 3' has a *Bam*HI site followed by Kozak sequence and start codon
Gp IL-2 reverse: gcggccgcttaagtcagtcttgacatg, 5' encloses stop codon after *Not*I site

After cloning and production of the recombinant gpIL-2, the supernatant containing the cytokine was harvested from the transduced murine cell line 38B9 culture (culture medium: SF-IMDM + 2 % FCS). It was tested for its functionality and titrated.

3.10.2 Primary T cell culture

On the day of blood collection, purified PBMCs (see section 3.7) were resuspended in SF-IMDM with 10 % autologous serum at a concentration of 1 x 10^6 cells/ml. Next, 100 µl cell suspension per well were filled in 96-well round bottom microtiter plates and 100 µl antigen preparation were added (final concentration CMEs 10 µg/ml, w/v; Tub12 30 IU/ml; serum 5 %). Some wells were seeded with cells and medium-only to control for basal growth in daily microscopic inspections. Microtiter plates were incubated at 37 °C and 5 % CO_2. After 5 days, 2 µl cell culture supernatant containing recombinant gpIL-2 (see section 3.10.1), 0.5 µl autologous serum and 7.5 µl SF-IMDM were added per well. After a further 5 days, 20 µl cell culture supernatant containing recombinant gpIL-2 and 10 µl autologous serum were added per well. In the days that followed, cells were inspected daily for medium color change. As soon as the medium turned orange, limiting dilution was performed.

3.10.3 Limiting dilution

Cells were harvested, washed with PBS + 1 % FCS (900 x *g*, 5 min, 15 °C), counted and resuspended in cloning mixture. The cloning mixture consisted of SF-IMDM, 5 % autologous serum, 1/10 cell culture supernatant containing recombinant gpIL-2 (see section 3.10.1), 4 x 10^6 irradiated guinea pig PBMCs per ml (see section 3.7.4) and 1 µg/ml PHA.

For generation of polyclonal T cell lines, cells were diluted in 96-well round bottom microtiter plates with concentrations of 600 or 6,000 potential T cells per ml and 50 µl per well. PBMCs for antigen presentation derived from inbred strain 2 or outbred Dunkin-Hartley guinea pigs.

For generation of oligo- or monoclonal T cell lines, cells were seeded either in 96-well round bottom microtiter plates (Thermo Fisher Scientific) with concentrations of 0.2 / 5 / 50 potential T cells per ml and 100 µl per well, or in 384-well microtiter plates (Thermo Fisher Scientific) with 10 / 50 / 250 potential T cells per ml and 20 µl per well. Inbred strain 2 guinea pigs were used for generation of irradiated, syngenic PBMCs for antigen presentation.

Cells were incubated at 37 °C with 5 % CO_2.

3.10.4 Maintenance, transfer and stimulation of T cell lines

T cell lines were inspected using a light microscope on a regular basis, often daily. If required, new SF-IMDM, serum and/or cell culture supernatant containing recombinant gpIL-2 were added. If cells grew out they were split or transferred to larger plates (96-well microtiter plates, 24-well microtiter plates). If proliferation stagnated, cell lines were stimulated with 0.05 µg/ml (w/v) PHA and irradiated PBMCs (see section 3.7.4) of outbred Dunkin-Hartley guinea pigs in a 1:1 ratio.

3.10.5 Specificity assays for guinea pig T cell lines

For determination of antigen specificity, T cell lines were subjected to specificity assays and subsequent microscopic and flowcytometric analysis. The supernatant was further tested by TNFα ELISA (see section 3.9). In these specificity assays, irradiated PBMCs (see section 3.7.4) of inbred strain 2 guinea pigs were used for syngenic presentation of antigens. T cells and irradiated, syngenic PBMCs were mixed in the same ratio and the cells were stimulated with the antigens and incubated as described for the *ex vivo* lymphocyte proliferation assay (see section 3.8.1). TNFα ELISA was performed as described above (see section 3.9).

In flowcytometric analysis, the count of living and blasting lymphocytes was determined if CFSE labeling had not been possible due to low cell numbers (see section 3.8.4).

3.10.6 Freezing of guinea pig T cell lines

Cells were frozen at each step in 90 % FCS + 10 % DMSO in cold cryo vials at –80 °C (see section 3.7.3). If required, cells were thawed and stimulated as described above.

3.11 Statistics

The statistical analyses were conducted with Microsoft Office Excel 2010 and Graph Pad Prism (version 5.04 and 6.0).

Each antigen was tested in duplicate per animal, if not stated otherwise. The arithmetic mean was calculated for each duplicate and used for further analyses.

The significance of difference between two groups was calculated using the two-tailed parametric student's *t* test. To calculate the significance of difference of one group to a defined value, one-sample *t* test was employed. Significances of differences between lymphocyte counts were calculated by ratio *t* test. The potential statistical values are depicted in **Table 3.3**.

Correlations were calculated using two-tailed Spearman correlation coefficients, assuming a non-Gaussian distribution of the values.

Table 3.3 Statistical values.

p value	Symbol	Explanation
$p > 0.05$	ns	not significant
$0.01 < p \leq 0.05$	*	slightly significant
$0.001 < p \leq 0.01$	**	moderately significant
$0.0001 < p \leq 0.001$	***	strongly significant
$p \leq 0.0001$	****	highly significant

4 Results

4.1 *Ex vivo* lymphocyte proliferative responses to tuberculins and CMEs

Bastian *et al.* (2008) and Seshadri *et al.* (2013) described a strong CD4-positive T cell response of TB-infected humans that was directed against mycobacterial lipopeptide-containing antigen preparations. The initial objective of the present study was therefore to investigate whether these results were reproducible with BCG-sensitized guinea pigs. Guinea pigs which were sensitized with inactivated wet mass of the virulent *M. bovis* strain AN5 were used for control purposes. Prior to and 30 days after sensitization (or as indicated), blood samples were obtained from the guinea pigs and PBMCs were purified by Ficoll gradient centrifugation. The PBMCs were labeled with CFSE and stimulated with different antigens in the *ex vivo* lymphocyte proliferation assay.

4.1.1 Lymphocyte proliferation in response to tuberculins

In the present study, Koch's Old Tuberculin standard Tub12 was used as the specific positive control. The stimulatory potential of Tub12 was analyzed in the *ex vivo* lymphocyte proliferation assay prior to and after sensitization of the guinea pigs, as well as in direct comparison with different PPDs.

To investigate whether lymphocytes of the sensitized guinea pigs proliferated in response to Koch's Old Tuberculin Tub12, CFSE-labeled lymphocytes of naïve guinea pigs and of the same guinea pigs 30 days after iAN5 or BCG sensitization were incubated with 30 IU/ml Tub12 in the *ex vivo* lymphocyte proliferation assay (CFSE assay). After 5 days of incubation, proliferation of lymphocytes was determined as the loss of CFSE fluorescence in flowcytometric analysis.

Figure 4.1 shows the proliferation results of 9 iAN5-sensitized guinea pigs and of 10 representative BCG-sensitized animals in response to Tub12 at day 0 and day 30 after sensitization. The experiment was performed with these 9 iAN5-sensitized animals and with a total of 29 BCG-sensitized guinea pigs.

Before sensitization (d0), no lymphocyte proliferation in response to Tub12 stimulation was observed in all assays (**Figure 4.1**). The percentages of $CFSE_{low}$ lymphocytes, i.e., cells that proliferated in response to the antigenic stimulus, were less than 20 % of the total lymphocyte population. The median value of the percentages of $CFSE_{low}$ lymphocytes from

all animals before sensitization (n = 38), but upon *ex vivo* Tub12-stimulation, was 1.9 % (range 0 to 12.2 %).

Thirty days after iAN5 or BCG sensitization (d30), *ex vivo* lymphocytes proliferated strongly in response to Tub12 as also depicted in **Figure 4.1**. The median value of the percentages of $CFSE_{low}$ lymphocytes of the iAN5-sensitized guinea pigs (n = 9) was 28.6 % (range 16.6 to 82.2 %) and of the BCG-sensitized guinea pigs (n = 29) 47.1 % (range 14.6 to 86.4 %). The median increase in $CFSE_{low}$ lymphocytes in response to Tub12 stimulation from d0 to d30 (d30/d0) was 18.5 (range 7.2 to 279,1) in the iAN5-sensitized animals and 23.3 (range 1.2 to 332.5) in the 29 BCG-sensitized guinea pigs. In 8 of 9 assays with PBMCs of iAN5-sensitized guinea pigs and in 26 of 29 assays with PBMCs of BCG-sensitized animals, the proliferating lymphocytes corresponded to more than 20 % of the total lymphocyte population. The PBMCs with less than 20 % $CFSE_{low}$ lymphocytes in the Tub12 positive control additionally showed only minor proliferative responses (< 20 %) to the other, strong antigen preparations CME_{BCG} and CME_{H37Rv} (data not shown). This finding supported the definition of the 20 % cut-off for the Tub12 positive control which was subsequently applied in the analyses of the *ex vivo* lymphocyte proliferation assay (see section 4.1.2), unless otherwise stated.

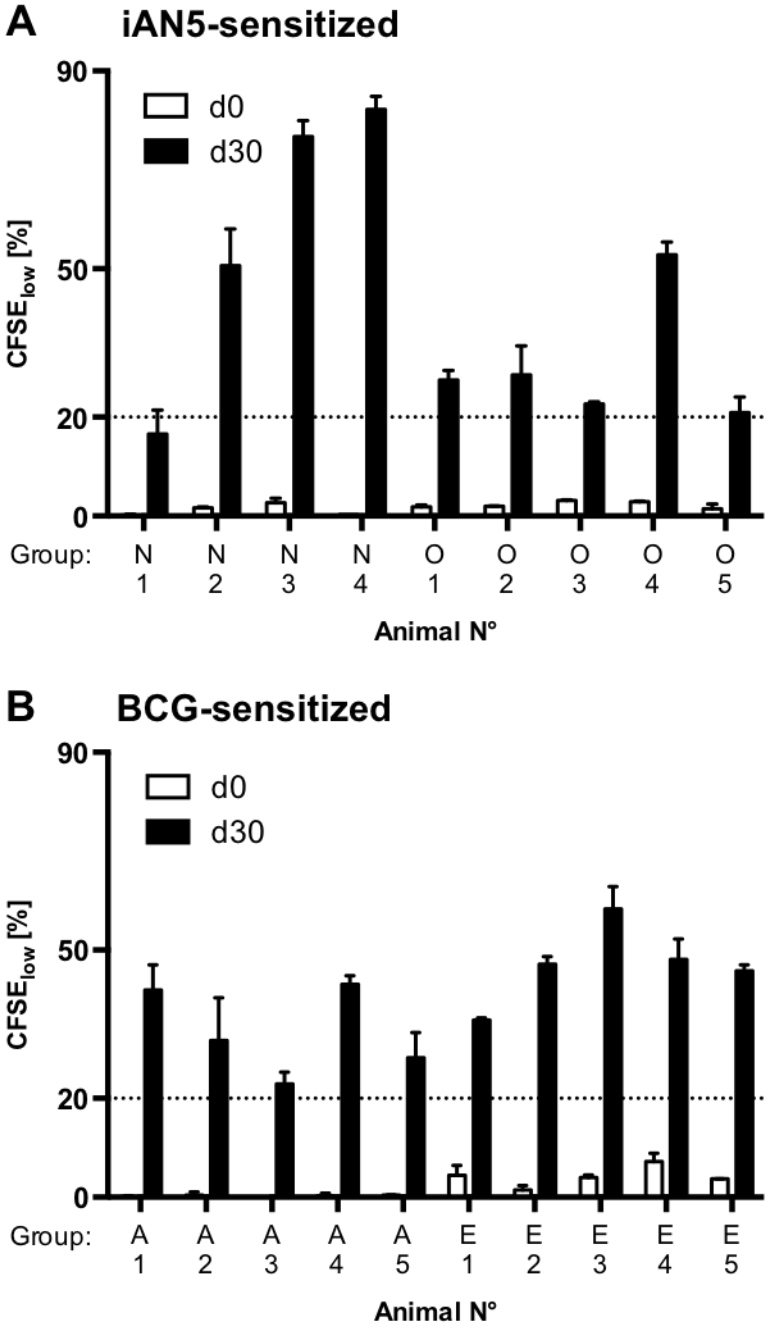

Figure 4.1 iAN5 as well as BCG sensitization induces *ex vivo* lymphocyte proliferation to Tub12 in previously naïve guinea pigs.

PBMCs were isolated, labeled with CFSE and incubated with 30 IU/ml Tub12 for 5 days. Proliferation was determined by flowcytometric analysis as the loss of CFSE fluorescence. The bars indicate the arithmetic mean percentages of $CFSE_{low}$ lymphocytes in the Tub12-stimulated duplicate per animal after 5 days of incubation. The PBMCs represented by the white bars were obtained at day 0 before sensitization. Black bars show PBMCs that were obtained at day 30 after sensitization. Error bars indicate the standard deviation. **A.** *Ex vivo* Tub12 reactivity of PBMCs obtained from 9 individual guinea pigs at day 0 and day 30 after iAN5 sensitization. **B.** *Ex vivo* Tub12 reactivity of PBMCs obtained from 10 individual guinea pigs at day 0 and day 30 after BCG sensitization.

Tub12 is a Koch's Old Tuberculin standard. Today, purified protein derivatives of tuberculin (PPDs) are usually used for tuberculosis diagnosis. However, based on its preparation procedure (European Directorate for the Quality of Medicine and Health Care 2013) the Old Tuberculin must contain a wider range of antigens than PPD, in particular lipid antigens.

To investigate the antigenic and stimulatory capacities of Old Tuberculin in comparison with PPDs, Tub12 was analyzed in parallel with different WHO PPD standards as well as commercially available veterinary PPDs. To this end, the proteins in the different tuberculins were separated by SDS-PAGE and visualized by Coomassie or silver staining. Furthermore, the tuberculins were analyzed by Western blotting using pooled sera of 10 BCG-sensitized guinea pigs. The lipid content was analyzed by thin layer chromatography with chloroform-methanol-water (65:25:4) as the mobile phase. The results are shown in **Figure 4.2**.

All tuberculins, except WHO_{hum}, demonstrated a high protein content (**Figure 4.2A** and **B**) and all tuberculins contained antibody-recognized antigens (**Figure 4.2C**). A similar pattern was observed in Western blot analysis of mannosylated lipoarabinomannan (ManLAM, compare **Figure 4.23**). It is remarkable that the WHO standard PPD for human tuberculosis (WHO_{hum}) had the lowest protein content but showed the most prominent signal in the Western blot analysis. As expected, the lipid content of the Koch's Old Tuberculin Tub12 was significantly higher than the lipid content of the PPDs. Some lipid content was also detectable in three commercially available *M. bovis* PPDs (*M. bovis* PPDs "1", "2", and "3" in **Figure 4.2D**). A chloroform-methanol extract of BCG and a BCG lysate were included for comparison.

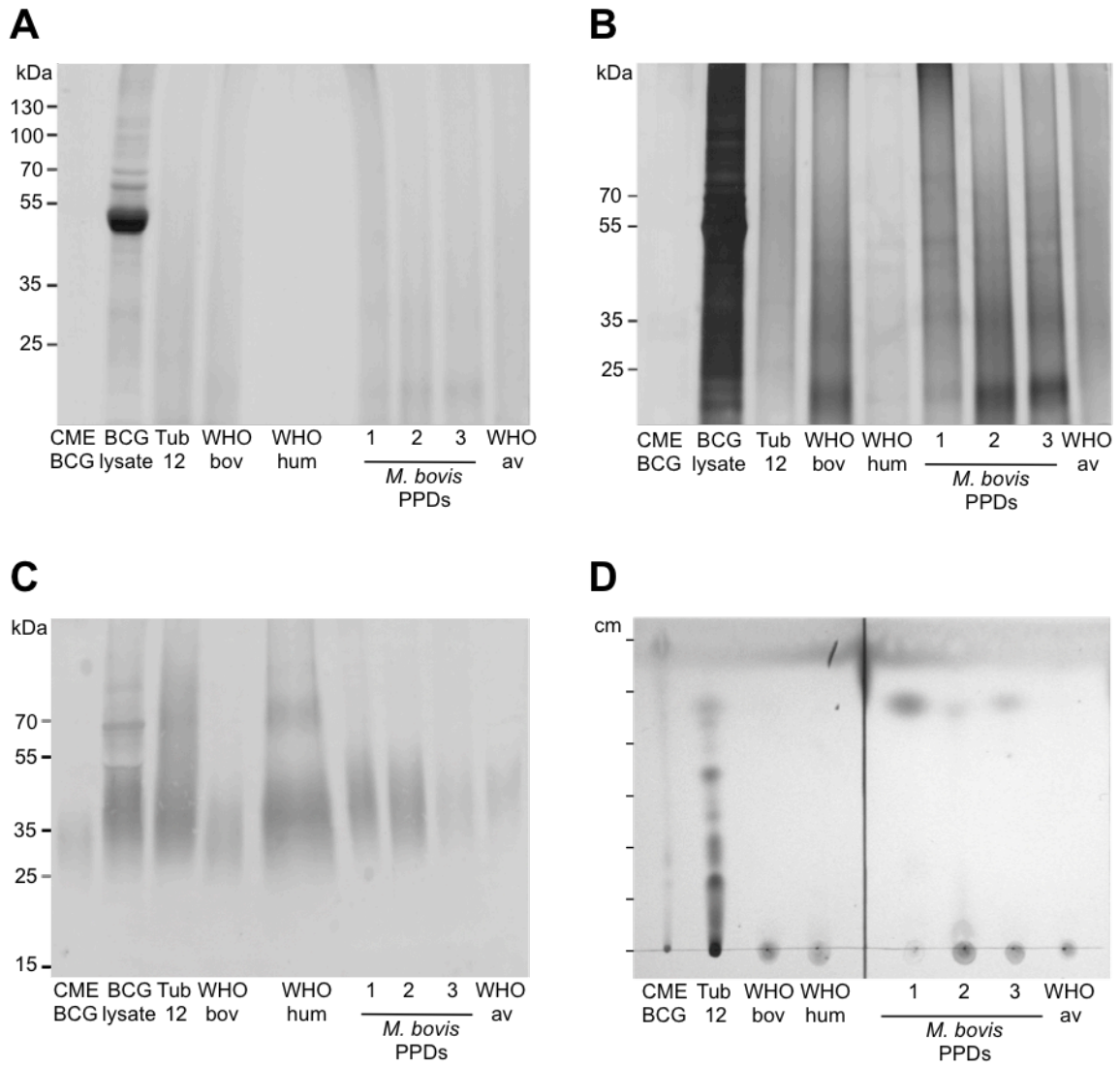

Figure 4.2 Characteristics of different tuberculins determined by Coomassie staining, silver staining, Western blot analysis and thin layer chromatography.

A. Visualization of proteins in different tuberculins and control samples by SDS-PAGE and Coomassie staining. Quantities used per slot: CME_{BCG} 80 µg; BCG lysate 50 µg; tuberculins 240 IU. **B.** Visualization of proteins in different tuberculins and control samples by SDS-PAGE and silver staining. Quantities used per slot: CME_{BCG} 10 µg; BCG lysate 25 µg; tuberculins 30 IU. **C.** Visualization of antigens in different tuberculins, which are recognized by antibodies in pooled sera of 10 BCG-sensitized guinea pigs. Quantities used per slot: CME_{BCG} 80 µg; BCG lysate 50 µg; tuberculins 240 IU. **D.** Visualization of lipids by thin layer chromatography with chloroform-methanol-water (65:25:4) as the mobile phase. Quantities used per slot: CME_{BCG} 83.3 µg; tuberculins 250 IU.
According to the stimulatory capacities in the guinea pig *ex vivo* lymphocyte proliferation assay, the quantities of CME_{BCG} and tuberculins matched in all cases (10 µg/ml CME_{BCG} corresponded to 30 IU/ml tuberculin).

All tuberculins were tested simultaneously in the *ex vivo* lymphocyte proliferation assay to determine their capacities to induce proliferation of lymphocytes from 13 iAN5- and 16 BCG-sensitized guinea pigs (**Figure 4.3**). In this analysis of all tuberculins in direct comparison, no validity criteria (see above and section 3.8.4) were applied on the Tub12 positive control to avoid any falsification of the results.

The proliferation results of the PBMCs from the outbred Dunkin-Hartley guinea pigs showed a large variance. However, as evident from **Figure 4.3**, the lymphocytes of one animal usually proliferated in a similar range within the stimulatory capacities of the antigen preparations, i.e., the lymphocytes of some animals showed proliferation in the upper ranges in response to all stimulatory antigen preparations, whereas the lymphocytes of other animals showed proliferation in the lower ranges. On average, the lymphocyte proliferation of iAN5-sensitized guinea pigs was stronger, but showed a larger variance than the lymphocyte proliferation of BCG-sensitized animals. However, the differences were only significant in samples stimulated with WHO_{bov} and the commercially available *M. bovis* PPD from the manufacturer "3" ($p \leq 0.01$, student's *t* test). WHO_{hum} and WHO_{av} have not been tested with the PBMCs of iAN5-sensitized guinea pigs.

A strong stimulatory potential was observed in Tub12 and all *M. tuberculosis* and *M. bovis* PPD preparations (medians significantly higher than 20 % $CFSE_{low}$ lymphocytes, $p \leq 0.01$, one-sample *t* test, see asterisks in **Figure 4.3**). On average, the WHO standard tuberculin of *M. avium* complex (MAC) (WHO_{av}) induced low proliferation of the lymphocytes from BCG-sensitized guinea pigs (median 20.9 %, range 12.3 to 42.6 %), but the median value did not significantly exceed the 20 % cut-off ($p > 0.05$, one-sample *t* test).

The strong stimulatory capacity of Tub12 (**Figure 4.1**) which is similar to *M. tuberculosis* and *M. bovis* PPDs (**Figure 4.3**) and the wider range of antigens available in Tub12 compared with PPDs (especially lipid antigens) (**Figure 4.2**) supported the selection of this antigen preparation as the specific positive control in the sense of a standardized whole antigen preparation throughout this study.

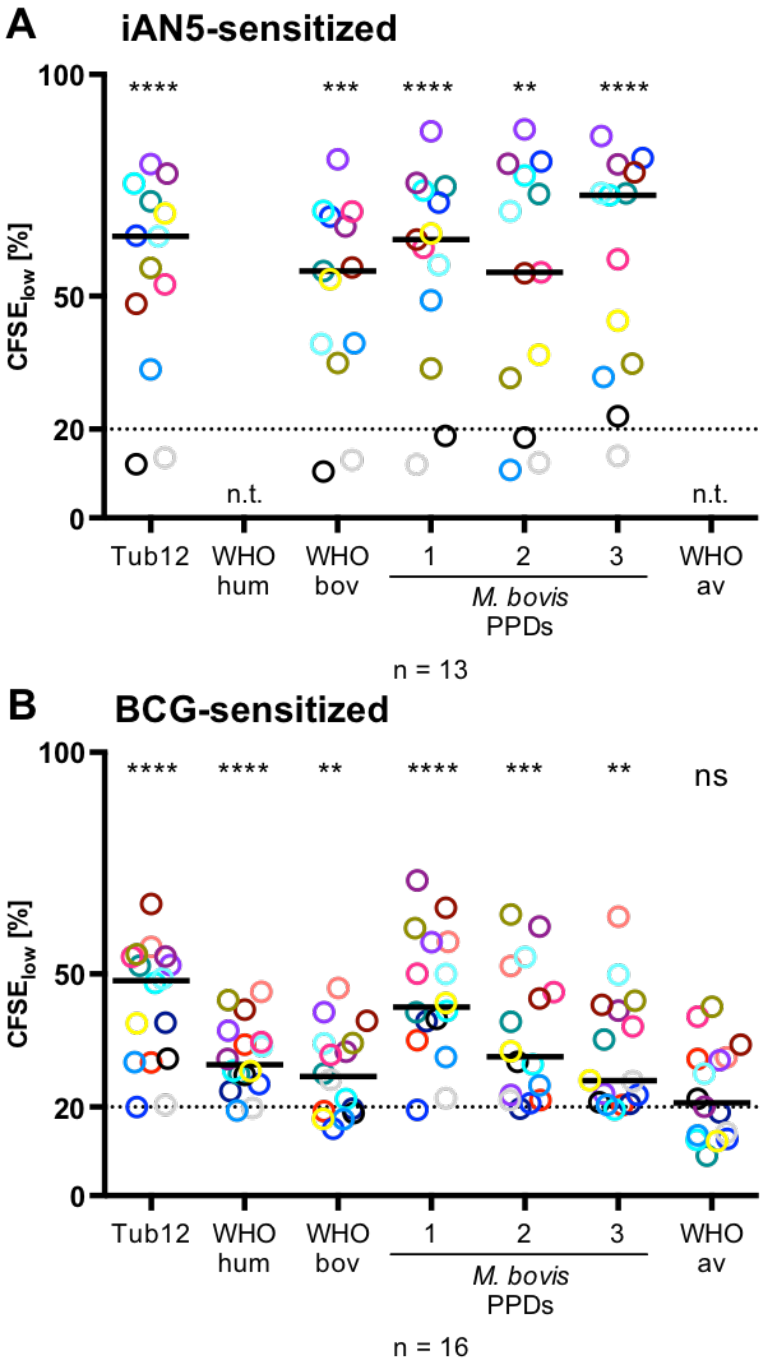

Figure 4.3 Different tuberculins induce strong lymphocyte proliferation in the PBMCs of sensitized guinea pigs.

Results of the *ex vivo* lymphocyte proliferation assay. PBMCs had been incubated with 30 IU/ml of different tuberculins for 5 days. The y-axis indicates the percentage of $CFSE_{low}$ lymphocytes compared with the total lymphocyte population after 5 days of incubation. Circles represent the arithmetic means of the duplicate tested per antigen, per animal. Each color represents the lymphocyte proliferation of one guinea pig. Black bars indicate the median values over all animals, per antigen. One sample t-test was used to calculate whether the results per group per antigen significantly exceeded the 20 % cut-off. No validity criteria were applied on the Tub12 positive control to avoid falsification of the results. n.t.: not tested. **A.** Lymphocyte proliferation of the PBMCs from 13 individual guinea pigs at day 60 after iAN5 sensitization. **B.** Lymphocyte proliferation of the PBMCs from 16 individual guinea pigs at day 30 after BCG sensitization.

4.1.2 Lymphocyte proliferation in response to chloroform-methanol extracts

In order to investigate the effect of BCG sensitization on the induction of lipid-reactive lymphocytes, PBMCs were isolated from guinea pigs before and 30 days after sensitization with BCG or with heat-inactivated, virulent *M. bovis* AN5 (iAN5). After CFSE labeling, the PBMCs were incubated with CME of the *M. bovis* vaccine strain BCG (CME_{BCG}) for 5 days. Loss of CFSE fluorescence as an indicator for proliferation was subsequently analyzed (*ex vivo* lymphocyte proliferation assay).

Figure 4.4 displays the lymphocyte proliferation in response to CME_{BCG} at day 0 and day 30 after sensitization of those animals whose lymphocyte responses to the Tub12 positive control have already been outlined in **Figure 4.1**. When analyzing the lymphocyte proliferation in response to CME_{BCG}, the iAN5-sensitized animal "N–1" (**Figure 4.1**) as well as 3 of the 29 described BCG-sensitized guinea pigs (see text in section 4.1.1) had to be excluded due to the general validity criterion of the assay which has been defined in section 4.1.1 (≥ 20 % $CFSE_{low}$ lymphocytes in Tub12 positive control).

Figure 4.4 shows the lymphocyte proliferation results of the 8 iAN5-sensitized guinea pigs and of 10 BCG-sensitized animals which were considered representatives of all 26 BCG-sensitized guinea pigs included in this analysis. Prior to sensitization, the median value of the lymphocyte proliferation of all animals (n = 34) in response to CME_{BCG} was 3.2 % (range 0.2 to 8.6 %). At day 30 after sensitization, the median value of the lymphocyte proliferation of the 8 iAN5-sensitized animals was 30.8 % (range 7.9 to 82.3 %) and 35.2 % (range 10.8 to 88.3 %) for the 26 BCG-sensitized animals. In PBMCs from 4 of 8 iAN5-sensitized animals and in PBMCs from 24 of 26 BCG-sensitized guinea pigs, the $CFSE_{low}$ population upon CME_{BCG} stimulation represented more than 20 % of the whole lymphocyte population in the assay. The median increase in $CFSE_{low}$ lymphocytes in response to CME_{BCG} stimulation from d0 to d30 (d30/d0) was 10.2 (range 2.2 to 70.3) in the 8 iAN5-sensitized animals and 16.9 (range 3.7 to 332.9) in the 26 BCG-sensitized guinea pigs.

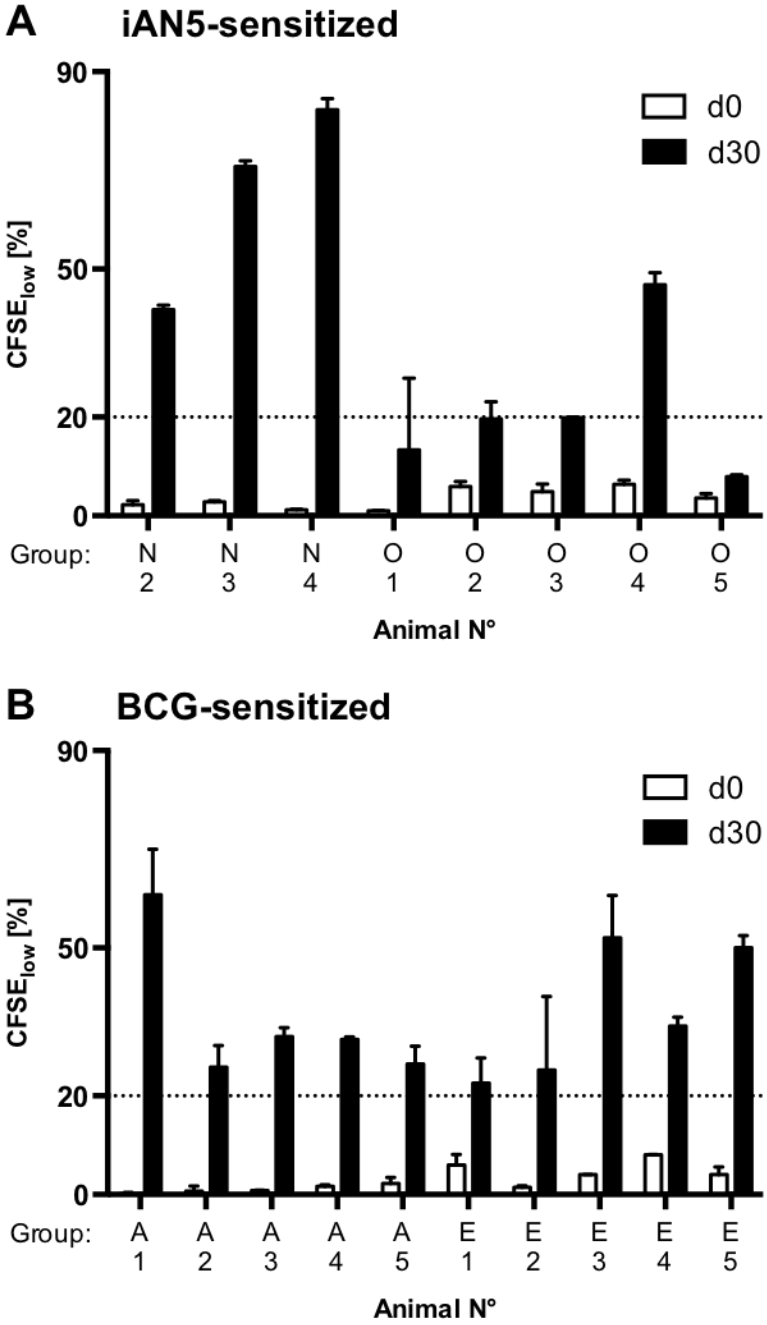

Figure 4.4 iAN5 as well as BCG sensitization induces *ex vivo* lymphocyte proliferation to CME_{BCG} in previously naïve guinea pigs.

Results of the *ex vivo* lymphocyte proliferation assay. PBMCs had been incubated with 10 µg/ml CME_{BCG} for 5 days. The bars indicate the arithmetic mean percentages of $CFSE_{low}$ lymphocytes in the CME_{BCG}-stimulated duplicate per animal after 5 days of incubation. The PBMCs represented by the white bars were obtained at day 0 before sensitization. Black bars show PBMCs that were obtained at day 30 after sensitization. Error bars indicate the standard deviation. **A.** CME_{BCG} reactivity of PBMCs obtained from 8 individual guinea pigs at day 0 and day 30 after iAN5 sensitization. **B.** CME_{BCG} reactivity of PBMCs obtained from 10 individual guinea pigs at day 0 and day 30 after BCG sensitization.

Next, it was tested whether not only CME_{BCG}, but also a lipid extract of the virulent laboratory *M. tuberculosis* strain H37Rv was able to stimulate a proliferative response in PBMCs from sensitized guinea pigs.

Figure 4.5 shows the proliferation results of the PBMCs from 35 iAN5-sensitized guinea pigs and from 45 BCG-sensitized guinea pigs in response to CME_{BCG} and CME_{H37Rv}. According to the validity criteria of the *ex vivo* lymphocyte proliferation assay (see section 3.8.4 and 4.1.1), assays from 5 iAN5-sensitized guinea pigs and from 9 BCG-sensitized animals were excluded because the lymphocyte proliferation in response to the Tub12 positive control accounted for less than 20 % $CFSE_{low}$ cells. No assays had to be excluded due to the validity criterion for the medium control (≤ 20 % $CFSE_{low}$ lymphocytes, see section 3.8.4).

The median value of the lymphocyte proliferation in response to CME_{BCG} was 46.9 % (range 4.8 to 88.6%) in the PBMCs from iAN5-sensitized guinea pigs and 43.9 % (range 10.8 to 88.3 %) in those from BCG-sensitized animals. The median value in response to CME_{H37Rv} was 39.6 % (range 3.8 to 73.1 %) and 26.8 % (range 10.8 to 87.3 %) for iAN5-sensitized and BCG-sensitized guinea pigs, respectively. In the iAN5-sensitized group as well as in the BCG-sensitized group, CME_{BCG}-stimulated PBMCs from 4 guinea pigs did not exceed the 20 % threshold. Similarly, the CME_{H37Rv}-stimulated lymphocyte proliferation in 8 animals of the iAN5 group and in 7 animals of the BCG group remained below 20 %. However, the overall lymphocyte proliferation in response to both CMEs differed significantly in all groups from the lymphocyte proliferation in the medium-only control ($p \leq 0.0001$; student's *t* test, **Figure 4.5**). Likewise, the overall lymphocyte proliferation in response to CME_{BCG} and CME_{H37Rv} significantly exceeded the 20 % threshold ($p \leq 0.0001$; one-sample *t* test). The lymphocyte proliferation in response to CME_{BCG} and CME_{H37Rv} did not differ significantly between the two groups (iAN5- and BCG-sensitized guinea pigs) ($p > 0.05$, student's *t* test). Remarkably, the lymphocytes of BCG-sensitized guinea pigs proliferated stronger in response to CME_{BCG} compared with CME_{H37Rv} ($p \leq 0.0001$, student's *t* test).

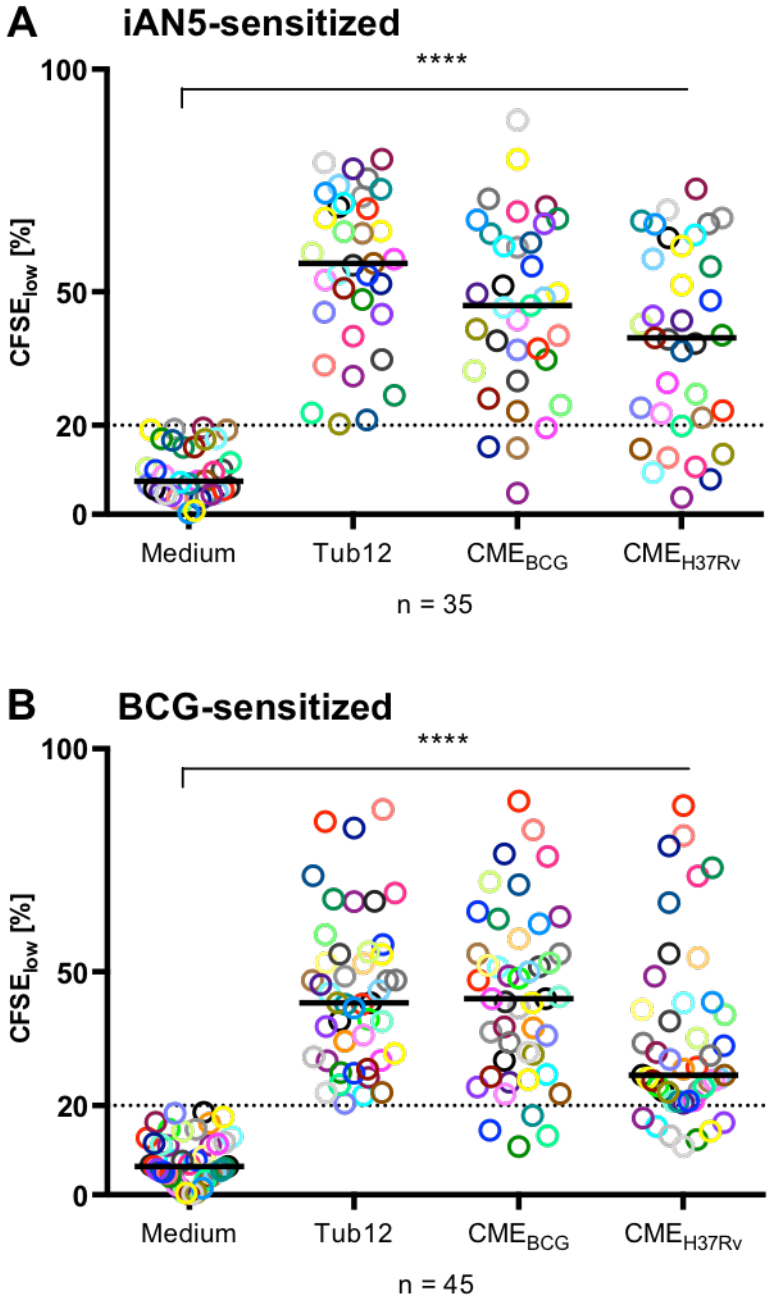

Figure 4.5 CME$_{BCG}$ and CME$_{H37Rv}$ induce strong lymphocyte proliferation in iAN5- and BCG-sensitized guinea pigs *ex vivo*.

Results of the *ex vivo* lymphocyte proliferation assay. PBMCs had been incubated with medium only or different antigens (Tub12 30 IU/ml; CMEs 10 µg/ml) for 5 days. The y-axis represents the percentage of CFSE$_{low}$ lymphocytes compared with the total lymphocyte population. Circles represent the arithmetic means of the duplicate tested per antigen, per animal. The black bars represent the median values over all animals, per antigen. **A.** Results of the PBMCs obtained from 35 individual guinea pigs at day 60 after iAN5 sensitization. **B.** Results of the PBMCs obtained from 45 individual guinea pigs at day 30 after BCG sensitization.

In the course of the adaption of the guinea pig *ex vivo* lymphocyte proliferation assay for CME antigen preparations, which was part of the present project, one aim was to assess whether 10 µg/ml CME constituted the optimal antigen concentration for stimulation of lymphocyte proliferation. To this end, the lymphocyte proliferation of the PBMCs from 5 and 8 BCG-sensitized guinea pigs was analyzed in response to serial dilutions of CME.

Figure 4.6 displays the dose-effect of CME antigens on the lymphocyte stimulation in a lower range (0.1, 1, 10 µg/ml) as well as in an upper range (10, 30, 50, 70, 90 µg/ml) of antigen concentrations. The median value of the lymphocyte proliferation in response to 10 µg/ml CME_{BCG} was 34.1 % (range 22.6 to 52.0 %) in the lower and 65.7 % (range 10.8 to 88.3 %) in the upper range analysis. Similarly, the median value of the lymphocyte proliferation in response to 10 µg/ml CME_{H37Rv} was 26.2 % (range 20.5 to 40.4 %) in the lower and 69.4 % (range 12.4 to 87.3 %) in the upper range analysis. For both CME_{BCG} and CME_{H37Rv}, lymphocyte proliferation in response to the antigen concentration of 10 µg/ml was significantly higher than that in response to the next tested lower (1 µg/ml) and higher (30 µg/ml) antigen concentration and it was also significantly higher than the lymphocyte proliferative response to all other tested antigen concentrations below and above ($p \leq 0.05$, student's *t* test).

In order to further investigate the conditions for the *ex vivo* lymphocyte proliferation assay, the proliferation capacities of the guinea pig PBMCs were tested at several time points after vaccination. The validity criterion for this experiment was only that the proliferation of the lymphocytes needed to be ≤ 20 % in the medium-only control, in order to detect any loss of Tub12-reactivity over time.

Figure 4.7 demonstrates the timelines elaborated for Tub12 and CME_{BCG} stimulation in both groups of guinea pigs. After iAN5 sensitization of 5 guinea pigs, the median value of the lymphocyte proliferation in response to Tub12 as well as in response to CME_{BCG} increased until day 90 (day 0 – Tub12: median 2.0 %, range 1.5 to 3.1 %; CME_{BCG}: median 4.9 %, range 1.0 to 6.4 %; day 90 – Tub12: median 53.4 %, range 29.7 to 82.2 %, CME_{BCG} 45.7 %, range 7.7 to 61.8 %). After day 90, it decreased continuously to values of around 20 % at day 150.

The peak of the lymphocyte proliferation after BCG sensitization of 11 guinea pigs was clearly at day 30 (Tub12: median 45.8 %; range 15.4 to 86.4 %; CME_{BCG}: median 25.2 % range 6.2 to 88.3 %). The median value of the lymphocyte proliferation decreased thereafter to values between 14 and 28 %, subsequently increased at day 120 and decreased again at day 150 (day 120 – Tub12: median 43.5 %, range 20.8 to 74.0 %; CME_{BCG} 28.7 %, range 12.0 to 68.6 %;).

In the iAN5-sensitized group, the lymphocyte proliferation at day 90 did not differ significantly from the lymphocyte proliferation at day 60 ($p > 0.05$, student's *t* test). The differences between day 90 and day 120 were only significant in the Tub12-stimulated samples ($p \leq 0.05$). The lymphocyte proliferation at day 30 and day 60 in the BCG-sensitized group did not differ significantly ($p > 0.05$).

Earlier time points have also been tested in our laboratory and indicated day 30 as the earliest possible time point to obtain reliable results (Spohr 2015).

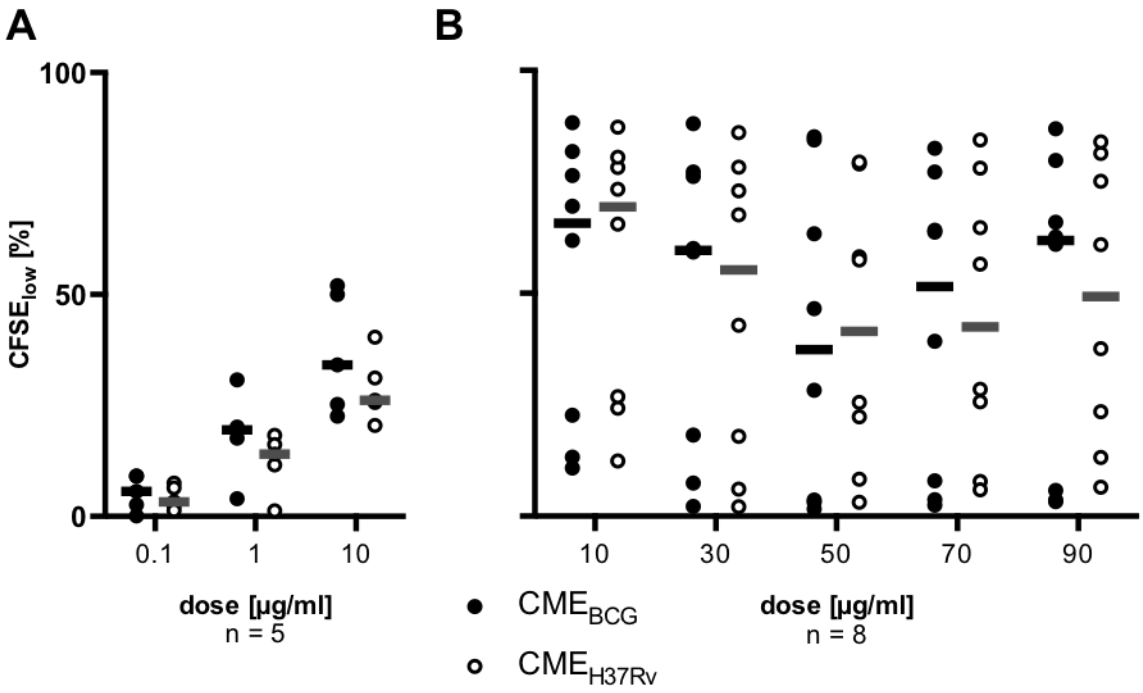

Figure 4.6 Lymphocyte proliferation in response to CMEs is dose-dependent.

Results of the *ex vivo* lymphocyte proliferation assay. Different doses of antigen were tested for their capacity to induce *ex vivo* proliferation in CFSE-labeled PBMCs over 5 days of incubation. Dots show the arithmetic means of the duplicate tested per indicated antigen per animal. Bars represent the medians over all animals, per antigen, per dose. **A.** Different doses of CMEs in the lower range (0.1, 1, 10 µg/ml) were tested with the PBMCs of 5 guinea pigs 30 days after BCG sensitization. **B.** Different high range doses (10, 30, 50, 70, 90 µg/ml) of CMEs were tested with the lymphocytes of 8 individual guinea pigs 30 days after BCG sensitization.

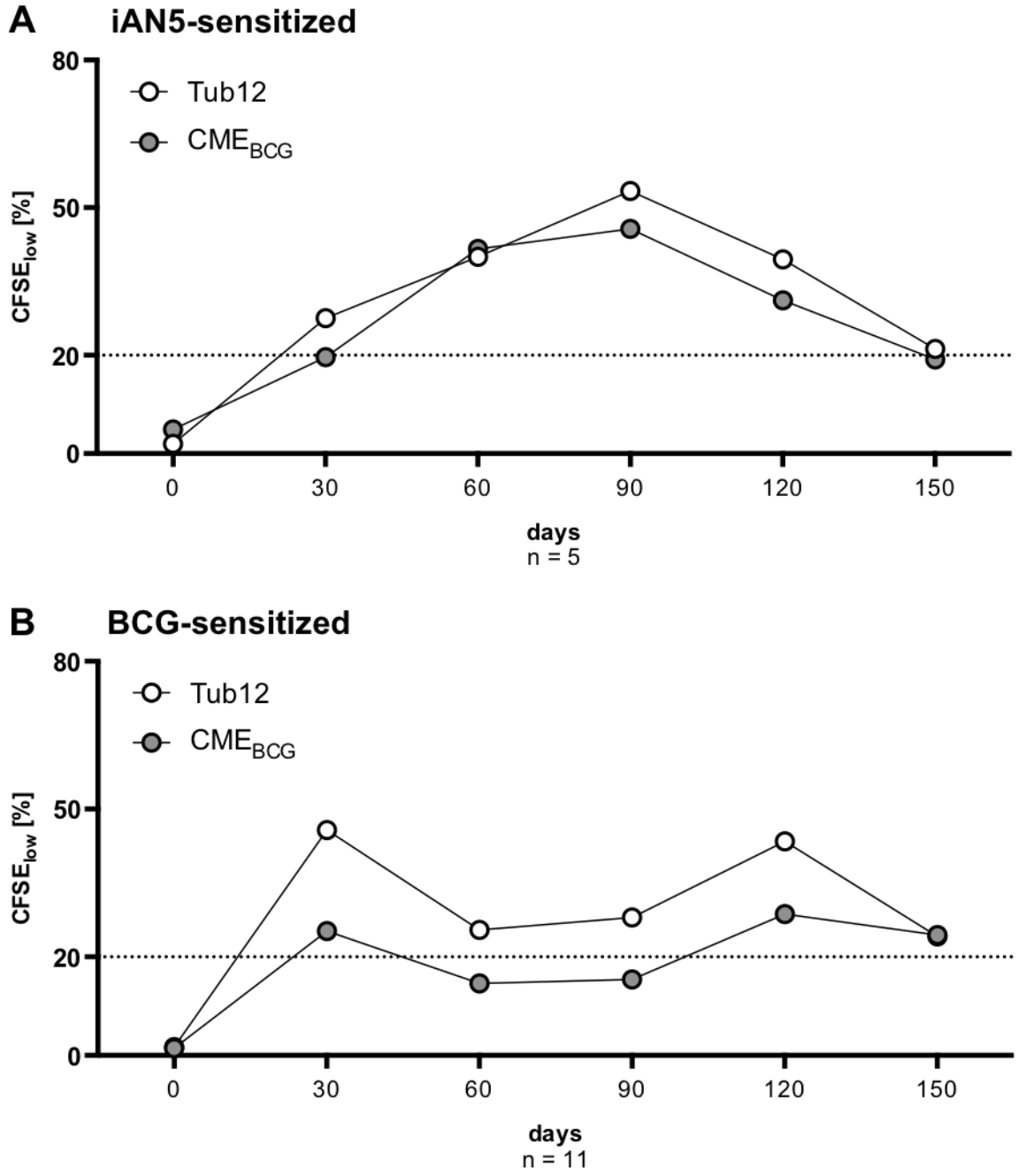

Figure 4.7 ***Ex vivo*** **lymphocyte proliferation varies over time depending on the type of sensitization.**

Results of the *ex vivo* lymphocyte proliferation assay. PBMCs were harvested at the indicated time points, labeled with CFSE and incubated with the described antigens (Tub12 30 IU/ml; CME_{BCG} 10 µg/ml) for 5 days. Dots represent the median values of the lymphocyte proliferation over all animals per antigen, per time point. Timeline of the *ex vivo* lymphocyte proliferative response using PBMCs from **A.** 5 iAN5-sensitized guinea pigs and **B.** 11 BCG-sensitized guinea pigs.

To investigate whether the strong lymphocyte proliferation observed after CME stimulation was related to innate immune activation, CFSE-labeled PBMCs were stimulated with lysates of the gram-negative bacteria *E. coli* and *S.* Typhi which contain large amounts of TLR-agonistic lipopolysaccharides (LPS).

Figure 4.8 displays the proliferation results of PBMCs from 21 BCG-sensitized guinea pigs. The median value of the lymphocyte proliferation in response to CME_{BCG} was 49.1 % (range 27.0 to 75.8 %), in response to *S.* Typhi lysate 17.0 % (range 2.6 to 30.6 %), and in response to *E. coli* lysate 21.6 % (range 5.5 to 50.1 %). Thus, on average, the proliferative responses to both bacterial lysates did not significantly exceed 20 % $CFSE_{low}$ lymphocytes ($p > 0.05$, one-sample *t* test). Furthermore, the percentages of $CFSE_{low}$ lymphocytes were significantly lower in response to the gram-negative bacterial lysates than in response to Tub12 and CME_{BCG} ($p \leq 0.0001$, student's *t* test). The lymphocyte proliferation in response to CME_{BCG} did not correlate with the stimulation by the bacterial lysates (Spearman correlation: $r = -0.1844$ for CME_{BCG} versus *S.* Typhi lysate and $r = -0.02727$ for CME_{BCG} versus *E. coli* lysate).

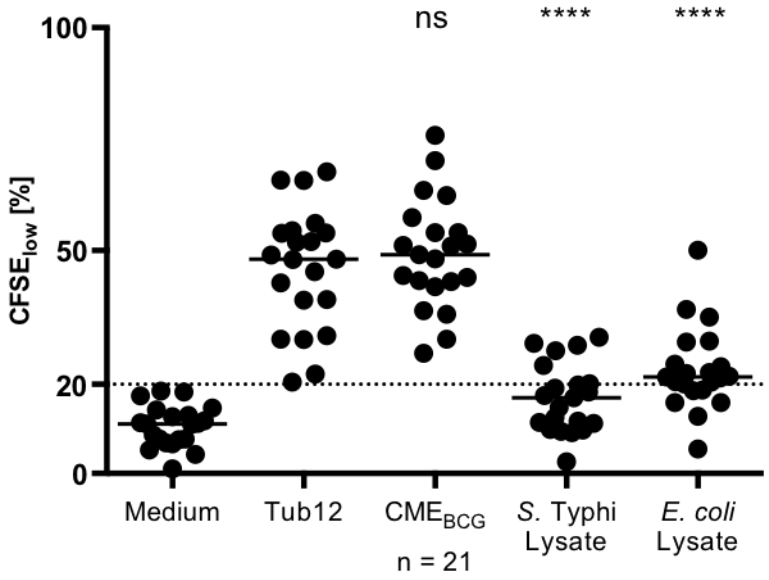

Figure 4.8 LPS stimulation does not induce strong lymphocyte proliferation.

Results of the *ex vivo* lymphocyte proliferation assay. CFSE-labeled PBMCs of 21 guinea pigs at day 30 after BCG sensitization had been incubated with different antigens for 5 days: Tub12 30 IU/ml; CME_{BCG} 10 µg/ml; *Salmonella* Typhi and *E. coli* lysates 1 µg/ml. Black dots represent the arithmetic means of the duplicate tested per antigen, per animal. Black bars represent the medians over all animals, per antigen. Asterisks indicate the significances of difference of the lymphocyte proliferation in response to the respective antigen compared with the Tub12-stimulated samples.

Several protein antigens of mycobacteria are well-known for their immunogenicity (see section 2.3.2). One of those potent proteins is AG85A. It is not deleted in BCG and it is one of the major secreted antigens (Nagai *et al.* 1991). For these reasons, vaccination with BCG should induce an immune response directed towards AG85A. To investigate this assumption, purified recombinant AG85A (Lionex) was tested in the *ex vivo* lymphocyte proliferation assay at the same concentration as the CME preparations (10 µg/ml).

The proliferation results of the PBMCs from 26 BCG-sensitized guinea pigs are depicted in **Figure 4.9**. The median value of the lymphocyte proliferation in response to AG85A was 11.4 % (range 2.4 to 24.6 %). As calculated by one-sample *t* test, the average lymphocyte proliferation in response to AG85A was significantly below the 20 % cut-off ($p \leq 0.0001$). Hence, it was also significantly lower than the lymphocyte proliferation in response to Tub12 and CMEs ($p \leq 0.0001$, student's *t* test). However, the lymphocyte proliferation after stimulation with AG85A was still significantly higher ($p \leq 0.05$, student's *t* test) than the lymphocyte response in the medium-only control (median 9.8 %, range 1.0 to 18.5 %).

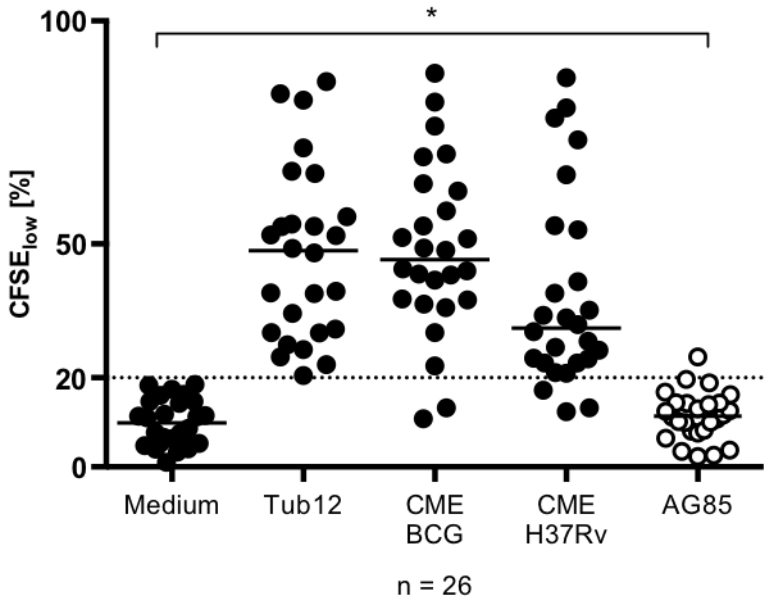

Figure 4.9 The defined strong antigen AG85A of *M. tuberculosis* induces significantly lower lymphocyte proliferation than Tub12 and CMEs.

Results of the *ex vivo* lymphocyte proliferation assay. PBMCs from guinea pigs 30 days after BCG sensitization had been labeled with CFSE and incubated with 30 IU/ml Tub12 or 10 µg/ml CME or 10 µg/ml recombinant AG85A for 5 days. Dots represent the arithmetic means of the duplicate tested per antigen, per animal. Black lines indicate the median values over all animals, per antigen. The asterisk marks the significance of difference between the proliferation in the medium-only control and in the AG85A-stimulated sample.

4.1.3 Phenotypical characterization of responding lymphocytes

In order to further assess the comparability of the results generated with guinea pig PBMCs with those obtained from human PBMCs, the phenotypes of the guinea pig lymphocytes were characterized after their stimulation with mycobacterial antigen preparations.

To this end, *ex vivo* PBMCs of 14 BCG-sensitized guinea pigs as well as the same PBMCs after 5 days of incubation with the respective antigens (Tub12, CME_{BCG}, CME_{H37Rv}) were stained with fluorescence-labeled antibodies directed against guinea pig pan T cell marker, guinea pig CD4, and guinea pig CD8. Subsequently, the stained cells were analyzed by flow cytometry.

Ex vivo, a median of 75.9 % of the gated lymphocytes (range 13.1 to 93.9 %) could be characterized as T cells. After 5 days of incubation, T cells made up for 91.8 % (median; range 81.7 to 98 %) of the Tub12-stimulated lymphocytes, 90.7 % (median; range 81.3 to 97.7 %) of the CME_{BCG}-stimulated lymphocytes, and 89.5 % (median; range 72.6 to 98.1 %) of the CME_{H37Rv}-stimulated lymphocytes. A median value of 28.1 % of the Tub12-stimulated T cells (range 13.3 to 74.8 %), a median value of 35.5 % of the CME_{BCG}-stimulated T cells (range 18.4 to 88.4 %), and a median value of 15.0 % of the CME_{H37Rv}-stimulated T cells (range 7.8 to 68.6 %) were recognized as $CFSE_{low}$.

The assessment of PBMCs before *in vitro* stimulation revealed that CD4-positive T cells constituted 56.1 % (median; range 38 to 67.2 %) and CD8-positive T cells 18.5 % (median; range 12 to 29.3 %) of the total T cell population in BCG-sensitized guinea pigs (**Figure 4.10**).

After 5 days of incubation with Tub12 or CME, the percentage of CD4-positive T cells among the proliferated ($CFSE_{low}$) T cells increased significantly compared with the *ex vivo* distribution ($p \leq 0.001$, student's *t* test), whereas the percentage of CD8-positive T cells decreased significantly ($p \leq 0.0001$) (**Figure 4.10**). In the Tub12-stimulated samples, a median of 77.3 % (range 48.4 to 93.8 %) of the whole $CFSE_{low}$ T cell population were CD4-positive T cells and 5.2 % (range 0.2 to 11.5 %) CD8-positive T cells. In the CME_{BCG}-stimulated samples, CD4-positive T cells constituted 83.2 % (median; range 62.4 to 94.2 %) and CD8-positive T cells 4.3 % (median; range 0.9 to 11.3 %) of the $CFSE_{low}$ T cells and in the CME_{H37Rv}-stimulated samples, CD4-positive T cells accounted for 74.9 % (median; range 39.3 to 89.5 %) and CD8-positive T cells for 6.3 % (median; range 1.2 to 14.3 %) of the proliferated T cells. On average, the percentage of CME_{BCG}-stimulated, $CFSE_{low}$, CD4-positive T cells was significantly higher than the percentages of $CFSE_{low}$, CD4-positive

T cells in the Tub12- and CME_{H37Rv}-stimulated samples ($p \leq 0.05$ and $p \leq 0.01$, respectively, student's *t* test).

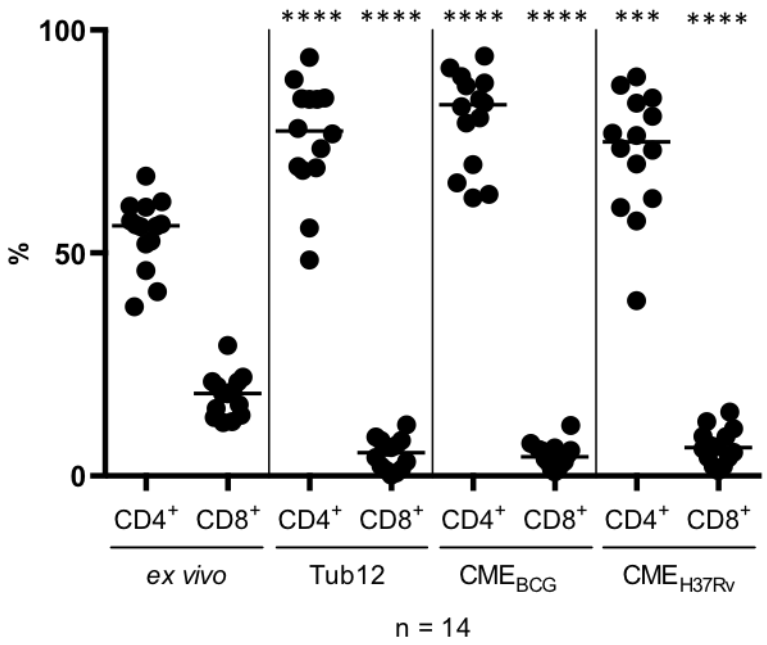

Figure 4.10 Proportions of CD4-positive and CD8-positive T cells before and after incubation with Tub12 or CMEs.

The flowcytometric analysis of CD4-positive and CD8-positive T cell proportions before and after stimulation is displayed. Lanes 1 and 2 represent the proportions of CD4-positive and CD8-positive cells, respectively, in the T cell subpopulation of PBMCs from 14 BCG-sensitized guinea pigs before stimulation. Lanes 3 through 8 show the proportions of CD4-positive and CD8-positive T cells among all proliferated T cells ($CFSE_{low}$, pan T cell marker-positive lymphocytes) after 5 days of incubation with the indicated antigen. Each black dot represents one guinea pig. Black bars delineate the medians. Asterisks indicate the significances of shift from *ex vivo* to post-stimulation percentages of CD4-positive and CD8-positive T cells, respectively. The data were generated with PBMCs from 14 guinea pigs at day 30 after BCG sensitization.

4.2 Specification of the stimulatory antigens

Biochemical degradation was used to investigate whether lipopeptides were responsible for the stimulatory capacities of the mycobacterial antigen preparations. Additionally, the stimulatory capacity of a lipopeptide-enriched subfraction of *M. tuberculosis* H37Rv (LppEL) was tested in the guinea pig *ex vivo* lymphocyte proliferation assay.

4.2.1 Biochemical degradation of antigens

Mild sodium hydroxide treatment was used for delipidation of the lipopeptides. Proteinase K and pronase E treatment was used to degrade the peptide moieties.

The effects of delipidation or proteinase treatment on the stimulatory capacities of Tub12 and CME_{BCG} were investigated using PBMCs from iAN5- and BCG-sensitized guinea pigs. To test for effects of the temperature treatment or the enzymes or chemicals themselves, controls with heat-inactivated enzyme or neutralized NaOH were included for each antigen sample. If enough guinea pig PBMCs were available, further temperature-only controls without any enzyme or chemical were tested.

Figure 4.11 displays the lymphocyte proliferation of 19 or 20 iAN5- and 20 or 21 BCG-sensitized guinea pigs, respectively, in response to mild sodium hydroxide treated Tub12 and CME_{BCG} as well as in response to control preparations (the original antigen preparation Tub12 or CME_{BCG}, the antigen preparations which were subjected to the temperature-control treatment, and the antigen preparations treated with neutralized sodium hydroxide).

Tub12 as well as of CME_{BCG} treated with mild sodium hydroxide stimulated *ex vivo* lymphocyte proliferation significantly less efficiently than the original antigen preparations, the antigen preparations which were subjected to the temperature-control treatment, and the antigen preparations treated with neutralized sodium hydroxide ($p \leq 0.0001$, student's *t* test). In all cases, the median values of the lymphocyte proliferation in the NaOH treated samples were less than 20 % $CFSE_{low}$ cells.

In detail, the median values and ranges of the lymphocyte proliferation in response to the indicated antigens are depicted in **Table 4.1**.

The lymphocyte proliferation in response to mild sodium hydroxide treated Tub12 was significantly lower in the BCG-sensitized group compared with the iAN5-sensitized animals ($p \leq 0.05$, student's *t* test). However, there was no significant difference between the two

groups in terms of lymphocyte stimulation by mild sodium hydroxide treated CME_{BCG} ($p > 0.05$).

Table 4.1 ***Ex vivo*** **proliferation of lymphocytes from iAN5- or BCG-sensitized guinea pigs to untreated, temperature-treated, neutralized NaOH-treated and mild NaOH-treated antigen preparations of Tub12 or CME_{BCG}.**

Source of PBMCs	Number of guinea pigs used	Antigen used for *ex vivo* stimulation		Percentage of $CFSE_{low}$ lymphocytes [%]		
		Antigen	Treatment	Median	Min	Max
iAN5-sensitized guinea pigs	19	Tub12	none	57.3	21.2	77.7
			temperature only	52.2	14.3	74.5
			neutralized NaOH	49.5	14.3	74.5
			mild NaOH	19.2	10.5	65.8
	20	CME_{BCG}	none	47.8	14.9	70.9
			temperature only	49.8	18.5	73.9
			neutralized NaOH	39.4	14.6	67.8
			mild NaOH	10.8	4.6	61.5
BCG-sensitized guinea pigs	20	Tub12	none	42.5	20.5	65.8
			neutralized NaOH	28.8	14.1	73.8
			mild NaOH	13.5	4.4	33.5
	21	CME_{BCG}	none	43.9	25.8	70.2
			neutralized NaOH	26.0	14.8	52.9
			mild NaOH	14.8	6.2	25.7

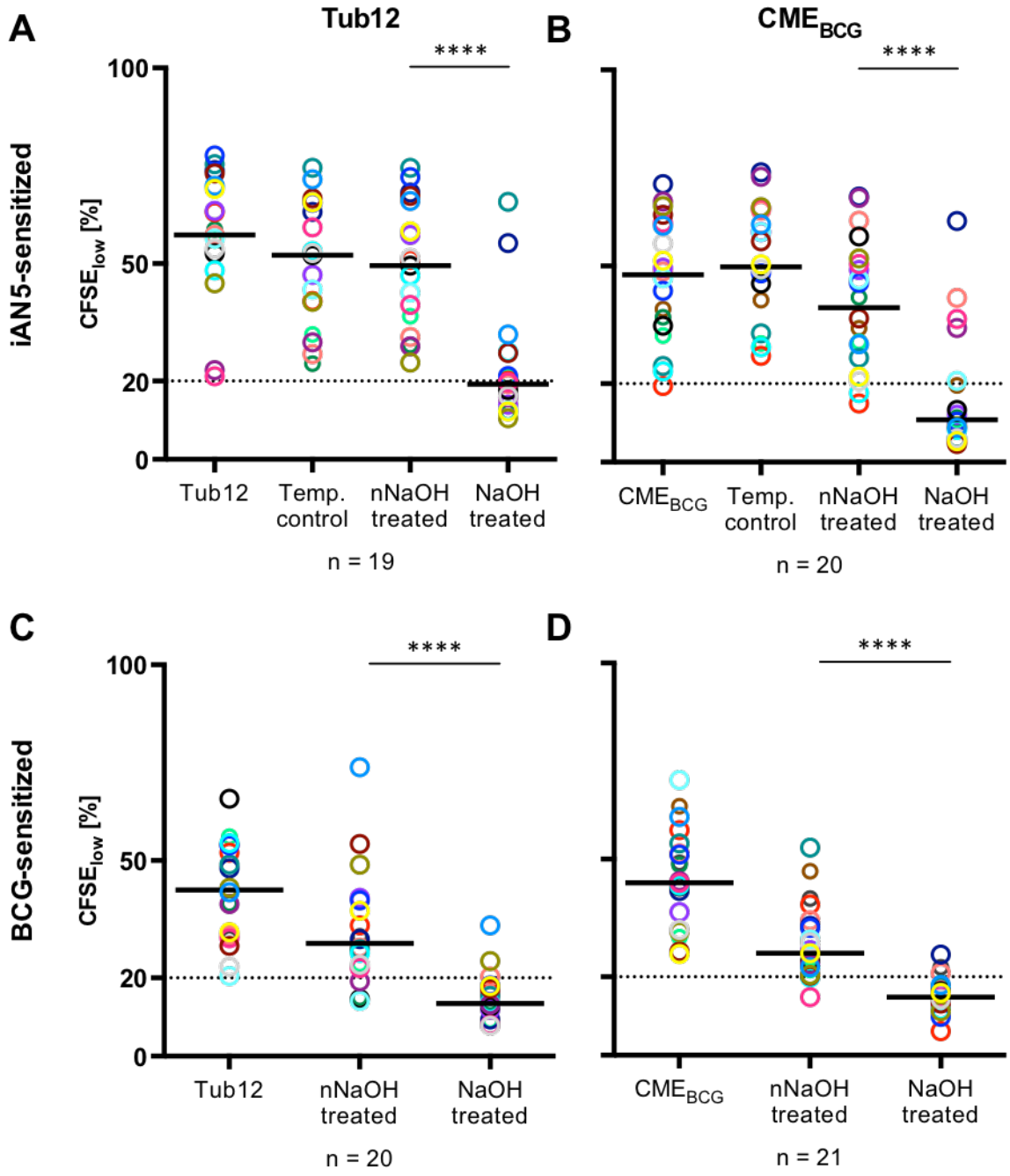

Figure 4.11 Mild NaOH treatment of Tub12 and CME$_{BCG}$ significantly decreases their stimulatory effects on lymphocyte proliferation *ex vivo*.

Results of the *ex vivo* lymphocyte proliferation assay. Proliferation in response to untreated Tub12 or CME$_{BCG}$, temperature-treated Tub12 or CME$_{BCG}$, Tub12 or CME$_{BCG}$ treated with neutralized mild NaOH and Tub12 or CME$_{BCG}$ treated with mild NaOH. Circles represent the arithmetic means of the duplicate tested per indicated antigen, per animal. Each color marks one animal in the specific plot. Bars represent the medians over all animals, per antigen. Asterisks indicate the significant differences between Tub12 or CME$_{BCG}$ treated with neutralized NaOH and Tub12 or CME$_{BCG}$ treated with mild NaOH. **A** and **B.** PBMCs obtained from guinea pigs at day 60 after iAN5 sensitization. **C** and **D.** PBMCs obtained from guinea pigs at day 30 after BCG sensitization.

An analogous experiment was conducted using proteinase K instead of mild sodium hydroxide for antigen treatment. **Figure 4.12** shows the lymphocyte proliferation results of 20 or 19 iAN5-sensitized guinea pigs and 17 or 16 BCG-sensitized animals, respectively, in response to Tub12 or CME_{BCG}, the antigen preparations subjected to temperature-control treatment, the antigen preparations treated with inactivated proteinase K, and the antigen preparations treated with the active enzyme.

In all groups, proteinase K treatment of Tub12 and CME_{BCG} reduced the median values of the lymphocyte proliferation to ≤ 20 % $CFSE_{low}$ cells. The reductions were significant compared with the proliferation in response to the untreated antigens, the antigens subjected to temperature-control treatment, as well as compared with the antigens treated with inactivated proteinase K ($p \leq 0.0001$, student's *t* test).

The median values of the lymphocyte proliferation using the indicated PBMCs and antigens are listed in **Table 4.2**.

The lymphocyte proliferation in response to Tub12 and CME_{BCG} degraded with proteinase K did not differ significantly between the iAN5- and the BCG-sensitized group.

Table 4.2 ***Ex vivo*** **proliferation of lymphocytes from iAN5- or BCG-sensitized guinea pigs to untreated, temperature-treated, inactivated proteinase K-treated and proteinase K-treated antigen preparations of Tub12 or CME_{BCG}.**

Source of PBMCs	Number of guinea pigs used	Antigen used for *ex vivo* stimulation		Percentage of $CFSE_{low}$ lymphocytes [%]		
		Antigen	Treatment	Median	Min	Max
iAN5-sensitized guinea pigs	19	Tub12	none	61.0	45.0	88.2
			temperature only	46.2	20.2	86.5
			inactivated proteinase K	48.0	16.2	88.5
			proteinase K	13.6	4.7	53.9
	20	CME_{BCG}	none	45.7	14.9	77.9
			temperature only	44.4	14.4	85.4
			inactivated proteinase K	44.0	12.3	87.5
			proteinase K	14.2	4.4	48.8
BCG-sensitized guinea pigs	20	Tub12	none	48.0	20.5	65.8
			inactivated proteinase K	32.5	14.0	57.9
			proteinase K	18.6	8.0	31.0
	21	CME_{BCG}	none	44.2	30.1	70.2
			inactivated proteinase K	44.4	6.0	70.5
			proteinase K	20.0	3.2	29.0

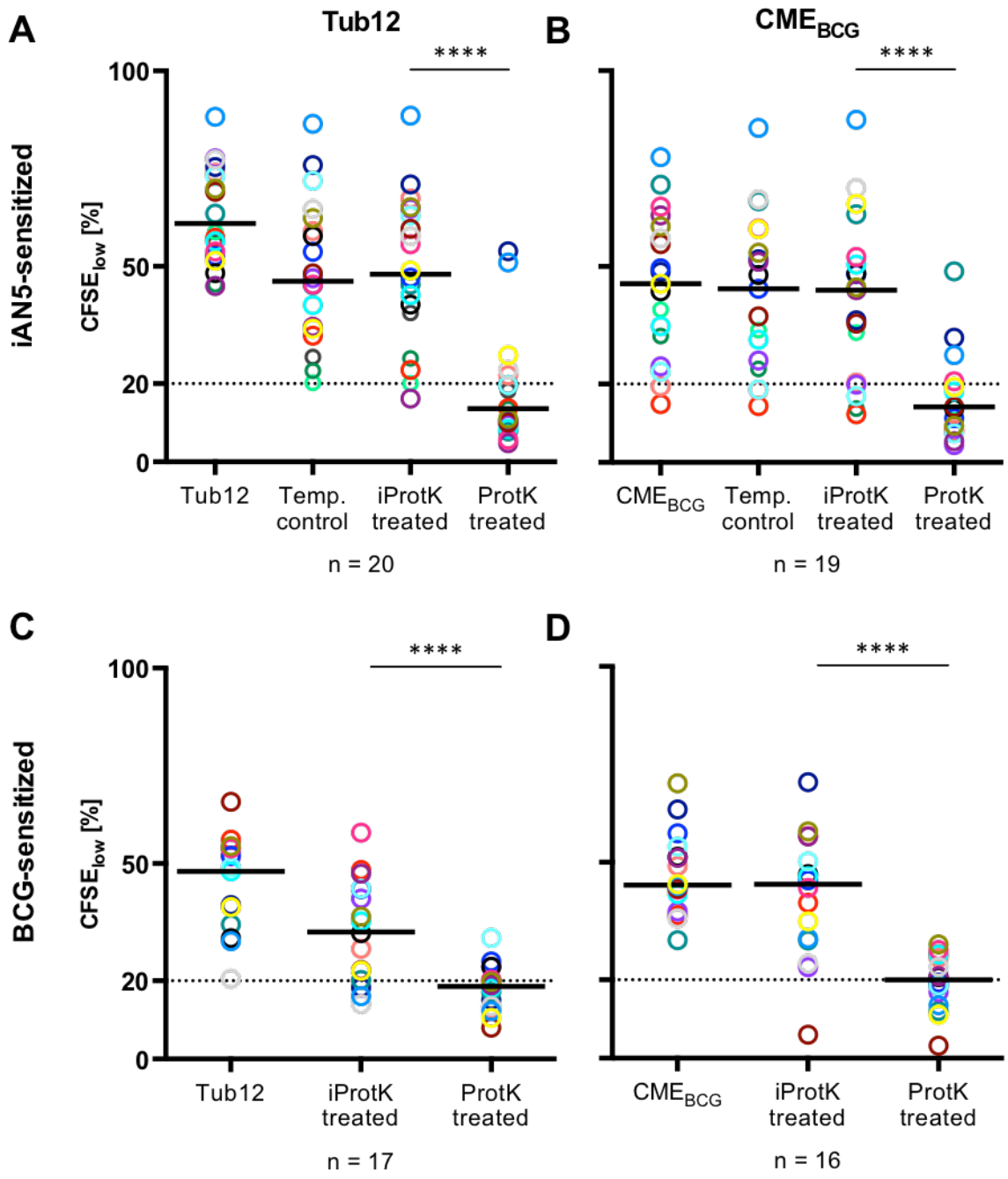

Figure 4.12 Proteinase K treatment of Tub12 and CME$_{BCG}$ significantly reduces its stimulatory effects on lymphocyte proliferation *ex vivo*.

Results of the *ex vivo* lymphocyte proliferation assay. Proliferation in response to untreated Tub12 or CME$_{BCG}$, temperature-treated Tub12 or CME$_{BCG}$, Tub12 or CME$_{BCG}$ treated with inactivated proteinase K (iProtK) and Tub12 or CME$_{BCG}$ treated with active proteinase K (ProtK). Circles represent the arithmetic means of the duplicate tested per indicated antigen, per animal. Each color marks one animal in the specific plot. Bars represent the medians over all animals, per antigen. Asterisks indicate the significant differences between Tub12 or CME$_{BCG}$ treated with inactivated proteinase K and Tub12 or CME$_{BCG}$ treated with active proteinase K. **A** and **B.** PBMCs obtained from guinea pigs at day 60 after iAN5 sensitization. **C** and **D.** PBMCs obtained from guinea pigs at day 30 after BCG sensitization.

To analyze the degradation effectivity of another protease, the experiment was repeated with pronase E. The effects of pronase E treatment of Tub12 and CME_{BCG} were tested with the PBMCs from 17 and 14 iAN5-sensitized animals, respectively (**Figure 4.13**).

Pronase E treatment of the antigen preparations Tub12 and CME_{BCG} resulted in a significant loss of their stimulatory effects on lymphocyte proliferation compared with the untreated antigen preparations, the antigen preparations subjected to temperature treatment only and the antigens treated with inactivated pronase E ($p \leq 0.0001$, student's *t* test) (**Figure 4.13**).

The obtained median values of lymphocyte proliferation in the PBMCs from iAN5-sensitized guinea pigs after stimulation with the indicated antigens are delineated in **Table 4.3**.

On average, the lymphocyte proliferation in response to pronase E-treated Tub12 and CME_{BCG} did not exceed the 20 % cut-off significantly ($p > 0.05$, one-sample *t* test). The proliferation in response to pronase E-treated Tub12 and CME_{BCG} did not differ significantly from the proliferation in response to the protease K-treated antigen preparations ($p > 0.05$, student's *t* test).

Table 4.3 ***Ex vivo*** **proliferation of lymphocytes from iAN5-sensitized guinea pigs to untreated, temperature-treated, inactivated pronase E-treated and pronase E-treated antigen preparations of Tub12 or CME_{BCG}.**

Source of PBMCs	Number of guinea pigs used	Antigen used for *ex vivo* stimulation		Percentage of $CFSE_{low}$ lymphocytes [%]		
		Antigen	Treatment	Median	Min	Max
iAN5-sensitized guinea pigs	19	Tub12	none	56.4	21.2	77.7
			temperature only	39.4	19.1	76.3
			inactivated pronase E	47.0	18.1	72.4
			pronase E	21.9	7.1	55.8
	20	CME_{BCG}	none	53.6	23.2	70.9
			temperature only	40.4	18.1	71.1
			inactivated pronase E	55.6	19.7	72.7
			pronase E	17.4	5.5	60.3

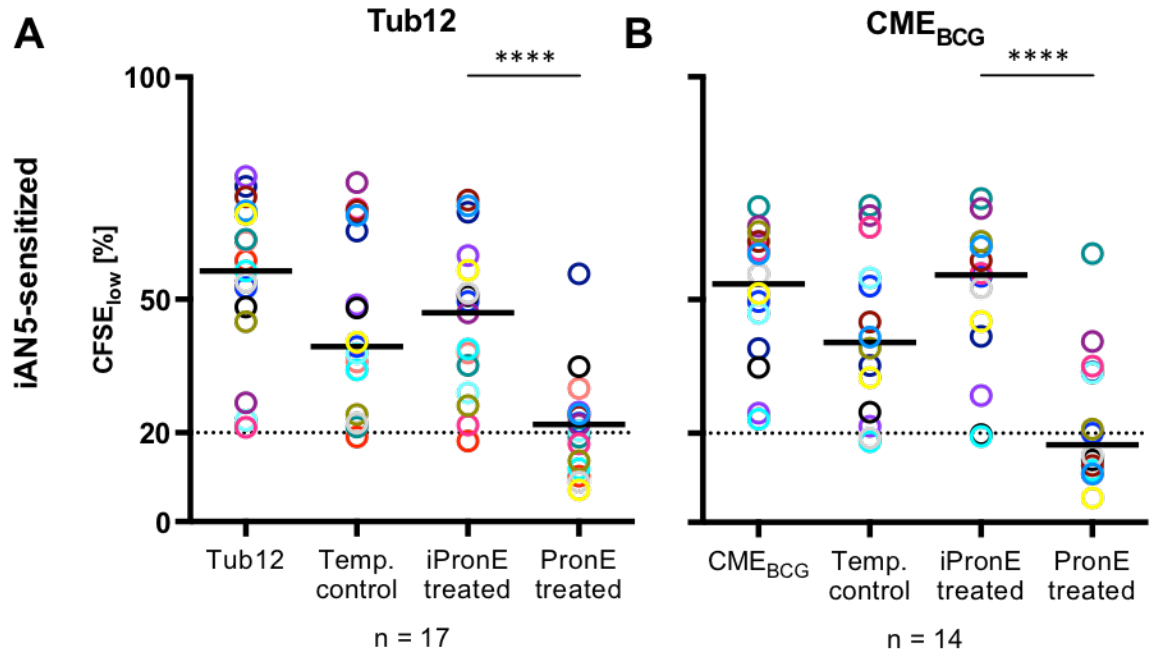

Figure 4.13 Pronase E treatment of Tub12 and CME$_{BCG}$ significantly lowers their stimulatory effects on lymphocyte proliferation *ex vivo*.

Results of the *ex vivo* lymphocyte proliferation assay. Proliferation in response to untreated Tub12 or CME$_{BCG}$, temperature-treated Tub12 or CME$_{BCG}$, Tub12 or CME$_{BCG}$ treated with inactivated pronase E (iPronE) and Tub12 or CME$_{BCG}$ treated with active pronase E (PronE). Circles represent the arithmetic means of the duplicate tested per indicated antigen, per animal. Each color marks one animal in the specific plot. Bars represent the medians over all animals, per antigen. Asterisks indicate the significant differences between Tub12 or CME$_{BCG}$ treated with inactivated pronase E and Tub12 or CME$_{BCG}$ treated with active pronase E. **A** and **B.** PBMCs obtained from guinea pigs at day 60 after iAN5 sensitization.

4.2.2 The stimulatory potential of a lipopeptide-enriched subfraction (LppEL)

The biochemical degradation experiments suggested that the relevant antigens in CME, and in Tub12 as well, must contain both an intact lipid and a peptide moiety. To corroborate the notion that the CME reactivity was induced by lipopeptides, the stimulatory potential of a subfraction of CME$_{H37Rv}$ which was specifically enriched in lipophilic peptides (LppEL) was investigated in the guinea pig *ex vivo* lymphocyte proliferation assay.

The stimulatory potential of this lipopeptide-enriched subfraction was analyzed in direct comparison with Tub12 and CME stimulation of PBMCs from 35 iAN5- and 45 BCG-sensitized guinea pigs (**Figure 4.14**). LppEL induced potent lymphocyte proliferation (median 43.8 %, range 9.1 to 84.1 %, in the iAN5-sensitized group and median 24.4 %, range 4.2 to 89.7 %, in the BCG-sensitized guinea pigs).

The lymphocyte proliferation of animals sensitized with the inactivated, virulent *M. bovis* AN5 was not only very strong in response to CME of the virulent *M. tuberculosis* strain H37Rv (median 39.6 %, range 3.8 to 73.1 %), but also in response to LppEL which derived from this strain. The proliferation results in response to these two antigen preparations did not differ significantly ($p > 0.05$, student's *t* test).

Although significantly lower than the proliferation observed with the PBMCs from iAN5-sensitized animals ($p \leq 0.05$, student's *t* test), a strong lymphocyte proliferation in response to LppEL was also observed in 29 of the 45 BCG-sensitized guinea pigs which led to an average proliferation in this group that was significantly above the 20 % cut-off ($p \leq 0.01$, one-sample *t* test). The median value of this LppEL stimulation (see above) manifested in the same range as the median value of the CME_{H37Rv} stimulation (median 26.8 %, range 10.8 to 87.3 %), whereas the lymphocyte proliferation in response to CME_{BCG} (median 43.9 %, range 10.8 to 88.3 %) was significantly higher than both of them ($p \leq 0.0001$, student's *t* test).

The variance of the lymphocyte proliferation results in response to LppEL was larger in BCG-sensitized animals compared with the iAN5-sensitized ones. However, the proportion of guinea pigs showing lymphocyte proliferation below 20 % $CFSE_{low}$ cells in the LppEL-stimulated samples was similar in both groups (11/35 iAN5-sensitized animals and 16/45 BCG-sensitized guinea pigs). As obvious from **Figure 4.14**, the cell samples which were located below the 20 % cut-off line belonged mainly to the same animals whose cells proliferated rather poorly in response to the other stimulatory antigen preparation as well.

The correlations associated with the lymphocyte proliferation in response to CME_{BCG}, CME_{H37Rv} and LppEL are depicted in **Figure 4.15**. The notion that the PBMCs of some animals responded well to the stimulatory antigens and that others responded only poorly to all preparations was corroborated by the highly significant positive correlations of the lymphocyte responses between the CME antigen preparations and LppEL.

In the iAN5-sensitized group, there were significant positive correlations of the lymphocyte proliferation in response to CME_{BCG} and CME_{H37Rv} ($r = 0.7$), CME_{BCG} and LppEL ($r = 0.6$), as well as in response to CME_{H37Rv} and LppEL ($r = 0.5$) ($p \leq 0.01$, Spearman correlation).

The correlation coefficients in the BCG-sensitized group were $r = 0.8$ for CME_{BCG} and CME_{H37Rv}, $r = 0.6$ for CME_{BCG} and LppEL, and $r = 0.6$ for CME_{H37Rv} and LppEL. All these correlations were highly significant ($p \leq 0.0001$, Spearman correlation).

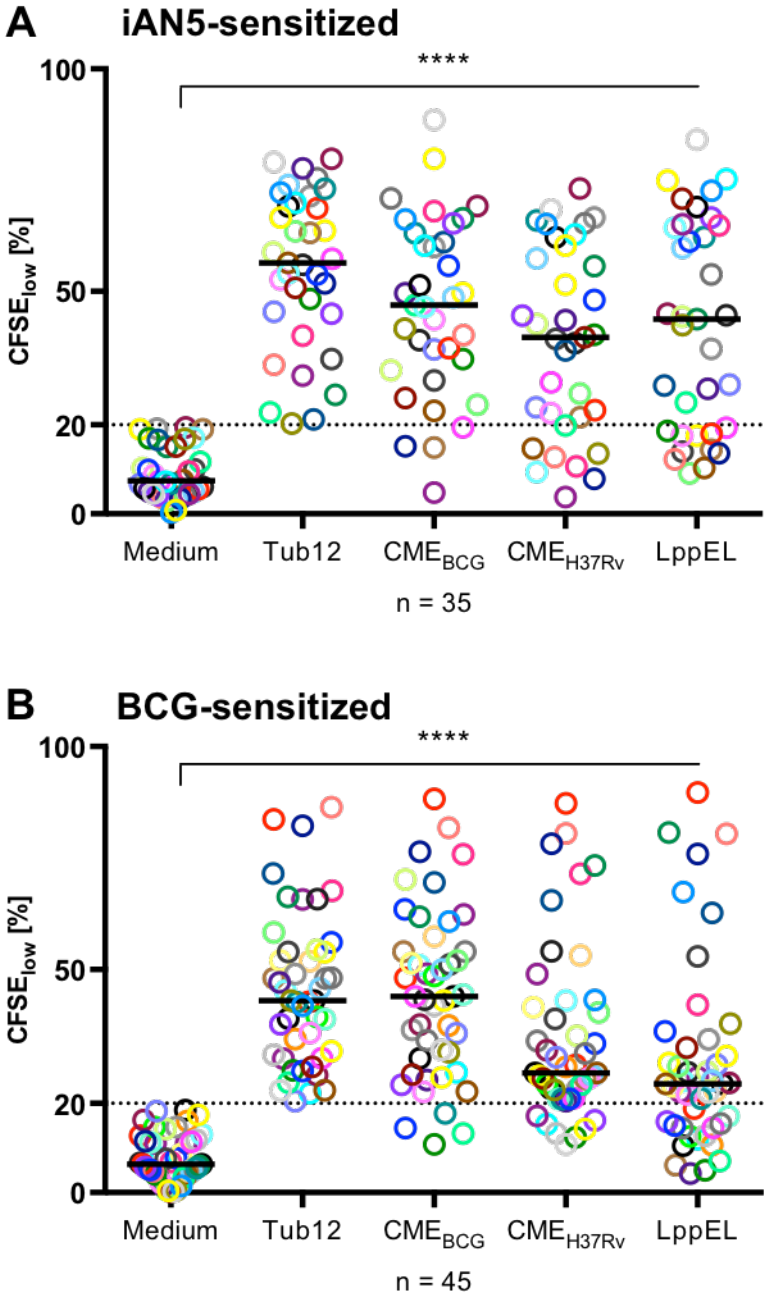

Figure 4.14 LppEL induces strong lymphocyte proliferation in iAN5- and BCG-sensitized guinea pigs *ex vivo*.

Results of the *ex vivo* lymphocyte proliferation assay. PBMCs were incubated with the different antigens (Tub12 30 IU/ml; CMEs and LppEL 10 µg/ml) for 5 days. The y-axis represents the percentage of $CFSE_{low}$ lymphocytes among all lymphocytes. Circles represent the arithmetic means of the duplicate tested per antigen, per animal. The black bars represent the median values over all animals, per antigen. **A.** PBMCs obtained from 35 individual guinea pigs at day 60 after iAN5 sensitization. **B.** PBMCs obtained from 45 individual guinea pigs at day 30 after BCG sensitization.

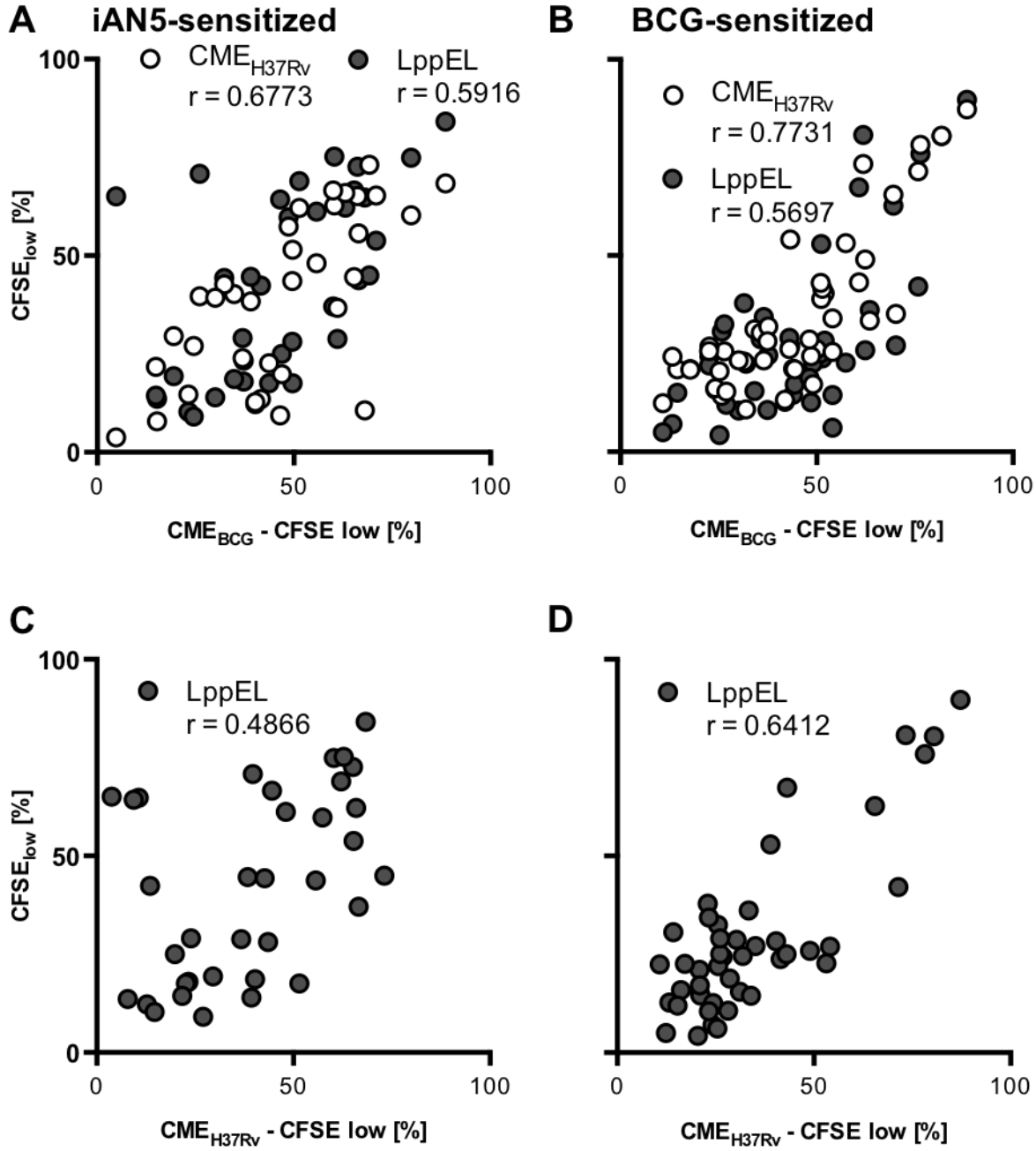

Figure 4.15 Lymphocyte proliferation in response to CME_{BCG} correlates with proliferation in response to CME_{H37Rv} and LppEL and lymphocyte proliferation in response to CME_{H37Rv} correlates with proliferation in response to LppEL.

Results of the *ex vivo* lymphocyte proliferation assay. The x-axis represents the percentage of $CFSE_{low}$ cells after 5 days of incubation with the indicated CME. On the y-axis, the dots display the percentage of $CFSE_{low}$ cells in the corresponding incubation with the indicated antigen preparation. Tub12 30 IU/ml; CMEs and LppEL 10 µg/ml. Dots represent the arithmetic means of the duplicate tested per indicated antigen, per animal. r indicates the non-parametric two-tailed Spearman correlation with a confidence interval of 95 %. **A** and **C.** PBMCs obtained from 35 guinea pigs at day 60 after iAN5 sensitization; **B** and **D.** PBMCs obtained from 45 guinea pigs 30 days after BCG sensitization.

4.3 Antigen specificity of the proliferating lymphocytes

4.3.1 Enrichment of expanded lymphocytes by magnetic sorting

To investigate the antigen specificity of the CME-responding lymphocytes, a novel method to sort for expanded lymphocytes was developed. After PBMC isolation, the cells were therefore extracellularly biotinylated and labeled with CFSE. Each mitotic division of the cell upon stimulation reduces the CFSE fluorescence by half (Lyons and Parish 1994; Quah *et al.* 2007). We hypothesized that the biotinylation of the cells followed the same pattern, and therefore, that the biotinylation of the cells correlated with the CFSE labeling. CFSE labeling can be directly measured by flow cytometry through detection of its characteristic green fluorescence. The degree of extracellular biotinylation was determined using a PE-Cy5.5-conjugated streptavidin, which binds biotin with high affinity.

For experimental proof of this concept, the MTC strain used for sensitization of guinea pigs, the days of blood collection and the stimulatory antigen preparations were considered irrelevant. Therefore, differentially sensitized and stimulated lymphocytes which were obtained at different days of blood collection were included in this analysis. However, each animal was considered only once to prevent any bias of particular individual proliferation properties.

Figure 4.16 demonstrates a strong correlation between the CFSE signal and the biotin signal on PBMCs after 5 days of incubation with mycobacterial antigen preparations. PBMCs had been obtained from 24 sensitized guinea pigs. The figure shows the positive correlation between the percentages of $CFSE_{high}$ cells (non-proliferated) and of $streptavidin^{PE\text{-}Cy5.5}{}_{positive}$ cells ($biotin_{positive}$) among all lymphocytes ($r = 0.9$). In contrast, the percentage of $CFSE_{low}$ cells (proliferated) correlated negatively with the portion of $streptavidin^{PE\text{-}Cy5.5}{}_{positive}$ cells ($r = –0.9$) ($biotin_{positive}$). These correlations were statistically highly significant ($p \leq 0.0001$, Spearman correlation).

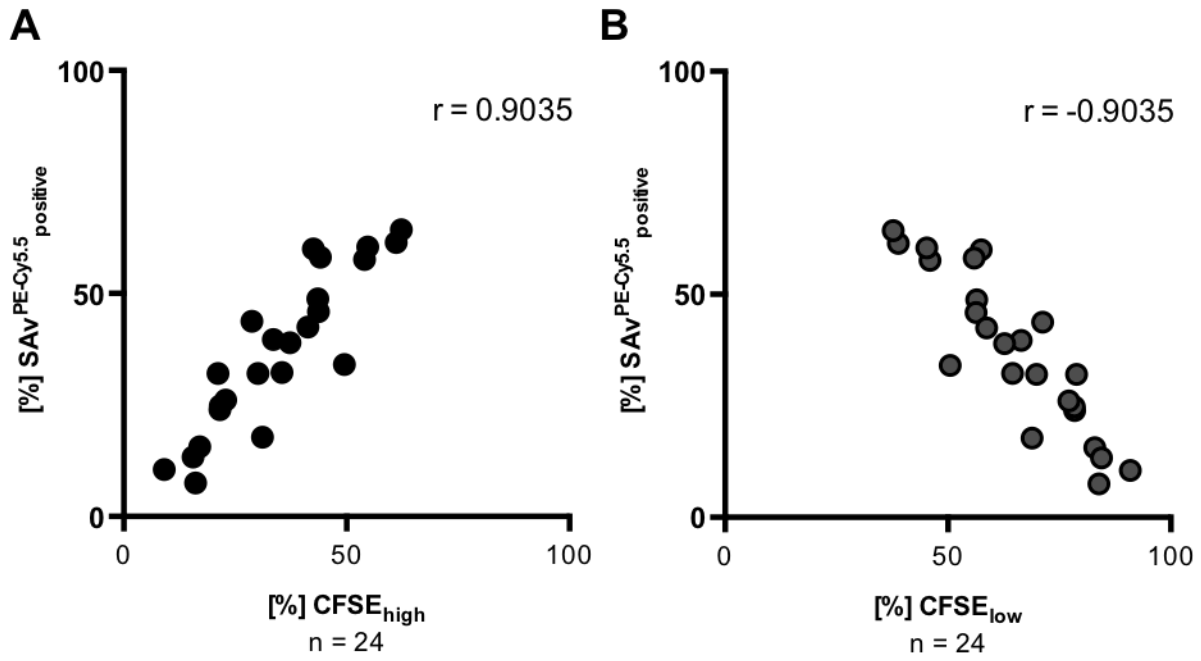

Figure 4.16 Correlation between loss of CFSE fluorescence and loss of biotinylation in antigen-stimulated lymphocytes *ex vivo*.

Ex vivo PBMCs were labeled with CFSE and biotinylated. After 6 days of incubation with a stimulatory antigen (Tub12 30 IU/ml; CME 10 µg/ml), cells were harvested and incubated with $SAv^{PE\text{-}Cy5.5}$, which bound to remaining biotin on the cells. In flowcytometric analysis, percentages of $CFSE_{high}$ and $CFSE_{low}$ as well as $SAv^{PE\text{-}Cy5.5}{}_{positive}$ lymphocytes were determined. Cells derived from 24 MTC-sensitized guinea pigs at different days of blood collection. Each dot represents one animal and only one stimulation per animal was displayed. **A.** Positive correlation of remaining CFSE fluorescence and $SAv^{PE\text{-}Cy5.5}$ binding. 100 % $CFSE_{high}$ indicates “no proliferation”. **B.** Negative correlation of the $CFSE_{low}$ cells and the binding of $SAv^{PE\text{-}Cy5.5}$. 100 % $CFSE_{low}$ equals “strong proliferation”.

Having demonstrated the correlation between loss of CFSE fluorescence and loss of biotinylation, biotinylation and subsequent incubation with streptavidin was assumed a valid method to sort for cells which were expanded by stimulation with an antigen of interest. To this end, *ex vivo* PBMCs of BCG-sensitized guinea pigs were labeled with CFSE and biotin, and were then expanded with Tub12, CME_{BCG} or CME_{H37Rv} for 6 days. Next, cells were incubated with streptavidin-coupled magnetic beads to label cells with remaining biotinylation. This magnetic labeling enabled the specific separation of those cells which did not proliferate in response to the respective antigen, by sorting the cell population through a magnetic column system (see section 3.8.2.2). The different fractions were collected as “$biotin_{negative}$ (proliferated) cells”, “flow-through” and “biotin-positive (non-proliferated) cells”.

To test for the efficacy of the procedure, samples were taken from each fraction and were analyzed by flow cytometry for their percentages of $CFSE_{low}$ cells, as displayed in **Figure 4.17**. Cells of the $biotin_{negative}$ population were enriched in $CFSE_{low}$ cells (98.7 %) compared with the initial population (61.9 %), whereas cells of the $biotin_{positive}$ population

showed a reduced $CFSE_{low}$ percentage (23.7 %). The $CFSE_{low}$ cells of the flow-through, which was collected after harvesting the $biotin_{negative}$ cells, were still enriched in $CFSE_{low}$ lymphocytes but to a slightly lesser extent (97.1 %) and there were only low cell numbers in this fraction. The flow-through was discarded to ensure high purity of the sorted cells.

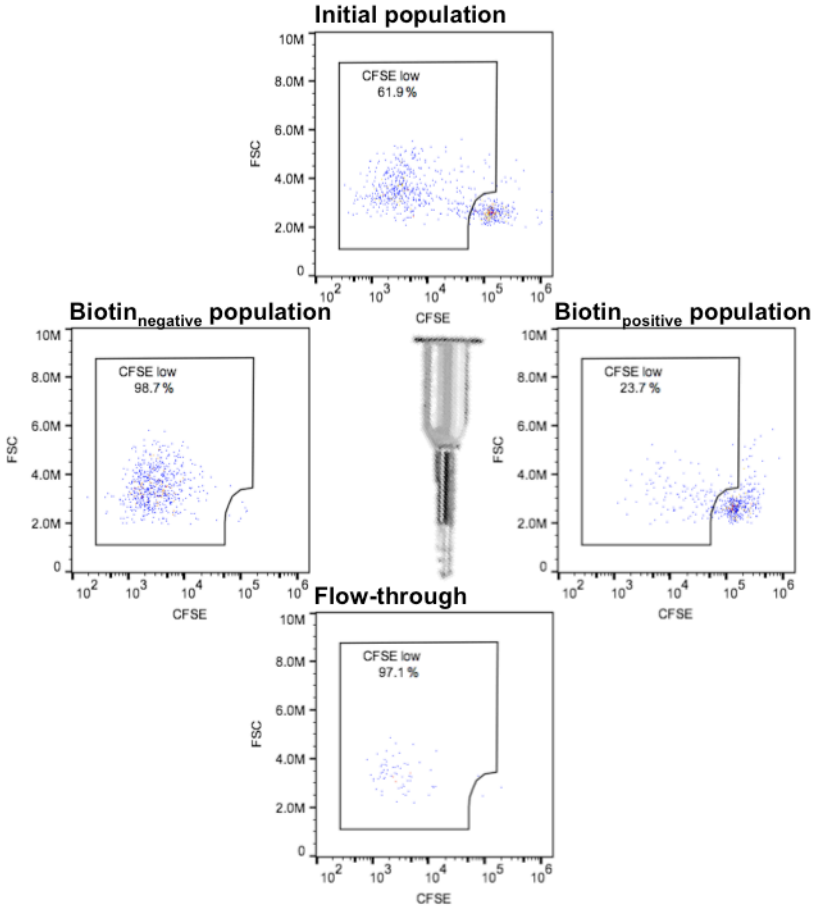

Figure 4.17 Enrichment of expanded lymphocytes by magnetic sorting.

Ex vivo PBMCs of sensitized guinea pigs were labeled with CFSE, biotinylated and expanded with a stimulatory antigen preparation (Tub12 30 IU/ml; CME 10 µg/ml). After 6 days, cells were incubated with streptavidin-coupled magnetic beads and sorted through a magnetic column (MiniMACS™). Samples of the initial population, the $biotin_{negative}$ and the $biotin_{positive}$ populations as well as of the flow-through were subsequently analyzed by flow cytometry for their $CFSE_{low}$ lymphocyte content. The plots have been illustrated using FlowJo Single Cell Analysis Software.

Figure 4.18 displays the results of the established enrichment procedure after it was applied on *in vitro*-expanded PBMCs obtained from 30 BCG-sensitized guinea pigs. The median value of $CFSE_{low}$ cells in the initial population was 62.7 % (range 15.7 to 84.7 %), which was significantly increased in the $biotin_{negative}$ (median 86.8 %, range 39.2 to 97.5 %) ($p \leq 0.0001$,

student's *t* test) and significantly decreased in the biotin$_{positive}$ population (median 12.6 %, range 3.4 to 56.3 %) ($p \leq 0.0001$).

To ensure the reliability of the restimulation results through high purity of the specifically expanded cell populations, only cell samples with ≥ 80 % CFSE$_{low}$ cells in the biotin$_{negative}$ fraction (filled symbols in **Figure 4.18**) were further processed.

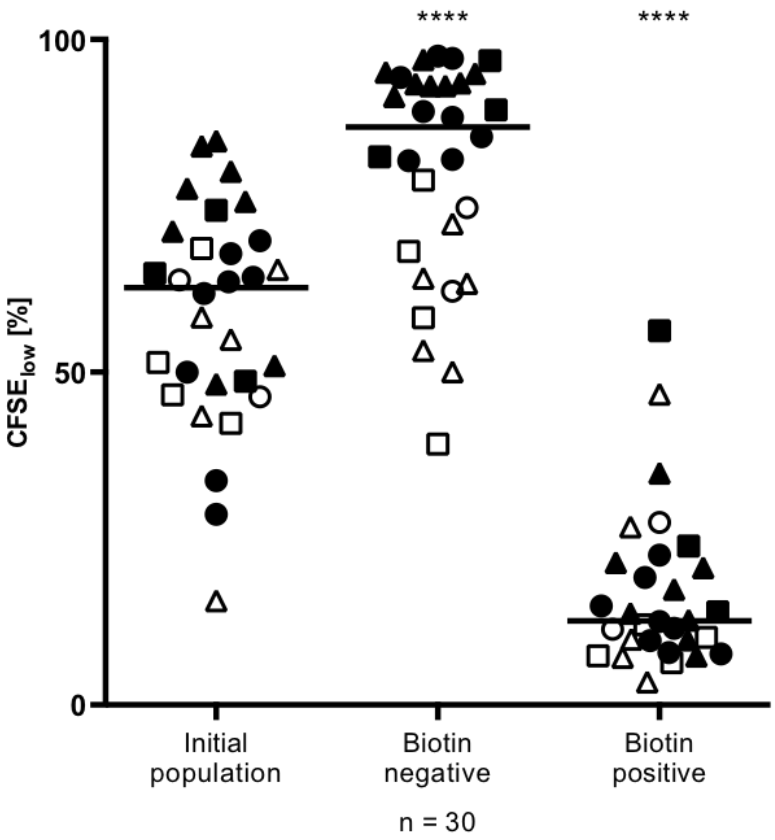

Figure 4.18 Enrichment of CFSE$_{low}$ lymphocytes in the biotin$_{negative}$ lymphocyte population.

Ex vivo guinea pig PBMCs were obtained at day 30 after BCG sensitization, labeled with CFSE, biotinylated and expanded with a stimulatory antigen preparation (Tub12 (Δ) 30 IU/ml; CME$_{BCG}$ (O) or CME$_{H37Rv}$ (□) 10 µg/ml). After 6 days, cells were incubated with streptavidin-coupled magnetic beads and sorted through a magnetic column (MiniMACS^{TM}). The figure represents the percentages of CFSE$_{low}$ lymphocytes (y-axis) in the initial population, in the biotin$_{negative}$ population and in the biotin$_{positive}$ population (x-axis) after incubation. Each symbol represents one expanded cell sample in the respective fractions. Expanded cell samples yielding ≥ 80 % CFSE$_{low}$ cells in the sorted biotin$_{negative}$ population are indicated by filled symbols.

4.3.2 Assessment of the antigen specificity of the sorted lymphocytes

$Biotin_{negative}$ lymphocyte populations with ≥ 80 % $CFSE_{low}$ cells were further analyzed in the restimulation assay. Thereto, cells were again labeled with CFSE and incubated for 5 days with the antigen preparations in the presence of irradiated autologous PBMCs as antigen presenting cells (APCs). The irradiated autologous PBMCs were used for efficient antigen processing and presentation (see below and **Figure 4.20**). After incubation, proliferation of the lymphocytes, as measured by loss of CFSE fluorescence, was again analyzed by flow cytometry (restimulation assay).

Figure 4.19 displays the proliferation results of 12 expanded and sorted lymphocyte populations from 9 BCG-sensitized guinea pigs. PBMCs obtained from 3 guinea pigs have been expanded with both Tub12 and CME, but in separate approaches. The resulting 2 populations per animal are marked by the same colors.

In particular, 2/6 samples of the CME-expanded cells did not proliferate upon restimulation anymore – irrespective of the antigen preparation used for restimulation (**Figure 4.19**). They did not even proliferate in response to PHA (data now shown).

However, those CME-expanded cell samples which showed proliferation upon restimulation with Tub12 (≥ 20 % $CFSE_{low}$ cells), demonstrated strong proliferation responses to all antigens (Tub12: median 76.4 %, range 32.2 to 93.9 %; CME_{BCG}: median 75.7 %, range 37.5 to 93.3 %; CME_{H37Rv}: median 72.6 %, range 23.1 to 89.3 %; LppEL: median 69.0 %, range 35.4 to 81.0 %). Similarly, the Tub12-expanded cells proliferated upon restimulation with all antigen preparations (Tub12: median 41.7 %, range 20.8 to 65.1 %; CME_{BCG}: median 43.4 %, range 15.4 to 72.0 %; CME_{H37Rv}: median 35.0 %, range 13.0 to 60.2 %; LppEL: median 45.5 %, range 19.2 to 80.0 %).

It is further remarkable that all sorted cell populations proliferated in an individual range which, however, was similar in response to all stimulatory antigen preparations (Tub12, CME_{BCG}, CME_{H37Rv}, LppEL). The proliferation results obtained upon restimulation with the different antigen preparations did not differ significantly from each other ($p > 0.05$, student's *t* test), except the proliferation in the LppEL-stimulated samples of Tub12-expanded lymphocytes which was significantly stronger than the proliferation in the CME_{H37Rv}-stimulated samples ($p \leq 0.05$). Thus, with this one exception, it had no effect on the extent of the proliferative response whether the same or different antigen preparations were used for lymphocyte expansion and restimulation.

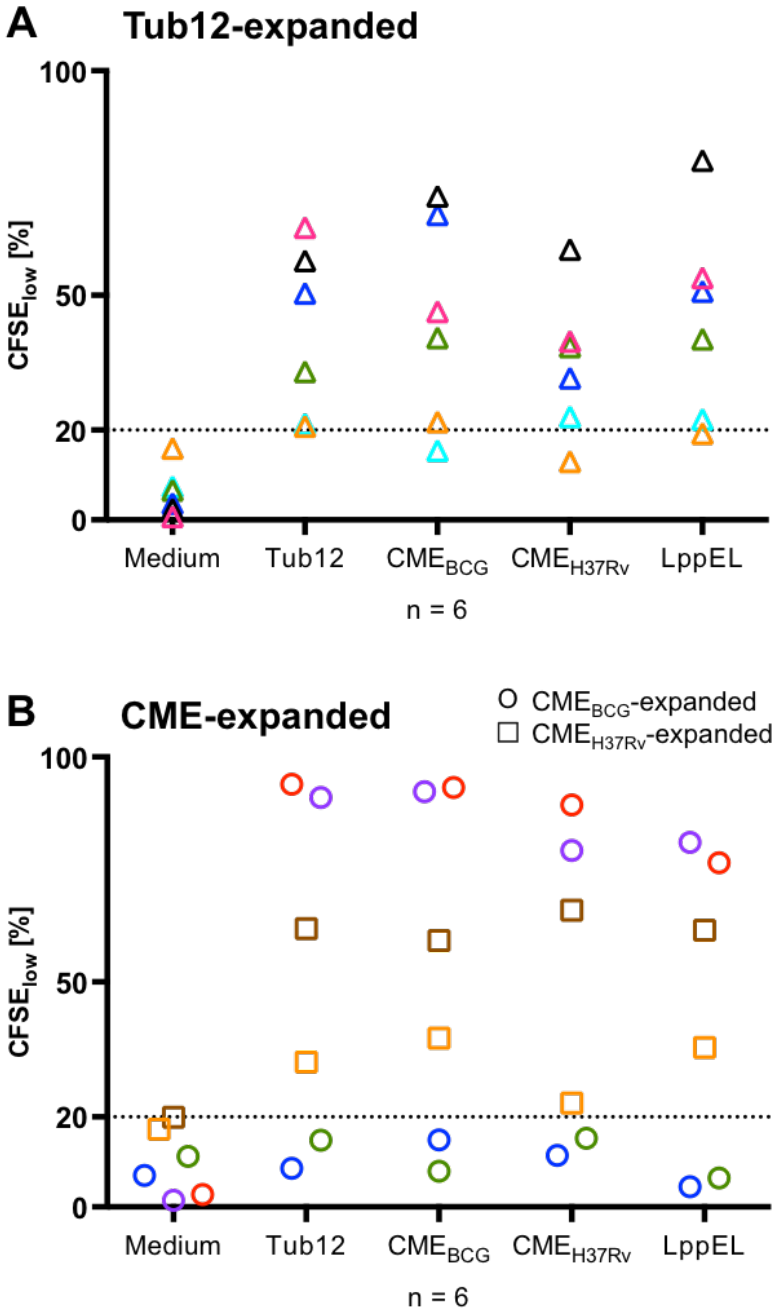

Figure 4.19 Proliferation responses of expanded and sorted biotin$_{negative}$ lymphocytes (co-incubated with irradiated autologous PBMCs) upon restimulation with mycobacterial antigens.

Results of the restimulation assay. PBMCs were obtained from 9 guinea pigs 30 days after BCG sensitization, labeled with CFSE and biotin and expanded with the antigen preparation as indicated in the title (Tub12 (Δ); CME$_{BCG}$ (O); CME$_{H37Rv}$ (☐)). After 6 days, cells were incubated with streptavidin-coupled magnetic beads and sorted via a MiniMACS^{TM} magnetic column. Biotin$_{negative}$ populations with ≥ 80 % CFSE$_{low}$ cells were CFSE labeled and mixed with irradiated autologous PBMCs and restimulated with the antigen preparations as indicated on the x-axis (Tub12 30 IU/ml; CME, LppEL 10 µg/ml). After 5 days, proliferation of these cells was determined by flow cytometry. Symbols represent the arithmetic means of the duplicate tested per antigen preparation, per biotin$_{negative}$ cell population. Each color represents one animal, n indicates the number of expanded cell populations displayed in the particular graph. **A.** Results of 6 Tub12-expanded cell populations in the restimulation assay. **B.** Results of 6 CME-expanded cell populations in the restimulation assay.

On the day of blood collection, *ex vivo* PBMCs were frozen to provide autologous APCs for antigen presentation in the restimulation assay. PBMCs mainly consist of lymphocytes, monocytes and macrophages. Sufficient numbers of cells which can act as APCs should therefore be available. PBMCs were irradiated to retain their function on short-term antigen processing and presentation but to exclude proliferation. Co-incubation of specialized lymphocytes with irradiated autologous PBMCs enabled proliferation of the lymphocytes as indicated in **Figure 4.19**. To control whether this proliferation was dependent on the presence of APCs or whether the irradiated PBMCs themselves were able to proliferate, these two populations were tested separately. The same total cell concentrations as for the co-incubations were used to achieve comparable results.

Figure 4.20 shows that no significant proliferation occurred when incubating 17 samples of expanded lymphocytes or 18 samples of irradiated PBMCs alone, not even in response to the strong and unspecific mitogen PHA. In both groups, there were no significant differences between the stimulated samples and the medium-only control ($p > 0.05$, student's *t* test) and, on average, all samples fell significantly below the 20 % cut-off line ($p \leq 0.05$, one-sample *t* test). Furthermore, there were no significant differences between the stimulation of lymphocytes only and irradiated PBMCs only ($p > 0.05$, student's *t* test).

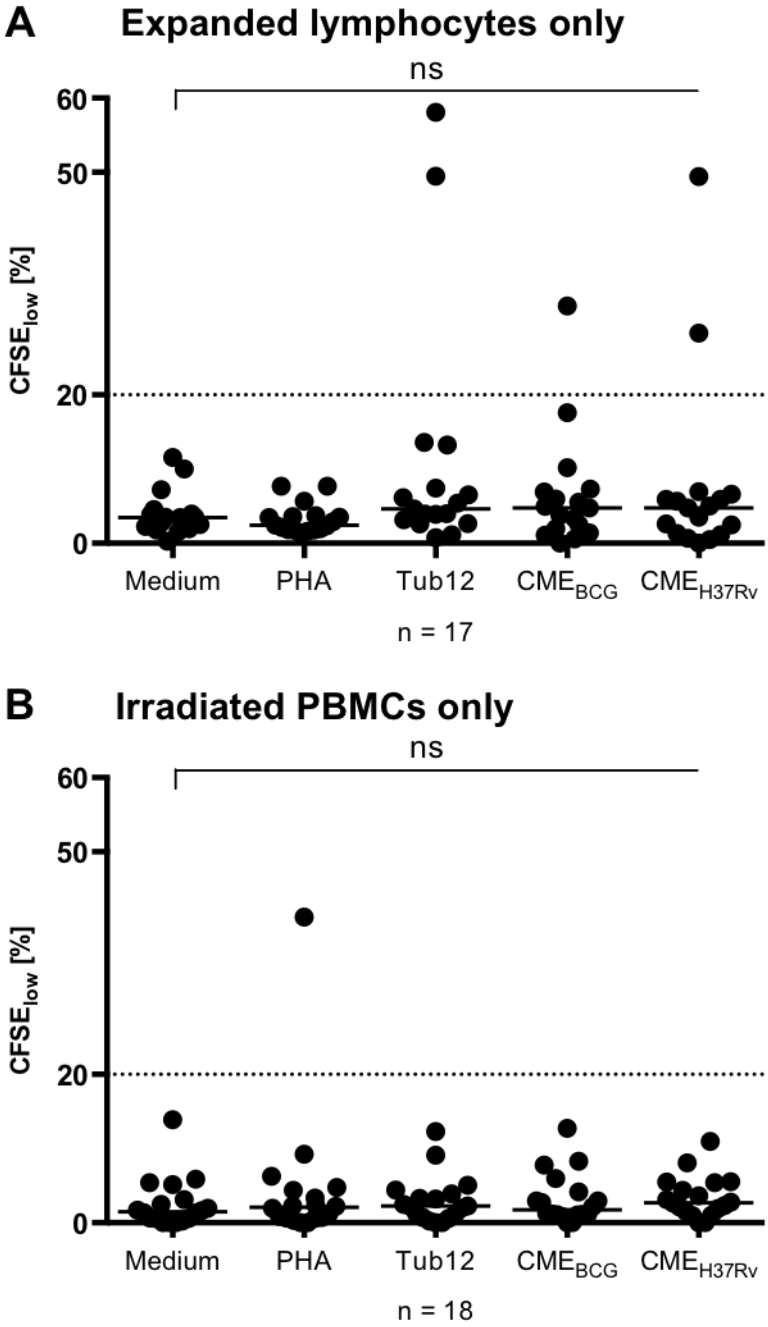

Figure 4.20 Proliferation responses of expanded and sorted biotin$_{negative}$ lymphocytes and irradiated autologous PBMCs upon (re)stimulation with mycobacterial antigens or PHA.

Control experiments corresponding to Fig. 4.9. Expanded and sorted biotin$_{negative}$ lymphocyte samples (n = 17, obtained from 10 guinea pigs), or irradiated PBMCs obtained from guinea pigs (n = 18) were labeled with CFSE and incubated separately with the antigens as indicated on the x-axis. After 5 days, proliferation of these cells was determined by flow cytometry. Lymphocytes and PBMCs derived from MTC-sensitized guinea pigs at different time points of blood collection and were expanded with Tub12, CME$_{BCG}$ or CME$_{H37Rv}$. Each kind of expansion is only displayed once per animal. Black lines mark the median values over all samples or guinea pigs, respectively, per antigen. Tub12 30 IU/ml; CME 10 µg/ml. **A.** Proliferative responses of expanded and sorted biotin$_{negative}$ lymphocytes, not co-incubated with irradiated autologous PBMCs; each dot represents the arithmetic mean of the duplicate tested per antigen, per cell sample. **B.** Proliferative responses of irradiated autologous PBMCs; each dot represents the arithmetic mean of the duplicate tested per antigen, per guinea pig.

4.4 Analysis of the stimulatory antigens

The strong lymphocyte proliferation in response to CME_{BCG} and CME_{H37Rv} after BCG sensitization prompted us to investigate to what extent the stimulatory antigens in these preparations are expressed over the genus *Mycobacterium*.

4.4.1 Characteristics of different CME preparations

The distribution of the stimulatory antigens among mycobacteria was investigated by analyzing the stimulatory potential of CME preparations produced from different mycobacterial strains (see **Table 3.2**) on the sensitized lymphocytes.

Although slightly different protocols were used to produce the different CMEs, no systematic differences with functional relevance could be identified between the preparations.

In detail, the protein content of the various CME preparations was analyzed by SDS-PAGE and subsequent Coomassie staining or silver staining and antigens were visualized by Western blotting. If separation was followed by Coomassie staining or Western blotting, 80 µg CME were used per slot in SDS-PAGE. This quantity corresponded to 80 times the amount of CME that was added in the *ex vivo* lymphocyte proliferation assay per well.

Although Coomassie staining is relatively insensitive (**Figure 4.21**), there were traces of a protein smear detectable within the *M. marinum* sample. This sample had the highest remaining protein content throughout all analyses. In all other CME preparations, there was no protein detectable with Coomassie staining.

For silver staining which is, according to the manufacturer of the kit (Life Technologies), approximately 30-fold more sensitive than Coomassie staining, only 10 µg CME were used per slot, which corresponded to the 10-fold CME amount that was applied in the *ex vivo* lymphocyte proliferation assay per well. Silver staining of the CMEs separated by SDS-PAGE revealed small amounts of proteins in individual preparations (**Figure 4.22**). These bands did not correspond to ManLAM. They were detected in particular in the MRL Fort Collins preparations of *M. tuberculosis* CDC 1551 and HN 878 as well as in the IPBS Toulouse preparations of *M. marinum* and *M. fortuitum*. Interestingly, the preparation protocols of IPBS Toulouse and MRL Fort Collins varied to the greatest extent among all preparation protocols (see section 3.3.3). No such protein traces were found within the samples prepared according to the PEI protocols which were adapted from the MRL protocol. However, the stimulatory capacities of the indicated strains in the *ex vivo* lymphocyte proliferation assay were high in the *M. tuberculosis* preparations and low in

M. marinum and in particular in *M. fortuitum* (**Figure 4.25**). It was therefore concluded that the observed substances were not stimulatory *per se*.

Western blotting was used to detect antigens separated by SDS-PAGE. After Western blotting, the nitrocellulose membrane with the proteins and peptides was incubated with pooled sera of 10 BCG-sensitized guinea pigs. Pooled sera were used to cover the broadest possible range of different antigens present in CMEs. Binding of serum antibodies was visualized by subsequent incubation with HRP-conjugated goat anti-guinea pig IgG. The HRP catalyzes the chromogenic reaction of 3-amino-9-ethylcarbazole (AEC).

Figure 4.23 shows that all CME preparations from IPBS Toulouse (CME_{BCG}, CME_{H37Rv}, as well as CME *M. marinum* and CME *M. fortuitum)* contained antibody-recognized antigens. Staining of the CME_{BCG} preparation was observable in the range of approximately 21 to 60 kDa with the strongest staining in the molecular weight range of ~ 24 to 40 kDa. CME_{H37Rv} was stained in the range from ~ 21 to 70 kDa with the strongest staining in the range of ~ 23 to 38 kDa. CME *M. marinum* was stained in a wide molecular weight range (~ 23 to 130 kDa) with the strongest staining being observable in the range of ~ 26 to 42 kDa. Staining of the CME *M. fortuitum* preparation was detectable within the range of ~ 15 to 100 kDa with 3 intensifications in decreasing strength: ~ 23 – 35 kDa, ~ 80 – 95 kDa, and ~ 40 – 55 kDa. For comparison purposes, the *M. tuberculosis* lipoglycan ManLAM stained in the range of ~ 22 to 120 kDa, with 4 intensifications in the ranges of (in decreasing order of intensity) ~ 55 – 70 kDa, ~ 23 – 35 kDa, ~ 95 – 100 kDa, and ~ 110 – 120 kDa. Among the other samples, antigens of similar sizes (approximately 25 to 35 kDa) were obvious in three CMEs prepared according to the PEI 2015 protocol (CME EIA 1797 and to a lower extent in CMEs Beijing 1934 and Haarlem 2336). These *M. tuberculosis* strains were all inactivated with chloroform-methanol 1:1 prior to shipment from the Research Center Borstel. This initial chloroform-methanol solution was dried off afterwards and the dried material was again extracted with chloroform-methanol 2:1 as described in the protocol “PEI 2015” (see section 3.3.3). It must be considered that the initial chloroform-methanol extraction already dissolved antigens, such as e.g., ManLAM, out of the bacterial cell wall, rendering them more easily dissolvable in chloroform-methanol 2:1 afterwards. However, again, stimulatory and non-stimulatory samples were found among these preparations showing staining in Western blot analysis (see **Figure 4.25**). Minute amounts of staining could furthermore be recognized in CME CDC 1551, CME HN 878, and CME MAP. The 15 kDa antigen in the CME from *M. canetti* was observed in all Western blots and is therefore not assumed an artifact caused by, e.g., accumulation of loading dye. The nature of this antigen could not be further determined.

Thin layer chromatography was performed to compare the lipid content of the preparations. Due to the low sensitivity of the detection on TLC plates, 500 µg of the CME preparations

were analyzed per lane. Chloroform-methanol-water (65:25:4) was used as the mobile phase. This solvent mixture favors the migration of amphiphilic molecules in the silica gel of the stationary phase, it is hence suited to separate lipopeptides (Symmank *et al.* 2002; Vater *et al.* 2002; Smyth *et al.* 2010). Among different solvent mixtures (chloroform-methanol-water 2:1:0 or 60:35:8 or 65:25:4), chloroform-methanol-water 65:25:4 produced the most distinct bands with the highest resolution (data not shown). Considering the signal intensities of the separated components, large amounts of mobile ingredients (putatively lipids and/or lipopeptides; subsequently summarized as “lipids”) were detectable in all CME preparations (**Figure 4.24**). The lowest lipid contents were observed in the “PEI 2014” preparations of which both the initial materials for chloroform-methanol extraction were heat-inactivated bacterial wet masses. This low lipid content was in accordance with a likewise non-detectable amount of proteins and antigens in the previous analyses (**Figure 4.22**, **Figure 4.23**, **Figure 4.24**). However, the low lipid content in both preparations did not correlate with the stimulatory potential on PBMCs of BCG-sensitized guinea pigs (high in CME AN5, low in CME MAA, **Figure 4.25**). The highest lipid contents were observed in all preparations from IPBS Toulouse and MRL Fort Collins with the overall highest lipid content displayed in the MRL Fort Collins preparation CME EAI 91/0079, which did not show strong silver staining (**Figure 4.22**). Since purified ManLAM was not detected at all in thin layer chromatography (**Figure 4.24**), it was assumed that the high lipid content observed in various CME preparations was not due to ManLAM. No systematic differences in the general lipid contents of MTC and NTM could be detected.

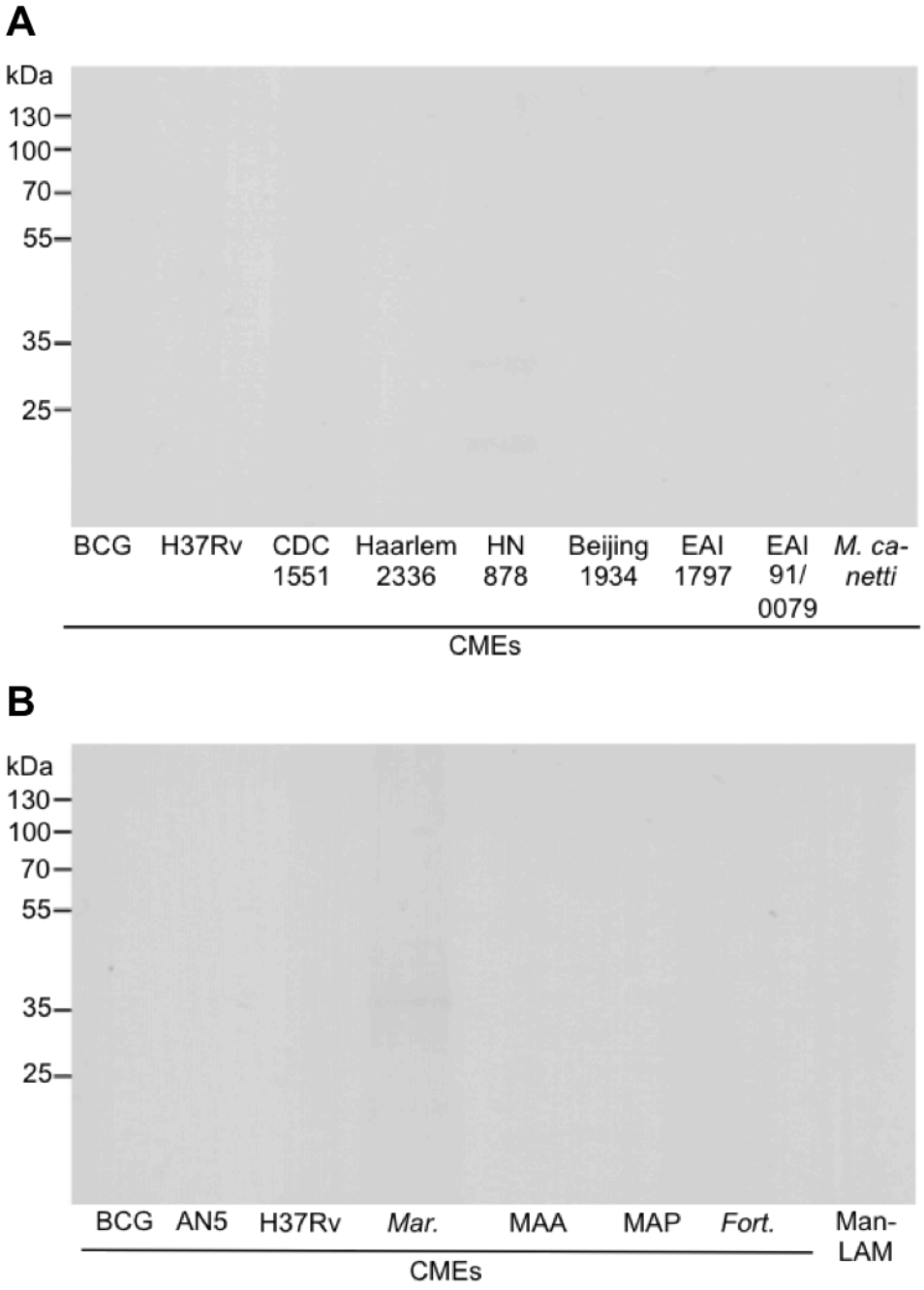

Figure 4.21 Comparison of the different chloroform-methanol extracts (CMEs) using SDS-PAGE and Coomassie staining.

A and B. Separation of 80 µg CME or 1 µg Man-LAM per slot by SDS-PAGE and subsequent staining with Coomassie Brilliant Blue G250.

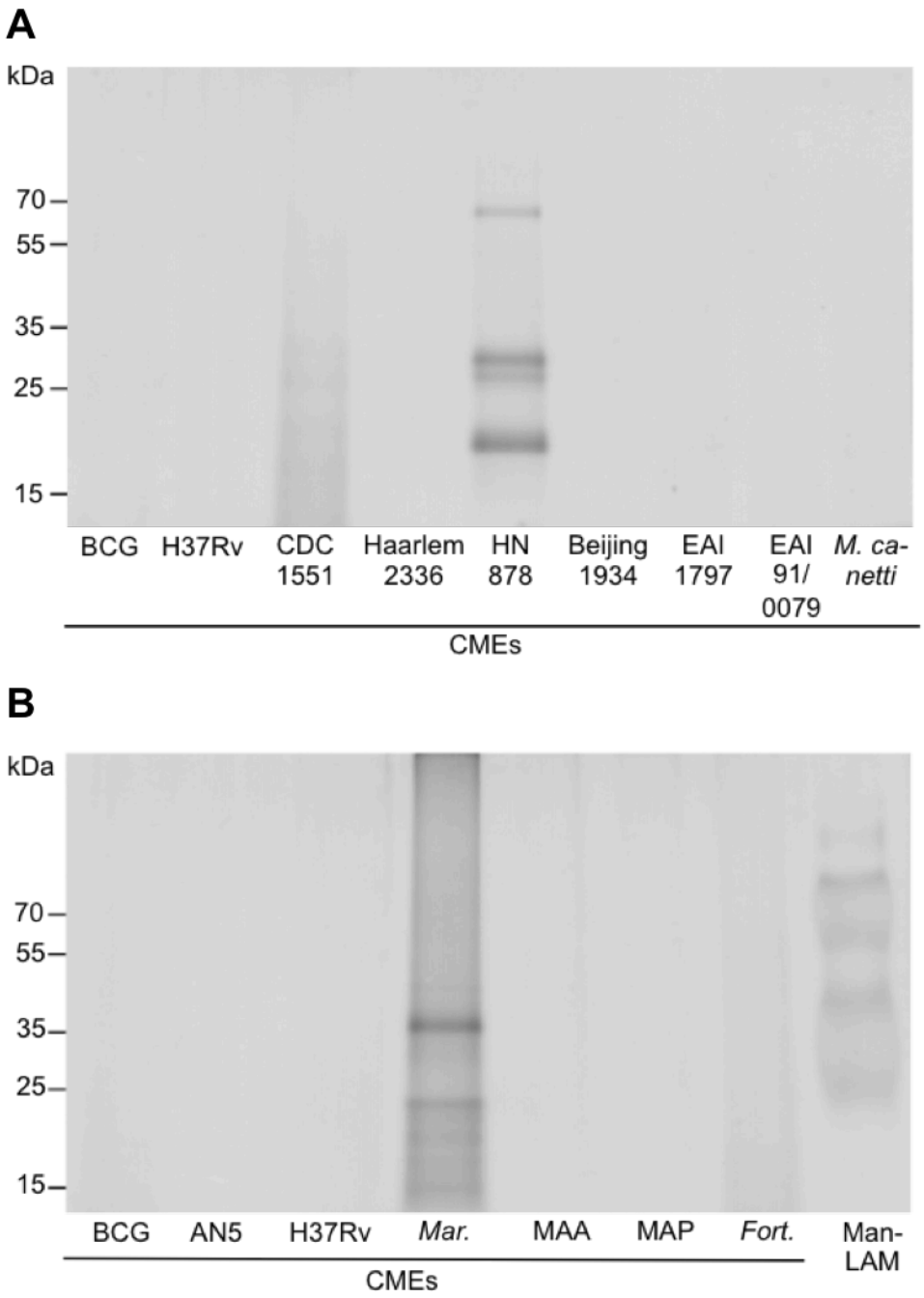

Figure 4.22 Comparison of the different chloroform-methanol extracts (CMEs) using SDS-PAGE and silver staining.

A and B. Separation of 10 µg CMEs or 0.5 µg Man-LAM per slot by SDS-PAGE and subsequent silver staining.

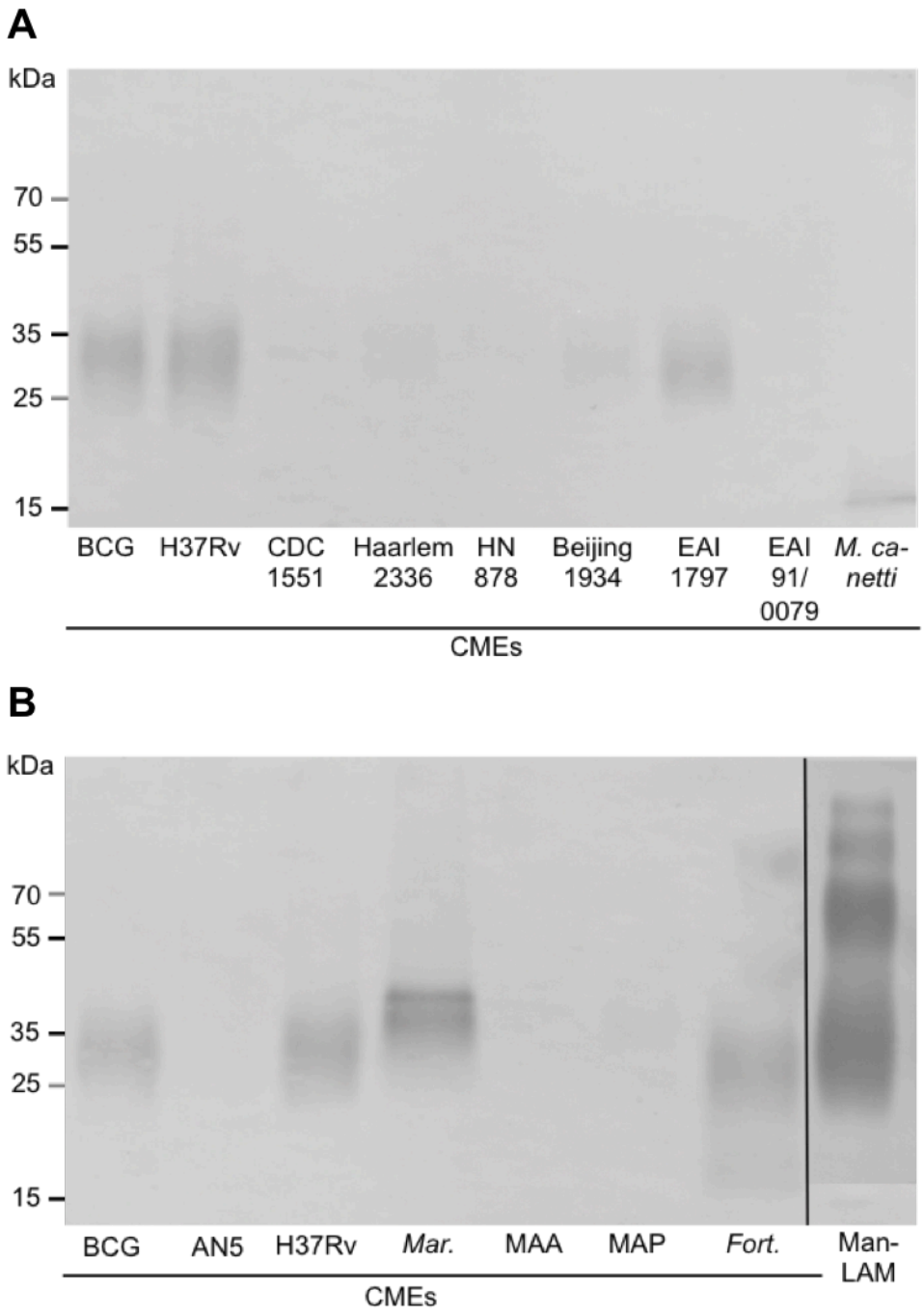

Figure 4.23 Comparison of the different chloroform-methanol extracts (CMEs) using Western blot analysis.

A and B. Separation of 80 µg CME or 1 µg Man-LAM per slot by SDS-PAGE. A Western blot was performed and developed with pooled sera of 10 BCG-sensitized guinea pigs, HRP-conjugated goat anti-guinea pig IgG and AEC.

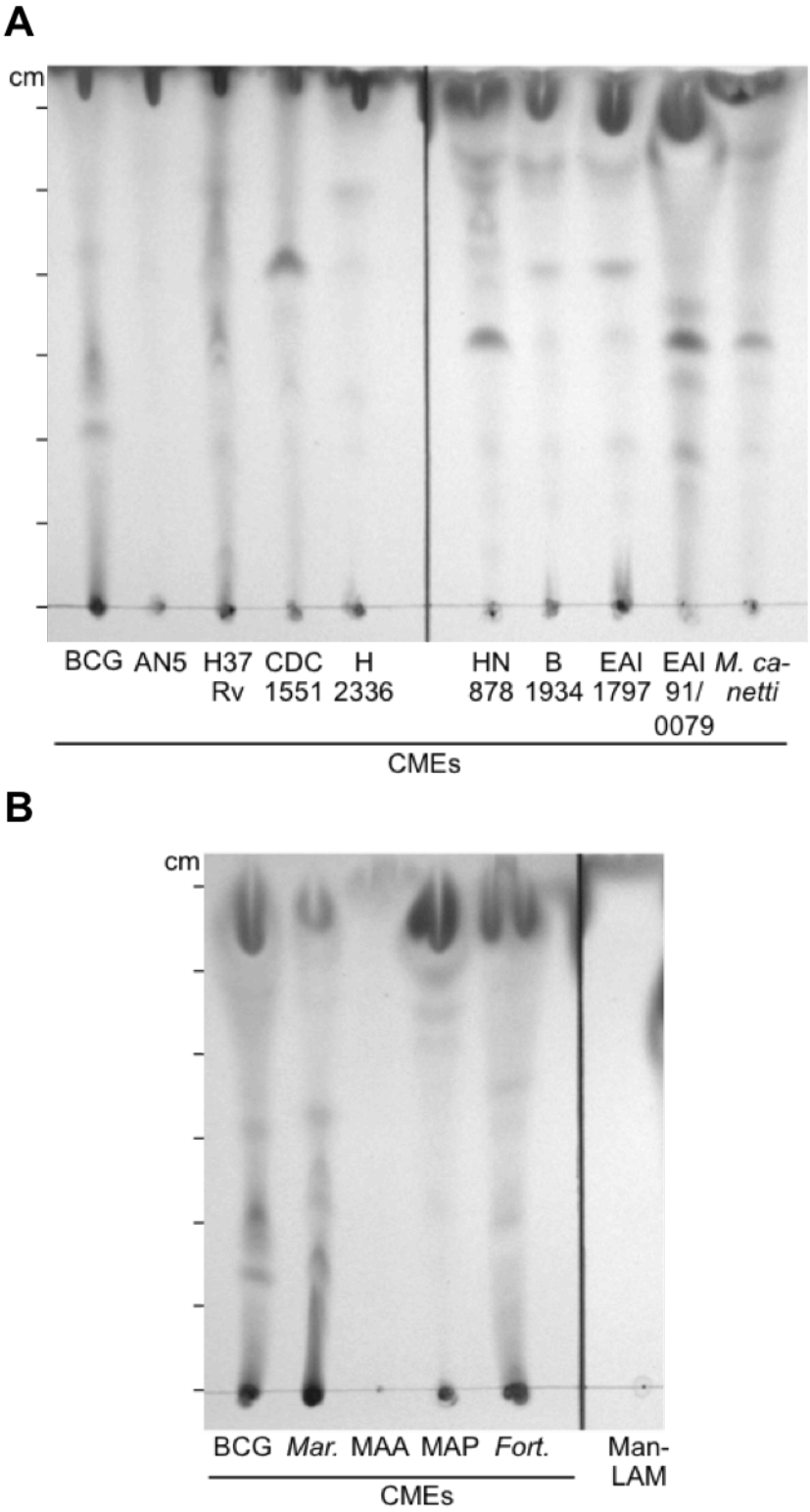

Figure 4.24 Comparison of the different chloroform-methanol extracts (CMEs) by thin layer chromatography.

A and B. Thin layer chromatography with chloroform-methanol-water (65:25:4) as the mobile phase. Quantity used per lane: 500 µg CME or 1 µg Man-LAM.

4.4.2 Strain specificity of the stimulatory antigens

BCG sensitization of guinea pigs induced T cells which proliferated upon stimulation with CME_{BCG} and CME_{H37Rv} (**Figure 4.5**). In contrast, they did not demonstrate such strong activation in response to lysates of *E. coli* and *S.* Typhi (**Figure 4.8**), suggesting specificity for mycobacteria. Therefore, the distribution of the stimulatory capacities among the genus *Mycobacterium* was investigated next.

To this end, CMEs prepared from strains of different mycobacterial species were tested in the *ex vivo* lymphocyte proliferation assay using PBMCs collected from 17 guinea pigs 30 days after BCG sensitization (**Figure 4.25**). The analysis revealed that all CMEs of MTC bacteria, except that of *M. canetti* which is remarkably not regularly listed as part of this complex (Whitman *et al.* 2012), stimulated strong lymphocyte proliferation which was significantly higher than the cut-off of 20 % $CFSE_{low}$ cells ($p \leq 0.05$, one-sample *t* test). The CME of *M. canetti* induced the relatively lowest lymphocyte proliferation among these preparations which did not exceed the 20 % cut-off significantly ($p > 0.05$).

All CME preparations of non-tuberculous mycobacteria (NTM) induced lymphocyte proliferation with the median below 20 % $CFSE_{low}$ cells with one exception – CME of *M. marinum* stimulated a marginal proliferation. On average, the proliferation in response to CME *M. marinum* did, however, not significantly differ from the 20 % cut-off ($p > 0.05$, one-sample *t* test). *M. marinum* is, based on the 16S rRNA, more closely related to the MTC bacteria than to the other NTM (Harmsen *et al.* 2003).

In detail, the median values and ranges of the *ex vivo* lymphocyte proliferation in response to the MTC- and NTM-derived CME preparations are listed in **Table 4.4**.

There were no specific proliferation patterns observable within the categories of MTC and NTM or within the individual mycobacterial species *M. bovis*, *M. tuberculosis*, and *M. avium*.

Table 4.4 ***Ex vivo*** **proliferation of lymphocytes from 17 BCG-sensitized guinea pigs in response to CME preparations of different strains of the** ***M. tuberculosis*** **complex and non-tuberculous mycobacteria.**

Antigen used for *ex vivo* stimulation		Percentage of $CFSE_{low}$ lymphocytes [%]		
Category	Antigen	Median	Min	Max
Negative control	Medium	11.4	1.0	18.5
Positive control	Tub12	48.0	20.5	65.8
M. tuberculosis complex-derived preparations	CME_{BCG}	44.4	30.1	70.2
	CME AN5	25.0	13.1	40.3
	CME_{H37Rv}	28.2	13.3	54.1
	CME CDC 1551	33.0	16.9	63.8
	CME Haarlem 2336	32.1	17.7	54.9
	CME HN 878	37.0	15.8	66.5
	CME Beijing 1934	27.5	14.4	57.4
	CME EAI 1797	43.1	10.1	64.4
	CME EAI 91/0079	33.0	13.0	46.4
	CME *M. canetti*	24.1	12.7	39.1
Non-tuberculous mycobacteria-derived preparations	CME *M. marinum*	21.3	4.9	50.7
	CME MAA	11.1	1.9	18.4
	CME MAP	18.3	8.0	33.8
	CME *M. leprae*	13.2	2.3	20.6
	CME *M. fortuitum*	13.0	3.4	16.3

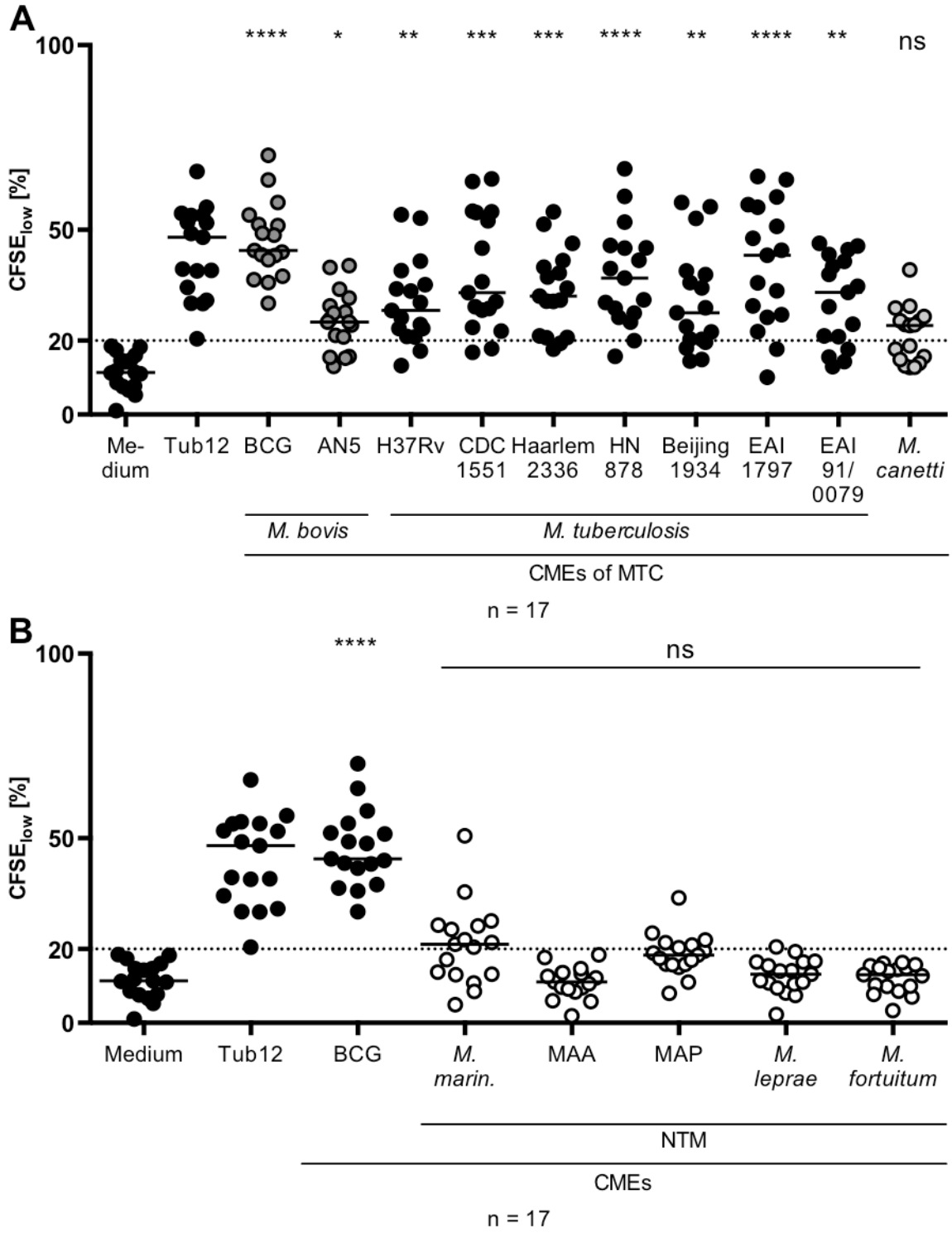

Figure 4.25 *Ex vivo* lymphocyte proliferation in response to CMEs is specific for the investigated bacteria of the *Mycobacterium tuberculosis* complex.

Results of the *ex vivo* lymphocyte proliferation assay. PBMCs of 17 guinea pigs 30 days after BCG sensitization were incubated with CMEs (10 µg/ml) or Tub12 (30 IU/ml) as the positive control or medium-only as the negative control. Dots represent the arithmetic means of the duplicate tested per antigen, per animal. Black lines indicate the median values over all animals, per antigen. One sample t-test was used to calculate whether the results per group significantly exceeded the 20 % cut-off. **A.** CME preparations obtained from members of the *M. tuberculosis* complex (MTC). **B.** CME preparations obtained from BCG and non-tuberculous mycobacteria (NTM).

4.4.3 Distribution of the stimulatory antigens within the bacterial cell

Young and Garbe (1991) and Wolfe *et al.* (2010) provided evidence that mycobacteria actively release strong antigens, such as lipoproteins. To test this in the context of *ex vivo* lymphocyte stimulation and the vaccine strain BCG, the PBMCs of BCG-sensitized guinea pigs were stimulated with different antigen preparations of BCG in the *ex vivo* lymphocyte proliferation assay.

Figure 4.26 displays the lymphocyte proliferation results of BCG-sensitized guinea pigs in response to different antigen preparations of BCG: live and heat-inactivated BCG bacteria, bacterial lysates deriving from BCG cultures in the exponential and static growth phase and culture supernatant obtained from a BCG culture in the exponential growth phase. BCG lysates represented the sterile-filtered soluble fractions of whole bacterial cells subjected to ultrasonication. Tub12, CME_{BCG}, and medium-only were used for control purposes.

Lysates of BCG bacteria, derived from cultures in either the exponential or static growth phase, BCG culture supernatant and CME_{BCG}, all induced very strong lymphocyte proliferation which was significantly above the 20 % cut-off ($p \leq 0.01$, one-sample *t* test) (CME_{BCG}: median 54.0 %, range 48.1 to 75.8 %; BCG lysate from the exponential growth phase: median 67.2 %, range 62.7 to 84 %; BCG lysate from the static growth phase: median 70.4 %, range 63.7 to 80.4 %). There were no significant differences between the lymphocyte proliferation results in response to the various BCG lysates and the culture supernatant preparation ($p > 0.05$, student's *t* test).

Furthermore, both live and heat-inactivated BCG bacteria induced lymphocyte proliferation in a dose-dependent manner. However, the lymphocyte proliferation in response to live BCG was significantly stronger in doses of 1 and 0.1 µl/ml ($p \leq 0.05$, student's *t* test).

The analysis of the lymphocyte proliferation stimulated by cell-free BCG culture supernatant harvested in the exponential growth phase (median 62.5 %, range 53.2 to 82.1 %) revealed that the strong antigens were not only directly associated with the bacterial cell but must also be actively released.

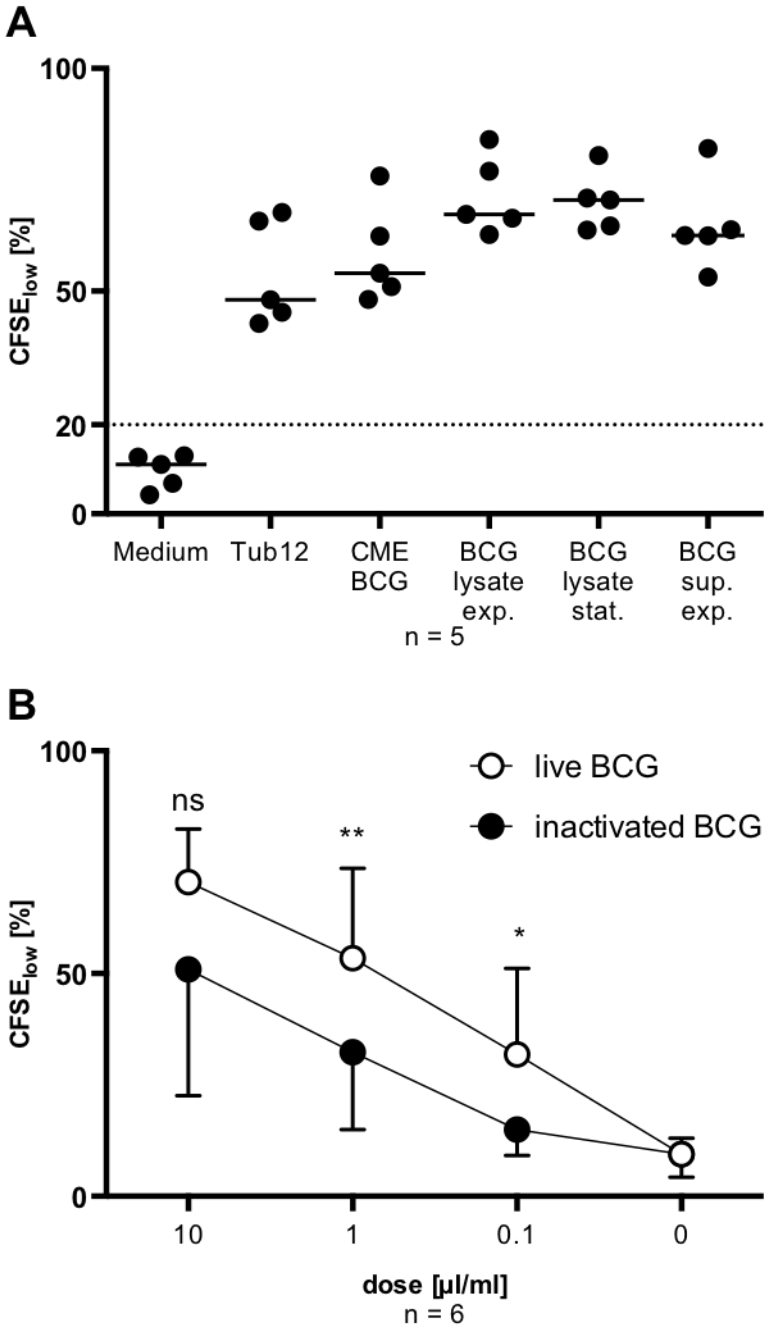

Figure 4.26 Relevant BCG antigens capable of inducing *ex vivo* lymphocyte proliferation are cell-associated as well as secreted.

Results of the *ex vivo* lymphocyte proliferation assay. PBMCs of guinea pigs 30 days after BCG sensitization were incubated with the different antigens for 5 days. **A.** Lymphocyte proliferation in response to different antigens (CME_{BCG} 10 µg/ml; BCG bacterial lysate deriving from exponential (exp.) or static (stat.) culture growth phases 100 µg/ml; BCG culture supernatant from a culture in the exponential growth phase (sup. exp.) 10 µl/well). Black dots represent the arithmetic means of the duplicate tested per antigen, per animal. Black bars represent the median values over all animals, per antigen. **B.** Lymphocyte proliferation in response to live or heat-inactivated BCG in doses of 10 / 1 / 0.1 µl/ml. The dots represent the median values over all animals, per antigen, per dose. Asterisks describe the significances of difference between the lymphocyte proliferation to the live BCG stimulus compared with the heat-inactivated BCG in the same dose (student's *t* test).

4.5 Approaches to identify individual mycobacterial lipopeptide antigens

So far, it could be demonstrated that MTC bacteria extensively express and secrete antigens capable of inducing strong proliferative responses in lymphocytes obtained from MTC-sensitized guinea pigs. Evidence from the present and previous studies suggested that those antigens were lipopeptides. This was in particular proposed by significantly reduced stimulatory capacities of the lipid preparations after either protease treatment or delipidation, and by the strong T cell response induced by stimulation with a lipopeptide-enriched subfraction of *M. tuberculosis* H37Rv. However, a distinct lipopeptide or a purified fraction of a few lipopeptides responsible for this strong stimulation has not yet been identified.

Tuberculin and chloroform-methanol extracts both constitute mixtures of large numbers of mycobacterial antigens. The antigens that they contain are not completely defined and neither are their proportions. To further characterize the strong antigens described in this study, individual antigens should be identified from the heterogeneous mixture contained in the CME. To this end, two complementary approaches were investigated:

1. Chromatographic purification of lipopeptides from CME;
2. Biochemical synthesis of N-terminal peptides of *M. tuberculosis* known, probable and possible lipoproteins.

4.5.1 Chromatographic purification of mycobacterial lipopeptide antigens

It was demonstrated in previous experiments that normal phase chromatography (Layre *et al.* 2009) as well as reversed phase chromatography (Dr. Max Bastian, personal communication) was suited to purify mycobacterial antigens which were capable of stimulating mycobacteria-reactive human T cell clones.

4.5.1.1 Solubility of CME antigens in different solvents

To investigate which solvent, suitable for RPC, was ideal to dissolve the antigens for subsequent chromatographic purification, CME_{BCG} was dried and resuspended in different concentrations of different solvents by ultrasound. After centrifugation of the samples, the supernatants were collected as soluble and the pellets as insoluble portions. The solvents

were dried off and the antigens resuspended in medium to test them in the *ex vivo* lymphocyte proliferation assay.

The results depicted in **Figure 4.27** demonstrate that the CME antigens were partially soluble in 17.5 % propanol/H_2O and 25 % AcN/H_2O. A higher concentration (25 %) of only AcN, but not methanol and propanol, seemed to be suited to dissolve stimulatory antigens.

In detail, the stimulatory ingredients of CME_{BCG} were insoluble in low AcN/H_2O concentrations (10 % and 17.5 %). However, their solubility increased at 25 % AcN/H_2O, although there were still significantly more insoluble antigens. When dissolving CME_{BCG} in propanol/H_2O, there was a slight increase in the solubility of the stimulatory antigens at a concentration of 17.5 % propanol. However, the solubility decreased in the higher concentration (25 %). The stimulatory antigens of CME_{BCG} were completely insoluble in 5 – 17.5 % methanol/H_2O. Furthermore, concentrations of 25 % propanol/H_2O and 25 % methanol/H_2O completely abrogated the stimulatory capacities of CME_{BCG}.

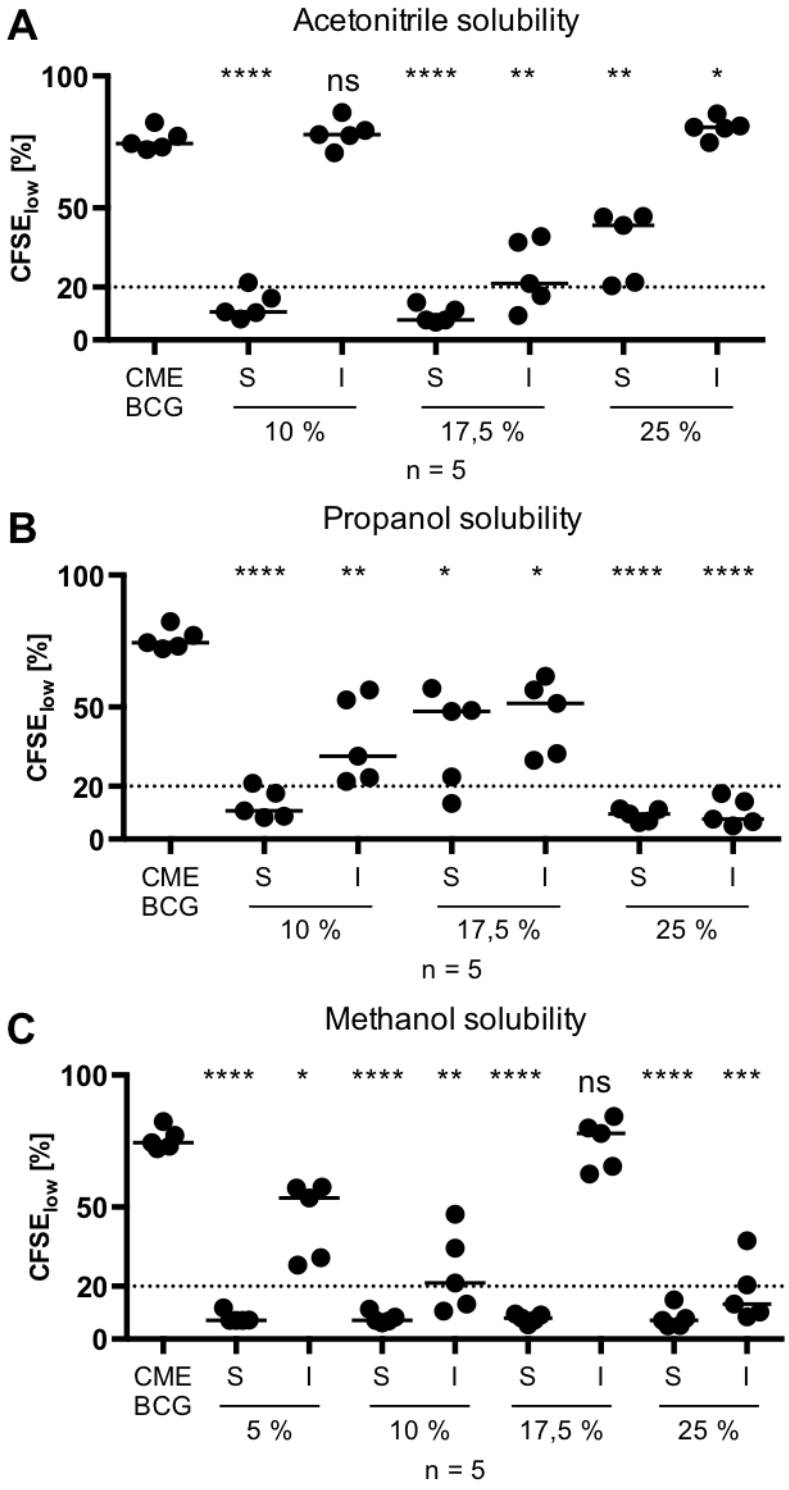

Figure 4.27 Solubility of chloroform-methanol-extracted BCG antigens in different solvents.

Results of the *ex vivo* lymphocyte proliferation assay. CME_{BCG} was dried and redissolved in the indicated solvents. After centrifugation, the soluble (S) and insoluble (I) portions were separated, dried and used for stimulation of PBMCs obtained from guinea pigs at day 60 after iAN5 sensitization. CME_{BCG} 10 µg/ml. Black dots represent the arithmetic means of the duplicate tested per antigen, per animal. Black bars represent the median values over all animals, per antigen. Asterisks indicate the significances of difference between the lymphocyte proliferation in response to the untreated CME_{BCG} and the extracted portions. Solubility and stimulatory capacities of CME_{BCG} in different concentrations of **A.** acetonitrile; **B.** propanol; **C.** methanol.

4.5.1.2 Chromatographic approaches and initial characterization of purified fractions

4.5.1.2.1 Chromatographic purification attempt with initial phenol partitioning

The first chromatographic purification attempt aimed at fractionizing a portion of CME which was already enriched in lipopeptides through phenol partitioning. To enrich the lipopeptides, a similar strategy as for the generation of LppEL was followed by partitioning CME_{BCG} with phenol (Lee *et al.* 2002). Due to its cytotoxicity the phenol was subsequently removed from the antigens by dialysis against water.

Though adaptive immune responses to lipopeptides were investigated in this study, triacylated lipopeptides are also well known for the induction of TLR2 signaling (Nakayama *et al.* 2012). The HEK TLR2 CD14 293 cell line is sensitive to TLR2 agonists and subsequently activates the transcription factor NF-κB which can be detected in the culture supernatant using Quanti-Blue™ dye. Therefore, a TLR2 assay was used as a functional screening test in the series of experiments presented here to verify whether TLR2 agonistic lipopeptides were still present after extraction or chromatographic fractionation of mycobacterial antigen mixtures.

As displayed in **Figure 4.28**, the phenol-partitioned CME_{BCG} in concentrations of 10 / 1 / 0.1 / 0.01 µg/ml induced strong TLR2 signaling, which was similar to the TLR2 activity stimulated by the control lipoprotein Pam3CSK4.

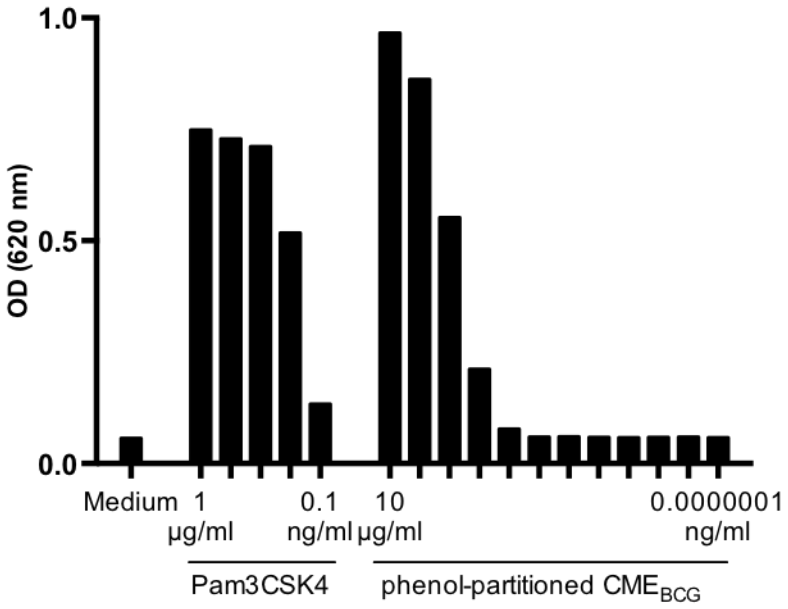

Figure 4.28 The phenol-partitioned CME_{BCG} contains TLR2 ligands.

Results of a 10-fold serial dilution of phenol-partitioned CME_{BCG} in the TLR2 assay. Medium-only served as the negative control. A 10-fold serial dilution of the synthetic lipopeptide Pam3CSK4 constituted the positive control for TLR2 ligands. Each black column represents the arithmetic mean value over the duplicate tested per antigen concentration.

Subsequently, the phenol-partitioned CME_{BCG} was subjected to a reversed phase chromatography using a C4 silica column and a gradient of 100 % H_2O to 100 % AcN. The column was re-equilibrated to 100 % H_2O in the same run.

Results of the chromatographic fractionation of phenol-partitioned CME_{BCG} are presented in **Figure 4.29**. A total of 24 fractions were collected in this run. The early and wide elevations of the chromatogram suggested that many analytes did not bind to the column. To investigate this assumption, all fractions, with the exception of F1, were tested as follows.

First, the concentration of total material dissolved in a particular fraction was obtained by drying a determined volume of the fraction, weighing the dried residues and back-calculating to their concentration per ml. The highest concentrations of total material were observed in the fractions F5 through F10 and F18 through F24. Some fractions contained virtually no material.

The peptide content in the fractions was determined using the Bradford assay. In accordance with the chromatogram and the concentrations of total material, highest peptide contents were detected in fractions F5 through F11 as well as in F21, F22, and F24.

The TLR2 activity within the fractions was analyzed by the TLR2 assay. The fractions were tested twice in this assay: first with an equal volume (10 µl/ml) and second, at equal

concentration (10 µg/ml) as far as a concentration could be determined. Similar to the above-mentioned results, the strongest TLR2 activity was observed in fractions F5 through F10 and F21 through F24. The reactivity pattern was the same regardless of whether the fractions were tested at equal volume or equal concentration.

A second and a third chromatography run were conducted with phenol-partitioned CME_{BCG} and phenol-partitioned CME_{H37Rv}. The elution time and the number of collected fractions were increased in order to achieve a better resolution, but these approaches did not yield sufficient resolution either (data not shown).

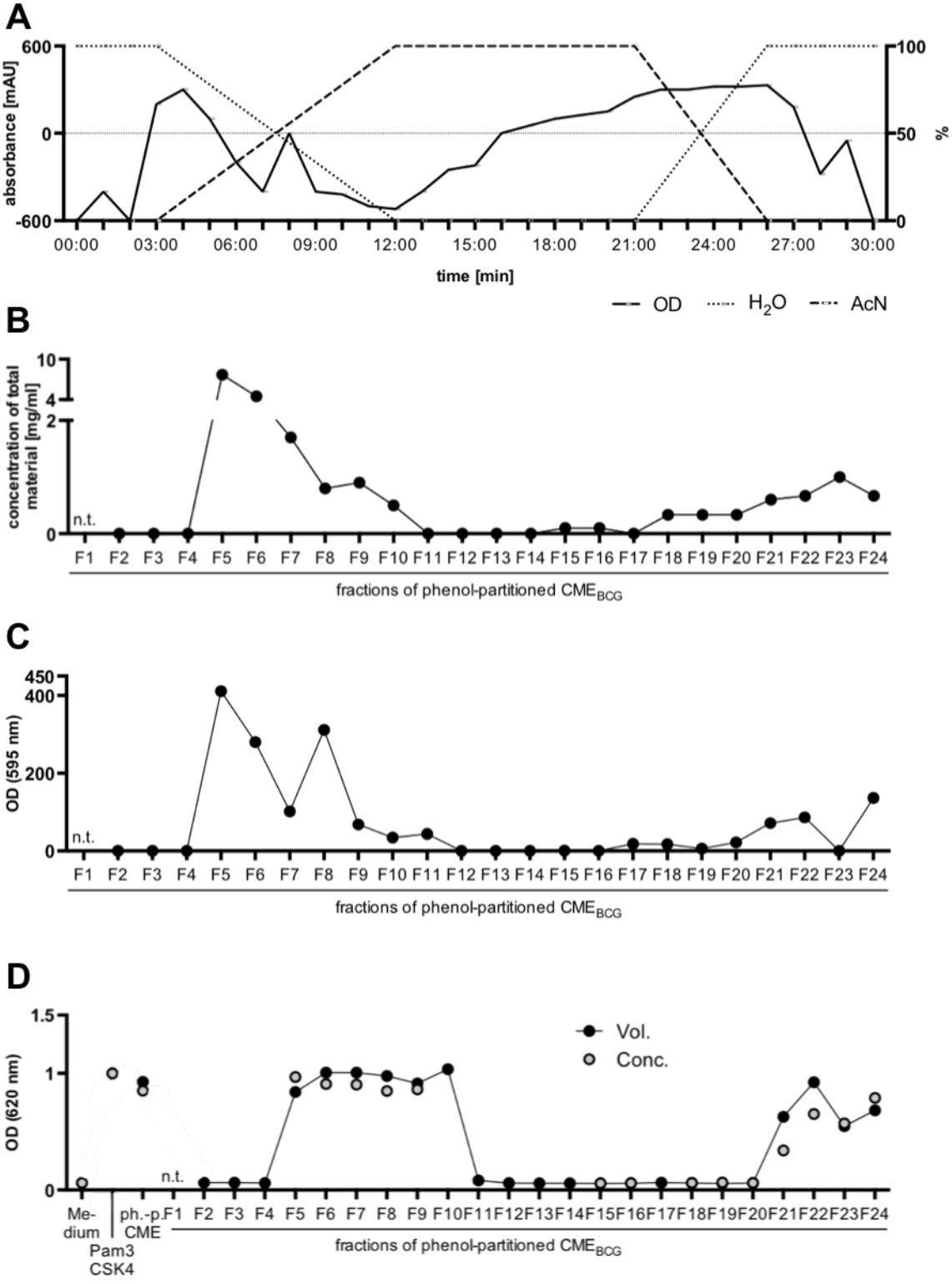

Figure 4.29 Characteristics of the fractions of the phenol-partitioned CME_{BCG} obtained by C4 reversed phase chromatography.

A. Chart of the C4 reversed phase chromatography of phenol-partitioned CME_{BCG} with gradients of 100 % H_2O to 100 % AcN and in reverse. **B.** Concentrations of total material. **C.** Peptide contents (results of the Bradford assay). **D.** Results of the TLR2 assay. Cells were stimulated with phenol-partitioned CME_{BCG} (ph.-p. CME) and fractions at equal volume (10 µl/ml, black dots) and, if a concentration could be determined, at equal concentration (10 µg/ml, grey dots) as well. Pam3CSK4 1 µg/ml.

4.5.1.2.2 Chromatographic purification attempt with preselection of lipophilic peptides

Another chromatographic approach to purify lipopeptides from CME was investigated. This approach aimed at preselection of lipophilic peptides and thereby reduction of the overall quantity of antigens through dissolving dried CME_{BCG} in 40 % AcN. The insoluble portion was discarded after centrifugation. A C18 column was used for high-performance liquid chromatography (HPLC) to achieve the most hydrophobic interactions between the column and the analytes. The gradient was adjusted to range from 40 to 97 % AcN/H_2O.

One distinct peak at approximately 50 % AcN/H_2O and 3 distinct peaks at approximately 80 % AcN were identified using this chromatographic approach (**Figure 4.30**). The pattern was reproducible and observed in several runs.

To investigate whether these peaks represented lipopeptides, the procedure was repeated using proteinase K-treated or delipidated CME_{BCG} (according to the protocols in section 3.3.9). The early peak at 50 % AcN was clearly reduced after proteinase K treatment and it was completely abolished after delipidation by mild sodium hydroxide treatment (**Figure 4.30**). These findings suggested that the early peak was indeed due to lipopeptides. The other peaks were not altered by the proteinase K, but destroyed by the mild sodium hydroxide treatment, indicating that these peaking analytes rather represented true lipid species. However, none of the corresponding fractions induced a clear reactivity in the guinea pig *ex vivo* lymphocyte proliferation assay (data not shown).

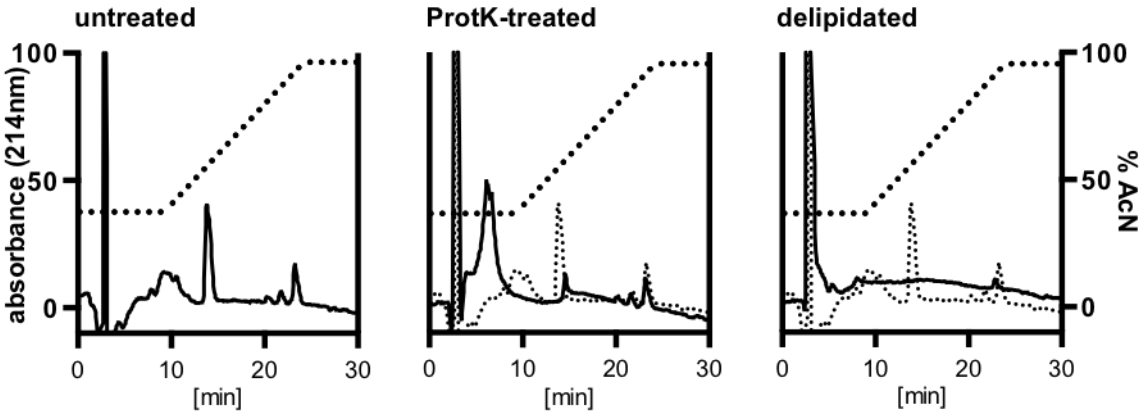

Figure 4.30 Chromatographic fractionation of mycobacterial antigens contained in CME_{BCG} after preselection of lipophilic peptides.

CME_{BCG} was dried and redissolved in 40 % AcN. A C18 reversed phase HPLC was performed with the AcN-soluble portion using an AcN/H_2O gradient of 40 to 97 % (left panel). Additionally, the same procedure was performed using proteinase K-treated (middle) or delipidated CME_{BCG} (right panel).

4.5.1.3 Lymphocyte stimulation by the chromatographically purified fractions

The fractions obtained during the first attempt of chromatographic fractionation of phenol-partitioned CME_{BCG} were screened for their antigenic potential in the *ex vivo* lymphocyte proliferation assay. No specific criteria were employed on the validity of these screening assays as they required many cells and were therefore performed only with low animal numbers (n = 2 in the *ex vivo* lymphocyte proliferation assay with reduced antigen concentrations, see below).

During the characterization in the TLR2 assay (**Figure 4.29**), the fractions, though possessing diverse concentrations of total material and peptides, did not induce principally different extents of TLR2 signaling in the target cells when being employed in equal volumes or equal concentrations. For feasibility reasons, equal volumes of all antigens were therefore employed in the guinea pig *ex vivo* lymphocyte proliferation assay (100 µl/ml). Comparison of concentrations of the respective fractions revealed that particularly high amounts of possibly antigenic material were used with the initial material of phenol-partitioned CME_{BCG} and with fractions F5 – F9, F21, F22, and F24. Flowcytometric analysis of the stimulated lymphocytes suggested that several of these fractions were cytotoxic. Cytotoxicity was determined by nearly abolished lymphocyte counts which were significantly lower than the count in the medium-only stimulated wells ($p \leq 0.05$ in F3, F5 – 7, F12, F21, and F22, ratio *t* test) (see section 3.8.4) (data not shown).

For this reason, the assay was repeated with a lower concentration of phenol-partitioned CME_{BCG} and chromatographic fractions (33 µl/ml) (**Figure 4.31**). At this concentration, the above-mentioned fractions (F3, F5 – 7, F12, F21, and F22) did not induce significantly reduced lymphocyte counts in comparison with the medium-only control ($p > 0.05$, ratio *t* test), though the lymphocyte counts, in particular in the fractions F5, F6, and F21, were still nearly abolished. Furthermore, the observed lymphocyte proliferation in response to the other fractions was low (< 20 % $CFSE_{low}$ cells) and most importantly, no major stimulatory fractions could be determined.

The same pattern was observed with the fractions obtained during the second and third attempts of chromatographic purification of antigens from phenol-partitioned CME as well as with the fractions obtained through chromatographic fractionation after preselection of lipophilic peptides (data not shown).

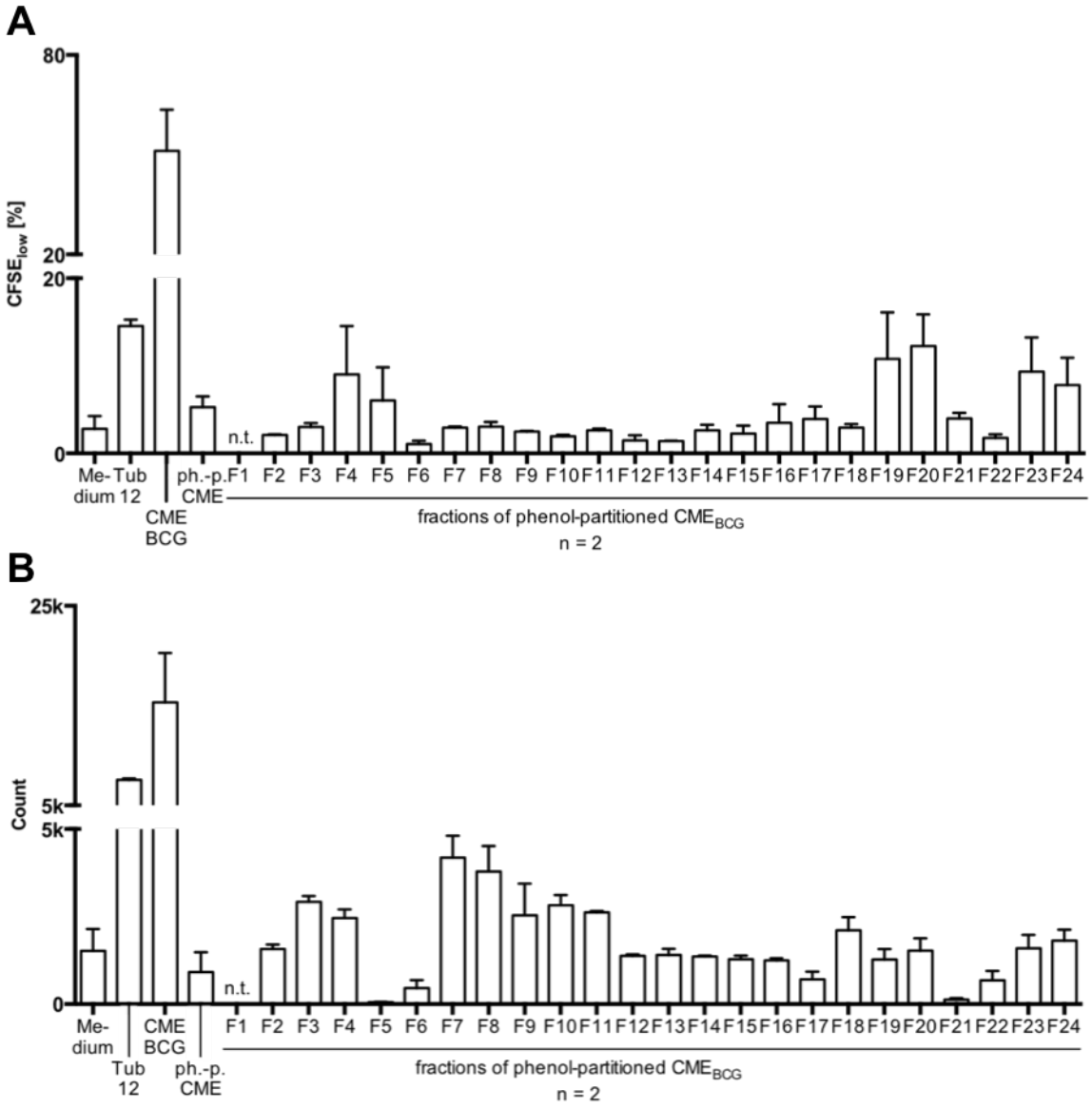

Figure 4.31 Guinea pig *ex vivo* lymphocyte proliferation in response to the fractions of the phenol-partitioned CME_{BCG} obtained by C4 reversed phase chromatography.

Ex vivo PBMCs from guinea pigs 60 days after iAN5 sensitization were labeled with CFSE and incubated with medium (negative control), Tub12 (30 IU/ml; positive control), CME_{BCG} (10 µg/ml), phenol-partitioned CME_{BCG} (ph.-p. CME, 33 µl/ml) or the fractions obtained from ph.-p. CME by chromatography (33 µl/ml). Each antigen was tested in duplicate per animal. Of this duplicate, the arithemtic mean was calculated and considered for median calculation over all animals, per antigen. This median value and the value range are displayed as columns and bars, respectively. Flowcytometric analysis of **A.** the percentage of $CFSE_{low}$ lymphocytes (*ex vivo* lymphocyte proliferation assay); **B.** the total count of lymphocytes to test for cytotoxicity of the antigens.

Apart from lymphocyte proliferation, stimulatory antigens might induce cytokine secretion by certain target cells which can be measured in specific ELISAs. To this end, the chromatographic fractions of the phenol-partitioned CME_{BCG} were tested for their capacity to induce TNFα secretion in cells of the guinea pig T cell line $H37_{2210}$-B10. This T cell line was established during this study (see section 4.6). The secreted levels of TNFα were determined using a commercially available guinea pig TNFα ELISA.

In accordance with the above-mentioned results, the TNFα secretion by the guinea pig T cell line revealed the majority of the stimulatory capacities within fractions of the first half of the chromatogram (F4 – F10) and minor stimulation in the last fractions (F22 – F24) (**Figure 4.32**). Additionally, the fractions F13 and F14 displayed stimulatory activity in this assay.

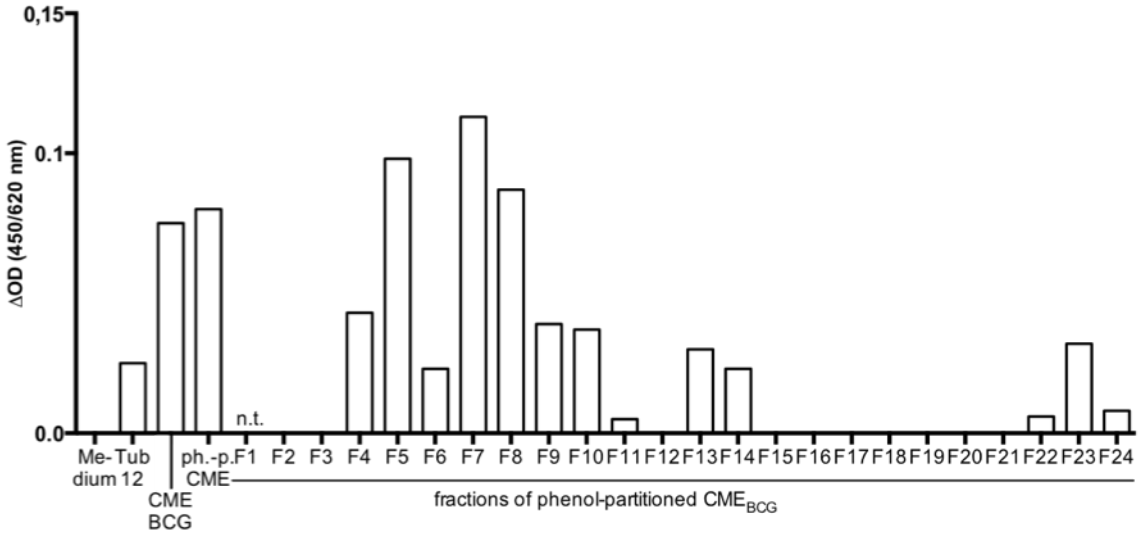

Figure 4.32 TNFα secretion by the guinea pig T cell line $H37_{2210}$-B10 upon stimulation with the fractions of the phenol-partitioned CME_{BCG} obtained by C4 reversed phase chromatography.

Cells of the guinea pig T cell line $H37_{2210}$-B10 were co-incubated overnight with syngenic irradiated PBMCs and the phenol-partitioned CME_{BCG}, the chromatographic fractions (11 µl/ml), Tub12 (30 IU/ml) or CME_{BCG} (10 µg/ml). The supernatants were collected and analyzed for their TNFα content in a guinea pig TNFα ELISA. The y-axis indicates the OD values normalized by background subtraction.

4.5.2 *Ex vivo* lymphocyte proliferation in response to synthetic N-terminal peptides of *M. tuberculosis* lipoproteins

The stimulatory potential of synthetic N-terminal peptides of *M. tuberculosis* lipoproteins was investigated complementary to the chromatographic purification attempts. According to our hypothesis, the actual immune response is directed to the N-terminus of the protein part of the triacylated lipoprotein while the lipid moiety is important for processing of the antigen through enhanced recognition by APCs. However, PBMC proliferation may also be inducible when MTC-sensitized lymphocytes are pulsed with large amounts of unlipidated N-terminal peptides of mycobacterial lipoproteins.

To this end, sequences of all *M. tuberculosis* proteins annotated as “putative lipoproteins” (n = 126) were extracted from the TBdatabase (http://www.tbdb.org; January 10, 2013) and scanned for lipobox motifs and for cysteins at approximately position 20 of the preprolipoprotein sequence. “Classical patterns” providing convincing evidence to represent lipoproteins, i.e., classical lipobox motifs [LVI][ASTVI][GAS][C]) (Babu *et al.* 2006) and a cystein at the above-described position, “non-classical patterns” which described sequences in front of cystein which differed in one position from the lipobox motif, as well as sequences which did neither display a lipobox motif nor a cystein at the anticipated position were identified. For testing in the guinea pig *ex vivo* lymphocyte proliferation assay, sequences of the N-termini of the mature proteins were synthesized with the length of 15 amino acids each (75 sequences displaying classical patterns, including one displaying a non-classical pattern in addition, and 3 sequences displaying non-classical patterns (see below). Additionally, the signal peptide sequences of the 9 best-characterized *M. tuberculosis* lipoproteins (see section 2.3.4.2) were synthesized with the length of 15 amino acids each and in an overlapping manner (AA1-15 and AA11-25). Peptide sequences are listed in Annex 5.

As depicted in **Figure 4.33**, the lymphocyte proliferation responses to the synthetic signal peptides of *M. tuberculosis* lipoproteins were generally low (< 10 % $CFSE_{low}$ cells). However, some signal peptide-derived epitopes induced a certain T cell reactivity. The respective peptides were in particular LppX-1 (AA1-15) (median 2.1 %, range 0.2 to 6.5 %), LprG-2 (AA11-25) (median 3.2 %, range 0.9 to 8.7 %) and PstS3-2 (AA11-25) (median 5.4 %, range 1.9 to 41.8 %). The lymphocyte proliferation stimulated by the LprG-2 peptide (AA11-25) was significantly stronger than the lymphocyte proliferation in the medium-only control ($p \leq 0.05$; student’s *t* test).

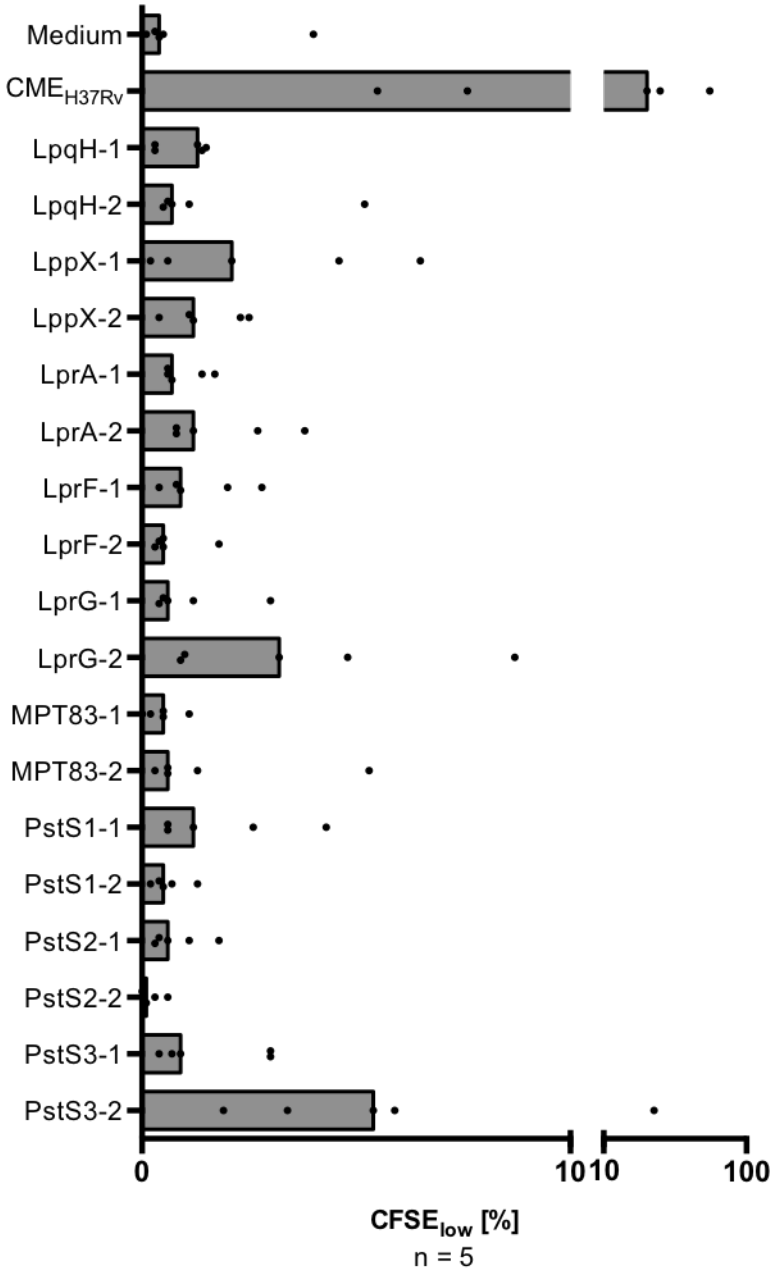

Figure 4.33 ***Ex vivo*** **lymphocyte proliferation in response to synthetic signal peptides of** ***M. tuberculosis*** **lipoproteins.**

Results of the *ex vivo* lymphocyte proliferation assay. PBMCs from 5 guinea pigs at day 30 after BCG sensitization were incubated with the indicated synthetic peptides (100 µg/ml) for 5 days. The two lines per peptide on the vertical axis represent the two overlapping, N-terminal signal peptide sequences of 15 amino acids each (see Annex 5). Black dots represent the arithmetic means of the duplicate tested per antigen, per animal. Grey columns represent the median over all animals, per antigen.

Apart from the signal peptides, the above-described unlipidated synthetic peptides representing the first 15 AA of the N-terminal domains of the mature lipoproteins were tested in the *ex vivo* lymphocyte proliferation assay. The proliferative responses to these peptides were significantly lower compared with stimulation by complex antigen mixtures such as CME and LppEL, but as with the signal peptides some reactivity could be observed upon stimulation with some of the N-terminal peptides.

To enhance the comprehensibility, presentation of the results with the individual peptides were stratified according to the description of the respective lipoprotein in the *M. tuberculosis* gene banks (TBdatabase and tuberculist, see Annex 5): Peptides derived from lipoproteins with known or assumed characteristics or function are shown in **Figure 4.34** and peptides of sequences annotated as “probable”, “probable conserved”, “possible”, or “possible conserved” lipoproteins are depicted in **Figure 4.35**.

Distinct proliferation patterns were observed in response to peptides derived from lipoproteins with described characteristics or functions (**Figure 4.34**), in particular upon stimulation with LppW (a probable conserved alanine-rich lipoprotein) and LpqL (a probable lipoprotein amino peptidase). LppW stimulated a median lymphocyte proliferation of 2.1 % $CFSE_{low}$ cells (range 0.7 to 5.3 %) which was significantly stronger than the lymphocyte proliferation in response to the medium-only control ($p \leq 0.05$, student’s *t* test). LpqL stimulated a median lymphocyte proliferation of 1.8 % (range 0 to 2.1 %) which did not differ significantly from the medium-only control ($p > 0.05$).

It is remarkable that the PBMCs of one of the 5 BCG-sensitized guinea pigs investigated in this series of experiments (guinea pig #3) proliferated much stronger in response to several peptides than the PBMCs of the other animals. CME_{H37Rv} and the peptides eliciting such strong proliferation (≥ 9.9 % $CFSE_{low}$ cells) are listed below. In this list, the first number after the colon indicates the percentage of $CFSE_{low}$ cells observed with the PBMCs of the particular animal, while the numbers behind the semicolon describe the median and range of $CFSE_{low}$ cell percentages in the remaining 4 guinea pigs.

- CME_{H37Rv}: 37.3 %; 26.7 % (range 5.5 to 76.8 %)
- LppJ (only defined as “lipoprotein”): 9.9 %; 0.75 % (range 0.2 to 1.4 %)
- LpqM (possible lipoprotein peptidase): 10.1 %; 0.9 % (range 0.5 to 1.4 %)
- LprL (possible mce-family lipoprotein): 20.9 %; 0.9 % (range 0.7 to 2.0 %)
- LprM (possible mce-family lipoprotein): 12.2 %; 0.5 % (range 0.1 to 0.8 %)
- ModA (probable molybdate-binding lipoprotein): 11.0 %; 0.8 % (range 0.2 to 3.6 %)
- Pitlp (probable periplasmic iron-transport lipoprotein): 27.5 %; 0.3 % (range 0.2 to 0.5 %)

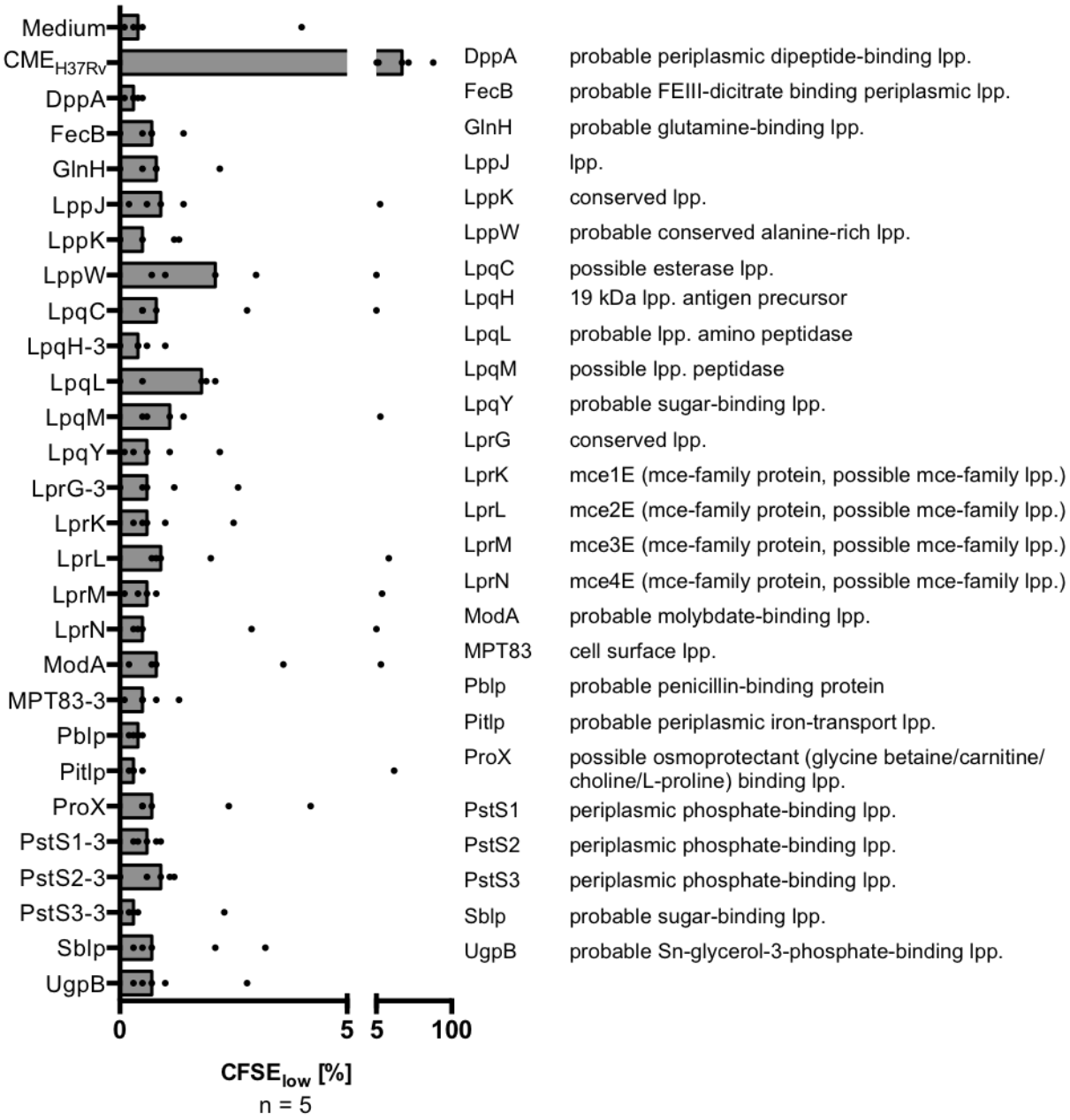

Figure 4.34 ***Ex vivo*** **lymphocyte proliferation in response to unlipidated synthetic N-terminal peptides of** ***M. tuberculosis*** **lipoproteins with known or assumed characteristics or function.**

Results of the *ex vivo* lymphocyte proliferation assay. PBMCs from 5 guinea pigs at day 30 after BCG sensitization were incubated with the indicated synthetic peptides (100 µg/ml) for 5 days. Characteristics or functions of the corresponding lipoproteins (lpp.) are listed on the right side. Black dots represent the arithmetic means of the duplicate tested per antigen, per animal. The grey columns represent the median over all animals, per antigen.

The lymphocyte proliferation in response to synthetic N-terminal peptides of possible and possible conserved or probable and probable conserved lipoproteins of *M. tuberculosis* is displayed in **Figure 4.35**. Again, the average lymphocyte proliferation in response to these

stimuli was very low (< 5 % $CFSE_{low}$ cells), yet outstanding proliferation rates could be observed with some peptides and/or some guinea pigs.

In the group of probable conserved lipoproteins, the strongest lymphocyte proliferation was detected with LpqN (median 1.8 %, range 0.6 to 5.4 %) and LppV (median 1.3 %, range 0 to 1.8 %). The stimulation with synthetic N-terminal peptides of possible conserved lipoproteins demonstrated LppE to induce the strongest proliferation (median 2.7 %, range 0.8 to 5.6 %). The synthetic N-terminal peptide of LppP exhibited the highest stimulatory capacity within the group of probable lipoproteins (median 1.6 %, range 0.8 to 3.7 %), and LpqQ within the group of possible lipoproteins (median 1.0 %, range 0.3 to 1.7 %). However, the lymphocyte proliferation in response to all these peptide preparations did not differ significantly from the medium-only control ($p > 0.05$).

Remarkably, there were again peptides which induced considerably stronger proliferation in the PBMCs obtained from particular guinea pigs. These peptides are listed below, sorted by the guinea pig which demonstrated the elevated lymphocyte proliferation. The first number after the colon indicates the percentage of $CFSE_{low}$ cells observed in PBMCs of this particular animal, the numbers behind the semicolon describe the median and range of $CFSE_{low}$ cell percentages in the remaining 4 guinea pigs.

Guinea pig #2:

- CME_{H37Rv}: 5.5 %; 41.5 % (range 7.6 to 76.8 %)
- LppM: 8.0 %; 0.6 % (range 0 to 1.9 %)
- LppE: 5.6 %; 1.9 % (range 0.8 to 4.4 %)

Guinea pig #3:

- CME_{H37Rv}: 37.3 %; 26.7 % (range 5.5 to 76.8 %)
- LpqN: 5.4 %; 1.3 % (range 0.6 to 2.1 %)
- LppC: 5.0 %; 1.1 % (range 0.6 to 1.4 %)
- LprJ: 15.0 %; 0.6 % (range 0.5 to 2.8 %)
- LppD: 29.7 %; 0.6 % (range 0.3 to 0.9 %)

Guinea pig #5:

- CME_{H37Rv}: 76.8 %; 22.5 % (range 5.5 to 45.7 %)
- DsbF: 17.0 %; 1.0 % (range 0 to 2.0 %)
- LpqT: 9.8 %; 0.5 % (range 0.2 to 0.7 %)
- LpqA: 7.3 %; 0.4 % (range 0 to 0.9 %)
- LprE: 17.3 %; 0.8 % (range 0 to 1.8 %)

The peptides deriving from sequences displaying a non-classical pattern at the position of the lipobox (see above) (**Figure 4.34**: ModA, Sblp; **Figure 4.35**: LppT, and LprO as the peptide deriving from the sequence displaying both a classical pattern and an alternative N-terminus) did neither stimulate lower nor higher lymphocyte proliferation than the other peptides, except for ModA which induced particularly strong lymphocyte proliferation in guinea pig #3 (see above).

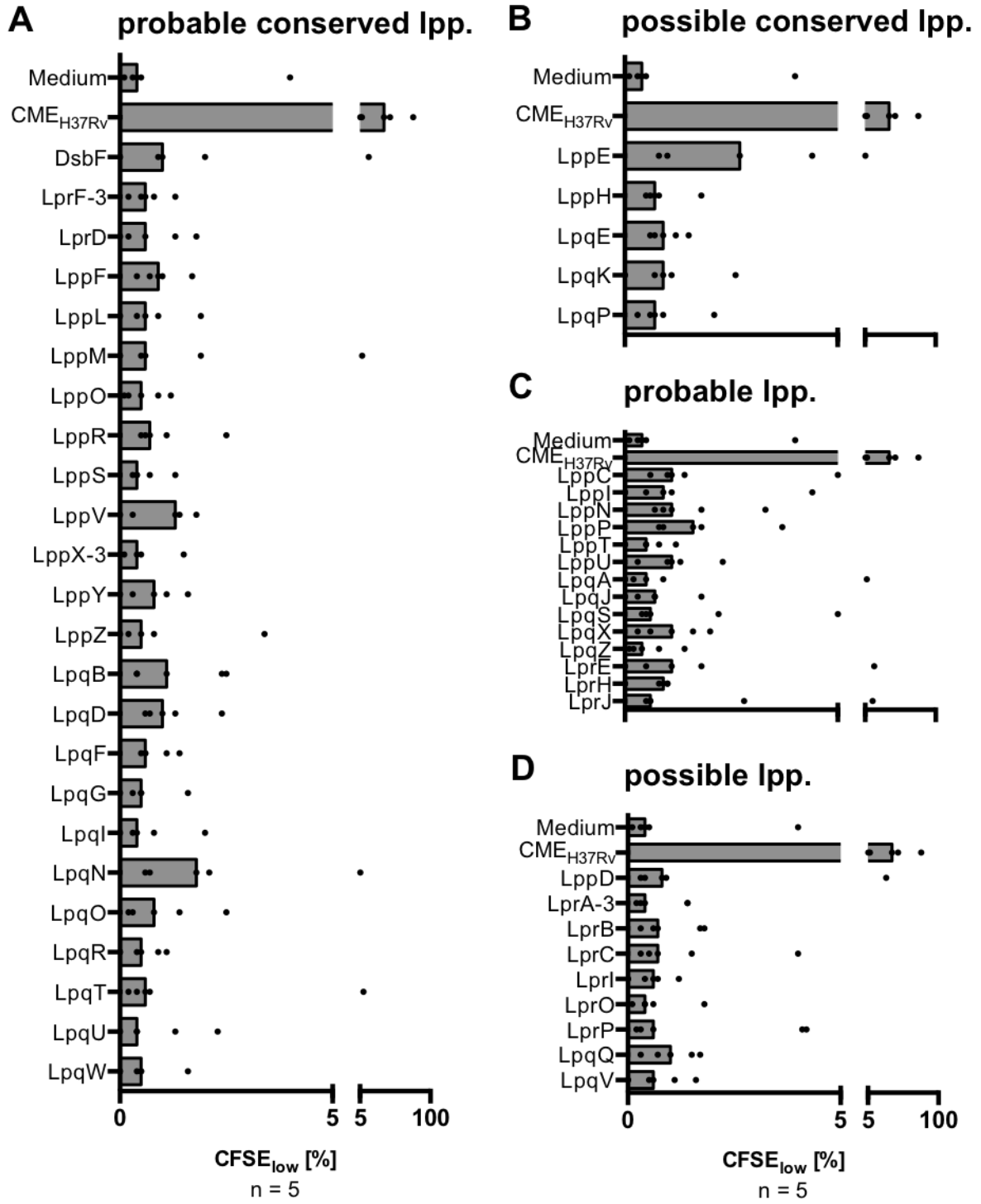

Figure 4.35 ***Ex vivo*** **lymphocyte proliferation in response to unlipidated synthetic N-terminal peptides of probable or possible** ***M. tuberculosis*** **lipoproteins.**

Results of the *ex vivo* lymphocyte proliferation assay. PBMCs from 5 guinea pigs at day 30 after BCG sensitization were incubated with the indicated synthetic peptides (100 µg/ml) for 5 days. Black dots represent the arithmetic means of the duplicate tested per antigen, per animal. Grey columns represent the median over all animals, per antigen. Proliferation results after stimulation with synthetic peptides of **A.** probable conserved; **B.** possible conserved; **C.** probable; **D.** possible *M. tuberculosis* lipoproteins.

4.6 Development and characterization of guinea pig T cell lines

Oligo- and monoclonal T cell lines with known specificity are valuable immunological tools to characterize antigen preparations. During their establishment, maintenance, expansion and functional characterization, compatible APCs are required for presentation of the antigen to the effector T lymphocytes. In contrast to humans, inbred animals can ensure the continuous availability of such APCs. Inbred strain 2 guinea pigs are histocompatible (Loeb and Wright 1927; Bauer 1958). This characteristic makes them valuable donors of PBMCs for the generation of guinea pig T cell lines and of the required APCs as they are recognized as syngenic by any other strain 2 guinea pig.

However, depending on the animal model and in particular in the guinea pig, there is still a limited availability of cytokines. A range of guinea pig cytokines, including the required IL-2, has therefore been produced in our laboratory (Spohr 2015) (see section 3.10.1). IL-2 is the most important growth factor for CD4-positive T cells (Oppenheim 2007).

In preliminary experiments, it was confirmed that the PBMCs obtained from MTC-sensitized inbred strain 2 guinea pigs proliferated to the same extent to Tub12 and CME stimuli as the PBMCs from MTC-sensitized outbred Dunkin Hartley guinea pigs (data not shown). Thereupon, those guinea pigs and their PBMCs were used for the generation of T cell lines. The final protocol, which reliably produced T cell lines, is described in section 3.10. This procedure was developed from protocols for human T cell lines (Mariotti and Nisini 2009) and by experimentation during this study.

From 6 initial approaches (primary T cell culture and limiting dilution), 51 polyclonal T cell lines as well as 11 putative oligoclonal and 2 putative monoclonal T cell lines which proliferated well at approximately 6–7 weeks of culturing were obtained. At this time, the cell lines were screened for their antigen specificity. This screening included the microscopic inspection of the cells and the determination of the total lymphocyte count in flowcytometric analysis upon antigen-specific stimulation of the cells, and a TNFα ELISA of the cell culture supernatant. The cell lines needed to provide positive results in at least 2 of these categories to be further propagated. Due to the low cell number which was available for these screening tests, only single tests could be performed per antigen, per cell line.

The characterization of three successfully established polyclonal guinea pig T cell lines, designated as $H37_{2210}$-B7, $H37_{2210}$-B10, and $H37_{2210}$-A6, by stimulation with Tub12 and CME_{BCG} is depicted in **Figure 4.36**. The T cell line $H37_{2210}$-B10 was the best-growing cell line which could therefore also be used for the screening of a range of chromatographic fractions (see below).

The CME_{H37Rv}-expanded guinea pig cell lines $H37_{2210}$-B7 and $H37_{2210}$-B10 proliferated upon Tub12 and CME_{BCG} stimulation as obvious from the percentages of FSC_{high} (blasting) cells within the living lymphocyte population (**Figure 4.36A**) as well as from the total lymphocyte count (**Figure 4.36B**). In particular, the cell line $H37_{2210}$-B10 showed strong proliferation in response to CME_{BCG} (12.0-fold increase in FSC_{high} cells and 2.8-fold increase in the absolute number of lymphocytes compared with the medium-only control), but less proliferation in response to Tub12 stimulation (3.8-fold increase in FSC_{high} cells and 1.1-fold increase in the absolute number of lymphocytes compared with the medium-only control). The cell line $H37_{2210}$-B7 demonstrated a 3.8-fold increase in FSC_{high} cells and a 2.8-fold increase in the absolute number of lymphocytes upon CME_{BCG} stimulation, and a 1.4-fold increase in FSC_{high} cells and 2.4-fold increase in the absolute number of lymphocytes when stimulated with Tub12, compared with the medium-only control. Upon stimulation, the cell line $H37_{2210}$-A6 demonstrated a more profound increase in TNFα secretion (see below) than in proliferation (1.1-fold increase in FSC_{high} cells and 2.1-fold increase in the absolute number of lymphocytes in response to CME_{BCG}, and 12.8 % decrease in FSC_{high} cells and 1.5-fold increase in the absolute number of lymphocytes in response to Tub12 stimulation compared with the medium-only control). Lymphocyte proliferation could not be determined in CFSE-based assays because of the limited availability of these cells.

In addition to the proliferative response, the described T cell lines secreted TNFα (**Figure 4.36C**). Compared with the medium-only control, the TNFα concentration in culture supernatants of all three T cell lines increased in response to CME_{BCG} and Tub12. The strongest increase was again observed with the cell line $H37_{2210}$-B10 (10.4-fold increase in TNFα concentration in response to CME_{BCG} and 3.6-fold increase upon Tub12 stimulation). There was a 5.1-fold increase in TNFα concentration upon CME_{BCG} stimulation and a 2.2-fold increase in response to Tub12 in the $H37_{2210}$-B7 cell line. A 2.3-fold increase in response to CME_{BCG} and a 1.8-fold increase in response to Tub12 stimulation was observed in the $H37_{2210}$-A6 cell line.

Furthermore, TNFα secretion of $H37_{2210}$-B10 could be observed in response to a range of individual fractions obtained from phenol-partitioned CME_{BCG} by reversed phase chromatography as displayed in **Figure 4.32**. These results were in accordance with the results obtained in the *ex vivo* lymphocyte proliferation assay of the described fractions using outbred Dunkin Hartley PBMCs. This accordance demonstrated that both *ex vivo* PBMCs of outbred guinea pigs as well as the inbred guinea pig T cell line $H37_{2210}$-B10 were stimulated by complex, putatively lipopeptide-containing antigen mixtures of BCG.

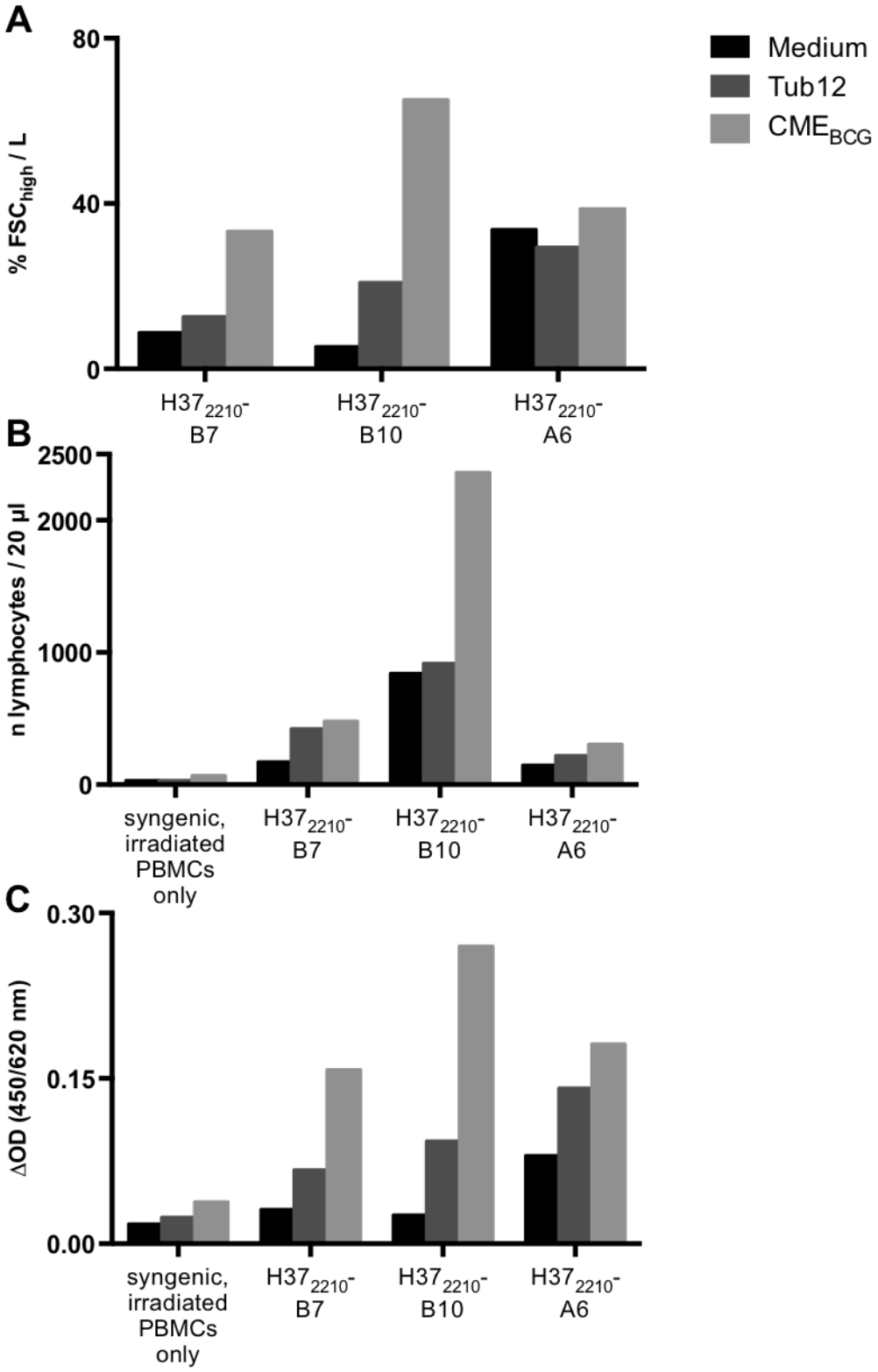

Figure 4.36 Response of three polyclonal guinea pig T cell lines to stimulation with mycobacterial antigens.

T cell lines derived from inbred strain 2 guinea pigs were incubated with syngenic, irradiated PBMCs and antigens Tub12 (30 IU/ml) and CME$_{BCG}$ (10 µg/ml) for 5 days. **A.** Flowcytometric analysis of the percentages of blasting, FSC$_{high}$ cells within the living lymphocytes. **B.** Flowcytometric analysis of the total count of lymphocytes per 20 µl. **C.** Analysis of the culture supernatant by TNFα ELISA, as shown by the corrected optical density at 450 nm.

The screening for antigen-specificity of two putatively oligoclonal guinea pig T cell lines, designated BCG_{2706}-#31 and BCG_{2706}-#34, as well as of one putatively monoclonal T cell line, BCG_{2706}-#36, is shown in **Figure 4.37**. Remarkably, the stimulations of the two putatively oligoclonal T cell lines were rather represented by TNFα secretion than by increased lymphocyte counts (BCG_{2706}-#31: 2.1-fold increase in CME_{BCG}-stimulated TNFα secretion compared with the medium-only control, but only 1.2-fold increase in the lymphocyte count; BCG_{2706}-#34: 1.4-fold increase in the CME_{BCG}-stimulated TNFα secretion compared with the medium-only control, but only 1.2-fold increase in the lymphocyte count). CME_{BCG}-specificity could not be assumed for the cell line BCG_{2706}-#36 as there was only a 1.1-fold increase in TNFα secretion as well as in the lymphocyte count observed in response to this antigen preparation compared with the medium-only control. There was a 1.3-fold increase in the lymphocyte count upon Tub12 stimulation of this cell line compared with the medium-only control, but no increase in TNFα secretion. Mono- or oligoclonality could not be confirmed until this time point. It was, however, probable due to the amount of cells seeded per well when performing the limiting dilution. It would have been interesting to investigate the stimulation of these cell lines by single mycobacterial antigens contained in CME and/or Tub12.

However, upon further culturing the cells decreased their proliferation, though they were split with medium containing guinea pig serum and guinea pig IL-2 and/or stimulated with guinea pig PBMCs and PHA when required. Upon culturing for 9–10 weeks from the initial isolation of the PBMCs, the majority of cell lines had to be discarded due to insufficient growth. Only 5 polyclonal T cell lines demonstrated further on adequate growth and 1 cell line grew slowly, but steadily. However, none of these cell lines proved antigen-specificity in subsequent screenings including the analysis of blasting lymphocytes and the loss of CFSE fluorescence in a CFSE-based stimulation test as well as in the associated TNFα ELISA of the cell culture supernatant (data not shown).

Samples of T cell lines were frozen at different time points, e.g., after the first screening. This procedure was well tolerated by the outbred guinea pig PBMCs and it was frequently applied to reserve autologous APCs for the restimulation assay. During the process of freezing and thawing the guinea pig T cell lines, however, became anergic – as in the continuous culture for more than 9 weeks – or, upon stimulation, the specific cells were overgrown by unspecific ones.

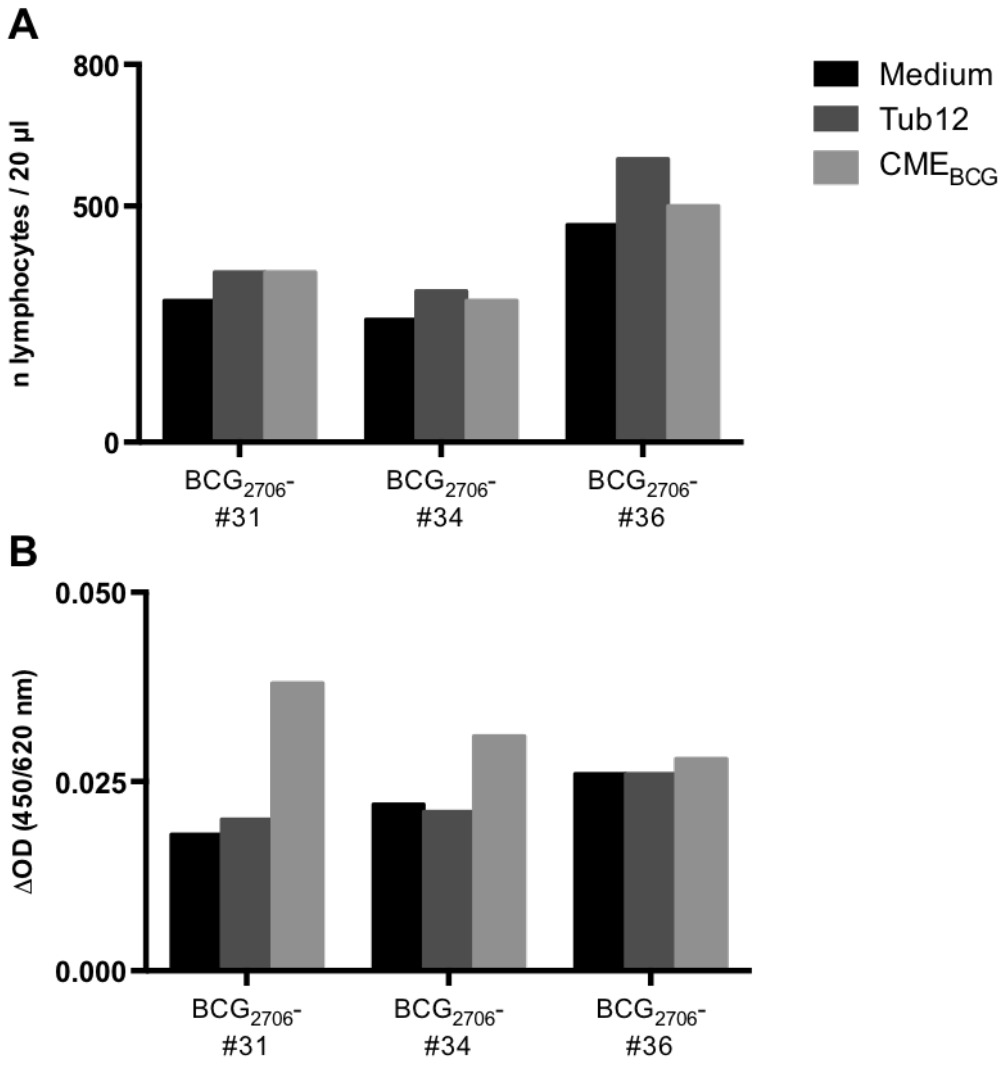

Figure 4.37 Response of two putative oligo- and one putative monoclonal guinea pig T cell line to stimulation with mycobacterial antigens.

T cell lines derived from inbred strain 2 guinea pigs were incubated with syngenic, irradiated PBMCs and antigens Tub12 (30 IU/ml) and CME_{BCG} (10 µg/ml) for 5 days. BCG_{2706}-#31 and BCG_{2706}-#34 were putative oligoclonal T cell lines, while BCG_{2706}-#36 was a putative monoclonal T cell line. **A.** Flowcytometric analysis of the total count of lymphocytes per 20 µl. **B.** Analysis of the culture supernatant by TNFα ELISA, as shown by the corrected optical density at 450 nm.

5 Discussion

5.1 Guinea pigs mount prominent lipid-reactive T cell responses upon sensitization with bacteria of the *Mycobacterium tuberculosis* complex

Infections with bacteria of the *M. tuberculosis* complex (MTC) induce a predominantly cell-mediated immune response (Cooper 2009). In this line, Bastian *et al.* (2008) recently demonstrated a strong CD4-positive T cell response of *M. tuberculosis*-infected humans that was directed against mycobacterial lipid preparations. The results were independently confirmed by Seshadri *et al.* (2013).

The aim of the present study was to investigate the lipid-reactive immune responses elicited by the important vaccine strain BCG in a defined experimental setting. The particular focus was on the BCG-induced T cell responses against lipid-rich antigen preparations of mycobacteria, the identification of strong antigen species within these preparations and the description of the distribution of these antigens. Guinea pigs were tested as a small animal model because many aspects of human tuberculosis including several immune responses have already proved reproducible in this host species (Smith and Harding 1977; Gupta and Katoch 2005; Williams *et al.* 2009; Clark *et al.* 2014).

To measure the *ex vivo* lymphocyte proliferation, a CFSE-based assay was adapted for use with guinea pig cells and CME preparations. CFSE labeling of lymphocytes for subsequent proliferation studies is recommended by many authors (Lyons and Parish 1994; Fulcher and Wong 1999; Lyons 1999; Parish 1999; Evrard *et al.* 2010; Faivre *et al.* 2014). It provides good correlation with, but also several advantages over other methods, such as the widely used [^{3}H]-thymidine incorporation: e.g., CFSE labeling enables the flowcytometric identification of single cell divisions over as many as 10 rounds, whereas [^{3}H]-thymidine incorporation, besides being potentially biohazardous, only quantifies the overall proliferation, but provides no information on individual cells (Lyons and Parish 1994; Fulcher and Wong 1999; Lyons 1999; Parish 1999; Evrard *et al.* 2010; Faivre *et al.* 2014). The CFSE assay was previously used, for example, to detect human immune responses upon CME stimulation (Bastian *et al.* 2008) as well as guinea pig PBMC proliferation to tuberculin (Spohr *et al.* 2015). Tuberculin was thereby shown to induce not only delayed type hypersensitivity reactions in iAN5-sensitized guinea pigs which can be measured in the tuberculin skin test, but also strong *ex vivo* lymphocyte proliferation (Spohr *et al.* 2015). To investigate the lipid-reactive immune responses elicited by BCG, guinea pigs were sensitized with either BCG or, for the purpose of comparison, with heat-inactivated bacteria of the virulent *M. bovis* strain

AN5 (iAN5). The latter should provide the antigen repertoire of mycobacteria which are capable of infecting the host.

In the CFSE-based *ex vivo* lymphocyte proliferation assay, the PBMCs of sensitized guinea pigs demonstrated profound median values of proliferation upon stimulation with CME of *M. tuberculosis* H37Rv and CME of BCG with the majority of the proliferated lymphocytes being CD4-positive T cells. The profound stimulation was characterized by median values of ≥ 20 % $CFSE_{low}$ lymphocytes. The overall proliferation rates were generally located within a wide range of $CFSE_{low}$ percentages, with those animals showing proliferation in the lower, upper, or middle areas of the range in response to one antigen preparation usually also demonstrating rather low, strong, or intermediate proliferation in response to the other antigen preparations, respectively, within the stimulatory capacities of the tested specimen. This finding could be attributed to the diverse genetic background of the outbred Dunkin-Hartley guinea pigs which perhaps mimics the diversity of immune responses of a heterogeneous population, such as humans, more closely than an inbred line such as strain 2 and strain 13 guinea pigs (Festing 1976; McKeand *et al.* 1994; Vaickus *et al.* 2010). The CME-induced lymphocyte proliferation was time- and antigen dose-dependent and could not be observed in non-immunized guinea pigs. Interestingly, the extent of lymphocyte proliferation in response to the CMEs was similar to that in response to tuberculin.

PBMCs of guinea pigs sensitized with either antigen, BCG or iAN5, proliferated to an equal extent in response to CME_{BCG}. Proliferation in response to CME_{H37Rv} was slightly stronger in PBMCs of guinea pigs sensitized with the virulent iAN5, but still robust in PBMCs of BCG-sensitized animals. This finding suggested that there were slight variations in the immunogenic antigen repertoire or content of both strains. Antigenic variation can be explained by the genetic differences between the attenuated BCG and other mycobacterial strains resulting from deletions and duplication (Brosch *et al.* 2007; Leung *et al.* 2008).

Bastian *et al.* (2008) and Seshadri *et al.* (2013) proposed that the relevant stimulatory antigens in the lipid preparations were lipoproteins, or rather lipopeptides. However, bacterial (including mycobacterial) lipoproteins are also known to be potent activators of innate immune mechanisms through TLR signaling (Brightbill *et al.* 1999; Hashimoto *et al.* 2006; Drage *et al.* 2009; Parra *et al.* 2010; Roux *et al.* 2011). It could therefore be suspected that the strong stimulation observed in the *ex vivo* lymphocyte proliferation assay was due to innate immune responses upon TLR signaling of mycobacterial lipoproteins. Prominent TLR stimulation is also achieved by LPS (Hoshino *et al.* 1999; Li *et al.* 2015; Theilacker *et al.* 2015). The stimulatory potential of LPS in *E. coli* and *S.* Typhi lysates was therefore investigated in the *ex vivo* lymphocyte proliferation assay in comparison with the CME preparations. The lymphocyte response to both bacterial lysates was significantly lower than

that to CME. The marginal, though not significant, proliferation of median 21.6 % $CFSE_{low}$ lymphocytes in response to *E. coli* lysate could be due to an adaptive immune response to these commensal bacteria. The finding that LPS-containing antigen preparations did not demonstrate strong stimulatory potential through TLR signaling in the guinea pig ex vivo lymphocyte proliferation assay was supported by the results of other investigators. Bastian *et al*. (2008) demonstrated that neither LPS nor the synthetic lipoprotein Pam3CSK4 induced proliferation in sensitized lymphocytes, though LPS – in contrast to CME – was shown to initiate DC maturation. Seshadri *et al.* (2013) reported that the lymphocyte response to the *M. tuberculosis* lipid preparation was not altered by TLR2-blocking antibodies. Furthermore, the lipid preparation of an *M. tuberculosis* strain deficient in mature lipoproteins failed to stimulate the lymphocytes, though many other TLR2 ligands, such as PIMs, were present (Seshadri *et al.* 2013).

The finding that TLR signaling was probably not directly involved in the lymphocyte proliferation observed in the *ex vivo* assay (see above) together with the result that CME responsiveness was only observed after sensitization of the guinea pigs, indicated that the *ex vivo* lymphocyte proliferation upon CME stimulation reflects an adaptive immune response of guinea pigs to *M. bovis* which is, at least, cross-reactive to *M. tuberculosis*. This adaptive immune response can be measured in the described *ex vivo* lymphocyte proliferation assay.

In addition to priming of T cells, it is however possible that lipopeptides direct the course of the adaptive immune response by promotion of Th1 development through TLR activation directly after infection or vaccination (Hsieh *et al.* 1993; Brightbill *et al.* 1999; Reba *et al.* 2014). The finding that CD4-positive Th1 cells were the principle responder cells upon stimulation with mycobacterial lipid preparations in humans (Bastian *et al.* 2008; Seshadri *et al.* 2013) strongly suggested such an innate immune system-mediated influence. Yet, regarding all of the above-described findings, TLR influence seemed not to play a direct role in the *ex vivo* proliferation assays using already sensitized cells as presented in this and previous studies (Bastian *et al.* 2008; Seshadri *et al.* 2013).

CD4-positive T cells recognize CD1- and MHC II-, but not MHC I-presented antigens. Lipids are usually presented through CD1 molecules and this presentation pathway has also been demonstrated for some lipopeptide antigens (Moody *et al.* 2004; van Rhijn *et al.* 2005; Van Rhijn *et al.* 2009b). Additionally, there are a number of MHC-restricted T cell epitopes described for mycobacterial lipoproteins (Vordermeier *et al.* 1991; da Fonseca *et al.* 1998; Mohagheghpour *et al.* 1998; Kao *et al.* 2012).

Heterogeneous mycobacterial lipid preparations containing diverse lipopeptides have clearly been demonstrated to activate a strong and predominantly MHC II-restricted CD4-positive

Th1 cell response in a TLR2-independent manner with only minor contribution of CD1 presentation in humans (Bastian *et al.* 2008; Seshadri *et al.* 2013). The guinea pig expresses MHC and several isoforms of most CD1 molecules (Dascher *et al.* 1999; Hiromatsu *et al.* 2002; Brigl and Brenner 2004). It thereby largely provides all pathways of presentation which are available in the human immune system. Unfortunately, a detailed characterization of the antigen presentation and recognition by the responding CD4-positive T cells was not possible in the present study. Available guinea pig anti-CD1 antibodies were suited to specifically stain CD1 molecules (Spohr 2015), but did not block antigen presentation through CD1 in the proliferation assay (data not shown). It is possible that the antibodies were not able to bind for the whole incubation period of 5 days which was required to measure proliferation. It was also not possible to perform blocking experiments with designated guinea pig anti-MHC antibodies as those antibodies did not show any binding at all (Dr. M. Bastian, personal communication). It was, however, assumed that the relevant antigens in the CMEs were mainly presented through MHC II in the guinea pig due to the following reasons: Antigen presentation was predominantly MHC II-restricted when human lymphocytes were stimulated with heterogeneous lipopeptide-containing lipid preparations in the presence of professional APCs which express CD1 as well as MHC molecules (Bastian *et al.* 2008; Seshadri *et al.* 2013). In the present study, specialized APCs were not utilized in the guinea pig *ex vivo* lymphocyte proliferation assay, but the antigen-presenting capacity depended on all cells present in PBMCs. PBMCs are a heterogeneous group of cells comprised of lymphocytes and monocytes (Simiele *et al.* 2011). Altogether these cells express less CD1 than MHC molecules, whereas professional APCs extensively express CD1 and MHC (Dascher *et al.* 1999; Hiromatsu *et al.* 2002; Brigl and Brenner 2004; Dougan *et al.* 2007; Murphy 2011). Nevertheless, a strong stimulation of guinea pig lymphocytes (median ≥ 20 % $CFSE_{low}$ cells) by the CME preparations in the *ex vivo* lymphocyte proliferation assay was observed. In this line, it was shown that defined mycobacterial lipids (GMM, PIM, ManLAM), in contrast to CME preparations, stimulated guinea pig T cell proliferation only if CD1-expressing APCs were added (Spohr 2015).

Similar *ex vivo* reactivities of guinea pig PBMCs compared with human PBMCs in response to mycobacterial lipid preparations were observed. The same types of lymphocytes responded upon stimulation of human and guinea pig PBMCs, as far as characterization was possible. These findings demonstrated the guinea pig to be not only a good model for the pathology of human tuberculosis (Gupta and Katoch 2005), but also for the investigation of immunological issues. Taken together, BCG as well as iAN5 sensitization of guinea pigs elicited an adaptive immune response which could be measured *ex vivo* as robust proliferation of CD4-positive T cells in response to stimulation with CMEs obtained from *M. tuberculosis* and BCG.

5.2 The guinea pig model provides immunological evidence for the stimulatory importance of lipopeptides in mycobacterial lipid preparations

Lipopeptides constitute important stimulatory antigens in mycobacterial lipid preparations for lymphocytes of MTC-infected humans (Bastian *et al.* 2008; Seshadri *et al.* 2013). To investigate whether lipopeptides represent the relevant antigens in CME preparations for BCG-sensitized guinea pig lymphocytes as well, three different immunological approaches were conducted.

The first approach was based on findings that protease degradation and delipidation both abolished the previous stimulatory capacities of a CME preparation (Bastian *et al.* 2008). Indeed, the biochemical degeneration of the protein backbone using proteinase K or pronase E as well as the delipidation of the antigens contained in CME by mild sodium hydroxide treatment diminished proliferation of the *ex vivo* guinea pig lymphocytes significantly. Furthermore, the same treatments could be demonstrated to significantly reduce the stimulatory potential of the Koch's Old Tuberculin Tub12. These findings suggested that lipopeptide antigens dominated not only the activity of the CMEs in the *ex vivo* lymphocyte proliferation assay, but at least also that of the Koch's Old Tuberculin which contains more lipid species than protein-enriched PPDs.

In the present study, mild sodium hydroxide treatment was used for delipidation of the antigens. This treatment breaks up the ester bonds at the glycerol and separates the peptide and the lipid moiety (Seid and Sadoff 1981), it does not destroy the lipid part as such. The observed significant decrease in the stimulatory effect of Tub12 and CME after delipidation therefore suggested that the general presence of peptide and lipid was not sufficient to induce lymphocyte proliferation – a lipidated peptide seemed to be crucial. This was also observed using PBMCs from MTC-infected or BCG-vaccinated humans (Bastian *et al.* 2008). The importance of the lipid moiety for the stimulatory capacities of mycobacterial lipopeptides was further demonstrated in several investigations on innate and adaptive immunity (Brightbill *et al.* 1999; Neyrolles *et al.* 2001; Hertz *et al.* 2001; Wilkinson *et al.* 2009; Van Rhijn *et al.* 2009b). The effects on innate immunity, including its influence on adaptive immunity, are due to the strong adjuvant activity of mycobacterial lipopeptides through TLR2 signaling (Stenger and Modlin 2002; Junqueira-Kipnis *et al.* 2014). Regarding adaptive immune mechanisms, the triacylation of peptides could provide direct advantages in the recognition of epitopes by host T cells through two mechanisms: influencing the intracellular trafficking of the antigen in APCs including access to certain presentation pathways (Neyrolles *et al.* 2001; Stittelaar *et al.* 2001) and/or stabilizing the antigen-MHC-TCR complex during presentation (Robinson *et al.* 1992). However, in contrast to the above-

mentioned findings on the crucial importance of the lipid moiety, some groups demonstrated a stimulatory capacity of the peptide part without lipidation as well (Faith *et al.* 1991; Lopez *et al.* 2003). When specifically investigating the influence of the peptide lipidation on MHC-mediated T cell proliferation, Rees *et al.* (1993) could reveal a sophisticated requirement. On the one hand, when stimulating heterogeneous PBMCs, enhanced T cell proliferation after lipidation of the peptide could be demonstrated, but only if initial recognition of the unlipidated peptide was observed as well. The authors suggested that the lipid part may indeed increase the activation of the T cells. Such an effect could, for example, be mediated through an enhanced stabilization of the T cell-APC interaction resulting in reduced requirements of adhesions molecules as proposed by Robinson *et al.* (1992), if it was not mandatory. On the other hand, when stimulating T cell clones, no such general enhancement of the proliferative response could be demonstrated. In contrast, depending on the location of the stimulatory epitope, lipidation could even abolish the T cell proliferation. This finding could simply be due to the size of the lipid part or its neutral charge, both which could interfere with the binding to the presentation molecule (Rees *et al.* 1993).

In the present study it could demonstrated that the delipidation of the lipopeptides in CMEs and Tub12 significantly reduced the T cell proliferative response to these antigen preparations. Whether the underlying mechanism was the removal of a general adjuvant-like activity as proposed by Rees *et al.* (1993) or the deletion of a moiety more generally required for peptide antigen recognition, processing and/or presentation in the first place, was not further investigated. A partial influence of both mechanisms is probable regarding the heterogeneity of the *ex vivo* PBMCs. However, it has also been demonstrated that the stimulatory capacity did not rely solely on the lipid as the mild sodium hydroxide treatment does not destroy the lipid as such and as protease treatment of the antigen preparation decreased the T cell proliferation as well.

To substantiate the findings on the relevance of lipopeptides, the investigation of lipopeptide-deficient strains is of great value. Seshadri *et al.* (2013) observed significantly decreased T cell activation after stimulation with the lipid preparation of an *M. tuberculosis* H37Rv strain lacking mature lipopeptides due to deletion of the gene encoding the signal peptidase LspA (Δ*lspA*) compared with the wild type and an *lspA*-complemented strain. It would be even more interesting to investigate a Δ*lgt* strain of MTC as the encoded enzyme Lgt (prolipoprotein diacylglyceryl transferase) catalyzes the first step of the post-translational modification of lipoproteins – coupling a diacylglycerol to the N-terminal cysteine – and mutant strains thus completely lack lipoproteins, not only mature lipoproteins. However, Lgt has been shown to be essential for the growth of *M. tuberculosis* (Tschumi *et al.* 2012). A mutant strain lacking lipidated proteins could so far only be generated using non-tuberculous *M. smegmatis* (Tschumi *et al.* 2012). As lipid preparations obtained from non-tuberculous

mycobacteria (NTM) did not induce T cell proliferation in the study design used here (see section 5.3), it appeared futile to investigate the influence of complete lipopeptide deficiency in one of those strains.

To further determine the significance of lipopeptides as antigens within the CME preparations, a subfraction of CME_{H37Rv}, which has been manufactured using a technique that had been described to purify lipoproteins (Bordier 1981; Lee *et al.* 2002; Gehring *et al.* 2003; Gehring *et al.* 2004; Målen *et al.* 2010), was tested in the guinea pig *ex vivo* lymphocyte proliferation assay. In detail, the manufacturing of CME_{H37Rv} consisted of a phase-separation with Triton X-114, precipitation with acetone and partitioning with phenol (Cala-De Paepe 2011). The resulting LppEL stimulated a 50 % increased IFN-γ secretion in a mycobacterial lipopeptide-responding human T cell clone ($-C2) (Cala-De Paepe 2011). When stimulating iAN5- or BCG-sensitized guinea pig PBMCs with LppEL, a strong lymphocyte proliferation was initiated. Interestingly, the strength of this proliferation was in the same range as the proliferation in response to the parental CME_{H37Rv}. This finding also strongly suggested that lipoproteins were mostly responsible for the stimulatory capacity of the CME_{H37Rv} preparation. The notion that the same antigens are stimulatory in CME and LppEL was further corroborated by the significant positive correlations between the proliferative responses to these antigen preparations. This finding suggested that both iAN5 as well as BCG sensitization induced lipopeptide-responsive lymphocytes that cross-recognize lipopeptides of virulent *M. tuberculosis* (see section 5.3).

Concerning the question whether the relevant antigens were rather lipoproteins or lipopeptides, it was hypothesized that the actual antigenic components were peptides of approximately 20 amino acids with an N-terminal triacylation. In view of the extraction capacities of chloroform-methanol (extraction of mainly neutral lipids such as triglycerides, waxes, and pigments by chloroform, and phospholipids, glycolipids, cholesterol, and lipopeptides by methanol (Ferraz *et al.* 2004; Zhang *et al.* 2012; Mandal *et al.* 2013)) and in accordance with Seshadri *et al.* (2013) it is rather unlikely that longer proteins are extracted into chloroform-methanol. Furthermore, in the present study nearly no protein content could be found in SDS-PAGE analysis of CME preparations but extensive lipid species were detectable by TLC. Herrmann *et al.* (1996) revealed the principle that proteolytic cleavage close to the acylated N-terminus of a lipoprotein in *M. tuberculosis* can release lower molecular size forms of this protein into the culture supernatant, while the lipid moiety containing the N-terminus with 19 to 22 amino acids remains anchored in the cell membrane. Other groups provided further evidence for such anchoring of lipopeptides (Andersen *et al.* 1990; Andersen and Doherty 2005; Wilkinson *et al.* 2009). Though T cell epitopes have also been found in the C-terminal part of lipoproteins (Vordermeier *et al.* 1991; Harris *et al.* 1993),

the N-terminal peptide provides an especially large density of such epitopes (Faith *et al.* 1991; Rees *et al.* 1993). Van Rhijn *et al.* (2009b) further demonstrated that degradation of the peptide moiety, though small, is possible by protease treatment which strongly supported the general feasibility of our approach. However, another CD1-restricted lipopeptide in their study (dideoxymycobactin) was not inactivated by the protease treatment (Van Rhijn *et al.* 2009b) indicating that lipopeptide antigens which are presented through CD1 molecules must not necessarily be degradable by proteases.

In the course of this project, a novel restimulation assay was established enabling the sorting and the testing of antigen-specific lymphocytes and thus the investigation of the importance of lipopeptide antigens. As in the guinea pig experiments the technique appears easily applicable in investigations using animal cells with only limited availability of immunological reagents. In this assay, *ex vivo* guinea pig PBMCs were CFSE-labeled, non-specifically biotinylated at the cell surface, stimulated with CME or Tub12 and expanded. Subsequently, expanded cells were sorted and restimulated. While designing this assay, we hypothesized that the cells lose their CFSE labeling, as already demonstrated, but also their biotinylation upon stimuli-induced proliferation stepwise from cell division to cell division. As streptavidin binds biotin with high affinity, paramagnetic-labeled streptavidin molecules could be used for sorting the non-proliferated from the proliferated cells in a magnetic column. The basis of such magnetic cell sorting was described by Miltenyi *et al.* (1990). Correlation between the loss of CFSE and the loss of biotin was not self-evident as cytokine secretion as well as granule exocytosis can lead to membrane turnover (Betts *et al.* 2003; Stow and Murray 2013), possibly affecting the biotin load of a cell, but usually not the intracellular CFSE load. The correlation between cellular loads with CFSE and biotin after expansion of the cells was determined by FACS staining with PE-Cy5.5-coupled streptavidin. In contrast to the above-mentioned possibility, it revealed a high correlation (r = 0.9) of loss of CFSE fluorescence and loss of biotin. Overall, the actual MACS-sorting achieved a substantial increase in $CFSE_{low}$ cells in the $biotin_{negative}$ population compared with the initial population. The purity after magnetic separation ranged from 39.2 to 97.5 % $CFSE_{low}$ cells in the $biotin_{negative}$ population with the median percentage of $CFSE_{low}$ cells being 86.8 %. The wide range could be due to technical reasons as the procedure required several incubations, leading to the cells to be handled multiple times, as well as a mechanical sorting step. For further experiments only $biotin_{negative}$ fractions with 80 % or more $CFSE_{low}$ lymphocytes were used to ensure the purity of the restimulated cell population. These cells were relabeled with CFSE and restimulated with either Tub12, CME or LppEL in the presence of irradiated, autologous PBMCs which acted as APCs.

APCs were critically required to initiate lymphocyte proliferation through presentation of the antigen in the restimulation assay with already expanded cells. As demonstrated in a specific experiment neither irradiated PBMCs nor expanded lymphocytes alone had the potential to proliferate.

Following incubation in the presence of irradiated, autologous PBMCs and the antigen in question, proliferation of the lymphocytes was determined. However, some cell samples no longer responded. A possible explanation could be that the cells became anergic due to the repeated strong stimulation in the short term. Anergy occurs in tuberculosis by chronic stimulation and exhaustion of the cells and is characterized by general unresponsiveness (Jin *et al.* 2011; Nunes-Alves *et al.* 2014). Anergy in tuberculosis patients can lead to the well-described phenomenon of false-negative TB tests during active disease (Huebner *et al.* 1993). Whether non-responsive lymphocytes in the restimulation assay occurred due to exhaustion because of the strong stimulation in a very short time frame, or whether they only occurred due to technical reasons could not be determined.

Nevertheless, the analysis of the proliferating lymphocytes in the restimulation assay yielded interesting insights into the specificity of the responding cells and the composition of the heterogeneous antigen preparations CME_{BCG}, CME_{H37Rv} and Koch's Old Tuberculin Tub12. The strong proliferation in response to the antigen preparation, which was also used for expansion, indicated that the expanded lymphocytes reacted antigen-specifically. The strong proliferation to the other preparations suggested that the relevant stimulatory antigens must be present in all these preparations. In detail, the cells expanded with the heterogeneous preparations CME and Tub12 demonstrated strong proliferation in response to the lipopeptide-enriched subfraction LppEL. Thus, expansion of lymphocytes with specificity to LppEL components must have occurred with the lipopeptides available in the less purified antigen preparations CME and Tub12. This finding corroborated the hypothesis that lipopeptides are relevant stimulatory antigens within CME and Koch's Old Tuberculin. In addition, the finding that these lipopeptide-reactive T cells responded equally strong to CME_{BCG}, CME_{H37Rv} and Tub12, regardless of which one was used for initial expansion, further supported the notion that cross-reactive lipopeptides must be contained in all CME preparations as well as in Koch's Old Tuberculin.

When considering the results of these three different series of experiments collectively, the guinea pig model provided substantial immunological evidence that lipopeptides indeed constitute strong and relevant stimulatory antigens within Koch's Old Tuberculin and, most importantly, in CME preparations of BCG and *M. tuberculosis* H37Rv. These findings obtained from BCG-sensitized guinea pigs are in accordance with previous findings of MTC-infected humans. It can be concluded that BCG vaccination, as MTC infection, sensitizes for

mycobacterial lipopeptide antigens. In addition, the results provided further evidence that the guinea pig represents a valid model to address immunological questions on human tuberculosis.

5.3 BCG sensitization induces lymphocyte responses against lipid antigens expressed by several tuberculous but only rarely by non-tuberculous mycobacteria

BCG is one of the most widely used vaccines and the only available one against human tuberculosis (Luca and Mihaescu 2013; Dye 2013). In order to obtain further insights into the immune responses elicited by this vaccine strain, it was investigated in the guinea pig model to which extent BCG-sensitized lymphocytes recognize CME-contained antigens of other mycobacterial species.

It was first tested whether BCG sensitization of guinea pigs elicited lymphocytes which were responsive to stimulation with a lipid preparation of the virulent *M. tuberculosis* strain H37Rv. The strong lymphocyte proliferation in response to the homologous CME_{BCG} was positively correlated with the lymphocyte proliferation in response to CME_{H37Rv}. The significantly positive correlation to the CME_{H37Rv}-derived lipopeptide-enriched subfraction LppEL further supported the stimulatory relevance of lipopeptide antigens within both CME preparations. These findings indicated that BCG is indeed capable of sensitizing lymphocytes for antigens provided by *M. tuberculosis*. This was not obvious because differences in the lipid expression of strains H37Rv and BCG exist, as investigations by Dr. Diane Cala-de Paepe revealed. She characterized a human T cell clone which was stimulated by CME_{H37Rv}, but not by CME_{BCG} (Cala-De Paepe 2011). Nevertheless, for many protein as well as lipoprotein antigens of *M. tuberculosis,* orthologs within other MTC strains, including BCG, as well as within NTM are described (see sections 2.3.2 and 2.3.4.2). This large number of conserved antigens could also be responsible for the partial cross-protection of BCG vaccination against leprosy (Richardus and Oskam 2015) and Buruli ulcer (Portaels *et al.* 2004) caused by *M. leprae* and *M. ulcerans*, respectively. Although there may be some beneficial cross-protection, other authors have explained the failure of BCG vaccination with the interference by cross-reactive NTM infections (Brandt *et al.* 2002; Andersen and Doherty 2005; Poyntz *et al.* 2014). Furthermore, false-positive skin tests are often attributed to cross-reactive T cell populations that have been elicited through exposure to NTM (Reyn *et al.* 1998).

The strong cross-reactivity between CMEs of *M. tuberculosis* H37Rv and *M. bovis* BCG in the context of BCG sensitization prompted us to study the pattern of this stimulatory capacity

across various strains of the *M. tuberculosis* complex and several non-tuberculous mycobacterial species. Due to the different providers of the antigens used in this series of experiments and because slightly differing protocols had been used for antigen extraction with chloroform-methanol, these antigen preparations were thoroughly analyzed by means of Coomassie and silver staining, Western blotting, and TLC prior to testing in the *ex vivo* lymphocyte proliferation assay. A striking finding was the presence of traces of possibly lipoarabinomannan (ManLAM) in some of the specimens. It is possible that the presence of these traces was due to the fact that for these particular preparations the bacterial pellets were initially resuspended in chloroform-methanol at a ratio of 1:1. However, this is rather speculative as it was not investigated systematically and in detail. ManLAM in *M. tuberculosis*, *M. bovis*, and *M. marinum* as well as the possibly differentially capped forms of LAM in other mycobacteria are described as pathogen-associated molecular patterns (PAMPs) important in the innate immune response to mycobacterial infection (Briken *et al.* 2004). So far, it could not be observed that innate immune responses influenced the *ex vivo* lymphocyte proliferation assay and some of these preparations did not stimulate proliferation either. It was therefore assumed that the presence of LAM had no significant influence on the T cell reactivity measured in this assay.

In some preparations (CMEs of *M. tuberculosis* CDC 1551, *M. tuberculosis* HN 878, and *M. fortuitum*) proteinaceous constituents could be detected by highly sensitive silver staining, but not with usual Coomassie staining. This indicated that any amounts of possible proteins were small. Again, as stimulatory and non-stimulatory CME preparations contained these trace amounts of proteins, it was concluded that they were irrelevant for the observed T cell reactivity. The highest amounts of silver and Coomassie detectable molecules were found in CME *M. marinum*. This finding is discussed below. The overall weakest visualization in both SDS-gels and TLC was achieved with CMEs of *M. avium* ssp. *avium* and *M. bovis* AN5. These CMEs were both generated from heat-inactivated bacterial wet mass. Although in both preparations only minute amounts of antigen were detectable, CME AN5 provoked a strong T cell response, while no reactivity was observed with the *M. avium* ssp. *avium*-derived CME (see below). Altogether, even though the preparations differed slightly in their antigen composition, the origin and the preparation method had no systematical and functional influence on the T cell response. Instead, it was concluded that the differences in the T cell reactivity were due to species-specific divergence in the expression of immunogenic lipopeptides.

The first interesting finding, when analyzing the stimulatory potentials of these CME preparations in the *ex vivo* lymphocyte proliferation assay, was that all CMEs obtained from *M. bovis* and *M. tuberculosis* strains caused profound T cell proliferation. This indicated that

BCG sensitized the lymphocytes of the guinea pigs for antigens which are ubiquitously expressed or cross-recognized within these species of the MTC. In this line, it was remarkable that *M. canetti* induced the lowest proliferation among the MTC strains. *M. canetti* separated early from a common ancestor of all MTC members (Brosch *et al.* 2002). It is a rare pathogen causing human tuberculosis and was assigned to the MTC (van Soolingen *et al.* 1997), but interestingly it is not regularly listed for this complex (Whitman *et al.* 2012). All other MTC CMEs caused strong lymphocyte proliferation in PBMCs of at least 13 of 17 guinea pigs tested, without any distinct pattern of differences observable.

The virulence features of three clinical strains, *M. tuberculosis* Beijing 1934, Haarlem 2336, and East-African Indian strain 1797, tested in the present study, have recently been characterized (Reiling *et al.* 2013). The Beijing strain accounted for very weak induction of cytokines in human MDMs and the bacterial uptake by human macrophages was low, but the bacteria showed substantial growth within these cells. In contrast, the Haarlem strain demonstrated substantial induction of cytokine responses and was extensively taken up by human macrophages where it also replicated strongly. The less virulent East-African Indian strain 1797 induced very weak cytokine responses and the uptake by human macrophages was low, as was the bacterial growth within these cells (Reiling *et al.* 2013). The *M. tuberculosis* strains H37Rv, HN 878 and CDC 1551 were analyzed for their virulence *in vitro* and *in vivo* (Manca *et al.* 1999). CDC 1551 was thereby shown to initially grow similar to the other strains *in vitro* and *in vivo* but to initiate more rapid and robust immune responses. Manca *et al.* (1999) and Neyrolles *et al.* (2011) suggested that differences in the lipid components of MTC strains could be associated with variation in immunogenicity and virulence. However, in the present study it was not possible in the guinea pig *ex vivo* lymphocyte proliferation assay to determine any relation between proliferation or probable lipopeptide expression and reported characteristics of the MTC strains.

Although all CMEs of MTC bacteria stimulated strong lymphocyte proliferation and no distinctive pattern could be observed to further differentiate between species or even strains within this complex, genetic polymorphisms between MTC strains have been described (Hershberg *et al.* 2008) as well as that these polymorphisms also affect lipoproteins (Fleischmann *et al.* 2002; Målen *et al.* 2010). Yet, the majority of these strong antigens seems to be ubiquitously expressed or cross-recognized over the *Mycobacterium tuberculosis* complex. This is in line with findings of Comas *et al.* (2010) who discovered that most human T cell epitopes of *M. tuberculosis* are hyperconserved among MTC species. They suggested that *M. tuberculosis* favors its recognition by the host immune system through the expression of such conserved antigens and that this recognition must be beneficial for the pathogen in terms of persistence (Comas *et al.* 2010). Recognition by the

host initiates a prominent and broad immune response during early infection which seems to be crucial for mature granuloma formation as the pathogen's niche for survival and replication (Ramakrishnan 2012), but also to protect the host and thereby to ensure the establishment of a long-standing MTC infection which is mandatory for efficient transmission of the pathogen to other individuals (Hunter 2011). The existence of conserved T cell epitopes could also explain the strong immune responses to mycobacterial lipopeptides. At present, however, the stimulatory epitopes in these lipopeptides have not yet been identified, so any consideration of conservation can only be based on functional analyses and not on sequencing data.

By contrast, CMEs of NTM did not cause strong lymphocyte proliferation. The only member of this group inducing a median proliferation above the threshold of 20 % $CFSE_{low}$ cells was *M. marinum*. Additionally, PBMCs of some guinea pigs displayed strong proliferation in response to CME of *M. avium* ssp. *paratuberculosis* (MAP), but the median proliferation remained below 20 %. Remarkably, *M. marinum* is rather closely related to MTC based on the 16S rRNA (Harmsen *et al.* 2003). The close resemblance of *M. marinum* infection in fish with *M. tuberculosis* infection in humans provides an interesting animal model (Hodgkinson *et al.* 2012; Cronan and Tobin 2014). However, the observed proliferation could also be due to the presence of residual protein which was highest in the CME preparation from *M. marinum* as detected by silver and Coomassie staining. It was therefore not possible to draw a final conclusion on the cause of the observed stimulatory effect of this antigen preparation. Regarding the MAP-stimulated samples, the observed proliferation of ≥ 20 % $CFSE_{low}$ cells in the PBMCs from 6 of 17 guinea pigs suggested that there may be low cross-reactivity between BCG and MAP lipid antigens. The lymphocyte proliferation in response to all other NTMs, including important pathogenic strains such as *M. avium* ssp. *avium* (MAA) and *M. leprae*, remained clearly below the 20 % cut-off line.

Specific T cell responses to mycobacterial lipids were also reported by van Rhijn *et al.* (2009a) when they investigated CD1-restricted T cells of *M. bovis*- or MAP-infected cattle. The T cell responses elicited by these infections were antigen-specific and in MAP-infected cattle preferentially directed against glucose monomycolate (GMM). A more hydrophilic compound of the *M. bovis* lipid preparation was the immunodominant substance for T cell activation of *M. bovis*-infected cattle, yet the authors could not determine a stimulatory protein part. T cells of *M. bovis*-infected cattle additionally recognized BCG lipid preparations but not MAP. *Vice versa*, T cells of MAP-infected cattle showed only a low cross-reactivity to the *M. bovis* preparation. These findings proposed the sensitization for different lipids by MTC and NTM (Van Rhijn *et al.* 2009a). No differences in the lipid reactivity could be observed when using different culture media for growth of these bacteria *in vitro* (Van Rhijn

et al. 2009a). The latter finding was in accordance with our own observations on CMEs of BCG and MAP grown in different media (data not shown).

The observation that CME obtained from *M. avium* ssp. *avium* (MAA) did not induce T cell proliferation in the guinea pig *ex vivo* lymphocyte proliferation assay was however surprising due to the fact that MAA expresses strong lipid antigens called glycopeptidolipids which should have been present in the CME preparation (Eckstein *et al.* 2003). However, both stimulatory and inhibitory potentials to modulate T cell immune responses have been described for glycopeptidolipids (Pourshafie *et al.* 1999; Kano *et al.* 2005; Schorey and Sweet 2008)

NTM infections are described to interfere with BCG vaccination (Brandt *et al.* 2002; Poyntz *et al.* 2014). In turn, despite high rates of BCG vaccination little information is available on BCG cross-protection against NTM infections and this information is mainly limited to leprosy and Buruli ulcer (Portaels *et al.* 2004; Richardus and Oskam 2015). Of great interest and importance in this regard and consistent with the observations of van Rhijn *et al.* (2009a) (see above) was the finding that NTM sensitizes for non-hyperconserved epitopes which partially stimulate cross-reactivity to less frequent epitopes in the MTC, whereas MTC sensitization for hyperconserved epitopes does not induce cross-reactivity to NTM (Lindestam Arlehamn *et al.* 2015). These findings could help to explain why NTM infections can interfere with generating a strong immune response to the attenuated BCG after vaccination (Brandt *et al.* 2002; Poyntz *et al.* 2014), but cannot confer protection against the more virulent *M. tuberculosis* (Andersen and Doherty 2005) and why BCG vaccination does not induce broad protection against NTM. More specifically, Herrmann *et al.* (1996) reported that the N-terminal peptide part which is responsible for the antigenic capacity of the 19 kDa lipoprotein is hypervariable with great differences between *M. tuberculosis* and *M. avium intracellulare*, though the actual protein parts displayed extensive conservation. Remarkably, a current vaccine candidate expressing the non-specific AG85A (McShane *et al.* 2004), which is presented by many mycobacterial species, did not offer protection against *M. tuberculosis* infection (Tameris *et al.* 2013). For future vaccine development, it could therefore be advantageous to favor MTC-specific antigens and thus the induction of specific immune responses. The detected strong proliferation of BCG-sensitized guinea pig lymphocytes in response to MTC but not NTM lipid preparations could be due to such specific antigens. Whether the stimulatory antigens recognized in MTC – presumably lipopeptides – were generally not expressed in NTM or whether their peptide sequences differed to such an extent that they were not cross-recognized by the BCG-primed T cells could not be deduced from this experiment. However, regarding the abundance of

M. tuberculosis protein and lipoprotein orthologs in NTM (see section 2.3.2 and 2.3.4.2), the latter explanation appears to be more likely.

In line with the specificity of lipid preparations, it has been demonstrated that the *ex vivo* PBMCs of MTC-sensitized guinea pigs reacted strongly to bovine PPD (derived from *M. bovis*), but not to PPD of MAA. The opposite was observed with the PBMCs of iMAA-sensitized guinea pigs (Spohr 2015). *In vivo*, a slightly stronger cross-recognition of the PPD preparations could be found (Reyn *et al.* 1998) which is taken into account in the simultaneous tuberculin skin test and which underlines the discriminatory potential of the *ex vivo* lymphocyte proliferation assay. These findings support the immunodominance of different antigens also on the protein level.

Altogether, the present findings indicated that BCG sensitizes for strong antigens which are probably ubiquitously present or at least cross-recognized in MTC but rarely in NTM. It is of note that such potent antigens were strongly expressed during the exponential as well as in the static culture growth phase of BCG. They were additionally found in the culture supernatant of the exponential growth phase. Assumed from the proliferative response of lymphocytes which was even stronger than in response to Tub12 and CME_{BCG}, the culture supernatant in particular contained large amounts of these antigens. Furthermore, the presentation of stimulatory antigens was actively supported by live bacteria. It has not yet been investigated whether the stimulatory activities in all these bacterial culture compartments originate from lipopeptides only. They may at least partially be due to proteins as well. A great amount of *M. tuberculosis* cell wall-associated proteins and even more lipoproteins have been described by Wolfe *et al.* (2010) who additionally identified secretion signals in many of them.

The abundant presentation of strong and conserved antigens could be an exposing signal of the bacterium supporting its detection and possibly being contributive to its life cycle through promotion and maintenance of the fine-tuned host-pathogen interplay (Comas *et al.* 2010). *M. tuberculosis* in its usual life cycle only temporarily profits from immunosuppression of its host. Most of the time an immunocompetent host seems to be favorable for the pathogen to persist and to establish cavities which are suited for effective transmission (Hunter 2011). The findings of the present study support the notion that strong lipopeptide antigens might be important features of mycobacteria causing tuberculosis in mammals. It may be that the described lipopeptides provide signals for the immune system that are required to form a robust adaptive, preferentially CD4-positive immune response which, as shown by Saunders *et al.* (2002), ensures containment of the pathogen in granulomas in the case of virulent infection. The presentation of lipoprotein antigens seems to represent a feature of a fine-tuned interaction of the pathogen with the host, because both a lack (Sander *et al.* 2004) and

the overexpression of lipoproteins (Rao *et al.* 2005; Hovav *et al.* 2006) alter the virulence of the bacterium (see sections 2.3.4.3 and 2.4.1.4).

The findings generated in the context of BCG sensitization revealed the formation of such a robust adaptive immune response also in the absence of virulent bacteria capable of hiding in granulomas. An advantage of this elicited immune response is the high efficacy of BCG vaccination against systemic forms of primary tuberculosis in infants (Trunz *et al.* 2006). However, the rather low efficacy of BCG vaccination against pulmonary infection with *M. tuberculosis* (Colditz *et al.* 1994; Fine 1995) indicates that these BCG-elicited cells are probably not suited to prevent or even support granuloma formation initiated by the virulent pathogen. Granulomas serve for the protection of the host from a fulminant infectious disease progression, but also support the persistence of the bacterium (Ehlers and Schaible 2013).

In humans, lipopeptide-reactive T cell responses generated upon *M. tuberculosis* infection were expressed as proliferation, cytokine secretion, and cytolytic functions (Bastian *et al.* 2008; Seshadri *et al.* 2013). *Ex vivo,* cytolytic CD4-positive T cells even exerted efficient killing of intracellular bacteria (Bastian *et al.* 2008). In general, it is well-established that cytokines, such as INF-γ and TNFα, as well as cytolytic effector functions are required for immune protection against tuberculosis (Cooper and Flynn 1995). However, these immune responses seem to be time- and location-dependent (Gideon *et al.* 2015) and usually not capable of clearing the pathogen from the host organism as most individuals infected with MTC mycobacteria progress to the latent form of the infection with the risk of reactivation (Shaler *et al.* 2012; Nunes-Alves *et al.* 2014). Such ambivalent outcomes of pro-inflammatory immune responses were observed upon lipoprotein sensitization in different experimental settings as well: In all cases strong immune responses were induced, but the protective efficacy varied to a great extent and was also influenced by the definition of “protection” (Abou-Zeid *et al.* 1997; Zhu *et al.* 1997; Hovav *et al.* 2003; Dascher 2003; Rao *et al.* 2005; Kao *et al.* 2012).

Regarding the significance of cytolytic CD4-positive T cells in tuberculosis (Ottenhoff *et al.* 1988; Lorgat *et al.* 1992; Mutis *et al.* 1993; Bastian *et al.* 2008), a possible reason for this T cell subset not leading to complete elimination of the pathogen upon infection might be their rather low frequency in the peripheral blood (Stegelmann *et al.* 2005). However, they seem to be much more abundant at the site of infection (Lorgat *et al.* 1992). Another possibility could be that their priming upon initial infection, like all adaptive immune responses in tuberculosis, takes too long (Shaler *et al.* 2012; Urdahl 2014) and in doing so allows the pathogen to create niches where it is no longer accessible (Shaler *et al.* 2013). Already the “innate granuloma” (see section 2.4.2.1) limits the accessibility of infected

macrophages for effector T cells (Shaler *et al.* 2013). This limitation is further extended during the development of the “immune granuloma” and caseation which can lead to central hypoxia (Tsai *et al.* 2006). Although the granuloma is in principle a dynamic structure allowing influx and dissemination of immune cells, T cells are particularly effective only in the outer layers and in the periphery, but not in the center (Ulrichs and Kaufmann 2006; Egen *et al.* 2008). In this line, Srivastava and Ernst (2013) reported recently that direct recognition of *M. tuberculosis*-infected cells by CD4-positive T cells and no long-range cytokine diffusion is crucial for infection control. A third possibility would be that specific cell populations are excessively down-regulated by anti-inflammatory mechanisms, e.g., T_{reg} cells (Marin *et al.* 2010). However, the distinct effect of T_{reg} cells on the cytolytic CD4-positive T cells still needs to be determined. Moreover, counter-regulation by anti-inflammatory mechanisms can also be advantageous by means of protection from excessive tissue damage through highly efficient cytolytic effectors (Nunes-Alves *et al.* 2014). The hypothesis of host protection but not pathogen elimination is in line with the difficulties to define reliable immunological correlates of protection in tuberculosis (Kagina *et al.* 2010; Nunes-Alves *et al.* 2014; Bhatt *et al.* 2015).

As noted above, similar T cell responses as in MTC infection are also observed after BCG vaccination (Esin *et al.* 1996; Vekemans *et al.* 2001; Mittrücker *et al.* 2007; Kaveh *et al.* 2011) which apparently does not reliably confer protection during the pulmonary course of the disease in humans (Colditz *et al.* 1994; Fine 1995). Novel vaccination strategies could therefore aim at strengthening those immune cell populations actually conferring protection through enhanced presentation of their specific priming antigens in subunit- but also live viral vector vaccines. Unfortunately, although a number of such vaccine candidates have been tested, no vaccine better than BCG could be developed so far (Delogu *et al.* 2014) and some vaccine candidates were even withdrawn due to safety issues (Moliva *et al.* 2015). A reason for safety-associated withdrawal can be exaggerated pro-inflammatory immune responses.

In general, already the biased pro-inflammatory cytokine response upon mycobacterial infection, though it is not as exaggerated, seems to be a problem. This milieu has been shown to be a crucial factor for granuloma formation which is associated with containment but also persistence of the pathogen. A pro-inflammatory immune response balanced with anti-inflammatory and regulatory elements seems to be required for sterilizing the granulomatous lesions (Gideon *et al.* 2015). Along that line, Nunes-Alves *et al.* (2014) proposed to investigate new vaccination approaches with the aim to induce broader, „unconventional“ immune responses. In this context, one strategy could be the development of live attenuated mycobacterial vaccine strains, e.g., by deletion of pro-inflammatory signals such as virulence-associated sulfatides (Brozna *et al.* 1991) or by reducing the abundant

expression of TLR2 agonists (Simmons *et al.* 2010). Alternatively, a more efficient immune response in terms of pathogen elimination could be achieved through adjuvanted subunit vaccines, which induce effector cells with a defined, favorable phenotype (Gideon *et al.* 2015). It needs to be investigated whether the described lipopetides constitute candidate antigens for deletion or provision in a subunit vaccine. In principle, they are favorable candidate vaccine antigens because they are strong immunogens, probably mainly expressed or cross-recognized in the MTC and available in the cell wall as well as in the culture supernatant (Strugnell *et al.* 2011). However, the experiences in humans and preliminary data with guinea pig T cells indicate that lipopeptide-reactive T cells express an exclusively pro-inflammatory phenotype (Bastian *et al.* 2008). So, the challenge is to develop a vaccine context for these antigens that induces T cells with a balanced, protective phenotype. It is possible that such a vaccine could also be administered to modulate pre-existing immune responses in latently infected donors and thus to influence the course of an already-established infection. This is a very promising strategy which is currently followed by a multistage subunit approach based on early and latency-associated antigens (Aagaard *et al.* 2011).

5.4 Synthetic peptides reveal potential stimulation by defined *M. tuberculosis* lipopeptide antigens

CMEs obtained from mycobacteria are heterogeneous mixtures of bacterial products despite enrichment in lipids including lipopeptides (Gunawardana *et al.* 1999; Ferraz *et al.* 2004; Cala-De Paepe 2011). The molecular identification of one or a few defined antigens which account for the strong stimulatory potential of these mixtures is important for further analysis of the role of lipopeptides in the immunopathology of tuberculosis. To this end, two complementary approaches to identify defined strong lipopeptide antigens were investigated: (i) the chromatographic purification of specifically enriched CME preparations and (ii) the production of synthetic N-terminal peptides of *M. tuberculosis* lipoproteins. For both approaches we were seeking for antigen-specific, oligo- or monoclonal T cell lines as they are most valuable immunological tools to pursue the purification of an antigen (Mariotti and Nisini 2009).

The aim was to generate these T cell lines from guinea pigs to obtain an immunological instrument for the characterization of mycobacterial antigens which was related to our animal model of human TB. Inbred strain 2 guinea pigs were used for this purpose because they are histocompatible (Bauer 1958). The advantage of using these syngenic animals instead of outbred guinea pigs is that the maintenance of the T cell lines is not dependent on APCs

collected from the same animal from which the line was initially generated, as MHC-compatible APCs can also be obtained from any other strain 2 guinea pig. The required guinea pig IL-2 for generation of such T cell lines was not commercially available. Therefore, the cytokine was first recombinantly produced in our laboratory (Spohr 2015) and the best-suited conditions for the stimulation, the sorting and the incubation of the anticipated T cells needed to be determined (data not shown). Using a modified version of the protocol of Mariotti and Nisini (2009), 64 guinea pig T cell lines were established and subsequently tested for their antigen specificity. One of these cell lines, the antigen-specific, adequately growing, but only polyclonal line $H37_{2210}$-B10, proved successful to further characterize a panel of chromatographic fractions of phenol-partitioned CME_{BCG}. Despite these promising results, the slow growth and the maintenance of the antigen specificity of the guinea pig T cell lines became the limiting factors. In the end, all generated guinea pig T cell lines were too fragile to be suited for sufficient expansion as required for serial antigen testing and for consideration as robust tools. In summary, the successful generation of guinea pig T cell lines with specificity to mycobacterial lipid antigens could be demonstrated within this study, but their maintenance requires further investigation. Guinea pig T cell lines were therefore not available for extensive screening of purified CME fractions or synthetic peptides. These screenings were then realized using *ex vivo* PBMCs of iAN5- or BCG-sensitized guinea pigs.

In mycobacteriology, preparative chromatography is widely used for the separation of either proteins or lipids. However, so far, only the chromatographic purification of single recombinant or synthetic lipopeptides has been demonstrated, but no extensive purification of lipopeptides from crude mycobacterial antigen extracts (Pecora *et al.* 2006; Van Rhijn *et al.* 2009b; Drage *et al.* 2010). Purification of lipopeptides through preparative chromatography suffers from several difficulties especially due to the presence of a large hydrophobic part covalently linked to a more hydrophilic proteinaceous domain. Peptides and hydrophobic molecules are usually separated using a hydrophobic stationary phase (Schmidt-Traub *et al.* 2012). Reversed phase chromatography (RPC) was therefore considered to be the method of choice.

Two complementary reversed phase chromatographic approaches to isolate antigenic lipopeptides from the mycobacterial CME preparations were pursued: (i) The first chromatographic purification attempt was a broad approach based on the initial enrichment of the CME preparation in lipopeptides through phenol partitioning. This step was also applied in the preparation procedure for LppEL, the lipopeptide-enriched subfraction of CME_{H37Rv}, which has been demonstrated to own a nearly identical stimulatory potential to its parental preparation. Using a TLR2 assay it was confirmed that phenol-partitioned CME still contained TLR2 ligands which were assumed to be the lipopeptides. A C4 column was

chosen for the preparative chromatography because it provides binding capacities for the widest range of antigens regarding their degree of hydrophobicity and molecular weight (Carr 2002). Due to the peptide moiety of the anticipated lipopeptides, a mobile phase gradually ranging from the most polar solvent available, H_2O, to a more apolar solvent, acetonitrile (AcN), was chosen. However, it was not possible to fractionate the phenol-partitioned CME preparation using this approach, probably because the binding between the column matrix and the analytes was not sufficient. This phenomenon of probably insufficient binding was observed with all phenol-partitioned CME preparations that were investigated and it was confirmed by determination of the concentrations (w/v) of total ingredients in the obtained fractions and their analysis in Bradford, TLR2 and *ex vivo* lymphocyte proliferation assays as well as by TNFα ELISA. The notion was supported by the fact that CME antigens were usually not soluble in low concentrations (10 and 17.5 %) of AcN/H_2O. In the present case, insufficient binding between the column and the analytes could possibly be provoked by saturation of the column due to an overload of antigen or by suboptimal binding characteristics of the C4 column to low molecular weight peptides. A true overload would present as a “shark fin”-shaped peak (Taylor 2013). Though the majority of eluents sorted right at the beginning of the run, there was no peak observable in this particular shape, rendering the first explanation rather unlikely. It was more likely that the lipopeptides, enriched through phenol partitioning of the CME preparations, were smaller than anticipated. Hence, the C4 column which is ideal to bind peptides in a size greater than 5,000 Da (Carr 2002) could perhaps not sufficiently retain these molecules.

(ii) The assumption that only very small peptide moieties were probably already present in the CMEs was considered in the second chromatographic approach. This approach aimed for a preselection of more lipophilic peptides and thereby an already more narrowed antigen spectrum. It was based on the specific sampling of CME-derived peptides in 40 % acetonitrile (AcN) and their subsequent fractionation using a C18 column and a gradient of 40 to 97 % AcN. As 40 % AcN is a rather polar solvent which solubilizes proteins and peptides, it was hypothesized that using dried CME as source material for the extraction, 40 % AcN would solubilize CME-contained lipopeptides. For sampling of these lipopeptides, CME_{BCG} was dried, redissolved in the 40 % AcN and centrifuged. The following chromatography of the supernatant displayed a distinct peak of eluents at approximately 80 % AcN which was degradable by proteinase K treatment as well as by delipidation. These results indicated that it was possible to purify mycobacterial lipopeptides by the described procedure. However, no particular lymphocyte proliferation could be observed when incubating sensitized guinea pig PBMCs with these fractions. It must therefore be assumed that the stimulatory lipopeptides were not solubilized in 40 % AcN but must have remained in

the pellet generated by the centrifugation step. It would be interesting to analyze the molecules present in this pellet, e.g., through further extraction with 75 or 100 % AcN.

A second, reverse approach to identify defined lipoprotein antigens was based on synthetic N-terminal peptides and synthetic signal peptides. The latter were additionally investigated because immunogenic T cell epitopes have also been described within this part of immature lipoproteins (Rees *et al.* 1993; Kovjazin *et al.* 2011). This approach was inspired by experimental evidence that all lipidated peptides inducing strong proliferation of heterogeneous PBMCs showed at least weak stimulatory activities without this lipidation (Rees *et al.* 1993). Wrong or displaced lipids could even be capable of sterically hindering T cell recognition of epitopes (Robinson *et al.* 1992; Rees *et al.* 1993). Rees *et al.* (1993) further suggested that the hydrophobic N-terminus of the lipoproteins could also bind to MHC II without processing so that excessive amounts of peptides could possibly overcome the putative adjuvant function of the lipid moiety for the mature peptides. Under this assumption, N-terminal peptides and signal peptides of *M. tuberculosis* lipoproteins were synthesized in a length of 15 amino acids each and tested in the guinea pig *ex vivo* lymphocyte proliferation assay.

A single, recombinant mycobacterial protein antigen, AG85A, which is usually a potent T cell stimulant (Hajizadeh *et al.* 2007), already demonstrated rather low stimulation in the *ex vivo* lymphocyte proliferation assay. Mixtures of antigens such as the lipopeptide-enriched subfraction (LppEL) induced significantly stronger lymphocyte proliferation. Hence, we did not expect strong proliferative responses to single synthetic peptides. We rather aimed to investigate whether particular peptides induced a more prominent proliferation than others. These peptides could be interesting for implementation in defined antigen mixtures to analyze their additive potential and the importance of polyclonal T cell responses upon mycobacterial stimulation. As expected, the overall proliferative response to the synthetic peptides was very low compared with the stimulation by complex antigen preparations such as Tub12, CME, and LppEL, but differences in the stimulatory capacities were observed. This is in accordance with reports describing a lower stimulatory capacity of the single mycobacterial antigen ESAT-6 in comparison with heterogeneous PPD and an *M. bovis* lipid preparation (van Pinxteren *et al.* 2000; Van Rhijn *et al.* 2009a). Furthermore, when directly comparing several recombinant proteins of *M. tuberculosis* for their capabilities to induce IFN-γ secretion in human PBMCs, Skjøt *et al.* (2000) could also reveal slight differences in their stimulatory potential. This supported the significance of our observations on synthetic peptides. It is probable that the heterogeneous antigen preparations stimulated a polyclonal proliferation, which was easily detected by ≥ 20 % $CFSE_{low}$ cells in the *ex vivo* lymphocyte

proliferation assay, whereas defined mycobacterial antigens induced a mono- or oligoclonal cell response.

Likewise to the lymphocyte proliferation observed in response to AG85A, the synthetic peptide representing the N-terminus of the mature lipoprotein LppW, a probable conserved alanine-rich lipoprotein, induced low lymphocyte stimulation which, however, was significantly stronger than the proliferation in the medium-only control. Nevertheless, regarding the overall low proliferation it must also be taken into consideration that the peptides with a length of 15 amino acids may possibly not have had the right size or did not exactly match the size and sequence of the cognate epitopes. To exclude this possibility, overlapping sequences need to be tested for all antigens. We already investigated such overlapping sequences for the signal peptides of the best-characterized mycobacterial lipoproteins (see literature section 2.3.4.2) and their associated mature peptides. Among the synthetic signal peptides, the most prominent T cell proliferations were induced by one N-terminal part of a signal peptide (LppX) and two C-terminal parts of signal peptides (LprG and PstS3). In all three cases the stimulation with the complementary signal peptide sequence resulted in clearly lower proliferation, although these differences were not statistically significant. In contrast, all mature peptides tested in overlapping sequences induced nearly equivalent T cell proliferation (data not shown). It can be assumed from these findings that these three described signal peptide sequences may indeed represent or contain specific T cell epitopes, but further investigations are required. In turn, similar T cell proliferation in response to the two overlapping sequences of the mature peptides must not indicate that these sequences were not stimulatory at all.

Interestingly, some peptide sequences of known, probable or possible *M. tuberculosis* lipoproteins (LppJ, LpqM, LprL, LprM, ModA, PitIb, LppM, LppE, LpqN, LppC, LprJ, LppD, DsbF, LpqT, LpqA, and LprE) induced much stronger proliferation in individual guinea pigs than in the others. Whether this finding was an artifact or a real result, e.g., due to the genetic background of the particular guinea pig, must be investigated using larger numbers of animals and, perhaps, with a more sensitive assay to assess lymphocyte proliferation.

Taken together, these experiments using synthetic peptides of mycobacterial lipoproteins yielded promising yet inconclusive results in that it was not possible to identify individual molecules that would explain the massive response to CME. For further interpretation of the achieved results, it is required to investigate the influence of the triacylation on these specific peptides. We assume that the triacylation would at least moderately strengthen the immune responses to the peptides. Such an enhancing effect of the lipid part could possibly only be observable if stimulating heterogeneous PBMCs, but not T cell clones recognizing only one specific epitope (Rees *et al.* 1993). In addition to this investigation, it would be interesting to

test whether the described peptides act additively or synergistically and thereby enhance the overall stimulatory activity if tested as a defined cocktail in the *ex vivo* lymphocyte proliferation assay.

The strong immune responses generated by the heterogeneous lipopeptide-containing mycobacterial CME preparations may lead to the assumption that the underlying stimulation might not be due to classical antigen recognition, processing and presentation, but to a superantigen effect. Superantigens are relatively frequent in other gram-positive bacteria such as *Staphylococcus* species and *Streptococcus* species (Spaulding *et al.* 2013). Superantigens induce a very strong, non-specific, polyclonal stimulation of T cells mainly through MHC II, in conjunction with the TCR Vβ region, but without requirement of processing by APCs. Stimulation by superantigens leads to extensive inflammation which can be fatal or possibly contributes to chronic autoimmune diseases as well (Langley and Renno 2011). The presence of mycobacterial superantigens was initially proposed by Ohmen *et al.* (1994). However, there are several facts that oppose the assumption that a superantigen was responsible for any findings in this study. First, no such mycobacterial superantigen has been identified so far (Langley and Renno 2011) and, in particular, despite the huge body of literature on mycobacterial lipid antigens, no such activity has ever been described for mycobacterial lipopeptides. *Ex vivo* proliferative T cell responses, e.g., to mycobacterial lipopeptides, have only been observed after infection or sensitization of the host with mycobacteria, but not in naïve individuals (Bastian *et al.* 2008; Seshadri *et al.* 2013; Spohr *et al.* 2015). This phenomenon is only consistent with adaptive T cell responses to mycobacterial antigens which require specific priming of the naïve T cells by professional APCs. Finally, experiments with expanded lymphocytes *in vitro* revealed that co-incubation with (irradiated) autologous PBMCs was essential to elicit a proliferative response to mycobacterial CMEs which would not be expected in the case of a superantigen.

Stimulating immune cells of MTC-sensitized hosts with complex antigen mixtures of mycobacterial origin, for instance lipid preparations or tuberculin, achieved a particularly strong activation of lymphocytes (Bastian *et al.* 2008; Seshadri *et al.* 2013; Spohr *et al.* 2015). These lymphocyte responses could be directed against a broad range of antigens or against a limited number of strong epitopes. As it was not possible until today to define single antigens accounting for this strong stimulation and as the PPD-based tuberculin skin test could not yet be improved by utilization of a defined antigen preparation, there is increasing evidence that synergistic effects between antigens are crucial for such a robust immune response. Synergistic effects can arise from innate as well as adaptive immune mechanisms. For instance, muramyl dipeptide (MDP), a degradation product of bacterial peptidoglycan, has been demonstrated to exert synergistic effects on numerous innate immune pathways

(Traub *et al.* 2006). The cell wall of mycobacteria contains a particularly thick layer of peptidoglycan (murein). Though the *ex vivo* lymphocyte proliferation assay investigated in the present and in previous studies (Bastian *et al.* 2008; Spohr *et al.* 2015) has been demonstrated to quantify only adaptive immune responses, it might be possible, that for example MDP in tuberculins sensitizes the PBMCs through innate mechanisms for the provided antigenic stimulus without directly inducing T cell stimulation. Due to its molecular nature MDP is rather unlikely to be present in the lipid preparations used here. However, other molecules might exert a similar function therein. It is rather unlikely that mycobacterial lipopeptides themselves account for such effects as it was shown that they, or at least a portion of them, elicit adaptive and antigen-specific immune responses and because lipopeptides influence the innate immune system mainly through TLR2 signaling which was specifically demonstrated not to be involved in the strong adaptive proliferative responses to mycobacterial lipopeptides observed in humans (Bastian *et al.* 2008; Seshadri *et al.* 2013). The phenomenon of heterogeneous antigen preparations eliciting strong immune responses *ex vivo* could also be due to the provision of diverse antigens, e.g., the investigated lipopeptides, each with a rather low stimulatory potential, which sensitize immune cells with different, but also same or similar effector functions. If common effector functions, e.g., proliferation, INF-γ or TNFα secretion, are subsequently analyzed, the heterogeneous nature of the underlying stimuli might become masked.

Some effector functions of such a heterogeneous activation of the immune system by *M. tuberculosis* certainly confer protection, e.g., by killing intracellular mycobacteria (Bastian *et al.* 2008), but can contribute to tissue damage as well (Orme 2014), and probably support granuloma formation (Shaler *et al.* 2013). The results of the present study indicated that the lipopeptides of MTC play an important role in the early activation of the immune system upon encountering bacteria of the *M. tuberculosis* complex, including BCG. The immune responses initiated during early infection usually lead to containment, but are in the majority of infected hosts not sufficient to eliminate the pathogen (Shaler *et al.* 2012; Nunes-Alves *et al.* 2014). Following the containment in granulomas, the pathogen enters into a stage of latency, or rather persistence (Orme 2014). This transition is associated with alterations in the antigenic repertoire (Demissie *et al.* 2006; Serra-Vidal *et al.* 2014). However, the immune system remains constantly exposed to antigenic activation in the dynamic structures of the granuloma (Shaler *et al.* 2011). Whether mycobacterial lipopeptide antigens still play a crucial role at this stage requires further investigations. Later stages of *M. tuberculosis* infection are often associated with exhaustion of the immune responses due to chronic stimulation (Jin *et al.* 2011; Nunes-Alves *et al.* 2014) which is represented by reversal of positive diagnostic TB tests and rapid disease progression (Huebner *et al.* 1993).

5.5 Conclusions

The present study led to the following conclusions:

- Both subcutaneous administration of BCG and intramuscular injection of an inactivated, virulent *M. bovis* strain sensitize lipopeptide-reactive CD4-positive T cells in the guinea pig.
- The induction of these T cells is part of a specific adaptive immune response towards mycobacteria of the MTC and can be quantitated by an *ex vivo* lymphocyte proliferation assay based on co-incubation of PBMCs with lipid-enriched extracts prepared from MTC bacteria.
- Lipopeptides are the dominating target antigens of the early *ex vivo* proliferative reactivity of lymphocytes to mycobacterial lipid preparations and Koch's Old Tuberculin (approximately 30 days after BCG and 60 days after iAN5 sensitization).
- The T cell stimulatory capacity of lipopeptides depends on intact lipid and peptide moieties covalently linked with each other.
- BCG sensitizes guinea pigs for structurally conserved or cross-reactive lipopeptide antigens which are expressed by strains of *M. tuberculosis* and *M. bovis*, and perhaps other members of the MTC. In non-tuberculous mycobacteria these lipopetides are either rarely present or hardly cross-recognized.
- Strong T cell-reactive antigens are abundantly expressed and secreted by BCG *in vitro*.
- Current protocols of reversed phase chromatography using C4 or C18 columns fail to purify from complex lipid preparations a particular antigenic lipopeptide capable of inducing a robust proliferative T cell response *ex vivo*.
- Screening of synthetic peptides with overlapping sequences is a promising approach to identify mycobacterial lipopeptides with T cell antigen activity.
- The protocol used for the development of guinea pig T cell lines requires further investigation particularly in terms of long-term cell line maintenance.
- Since all immune responses described in this study resemble those observed in MTC-infected humans, the guinea pig appears to be a well-suited animal model to investigate adaptive immune responses elicited by MTC bacteria and, in particular, BCG vaccination and mycobacterial lipid antigens.

The present study raised the following questions of particular interest for further investigation of the topic:

- Is an antigen preparation consisting of a few single mycobacterial antigens with outstanding stimulatory potentials capable of inducing equally strong immune responses as observed upon stimulation with the heterogeneous preparations? What is the molecular nature of these antigens?
- What are the specific functions of lipopeptide-reactive T cells in the host-pathogen interplay in tuberculosis? To which degree do these cells confer protection or damage host tissues?
- How does a vaccine which stimulates a broad immune response which does not only rely on pro-inflammatory T cells influence the outcome of *M. tuberculosis* infection? Would it be beneficial to exclude or include lipopeptides from/in mycobacterial vaccine formulations?

6 Summary

The only available vaccine against TB – the Bacille Calmette-Guérin (BCG) vaccine – provides reliable protection against severe manifestations of childhood TB, but not against pulmonary tuberculosis in adults. Despite many attempts, no improved alternative TB vaccine has been fully licensed so far. It may be crucial for future vaccine development to gain further knowledge on the stimulatory antigens of this vaccine strain and their elicited immune responses.

The aim of the current study was to investigate the BCG-mediated adaptive immune responses directed against lipid preparations (chloroform-methanol extracts, CMEs) of bacteria of the *Mycobacterium tuberculosis* complex (MTC). To this end, the BCG-sensitized guinea pig was employed as a model for human BCG vaccination. In particular, the present study addressed whether lipopeptides in the CME preparations constitute relevant stimulatory antigens for adaptive cellular immune responses upon BCG sensitization and whether the expression of stimulatory lipid antigens varies across the genus *Mycobacterium*. It was further attempted to identify the molecular nature of the stimulatory antigens present in CME.

Outbred Dunkin-Hartley guinea pigs were sensitized with BCG or, for comparison purposes, with heat-inactivated wet mass of the virulent *M. bovis* strain AN5. *Ex vivo*, the proliferation of peripheral blood mononuclear cells (PBMCs) was investigated in a CFSE-based proliferation assay which was subsequently analyzed by flow cytometry. In this assay, CMEs of *M. bovis* BCG and *M. tuberculosis* H37Rv and, in addition, a Koch's "Old Tuberculin" standard were used as antigenic stimuli. The molecular nature of the relevant stimulatory antigens within these preparations was investigated by means of delipidation and protease treatment. Furthermore, the stimulatory potentials of a lipopeptide-enriched subfraction of CME_{H37Rv} (LppEL), of a defined mycobacterial protein antigen (AG85A), and of different BCG preparations (live or heat-inactivated bacteria, bacterial lysates derived from BCG cultures in the exponential as well as in the static growth phase, and culture supernatant) were tested for their stimulatory potentials in the *ex vivo* lymphocyte proliferation assay. A restimulation assay based on the antigen-specific expansion of *ex vivo* lymphocytes, the sorting for expanded lymphocytes and the restimulation of these cells, was established in this study and served subsequently for determination of the antigen-specificity of the stimulated lymphocytes as well as for investigating the distribution of the stimulatory antigens among the tested preparations (Tuberculin, CME_{BCG}, CME_{H37Rv}, LppEL). The distribution of the stimulatory antigens was further analyzed among the genus *Mycobacterium* using CMEs of several MTC strains, including clinical ones, (*M. bovis* AN5, *M. tuberculosis* CDC 1551,

Haarlem 2336, HN 878, Beijing 1934, East African-Indian strains 1797 and 91/0079, *M. canetti*) and of non-tuberculous mycobacteria (NTM) (*M. marinum*, *M. avium* ssp. *avium* and *M. avium* ssp. *paratuberculosis*, *M. leprae*, *M. fortuitum*). It was attempted to identify the molecular nature of the stimulatory antigens in the lipid preparations by two complementary approaches: the purification of lipopeptides from enriched antigen preparations by means of reversed phase chromatography and the investigation of the stimulatory potentials of synthetic, N-terminal peptides of *M. tuberculosis* lipoproteins.

Flowcytometric analysis of the *ex vivo* lymphocyte proliferation assay revealed that guinea pigs mount strong, adaptive lymphocyte responses upon sensitization with both BCG and inactivated, virulent *M. bovis* AN5. The lymphocytes proliferated upon stimulation with CME preparations of *M. bovis* BCG and *M. tuberculosis* H37Rv. The CME_{BCG}-stimulated proliferation manifested in a similar range as lymphocyte responses elicited by tuberculin with the median proliferation being represented by ~ 45 % $CFSE_{low}$ lymphocytes in BCG-sensitized guinea pigs. This proliferation was significantly stronger than the lymphocyte responses to the defined mycobacterial protein antigen AG85A ($p \leq 0.0001$, student's *t* test). The above-mentioned preparations of BCG bacteria, however, stimulated strong proliferation as well (significantly above 20 % $CFSE_{low}$ cells, $p \leq 0.001$, one-sample *t* test). The CME_{BCG}-responding lymphocytes were predominantly (~ 83 %) CD4-positive T cells. Delipidation as well as protease treatment of CME_{BCG} decreased the stimulatory capacities significantly ($p \leq 0.0001$, student's *t* test) to median levels below 20 % $CFSE_{low}$ cells. The same effect on the *ex vivo* lymphocyte proliferation was observed upon delipidation as well as proteinase K treatment of tuberculin. Furthermore, when stimulating the *ex vivo* PBMCs with a lipopeptide-enriched subfraction of CME_{H37Rv} (LppEL), the median lymphocyte proliferation manifested similar to the lymphocyte response to the parental CME_{H37Rv} preparation and both proliferative responses were positively correlated ($r = 0.64$, Spearman correlation). Using the restimulation assay, it could be confirmed that the proliferated T cells responded specifically to antigens present in tuberculin, CME_{BCG} and CME_{H37Rv}, as well as in LppEL. Strong proliferative responses (on average significantly above 20 % $CFSE_{low}$ cells, $p \leq 0.05$, one-sample *t* test) were, however, only observed in response to CME preparations of MTC bacteria. In contrast, the average proliferative response to CME preparations of NTM did not exceed the 20 % cut-off significantly ($p > 0.05$). So far, it was not possible to identify single lipopeptides which accounted for the observed, strong lymphocyte proliferation. However, it is remarkable that some synthetic N-terminal peptides of *M. tuberculosis* lipoproteins (LprG, PstS3, LppW, LprL, PitIp, and LppD) stimulated stronger lymphocyte proliferation on average in the group or in individual guinea pigs.

The results demonstrate that the guinea pig is well-suited to investigate adaptive immune responses elicited by MTC bacteria and, in particular, it is a good model to investigate BCG vaccination in a defined experimental setting. All findings were in full accordance with the observations in *M. tuberculosis*-infected humans. Strong evidence for the stimulatory potential and the relevance of lipopeptides in CME preparations was provided by three independent immunological approaches. Moreover, it could be demonstrated that lipopeptides account for a majority of the stimulatory capacities not only of CME, but also of Koch's Old Tuberculin. The extensive expression and the release of strong antigens, such as the putative lipopeptides, by BCG is supported by the data. Furthermore, the putative stimulatory lipopeptides must be specifically expressed or cross-recognized within the *Mycobacterium tuberculosis* complex, but only rarely in non-tuberculous mycobacteria. However, the identification of single strong lipopeptide antigens requires further investigation. In this line, it must be considered that antigen mixtures of several single, strong lipopeptide antigens, whose existence has been suggested by the present results, might be necessary to elicit similar strong lymphocyte responses as observed upon stimulation with complex, lipopeptide-containing antigen mixtures such as CME.

7 Zusammenfassung

Der einzige, verfügbare Impfstoff gegen Tuberkulose – der Bacille Calmette-Guérin (BCG)-Impfstoff – schützt verlässlich vor schweren Formen der Tuberkulose im Kindesalter, aber nicht vor Lungentuberkulose bei Erwachsenen. Trotz vieler Versuche konnte bisher noch kein verbesserter, alternativer TB-Impfstoff zugelassen werden. Für die zukünftige Impfstoffentwicklung kann der weitere Erkenntnisgewinn über die stimulatorischen Antigene dieses Impfstammes und die durch sie hervorgerufenen Immunantworten entscheidend sein.

Das Ziel der hier beschriebenen Studie war die Untersuchung der BCG-vermittelten adaptiven Immunantwort, die sich gegen Lipidpräparationen (Chloroform-Methanol-Extrakte, CME) von Bakterien des *Mycobacterium tuberculosis*-Komplexes (MTC) richtet. Mit BCG sensibilisierte Meerschweinchen wurden als Modell für die BCG-Impfung im Menschen eingesetzt. Die hier vorliegende Studie befasst sich im Speziellen mit der Frage, ob Lipopeptide in CME-Präparationen relevante stimulatorische Antigene für die adaptive, zelluläre Immunantwort nach BCG-Impfung darstellen und ob die Expression von stimulatorischen Lipidantigenen innerhalb des Genus *Mycobacterium* variiert. Eine weitere Intention war, die molekulare Struktur der stimulatorischen Antigene in CME zu identifizieren.

Auszucht-Dunkin-Hartley-Meerschweinchen wurden mit BCG oder – zu Vergleichszwecken – mit hitze-inaktivierter Feuchtmasse des virulenten *M. bovis*-Stamms AN5 sensibilisiert. Die *ex vivo* Proliferation von mononukleären Zellen aus dem peripheren Blut (peripheral blood mononuclear cells, PBMCs) wurde in einem auf CFSE-Färbung basierenden Proliferationsassay untersucht, der mittels Durchflusszytometrie analysiert wurde. In diesem Assay wurden CMEs von *M. bovis* BCG und *M. tuberculosis* H37Rv sowie zusätzlich ein Kochscher Alttuberkulin-Standard als antigene Stimuli verwendet. Die Untersuchung der molekularen Struktur der relevanten, stimulatorischen Antigene in diesen Präparationen erfolgte mit Hilfe von Delipidierung und Protease-Behandlung. Darüber hinaus wurden die stimulatorischen Potenziale von einer Lipopeptid-angereicherten CME_{H37Rv}-Subfraktion (LppEL), einem definierten, mykobakteriellen Protein-Antigen (AG85A) und verschiedenen BCG-Präparationen (lebende oder Hitze-inaktivierte Bakterien, bakterielle Lysate von BCG-Kulturen in der exponentiellen als auch in der statischen Wachstumsphase, Kulturüberstand) im *ex vivo*-Lymphozytenproliferationsassay getestet. Ein Restimulationsassay, der auf der antigen-spezifischen Vermehrung von *ex vivo* Lymphozyten, der Sortierung der vermehrten Lymphozyten und der Restimulierung dieser Zellen basierte, wurde im Zuge dieser Studie etabliert und diente daraufhin zur Feststellung der Antigenspezifität der stimulierten Lymphozyten sowie zur Untersuchung der Verteilung der stimulatorischen Antigene in den verschiedenen, getesteten Präparationen (Tuberkulin, CME_{BCG}, CME_{H37Rv}, LppEL). Die

Verteilung der stimulatorischen Antigene wurde zusätzlich innerhalb des Genus *Mycobacterium* unter Verwendung von CMEs von verschiedenen MTC-Stämmen, einschließlich klinischer, (*M. bovis* AN5, *M. tuberculosis* CDC 1551, Haarlem 2336, HN 878, Beijing 1934, East African-Indian strains 1797 and 91/0079, *M. canetti*), und CMEs von nicht-tuberkulösen Mykobakterien (NTM) (*M. marinum*, *M. avium* ssp. *avium* and *M. avium* ssp. *paratuberculosis*, *M. leprae*, *M. fortuitum*) untersucht. Es wurde angestrebt, die molekulare Struktur der stimulatorischen Antigene in den Lipidpräparationen durch zwei komplementäre Ansätze zu identifizieren: Aufreinigung von Lipopeptiden aus angereicherten Präparationen mittels Umkehrphasen-Chromatographie und Untersuchung des stimulatorischen Potenzials von synthetischen, N-terminalen Peptiden von *M. tuberculosis*-Lipoproteinen.

Die durchflusszytometrische Auswertung des *ex vivo*-Lymphozytenproliferationsassays zeigte, dass Meerschweinchen starke adaptive Lymphozytenreaktionen nach Sensibilisierung mit sowohl BCG als auch inaktiviertem, virulentem *M. bovis* AN5 entwickeln. Die Lymphozyten proliferierten nach Stimulierung mit CME-Präparationen von *M. bovis* BCG und *M. tuberculosis* H37Rv. Die CME_{BCG}-stimulierte Proliferation war ähnlich stark wie die durch Tuberkulin hervorgerufene Lymphozytenreaktion und wurde durch ca. 45 % nur noch schwach CFSE-gefärbte Lymphozyten aus BCG-sensibilisierten Meerschweinchen repräsentiert. Diese Proliferation war signifikant stärker als die Lymphozytenreaktion auf das definierte mykobakterielle Protein-Antigen AG85A ($p \leq 0.0001$, Students *t*-Test). Jedoch stimulierten die oben aufgeführten Präparationen von BCG-Bakterien ebenfalls eine starke Proliferation (signifikant über 20 % CFSE-schwache Zellen, $p \leq 0.001$, *t*-Test mit einer Stichprobe). Die CME_{BCG}-reaktiven Lymphozyten waren vorwiegend (ca. 83 %) CD4-positive T-Zellen. Delipidierung als auch Protease-Behandlung von CME_{BCG} verminderte das stimulatorische Potenzial signifikant ($p \leq 0.0001$, Students *t*-Test) zu Medianwerten unter 20 % CFSE-schwachen Zellen. Den gleichen Effekt auf die *ex vivo* Lymphozytenproliferation hatte die Delipidierung als auch die Proteinase K-Behandlung von Tuberkulin. Weiterhin zeigte sich eine ähnlich starke mediane Lymphozytenproliferation wie in der Reaktion auf die ursprüngliche CME_{H37Rv}-Präparation, wenn *ex vivo* PBMCs mit der Lipopeptid-angereicherten Subfraktion von CME_{H37Rv} (LppEL) stimuliert wurden. Die beiden proliferativen Reaktionen waren positiv korreliert ($r = 0.64$, Spearman-Korrelation). Es konnte unter Verwendung des Restimulationsassays bestätigt werden, dass die proliferierenden T-Zellen spezifisch auf in Tuberkulin, CME_{BCG}, CME_{H37Rv} als auch in LppEL vorhandene Antigene reagierten. Starke Proliferation (im Mittel signifikant über 20 % CFSE-schwache Zellen, $p \leq 0.05$, *t*-Test mit einer Stichprobe) ließ sich jedoch ausschließlich als Reaktion auf CME-Präparationen von MTC-Bakterien beobachten. Im Gegensatz dazu überstieg die mittlere proliferative Reaktion auf CME-Präparationen von NTM die 20-%-Grenze nicht signifikant ($p > 0.05$). Bis zum jetzigen Zeitpunkt war es nicht möglich, einzelne Lipopeptide, welche die beobachtete,

starke Lymphozytenproliferation ausmachten, zu identifizieren. Es ist jedoch bemerkenswert, dass einige synthetische N-terminale Peptide von *M. tuberculosis*-Lipoproteinen (LprG, PstS3, LppW, LprL, Pitlp und LppD) im Mittel oder in einzelnen Meerschweinchen stärkere Lymphozytenproliferation stimulierten.

Die Ergebnisse zeigen, dass das Meerschweinchen für Studien über adaptive Immunantworten auf MTC-Bakterien geeignet ist und im Speziellen ein gutes Modell zur Untersuchung der BCG-Impfung unter definierten experimentellen Bedingungen darstellt. Alle Ergebnisse spiegeln die Beobachtungen in *M. tuberculosis*-infizierten Menschen wider. Starke Evidenz für das stimulatorische Potenzial und die Relevanz von Lipopeptiden in den CME-Präparationen wurde durch drei unabhängige, immunologische Ansätze geliefert. Darüber hinaus konnte gezeigt werden, dass Lipopeptide einen Großteil des stimulatorischen Potenzials nicht nur von CME, sondern auch von Kochschem Alttuberkulin ausmachen. Die Daten unterstützen die Annahme, dass BCG starke Antigene, wie z.B. die mutmaßlichen Lipopeptide, in großen Mengen exprimiert und freisetzt. Die vermuteten Lipopeptide werden anscheinend spezifisch innerhalb des *Mycobacterium-tuberculosis*-Komplexes exprimiert oder erkannt; in nicht-tuberkulösen Mykobakterien jedoch nur selten. Die Identifizierung einzelner starker Lipopeptid-Antigene bedarf weiterer Untersuchungen. In diesem Zusammenhang ist in Betracht zu ziehen, dass zur Stimulierung von ähnlich starken Lymphozytenreaktionen, wie sie nach Inkubation mit komplexen, Lipopeptid-haltigen Antigengemischen, wie z.B. CME, beobachtet wurden, gegebenenfalls Antigengemische verschiedener, starker Lipopeptid-Einzelantigene benötigt werden, deren Existenz die hier beschriebenen Ergebnisse nahelegen.

8 References

Aagaard C, Hoang T, Dietrich J, Cardona P-J, Izzo A, Dolganov G, Schoolnik GK, Cassidy JP, Billeskov R, Andersen P (2011) A multistage tuberculosis vaccine that confers efficient protection before and after exposure. Nat Med. 17:189–194.

Aaron L, Saadoun D, Calatroni I, Launay O, Mémain N, Vincent V, Marchal G, Dupont B, Bouchaud O, Valeyre D, Lortholary O (2004) Tuberculosis in HIV-infected patients: a comprehensive review. Clin Microbiol Infect. 10:388–398.

Abel B, Tameris M, Mansoor N, Gelderbloem S, Hughes J, Abrahams D, Makhethe L, Erasmus M, Kock M de, van der Merwe L, Hawkridge A, Veldsman A, Hatherill M, Schirru G, Pau MG, Hendriks J, Weverling GJ, Goudsmit J, Sizemore D, McClain JB, Goetz M, Gearhart J, Mahomed H, Hussey GD, Sadoff JC, Hanekom WA (2010) The novel tuberculosis vaccine, AERAS-402, induces robust and polyfunctional $CD4^+$ and $CD8^+$ T cells in adults. Am J Respir Crit Care Med. 181:1407–1417.

Abou-Zeid C, Gares MP, Inwald J, Janssen R, Zhang Y, Young DB, Hetzel C, Lamb JR, Baldwin SL, Orme IM, Yeremeev V, Nikonenko BV, Apt AS (1997) Induction of a type 1 immune response to a recombinant antigen from *Mycobacterium tuberculosis* expressed in *Mycobacterium vaccae*. Infect Immun. 65:1856–1862.

Abou-Zeid C, Ratliff TL, Wiker HG, Harboe M, Bennedsen J, Rook GA (1988) Characterization of fibronectin-binding antigens released by *Mycobacterium tuberculosis* and *Mycobacterium bovis* BCG. Infect Immun. 56:3046–3051.

Agger EM, Rosenkrands I, Hansen J, Brahimi K, Vandahl BS, Aagaard C, Werninghaus K, Kirschning C, Lang R, Christensen D, Theisen M, Follmann F, Andersen P (2008) Cationic liposomes formulated with synthetic mycobacterial cordfactor (CAF01): a versatile adjuvant for vaccines with different immunological requirements. PLoS ONE 3:e3116.

Aguiló N, Marinova D, Martín C, Pardo J (2013) ESX-1-induced apoptosis during mycobacterial infection: to be or not to be, that is the question. Front Cell Infect Microbiol. 3:88.

Akira S (2003) Toll-like receptor signaling. J Biol Chem. 278:38105–38108.

Albrecht M, Kühne Y, Ballmer-Weber BK, Becker W-M, Holzhauser T, Lauer I, Reuter A, Randow S, Falk S, Wangorsch A, Lidholm J, Reese G, Vieths S (2009) Relevance of IgE binding to short peptides for the allergenic activity of food allergens. J Allergy Clin Immunol. 124:328–336.

Alexander KA, Laver PN, Michel AL, Williams M, van Helden PD, Warren RM, Gey van Pittius NC (2010) Novel *Mycobacterium tuberculosis* complex pathogen, *M. mungi*. Emerg Infect Dis. 16:1296–1299.

Altare F, Durandy A, Lammas D, Emile JF, Lamhamedi S, Le Deist F, Drysdale P, Jouanguy E, Döffinger R, Bernaudin F, Jeppsson O, Gollob JA, Meinl E, Segal AW, Fischer A, Kumararatne D, Casanova JL (1998) Impairment of mycobacterial immunity in human interleukin-12 receptor deficiency. Science 280:1432–1435.

Andersen AB, Hansen EB (1989) Structure and mapping of antigenic domains of protein antigen b, a 38,000-molecular-weight protein of *Mycobacterium tuberculosis*. Infect Immun. 57:2481–2488.

Andersen AB, Ljungqvist L, Olsen M (1990) Evidence that protein antigen b of *Mycobacterium tuberculosis* is involved in phosphate metabolism. J Gen Microbiol. 136:477–480.

Andersen P, Doherty TM (2005) The success and failure of BCG – implications for a novel tuberculosis vaccine. Nat Rev Microbiol. 3:656–662.

Andersen P, Munk ME, Pollock JM, Doherty TM (2000) Specific immune-based diagnosis of tuberculosis. The Lancet 356:1099–1104.

Appelmelk BJ, Dunnen den J, Driessen NN, Ummels R, Pak M, Nigou J, Larrouy-Maumus G, Gurcha SS, Movahedzadeh F, Geurtsen J, Brown EJ, Eysink Smeets MM, Besra GS, Willemsen PTJ, Lowary TL, van Kooyk Y, Maaskant JJ, Stoker NG, van der Ley P, Puzo G, Vandenbroucke-Grauls CMJE, Wieland CW, van der Poll T, Geijtenbeek TBH, van der Sar AM, Bitter W (2008) The mannose cap of mycobacterial lipoarabinomannan does not dominate the mycobacterium-host interaction. Cell Microbiol. 10:930–944.

Arbues A, Aguilo JI, Gonzalo-Asensio J, Marinova D, Uranga S, Puentes E, Fernandez C, Parra A, Cardona P-J, Vilaplana C, Ausina V, Williams A, Clark S, Malaga W, Guilhot C, Gicquel B, Martín C (2013) Construction, characterization and preclinical evaluation of MTBVAC, the first live-attenuated *M. tuberculosis*-based vaccine to enter clinical trials. Vaccine 31:4867–4873.

Arend SM, Andersen P, van Meijgaarden KE, Skjøt RL, Subronto YW, van Dissel JT, Ottenhoff TH (2000) Detection of active tuberculosis infection by T cell responses to early-secreted antigenic target 6 kDa protein and culture filtrate protein 10. J Infect Dis. 181:1850–1854.

Aronson JD (1926) Spontaneous tuberculosis in salt water fish. J Infect Dis. 39:315–320.

Azuma I, Yamamura Y, Fukushi K (1968) Fractionation of mycobacterial cell wall. Isolation of arabinose mycolate and arabinogalactan from cell wall fraction of *Mycobacterium tuberculosis* strain Aoyama B. J Bacteriol. 96:1885–1887.

Babu MM, Priya ML, Selvan AT, Madera M, Gough J, Aravind L, Sankaran K (2006) A database of bacterial lipoproteins (DOLOP) with functional assignments to predicted lipoproteins. J Bacteriol. 188:2761–2773.

Baess I (1979) Deoxyribonucleic acid relatedness among species of slowly-growing mycobacteria. Acta Pathologica Microbiologica Scandinavica Section B Microbiology 87B:221–226.

Bakke AC (2001) The principles of flow cytometry. Laboratory Medicine 32:207–211.

Balasubramanian V, Wiegeshaus EH, Taylor BT, Smith DW (1994) Pathogenesis of tuberculosis: pathway to apical localization. Tuber Lung Dis. 75:168–178.

Baldwin SL, Bertholet S, Reese VA, Ching LK, Reed SG, Coler RN (2012) The importance of adjuvant formulation in the development of a tuberculosis vaccine. J Immunol. 188:2189–2197.

Banaiee N, Kincaid EZ, Buchwald U, Jacobs WR, Ernst JD (2006) Potent inhibition of macrophage responses to IFN-gamma by live virulent *Mycobacterium tuberculosis* is independent of mature mycobacterial lipoproteins but dependent on TLR2. J Immunol. 176:3019–3027.

Bandera A, Gori A, Catozzi L, Degli Esposti A, Marchetti G, Molteni C, Ferrario G, Codecasa L, Penati V, Matteelli A, Franzetti F (2001) Molecular epidemiology study of exogenous reinfection in an area with a low incidence of tuberculosis. J Clin Microbiol. 39:2213–2218.

Barreto ML, Rodrigues LC, Silva RCR, Assis AMO, Reis MG, Cast S, Blanton RE (2000) Lower hookworm incidence, prevalence, and intensity of infection in children with a Bacillus Calmette-Guérin vaccination scar. J Infect Dis 182:1800–1803.

Barry CE, Lee RE, Mdluli K, Sampson AE, Schroeder BG, Slayden RA, Yuan Y (1998) Mycolic acids: structure, biosynthesis and physiological functions. Prog Lipid Res. 37:143–179.

Basaraba RJ, Bielefeldt-Ohmann H, Eschelbach EK, Reisenhauer C, Tolnay AE, Taraba LC, Shanley CA, Smith EA, Bedwell CL, Chlipala EA, Orme IM (2008) Increased expression of host iron-binding proteins precedes iron accumulation and calcification of primary lung lesions in experimental tuberculosis in the guinea pig. Tuberculosis 88:69–79.

Basaraba RJ, Dailey DD, McFarland CT, Shanley CA, Smith EE, McMurray DN, Orme IM (2006a) Lymphadenitis as a major element of disease in the guinea pig model of tuberculosis. Tuberculosis 86:386–394.

Basaraba RJ, Smith EE, Shanley CA, Orme IM (2006b) Pulmonary lymphatics are primary sites of *Mycobacterium tuberculosis* infection in guinea pigs infected by aerosol. Infect Immun 74:5397–5401.

Bastian M, Braun T, Bruns H, Röllinghoff M, Stenger S (2008) Mycobacterial lipopeptides elicit $CD4^+$ CTLs in *Mycobacterium tuberculosis*-infected humans. J Immunol. 180:3436–3446.

Bauer JA (1958) Histocompatibility in inbred strains of guinea pigs. Ann N Y Acad Sci. 73:663–672.

Bazzi S, Modjtahedi H, Mudan S, Akle C, Bahr GM (2015) Analysis of the immunomodulatory properties of two heat-killed mycobacterial preparations in a human whole blood model. Immunobiology 220:1293-304.

Beaulieu AM, Rath P, Imhof M, Siddall ME, Roberts J, Schnappinger D, Nathan CF (2010) Genome-wide screen for *Mycobacterium tuberculosis* genes that regulate host immunity. PLoS ONE 5:e15120.

Beckman EM, Porcelli SA, Morita CT, Behar SM, Furlong ST, Brenner MB (1994) Recognition of a lipid antigen by CD1-restricted alpha $beta^+$ T cells. Nature 372:691–694.

Behr MA (2001a) Comparative genomics of BCG vaccines. Tuberculosis 81:165–168.

Behr MA (2001b) Correlation between BCG genomics and protective efficacy. Scand J Infect Dis. 33:66–69.

Behr MA, Small PM (1999) A historical and molecular phylogeny of BCG strains. Vaccine 17:915–922.

Belisle JT, Vissa VD, Sievert T, Takayama K, Brennan PJ, Besra GS (1997) Role of the major antigen of *Mycobacterium tuberculosis* in cell wall biogenesis. Science 276:1420–1422.

Berrington WR, Hawn TR (2007) *Mycobacterium tuberculosis*, macrophages, and the innate immune response: does common variation matter? Immunol Rev. 219:167–186.

Berthet FX, Rasmussen PB, Rosenkrands I, Andersen P, Gicquel B (1998) A *Mycobacterium tuberculosis* operon encoding ESAT-6 and a novel low-molecular-mass culture filtrate protein (CFP-10). Microbiology 144:3195–3203.

Besra GS, Khoo K-H, McNeil MR, Dell A, Morris HR, Brennan PJ (1995) A new interpretation of the structure of the mycolyl-arabinogalactan complex of *Mycobacterium tuberculosis* as revealed through characterization of oligoglycosylalditol fragments by fast-atom bombardment mass spectrometry and 1H nuclear magnetic resonance spectroscopy. Biochemistry 34:4257–4266.

Betts JC, Lukey PT, Robb LC, McAdam RA, Duncan K (2002) Evaluation of a nutrient starvation model of *Mycobacterium tuberculosis* persistence by gene and protein expression profiling. Mol Microbiol. 43:717–731.

Betts MR, Brenchley JM, Price DA, De Rosa SC, Douek DC, Roederer M, Koup RA (2003) Sensitive and viable identification of antigen-specific $CD8^+$ T cells by a flow cytometric assay for degranulation. Journal Immunol Methods 281:65–78.

Bhatt K, Verma S, Ellner JJ, Salgame P (2015) Quest for correlates of protection against tuberculosis: FIG 1. Clin Vaccine Immunol. 22:258–266.

Bigi F, Alito A, Romano MI, Zumarraga M, Caimi K, Cataldi A (2000) The gene encoding P27 lipoprotein and a putative antibiotic-resistance gene form an operon in *Mycobacterium tuberculosis* and *Mycobacterium bovis*. Microbiology 146:1011–1018.

Bigi F, Espitia C, Alito A, Zumarraga M, Romano MI, Cravero S, Cataldi A (1997) A novel 27 kDa lipoprotein antigen from *Mycobacterium bovis*. Microbiology 143:3599–3605.

Bigi F, Gioffré A, Klepp L, de la Paz Santangelo M, Alito A, Caimi K, Meikle V, Zumárraga M, Taboga O, Romano MI, Cataldi A (2004) The knockout of the lprG-Rv1410 operon produces strong attenuation of *Mycobacterium tuberculosis*. Microbes Infect. 6:182–187.

Bligh EG, Dyer WJ (1959) A rapid method of total lipid extraction and purification. Can J Biochem Physiol. 37:911–917.

Boldrin F, Ventura M, Degiacomi G, Ravishankar S, Sala C, Svetlikova Z, Ambady A, Dhar N, Korduláková J, Zhang M, Serafini A, Vishwas KG, Vishwas VG, Kolly GS, Kumar N, Palù G, Guerin ME, Mikusova K, Cole ST, Manganelli R (2014) The phosphatidyl-*myo*-inositol mannosyltransferase PimA is essential for *Mycobacterium tuberculosis* growth *in vitro* and *in vivo*. J Bacteriol. 196:3441–3451.

Bordier C (1981) Phase separation of integral membrane proteins in Triton X-114 solution. J Biol Chem. 256:1604–1607.

Borremans M, de Wit L, Volckaert G, Ooms J, de Bruyn J, Huygen K, van Vooren JP, Stelandre M, Verhofstadt R, Content J (1989) Cloning, sequence determination, and expression of a 32-kilodalton-protein gene of *Mycobacterium tuberculosis*. Infect Immun. 57:3123–3130.

Borsuk S, Newcombe J, Mendum TA, Dellagostin OA, McFadden J (2009) Identification of proteins from tuberculin purified protein derivative (PPD) by LC-MS/MS. Tuberculosis 89:423–430.

Bowdish DME, Sakamoto K, Kim M-J, Kroos M, Mukhopadhyay S, Leifer CA, Tryggvason K, Gordon S, Russell DG (2009) MARCO, TLR2, and CD14 are required for macrophage cytokine responses to mycobacterial trehalose dimycolate and *Mycobacterium tuberculosis*. PLoS Pathog. 5:e1000474.

Böddinghaus B, Rogall T, Flohr T, Blöcker H, Böttger EC (1990) Detection and identification of mycobacteria by amplification of rRNA. J Clin Microbiol. 28:1751–1759.

Bradford MM (1976) A rapid and sensitive method for the quantitation of microgram quantities of protein utilizing the principle of protein-dye binding. Anal Biochem. 72:248-254.

Braibant M, Lefèvre P, de Wit L, Ooms J, Peirs P, Huygen K, Wattiez R, Content J (1996a) Identification of a second *Mycobacterium tuberculosis* gene cluster encoding proteins of an ABC phosphate transporter. FEBS Lett. 394:206–212.

Braibant M, Lefèvre P, de Wit L, Peirs P, Ooms J, Huygen K, Andersen AB, Content J (1996b) A *Mycobacterium tuberculosis* gene cluster encoding proteins of a phosphate transporter homologous to the *Escherichia coli* Pst system. Gene 176:171–176.

Brandt L, Feino Cunha J, Weinreich Olsen A, Chilima B, Hirsch P, Appelberg R, Andersen P (2002) Failure of the *Mycobacterium bovis* BCG vaccine: some species of environmental mycobacteria block multiplication of BCG and induction of protective immunity to tuberculosis. Infect Immun. 70:672–678.

Brandt L, Oettinger T, Holm A, Andersen AB, Andersen P (1996) Key epitopes on the ESAT-6 antigen recognized in mice during the recall of protective immunity to *Mycobacterium tuberculosis*. J Immunol. 157:3527–3533.

Brennan PJ, Nikaido H (1995) The envelope of mycobacteria. Annu Rev Biochem. 64:29–63.

Brewer TF (2000) Preventing tuberculosis with Bacillus Calmette-Guérin vaccine: a meta-analysis of the literature. Clin Infect Dis. 31:S64–S67.

Brightbill HD, Libraty DH, Krutzik SR, Yang R-B, Belisle JT, Bleharski JR, Maitland M, Norgard MV, Plevy SE, Smale ST, Brennan PJ, Bloom BR, Godowski PJ, Modlin RL (1999) Host defense mechanisms triggered by microbial lipoproteins through Toll-like receptors. Science 285:732–736.

Brigl M, Brenner MB (2004) CD1: antigen presentation and T cell function. Annu Rev Immunol. 22:817–890.

Briken V, Porcelli SA, Besra GS, Kremer L (2004) Mycobacterial lipoarabinomannan and related lipoglycans: from biogenesis to modulation of the immune response. Mol Microbiol. 53:391–403.

Brock I, Munk ME, Kok-Jensen A, Andersen P (2001) Performance of whole blood IFN-gamma test for tuberculosis diagnosis based on PPD or the specific antigens ESAT-6 and CFP-10. Int J Tuberc Lung Dis. 5:462–467.

Brosch R, Gordon SV, Buchrieser C, Pym AS, Garnier T, Cole ST (2000) Comparative genomics uncovers large tandem chromosomal duplications in *Mycobacterium bovis* BCG Pasteur. Yeast 17:111–123.

Brosch R, Gordon SV, Garnier T, Eiglmeier K, Frigui W, Valenti P, Santos Dos S, Duthoy S, Lacroix C, Garcia-Pelayo C, Inwald JK, Golby P, Garcia JN, Hewinson RG, Behr MA, Quail MA, Churcher C, Barrell BG, Parkhill J, Cole ST (2007) Genome plasticity of BCG and impact on vaccine efficacy. Proc Natl Acad Sci USA. 104:5596–5601.

Brosch R, Gordon SV, Marmiesse M, Brodin P, Buchrieser C, Eiglmeier K, Garnier T, Gutierrez C, Hewinson G, Kremer K, Parsons LM, Pym AS, Samper S, van Soolingen D, Cole ST (2002) A new evolutionary scenario for the *Mycobacterium tuberculosis* complex. Proc Natl Acad Sci USA. 99:3684–3689.

Brosch R, Pym AS, Gordon SV, Cole ST (2001) The evolution of mycobacterial pathogenicity: clues from comparative genomics. Trends Microbiol. 9:452–458.

Brown M, Wittwer C (2000) Flow cytometry: principles and clinical applications in hematology. Clin Chem. 46:1221–1229.

Brozna JP, Horan M, Rademacher JM, Pabst KM, Pabst MJ (1991) Monocyte responses to sulfatide from *Mycobacterium tuberculosis*: inhibition of priming for enhanced release of superoxide, associated with increased secretion of interleukin-1 and tumor necrosis factor alpha, and altered protein phosphorylation. Infect Immun. 59:2542–2548.

Buddle BM, Parlane NA, Keen DL, Aldwell FE, Pollock JM, Lightbody K, Andersen P (1999) Differentiation between *Mycobacterium bovis* BCG-vaccinated and *M. bovis*-infected cattle by using recombinant mycobacterial antigens. Clin Diagn Lab Immunol. 6:1–5.

Cala-De Paepe D (2011) Les glycolipides mycobactériens multi-acylés: de la structure à la présentation antigénique. Dissertation, l'université de Toulouse, France.

Calmette A (1931) Preventive vaccination against tuberculosis with BCG. Proc R Soc Med. 24:1481–1490.

Cambier CJ, Takaki KK, Larson RP, Hernandez RE, Tobin DM, Urdahl KB, Cosma CL, Ramakrishnan L (2014) Mycobacteria manipulate macrophage recruitment through coordinated use of membrane lipids. Nature 505:218–222.

Carr D (2002) The handbook of analysis and purification of peptides and proteins by reversed phase HPLC, 3rd edition. Grace Vydac.

Cassidy JP (2006) The pathogenesis and pathology of bovine tuberculosis with insights from studies of tuberculosis in humans and laboratory animal models. Vet Microbiol. 112:151–161.

Cavalcanti YVN, Brelaz MCA, Neves JK de AL, Ferraz JC, Pereira VRA (2012) Role of TNF-alpha, IFN-gamma, and IL-10 in the development of pulmonary tuberculosis. Pulmonary Medicine 2012:745483–10.

Cegielski JP, McMurray DN (2004) The relationship between malnutrition and tuberculosis: evidence from studies in humans and experimental animals. Int J Tuberc Lung Dis. 8:286–298.

Chakhaiyar P, Nagalakshmi Y, Aruna B, Murthy KJR, Katoch VM, Hasnain SE (2004) Regions of high antigenicity within the hypothetical PPE major polymorphic tandem repeat open-reading frame, Rv2608, show a differential humoral response and a low T cell response in various categories of patients with tuberculosis. J Infect Dis. 190:1237–1244.

Chanwong S, Maneekarn N, Makonkawkeyoon L, Makonkawkeyoon S (2007) Intracellular growth and drug susceptibility of *Mycobacterium tuberculosis* in macrophages. Tuberculosis 87:130–133.

Chaparas SD, Maloney CJ, Hedrick SR (1970) Specificity of tuberculins and antigens from various species of mycobacteria. Am Rev Respir Dis. 101:74–83.

Chapman ALN, Munkanta M, Wilkinson KA, Pathan AA, Ewer K, Ayles H, Reece WH, Mwinga A, Godfrey-Faussett P, Lalvani A (2002) Rapid detection of active and latent tuberculosis infection in HIV-positive individuals by enumeration of *Mycobacterium tuberculosis*-specific T cells. AIDS 16:2285–2293.

Chatterjee D, Lowell K, Rivoire B, McNeil MR, Brennan PJ (1992) Lipoarabinomannan of *Mycobacterium tuberculosis*. Capping with mannosyl residues in some strains. J Biol Chem. 267:6234–6239.

Chester FD (1901) A manual of determinative bacteriology. MacMillan.

Chiodini RJ (1989) Crohn's disease and the mycobacterioses: a review and comparison of two disease entities. Clin Microbiol Rev. 2:90–117.

Cho SH, Warit S, Wan B, Hwang CH, Pauli GF, Franzblau SG (2007) Low-oxygen-recovery assay for high-throughput screening of compounds against nonreplicating *Mycobacterium tuberculosis*. Antimicrob Agents Chemother. 51:1380–1385.

Cho YS, Dobos KM, Prenni J, Yang H, Hess A, Rosenkrands I, Andersen P, Ryoo SW, Bai G-H, Brennan MJ, Izzo A, Bielefeldt-Ohmann H, Belisle JT (2012) Deciphering the proteome of the *in vivo* diagnostic reagent “purified protein derivative” from *Mycobacterium tuberculosis*. Proteomics 12:979–991.

Christie WW, Han X (2010) Lipid Analysis. Elsevier.

Ciaramella A, Cavone A, Santucci MB, Garg SK, Sanarico N, Bocchino M, Galati D, Martino A, Auricchio G, D’Orazio M, Stewart GR, Neyrolles O, Young DB, Colizzi V, Fraziano M (2004) Induction of apoptosis and release of interleukin-1β by cell wall-associated 19 kDa lipoprotein during the course of mycobacterial infection. J Infect Dis. 190:1167–76.

Clark RB, Shevach EM (1982) Generation of T cell colonies from responder strain 2 guinea pigs that recognize the copolymer L-glutamic acid, L-lysine in association with nonresponder strain 13 Ia antigens. J Exp Med. 155:635–640.

Clark S, Hall Y, Williams A (2014) Animal models of tuberculosis: guinea pigs. In: Kaufmann SHE, Rubin EJ, Zumla A (eds) Tuberculosis. Cold Spring Harbor Laboratory Press.

Clay H, Davis JM, Beery D, Huttenlocher A, Lyons SE, Ramakrishnan L (2007) Dichotomous role of the macrophage in early *Mycobacterium marinum* infection of the zebrafish. Cell Host Microbe 2:29–39.

Clemens DL, Horwitz MA (1996) The *Mycobacterium tuberculosis* phagosome interacts with early endosomes and is accessible to exogenously administered transferrin. J Exp Med 184:1349–1355.

Colditz GA, Brewer TF, Berkey CS, Wilson ME, Burdick E, Fineberg HV, Mosteller F (1994) Efficacy of BCG vaccine in the prevention of tuberculosis. Meta-analysis of the published literature. JAMA 271:698–702.

Cole ST (1999) Learning from the genome sequence of mycobacterium tuberculosis H37Rv. FEBS Lett. 452:7–10.

Cole ST, Brosch R, Parkhill J, Garnier T, Churcher C, Harris D, Gordon SV, Eiglmeier K, Gas S, Barry CE, Tekaia F, Badcock K, Basham D, Brown D, Chillingworth T, Connor R, Davies R, Devlin K, Feltwell T, Gentles S, Hamlin N, Holroyd S, Hornsby T, Jagels K, Krogh A, McLean J, Moule S, Murphy L, Oliver K, Osborne J, Quail MA, Rajandream MA, Rogers J, Rutter S, Seeger K, Skelton J, Squares R, Squares S, Sulston JE, Taylor K, Whitehead S, Barrell BG (1998) Deciphering the biology of *Mycobacterium tuberculosis* from the complete genome sequence. Nature 393:537–544.

Coler RN, Skeiky YA, Ovendale PJ, Vedvick TS, Gervassi L, Guderian J, Jen S, Reed SG, Campos-Neto A (2000) Cloning of a *Mycobacterium tuberculosis* gene encoding a purifed protein derivative protein that elicits strong tuberculosis-specific delayed-type hypersensitivity. J Infect Dis. 182:224–233.

Collins CH, Grange JM (1983) The bovine tubercle bacillus. J Appl Bacteriol. 55:13–29.

Collison LW, Vignali DAA (2011) *In vitro* Treg suppression assays. Methods Mol Biol. 707:21–37.

Comas I, Chakravartti J, Small PM, Galagan J, Niemann S, Kremer K, Ernst JD, Gagneux S (2010) Human T cell epitopes of *Mycobacterium tuberculosis* are evolutionarily hyperconserved. Nat Genet. 42:498–503.

Comas I, Coscolla M, Luo T, Borrell S, Holt KE, Kato-Maeda M, Parkhill J, Malla B, Berg S, Thwaites G, Yeboah-Manu D, Bothamley G, Mei J, Wei L, Bentley S, Harris SR, Niemann S, Diel R, Aseffa A, Gao Q, Young D, Gagneux S (2013) Out-of-Africa migration and neolithic coexpansion of *Mycobacterium tuberculosis* with modern humans. Nat Genet. 45:1176–1182.

Content J, la Cuvellerie de A, de Wit L, Vincent-Levy-Frébault V, Ooms J, de Bruyn J (1991) The genes coding for the antigen 85 complexes of *Mycobacterium tuberculosis* and *Mycobacterium bovis* BCG are members of a gene family: cloning, sequence determination, and genomic organization of the gene coding for antigen 85-C of *M. tuberculosis*. Infect Immun. 59:3205–3212.

Converse PJ, Jones SL, Astemborski J, Vlahov D, Graham NMH (1997) Comparison of a tuberculin interferon-γ assay with the tuberculin skin test in high-risk adults: effect of human immunodeficiency virus infection. J Infect Dis. 176:144–150.

Cooper AM (2009) Cell-mediated immune responses in tuberculosis. Annu Rev Immunol. 27:393–422.

Cooper AM, Flynn JL (1995) The protective immune response to *Mycobacterium tuberculosis*. Curr Opin Immunol. 7:512–516.

Cooper PJ, Chico ME, Gaus D, Griffin GE (2003) Relationship between Bacille Calmette-Guérin vaccination, Mantoux test positivity, and geohelminth infection. Trans R Soc Trop Med Hyg. 97:473–476.

Corbel MJ, Fruth U, Griffiths E, Knezevic I (2004) Report on a WHO Consultation on the characterisation of BCG strains, Imperial College, London 15-16 December 2003. Vaccine 22:2675–2680.

Corman ML (1989) Thomas Kennedy Dalziel 1861-1924. Chronic interstitial enteritis. Dis Colon Rectum. 32:1076–1078.

Cousins DV, Bastida R, Cataldi A, Quse V, Redrobe S, Dow S, Duignan P, Murray A, Dupont C, Ahmed N, Collins DM, Butler WR, Dawson D, Rodríguez D, Loureiro J, Romano MI, Alito A, Zumarraga M, Bernardelli A (2003) Tuberculosis in seals caused by a novel member of the *Mycobacterium tuberculosis* complex: *Mycobacterium pinnipedii* sp. nov. Int J Syst Evol Microbiol. 53:1305–1314.

Cox JS, Chen B, McNeil M, Jacobs WR (1999) Complex lipid determines tissue-specific replication of *Mycobacterium tuberculosis* in mice. Nature 402:79–83.

Cronan MR, Tobin DM (2014) Fit for consumption: zebrafish as a model for tuberculosis. Dis Model Mech. 7:777–784.

Cruz JC (1938) *Mycobacterium fortuitum*: um novo bacilo acido-resistente patogenico para o homem. Acta Med Rio de Janeiro. 1:297–301.

da Fonseca DP, Joosten D, van der Zee R, Jue DL, Singh M, Vordermeier HM, Snippe H, Verheul AF (1998) Identification of new cytotoxic T cell epitopes on the 38-kilodalton lipoglycoprotein of *Mycobacterium tuberculosis* by using lipopeptides. Infect Immun. 66:3190–3197.

Daffé M, Brennan PJ, McNeil M (1990) Predominant structural features of the cell wall arabinogalactan of *Mycobacterium tuberculosis* as revealed through characterization of oligoglycosyl alditol fragments by gas chromatography/mass spectrometry and by 1H and 13C NMR analyses. J Biol Chem. 265:6734–6743.

Daffé M, Draper P (1998) The envelope layers of mycobacteria with reference to their pathogenicity. Adv Microb Physiol. 39:131–203.

Daffé M, Lanéelle MA (1988) Distribution of phthiocerol diester, phenolic mycosides and related compounds in mycobacteria. J Gen Microbiol. 134:2049–2055.

Daniel TM (2006) The history of tuberculosis. Respiratory Medicine 100:1862–1870.

Dannenberg AM (2001) Pathogenesis of pulmonary *Mycobacterium bovis* infection: basic principles established by the rabbit model. Tuberculosis 81:87–96.

Dascher CC (2003) Immunization with a mycobacterial lipid vaccine improves pulmonary pathology in the guinea pig model of tuberculosis. Int Immunol. 15:915–925.

Dascher CC, Hiromatsu K, Naylor JW, Brauer PP, Brown KA, Storey JR, Behar SM, Kawasaki ES, Porcelli SA, Brenner MB, LeClair KP (1999) Conservation of a CD1 multigene family in the guinea pig. J Immunol. 163:5478–5488.

Davidsen J, Rosenkrands I, Christensen D, Vangala A, Kirby D, Perrie Y, Agger EM, Andersen P (2005) Characterization of cationic liposomes based on dimethyldioctadecylammonium and synthetic cord factor from *M. tuberculosis* (trehalose 6,6′-dibehenate) – a novel adjuvant inducing both strong CMI and antibody responses. BBA – Biomembranes 1718:22–31.

de Souza GA, Leversen NA, Målen H, Wiker HG (2011) Bacterial proteins with cleaved or uncleaved signal peptides of the general secretory pathway. J Proteomics. 75:502–510.

Delogu G, Manganelli R, Brennan MJ (2014) Critical research concepts in tuberculosis vaccine development. Clin Microbiol Infect. 20:59–65.

Demissie A, Leyten EMS, Abebe M, Wassie L, Aseffa A, Abate G, Fletcher H, Owiafe P, Hill PC, Brookes R, Rook G, Zumla A, Arend SM, Klein M, Ottenhoff THM, Andersen P, Doherty TM (2006) Recognition of stage-specific mycobacterial antigens differentiates between acute and latent infections with *Mycobacterium tuberculosis*. Clin Vaccine Immunol. 13:179–186.

Dey B, Bishai WR (2014) Crosstalk between *Mycobacterium tuberculosis* and the host cell. Semin Immunol. 26:486–496.

Diel R, Nienhaus A, Lange C, Meywald-Walter K, Forssbohm M, Schaberg T (2006) Tuberculosis contact investigation with a new, specific blood test in a low-incidence population containing a high proportion of BCG-vaccinated persons. Respir Res. 7:77.

Dietrich J, Aagaard C, Leah R, Olsen AW, Stryhn A, Doherty TM, Andersen P (2005) Exchanging ESAT-6 with TB10.4 in an Ag85B fusion molecule-based tuberculosis subunit vaccine: efficient protection and ESAT-6-based sensitive monitoring of vaccine efficacy. J Immunol. 174:6332–6339.

DiGiuseppe Champion PA, Cox JS (2007) Protein secretion systems in mycobacteria. Cell Microbiol. 9:1376–1384.

Dillon DC, Alderson MR, Day CH, Lewinsohn DM, Coler R, Bement T, Campos-Neto A, Skeiky YA, Orme IM, Roberts A, Steen S, Dalemans W, Badaro R, Reed SG (1999) Molecular characterization and human T cell responses to a member of a novel *Mycobacterium tuberculosis* MTB39 gene family. Infect Immun. 67:2941–2950.

Ding AH, Nathan CF, Stuehr DJ (1988) Release of reactive nitrogen intermediates and reactive oxygen intermediates from mouse peritoneal macrophages. Comparison of activating cytokines and evidence for independent production. J Immunol. 141:2407–2412.

Dobos KM (2015) Dobos lab production manuals, SOP PP01108, Isolation of total lipid. In: csu-cvmbs.colostate.edu. http://csu-cvmbs.colostate.edu/academics/mip/research/Pages/dobos-lab-production-manuals-sops.aspx. Accessed 23 Jun 2015.

Dobos KM, Khoo KH, Swiderek KM, Brennan PJ, Belisle JT (1996) Definition of the full extent of glycosylation of the 45-kilodalton glycoprotein of *Mycobacterium tuberculosis*. J Bacteriol. 178:2498–2506.

Dommergues MA, Rocque F de L, Guy C, Lécuyer A, Jacquet A, Guérin N, Fagot JP, Boucherat M, d'Athis P, Cohen R (2009) Local and regional adverse reactions to BCG-SSI® vaccination: a 12-month cohort follow-up study. Vaccine 27:6967–6973.

Dougan SK, Kaser A, Blumberg RS (2007) CD1 expression on antigen-presenting cells. In: Moody DB (ed) T cell activation by CD1 and lipid antigens. Springer.

Drage MG, Pecora ND, Hise AG, Febbraio M, Silverstein RL, Golenbock DT, Boom WH, Harding CV (2009) TLR2 and its co-receptors determine responses of macrophages and dendritic cells to lipoproteins of *Mycobacterium tuberculosis*. Cell Immunol. 258:29–37.

Drage MG, Tsai H-C, Pecora ND, Cheng T-Y, Arida AR, Shukla S, Rojas RE, Seshadri C, Moody DB, Boom WH, Sacchettini JC, Harding CV (2010) *Mycobacterium tuberculosis* lipoprotein LprG (Rv1411c) binds triacylated glycolipid agonists of Toll-like receptor 2. Nat Struct Mol Biol. 17:1088–1095.

Dubnau E, Chan J, Raynaud C, Mohan VP, Lanéelle MA, Yu K, Quémard A, Smith I, Daffé M (2000) Oxygenated mycolic acids are necessary for virulence of *Mycobacterium tuberculosis* in mice. Mol Microbiol. 36:630–637.

Dye C (2013) Making wider use of the world's most widely used vaccine: Bacille Calmette-Guerin revaccination reconsidered. J R Soc Interface. 10:20130365.

Eastwood A, Cobbett L, Griffith F, Griffith A, Power WH (1911) Final report of the Royal Commission appointed to inquire into the relations of human and animal tuberculosis. H.M. Stationary Office.

Eckstein TM, Belisle JT, Inamine JM (2003) Proposed pathway for the biosynthesis of serovar-specific glycopeptidolipids in *Mycobacterium avium* serovar 2. Microbiology 149:2797–2807.

Egen JG, Rothfuchs AG, Feng CG, Winter N, Sher A, Germain RN (2008) Macrophage and T cell dynamics during the development and disintegration of mycobacterial granulomas. Immunity 28:271–284.

Ehlers S (2010) DC-SIGN and mannosylated surface structures of *Mycobacterium tuberculosis* – a deceptive liaison. Eur J Cell Biol. 89:95–101.

Ehlers S, Schaible UE (2013) The granuloma in tuberculosis: dynamics of a host-pathogen collusion. Front Immunol. 3:411.

Ekdahl MO, Smith BL, Money DFL (1970) Tuberculosis in some wild and ferral animals in New Zealand. N Z Vet J. 18:44–45.

Elhay MJ, Oettinger T, Andersen P (1998) Delayed-type hypersensitivity responses to ESAT-6 and MPT64 from *Mycobacterium tuberculosis* in the guinea pig. Infect Immun. 66:3454–3456.

Elliott AM, Nakiyingi J, Quigley MA, French N, Gilks CF, Whitworth JA (1999) Inverse association between BCG immunisation and intestinal nematode infestation among HIV-1-positive individuals in Uganda. The Lancet 354:1000–1001.

Esin S, Batoni G, Källenius G, Gaines H, Campa M, Svenson SB, Andersson R, Wigzell H (1996) Proliferation of distinct human T cell subsets in response to live, killed or soluble extracts of *Mycobacterium tuberculosis* and *Myco. avium*. Clin Exp Immunol. 104:419–425.

European Directorate for the Quality of Medicine and Health Care (2013) European Pharmacopoeia 8.0.

Evrard B, Dosgilbert A, Jacquemot N, Demeocq F, Gilles T, Chassagne J, Berger M, Tridon A (2010) CFSE flow cytometric quantification of lymphocytic proliferation in extracorporeal photopheresis: use for quality control. Transfus Apher Sci. 42:11–19.

Ewer K, Deeks J, Alvarez L, Bryant G, Waller S, Andersen P, Monk P, Lalvani A (2003) Comparison of T cell-based assay with tuberculin skin test for diagnosis of *Mycobacterium tuberculosis* infection in a school tuberculosis outbreak. The Lancet 361:1168–1173.

Faith A, Moreno C, Lathigra R, Roman E, Fernandez M, Brett S, Mitchell DM, Ivanyi J, Rees AD (1991) Analysis of human T-cell epitopes in the 19,000 MW antigen of *Mycobacterium tuberculosis*: influence of HLA-DR. Immunology 74:1–7.

Faivre L, Lecouflet L, Liu W-Q, Khadher I, Lahaie C, Vidal M, Legouvello S, Beaumont J-L, Bierling P, Rouard H, Birebent B (2014) Quality control of extracorporeal photochemotherapy: proliferation assay using CFSE validated according to ISO 15189:2007 standards. Cytometry 88:30–39.

Farhat M, Greenaway C, Pai M, Menzies D (2006) False-positive tuberculin skin tests: what is the absolute effect of BCG and non-tuberculous mycobacteria? Int J Tuberc Lung Dis. 10:1192–1204.

Ferraz TPL, Fiúza MC, Santos dos MLA, Pontes de Carvalho L, Soares NM (2004) Comparison of six methods for the extraction of lipids from serum in terms of effectiveness and protein preservation. J Biochem Biophys Methods. 58:187–193.

Festing MF (1976) Phenotypic variability of inbred and outbred mice. Nature 263:230–232.

Fine PEM (1995) Variation in protection by BCG: implications of and for heterologous immunity. The Lancet 346:1339–1345.

Fine PEM (2001) BCG: The challenge continues. Scand J Infect Dis. 33:243–245.

Fleischmann RD, Alland D, Eisen JA, Carpenter L, White O, Peterson J, DeBoy R, Dodson R, Gwinn M, Haft D, Hickey E, Kolonay JF, Nelson WC, Umayam LA, Ermolaeva M, Salzberg SL, Delcher A, Utterback T, Weidman J, Khouri H, Gill J, Mikula A, Bishai W, Jacobs WR Jr, Venter JC, Fraser CM (2002) Whole-genome comparison of *Mycobacterium tuberculosis* clinical and laboratory strains. J Bacteriol. 184:5479–5490.

Flesch I, Hess JH, Oswald IP, Kaufmann S (1994) Growth-inhibition of *Mycobacterium bovis* by IFN-gamma stimulated macrophages – regulation by endogenous tumor-necrosis-factor-alpha and by Il-10. Int Immunol. 6:693–700.

Fletcher HA (2015) Profiling the host immune response to tuberculosis vaccines. Vaccine 33:5313–5315.

Fok JS, Ho RS, Arora PK, Harding GE, Smith DW (1976) Host-parasite relationships in experimental airborne tuberculosis. V. Lack of hematogenous dissemination of *Mycobacterium tuberculosis* to the lungs in animals vaccinated with Bacille Calmette-Guérin. J Infect Dis. 133:137–144.

Folch J, LEES M, Sloane Stanley GH (1957) A simple method for the isolation and purification of total lipides from animal tissues. J Biol Chem. 226:497–509.

Fox W (1868) A lecture on the artificial production of tubercle in the lower animals. Br Med J. 1:551–554.

Francis J (1958) Tuberculosis in animals and man. Cassell & Co., Ltd.

Francis J (1959) The work of the British Royal Commission on tuberculosis, 1901-1911. Tubercle 40:124–132.

Francis J (1947) Bovine tuberculosis. Staples Press Limited.

Fratti RA, Backer JM, Gruenberg J, Corvera S, Deretic V (2001) Role of phosphatidylinositol 3-kinase and Rab5 effectors in phagosomal biogenesis and mycobacterial phagosome maturation arrest. J Cell Biol. 154:631–644.

Fratti RA, Chua J, Vergne I, Deretic V (2003) *Mycobacterium tuberculosis* glycosylated phosphatidylinositol causes phagosome maturation arrest. Proc Natl Acad Sci USA. 100:5437–5442.

Frigui W, Bottai D, Majlessi L, Monot M, Josselin E, Brodin P, Garnier T, Gicquel B, Martín C, Leclerc C, Cole ST, Brosch R (2008) Control of *M. tuberculosis* ESAT-6 secretion and specific T cell recognition by PhoP. PLoS Pathog. 4:e33.

Frothingham R, Hills HG, Wilson KH (1994) Extensive DNA sequence conservation throughout the *Mycobacterium tuberculosis* complex. J Clin Microbiol. 32:1639–1643.

Fulcher DA, Wong SWJ (1999) Carboxyfluorescein succinimidyl ester-based proliferative assays for assessment of T cell function in the diagnostic laboratory. Immunol Cell Biol. 77:559–564.

Fulton SA, Reba SM, Pai RK, Pennini M, Torres M, Harding CV, Boom WH (2004) Inhibition of major histocompatibility complex II expression and antigen processing in murine alveolar macrophages by *Mycobacterium bovis* BCG and the 19-kilodalton mycobacterial lipoprotein. Infect Immun. 72:2101–2110.

Galagan JE, Minch K, Peterson M, Lyubetskaya A, Azizi E, Sweet L, Gomes A, Rustad T, Dolganov G, Glotova I, Abeel T, Mahwinney C, Kennedy AD, Allard R, Brabant W, Krueger A, Jaini S, Honda B, Yu W-H, Hickey MJ, Zucker J, Garay C, Weiner B, Sisk P, Stolte C, Winkler JK, Van de Peer Y, Iazzetti P, Camacho D, Dreyfuss J, Liu Y, Dorhoi A, Mollenkopf H-J, Drogaris P, Lamontagne J, Zhou Y, Piquenot J, Park ST, Raman S, Kaufmann SHE, Mohney RP, Chelsky D, Moody DB, Sherman DR, Schoolnik GK (2013) The *Mycobacterium tuberculosis* regulatory network and hypoxia. Nature 499:178–183.

Galagan JE, Sisk P, Stolte C, Weiner B, Koehrsen M, Wymore F, Reddy TBK, Zucker JD, Engels R, Gellesch M, Hubble J, Jin H, Larson L, Mao M, Nitzberg M, White J, Zachariah ZK, Sherlock G, Ball CA, Schoolnik GK (2010) TB database 2010: overview and update. Tuberculosis 90:225–235.

Garnier T, Eiglmeier K, Camus J-C, Medina N, Mansoor H, Pryor M, Duthoy S, Grondin S, Lacroix C, Monsempe C, Simon S, Harris B, Atkin R, Doggett J, Mayes R, Keating L, Wheeler PR, Parkhill J, Barrell BG, Cole ST, Gordon SV, Hewinson RG (2003) The complete genome sequence of *Mycobacterium bovis*. Proc Natl Acad Sci USA. 100:7877–7882.

Gehring AJ, Dobos KM, Belisle JT, Harding CV, Boom WH (2004) *Mycobacterium tuberculosis* LprG (Rv1411c): a novel TLR-2 ligand that inhibits human macrophage class II MHC antigen processing. J Immunol. 173:2660–2668.

Gehring AJ, Rojas RE, Canaday DH, Lakey DL, Harding CV, Boom WH (2003) The *Mycobacterium tuberculosis* 19-kilodalton lipoprotein inhibits gamma interferon-regulated HLA-DR and Fc gamma R1 on human macrophages through Toll-like receptor 2. Infect Immun. 71:4487–4497.

Geijtenbeek TBH, Van Vliet SJ, Koppel EA, Sanchez-Hernandez M, Vandenbroucke-Grauls CMJE, Appelmelk B, Van Kooyk Y (2003) Mycobacteria target DC-SIGN to suppress dendritic cell function. J Exp Med. 197:7–17.

Geisel RE, Sakamoto K, Russell DG, Rhoades ER (2005) *In vivo* activity of released cell wall lipids of *Mycobacterium bovis* Bacillus Calmette-Guérin is due principally to trehalose mycolates. J Immunol. 174:5007–5015.

Geldenhuys H, Mearns H, Miles DJC, Tameris M, Hokey D, Shi Z, Bennett S, Andersen P, Kromann I, Hoff ST, Hanekom WA, Mahomed H, Hatherill M, Scriba TJ, Group THITS, van Rooyen M, McClain JB, Ryall R, de Bruyn G (2015) The tuberculosis vaccine H4:IC31 is safe and induces a persistent polyfunctional CD4 T cell response in South African adults: A randomized controlled trial. Vaccine 33:3592–3599.

Germanier R, Fürer E (1975) Isolation and characterization of Gal E mutant Ty 21a of Salmonella typhi: a candidate strain for a live, oral typhoid vaccine. J Infect Dis. 131:553–558.

Getahun H, Matteelli A, Chaisson RE, Raviglione M (2015) Latent *Mycobacterium tuberculosis* Infection. N Engl J Med. 372:2127–2135.

Geurtsen J, Chedammi S, Mesters J, Cot M, Driessen NN, Sambou T, Kakutani R, Ummels R, Maaskant J, Takata H, Baba O, Terashima T, Bovin N, Vandenbroucke-Grauls CMJE, Nigou J, Puzo G, Lemassu A, Daffé M, Appelmelk BJ (2009) Identification of mycobacterial alpha-glucan as a novel ligand for DC-SIGN: involvement of mycobacterial capsular polysaccharides in host immune modulation. J Immunol. 183:5221–5231.

Gideon HP, Phuah J, Myers AJ, Bryson BD, Rodgers MA, Coleman MT, Maiello P, Rutledge T, Marino S, Fortune SM, Kirschner DE, Lin PL, Flynn JL (2015) Variability in tuberculosis granuloma T cell responses exists, but a balance of pro- and anti-inflammatory cytokines is associated with sterilization. PLoS Pathog. 11:e1004603.

Gilleron M, Jackson M, Nigou J, Puzo G (2008) Structure, biosynthesis, and activities of the phosphatidyl-*myo*-inositol-based lipoglycans. In: Daffé M, Reyrat J-M (eds) The mycobacterial cell envelope. American Society of Microbiology.

Gilleron M, Quesniaux VFJ, Puzo G (2003) Acylation state of the phosphatidylinositol hexamannosides from *Mycobacterium bovis* Bacillus Calmette-Guérin and mycobacterium tuberculosis H37Rv and its implication in Toll-like receptor response. J Biol Chem. 278:29880–29889.

Girard R, Pedron T, Uematsu S, Balloy V, Chignard M, Akira S, Chaby R (2003) Lipopolysaccharides from *Legionella* and *Rhizobium* stimulate mouse bone marrow granulocytes via Toll-like receptor 2. J Cell Sci. 116:293–302.

Godfrey HP, Feng Z, Mandy S, Mandy K, Huygen K, de Bruyn J, Abou-Zeid C, Wiker HG, Nagai S, Tasaka H (1992) Modulation of expression of delayed hypersensitivity by mycobacterial antigen 85 fibronectin-binding proteins. Infect Immun. 60:2522–2528.

Goodfellow M, Magee JG (1998) Taxonomy of mycobacteria. In: Mycobacteria. Springer US.

Grange JM (2001) *Mycobacterium bovis* infection in human beings. Tuberculosis 81:71–77.

Grange JM, Collins CH (1997) Tuberculosis and the cow. J R Soc Health. 117:119–122.

Grange JM, Collins CH (1987) Bovine tubercle bacilli and disease in animals and man. Epidemiology and Infection 99:221–234.

Griffith AS (1937) Bovine tuberculosis in man. Tubercle 18:529–543.

Grode L, Ganoza CA, Brohm C, Weiner J, Eisele B, Kaufmann SHE (2013) Safety and immunogenicity of the recombinant BCG vaccine VPM1002 in a phase 1 open-label randomized clinical trial. Vaccine 31:1340–1348.

Grode L, Seiler P, Baumann S, Hess J, Brinkmann V, Nasser Eddine A, Mann P, Goosmann C, Bandermann S, Smith D, Bancroft GJ, Reyrat J-M, van Soolingen D, Raupach B, Kaufmann SHE (2005) Increased vaccine efficacy against tuberculosis of recombinant *Mycobacterium bovis* Bacille Calmette-Guérin mutants that secrete listeriolysin. J Clin Invest. 115:2472–2479.

Guerardel Y, Maes E, Elass E, Leroy Y, Timmerman P, Besra GS, Locht C, Strecker G, Kremer L (2002) Structural study of lipomannan and lipoarabinomannan from *Mycobacterium chelonae*. Presence of unusual components with alpha 1,3-mannopyranose side chains. J Biol Chem. 277:30635–30648.

Guidry TV, Hunter RL, Actor JK (2007) Mycobacterial glycolipid trehalose 6,6'-dimycolate-induced hypersensitive granulomas: contribution of $CD4^+$ lymphocytes. Microbiology 153:3360–3369.

Guinn KM, Hickey MJ, Mathur SK, Zakel KL, Grotzke JE, Lewinsohn DM, Smith S, Sherman DR (2004) Individual RD1-region genes are required for export of ESAT-6/CFP10 and for virulence of *Mycobacterium tuberculosis*. Mol Microbiol. 51:359–370.

Gunawardana G, Chatterjee D, George KM, Brennan P, Whittern D, Small PLC (1999) Characterization of novel macrolide toxins, mycolactones A and B, from a human pathogen, *Mycobacterium ulcerans*. J Am Chem Soc. 121:6092–6093.

Guo S, Xue R, Li Y, Wang SM, Ren L, Xu JJ (2012) The CFP10/ESAT-6 complex of *Mycobacterium tuberculosis* may function as a regulator of macrophage cell death at different stages of tuberculosis infection. Medical Hypotheses 78:389–392.

Gupta UD, Katoch VM (2005) Animal models of tuberculosis. Tuberculosis 85:277–293.

Gutierrez MC, Brisse S, Brosch R, Fabre M, Omaïs B, Marmiesse M, Supply P, Vincent V (2005) Ancient origin and gene mosaicism of the progenitor of *Mycobacterium tuberculosis*. PLoS Pathog. 1:e5.

Haites RE, Morita YS, McConville MJ, Billman-Jacobe H (2005) Function of phosphatidylinositol in mycobacteria. J Biol Chem. 280:10981–10987.

Hajizadeh R, Sato H, Carlisle J, Nadaf MT, Evans W, Shepherd BE, Miller RF, Kalams SA, Drake WP (2007) *Mycobacterium tuberculosis* antigen 85A induces Th1 immune responses in systemic sarcoidosis. J Clin Immunol. 27:445–454.

Hansen DGA (1880) Bacillus leprae. Archiv für Pathologische Anatomie und Physiologie und für Klinische Medicin 79:32–42.

Harboe M, Oettinger T, Wiker HG, Rosenkrands I, Andersen P (1996) Evidence for occurrence of the ESAT-6 protein in *Mycobacterium tuberculosis* and virulent *Mycobacterium bovis* and for its absence in *Mycobacterium bovis* BCG. Infect Immun. 64:16–22.

Harboe M, Whelan AO, Ulvund G, McNair J, Pollock JM, Hewinson RG, Wiker HG (2002) Generation of antibodies to the signal peptide of the MPT83 lipoprotein of *Mycobacterium tuberculosis*. Scand J Immunol. 55:82–87.

Harding GE, Smith DW (1977) Host-parasite relationships in experimental airborne tuberculosis. VI. Influence of vaccination with Bacille Calmette-Guérin on the onset and/or extent of hematogenous dissemination of virulent *Mycobacterium tuberculosis* to the lungs. J Infect Dis. 136:439–443.

Harmsen D, Dostal S, Roth A, Niemann S, Rothgänger J, Sammeth M, Albert J, Frosch M, Richter E (2003) RIDOM: comprehensive and public sequence database for identification of *Mycobacterium* species. BMC Infect Dis. 3:26.

Harris DP, Vordermeier HM, Friscia G, Roman E, Surcel HM, Pasvol G, Moreno C, Ivanyi J (1993) Genetically permissive recognition of adjacent epitopes from the 19 kDa antigen of *Mycobacterium tuberculosis* by human and murine T cells. J Immunol. 150:5041–5050.

Harris J, Keane J (2010) How tumour necrosis factor blockers interfere with tuberculosis immunity. Clin Exp Immunol. 161:1–9.

Hashimoto M, Tawaratsumida K, Kariya H, Aoyama K, Tamura T, Suda Y (2006) Lipoprotein is a predominant Toll-like receptor 2 ligand in *Staphylococcus aureus* cell wall components. Int Immunol. 18:355–362.

Herrmann JL, O'Gaora P, Gallagher A, Thole JE, Young DB (1996) Bacterial glycoproteins: a link between glycosylation and proteolytic cleavage of a 19 kDa antigen from *Mycobacterium tuberculosis*. EMBO J. 15:3547–3554.

Hershberg R, Lipatov M, Small PM, Sheffer H, Niemann S, Homolka S, Roach JC, Kremer K, Petrov DA, Feldman MW, Gagneux S (2008) High functional diversity in *Mycobacterium tuberculosis* driven by genetic drift and human demography. Plos Biol. 6:e311.

Hertz CJ, Kiertscher SM, Godowski PJ, Bouis DA, Norgard MV, Roth MD, Modlin RL (2001) Microbial lipopeptides stimulate dendritic cell maturation via Toll-like receptor 2. J Immunol. 166:2444–2450.

Hewinson RG, Michell SL, Russell WP, McAdam RA, Jacobs WR (1996) Molecular characterization of MPT83: a seroreactive antigen of *Mycobacterium tuberculosis* with homology to MPT70. Scand J Immunol. 43:490–499.

Higgins DM, Sanchez-Campillo J, Rosas-Taraco AG, Lee EJ, Orme IM, Gonzalez-Juarrero M (2009) Lack of IL-10 alters inflammatory and immune responses during pulmonary *Mycobacterium tuberculosis* infection. Tuberculosis 89:149–157.

Hiromatsu K, Dascher CC, Sugita M, Gingrich-Baker C, Behar SM, LeClair KP, Brenner MB, Porcelli SA (2002) Characterization of guinea pig group 1 CD1 proteins. Immunology 106:159–172.

Ho RS, Fok JS, Harding GE, Smith DW (1978) Host-parasite relationships in experimental airborne tuberculosis. VII. Fate of *Mycobacterium tuberculosis* in primary lung lesions and in primary lesion-free lung tissue infected as a result of bacillemia. J Infect Dis. 138:237–241.

Hodgkinson JW, Ge J-Q, Grayfer L, Stafford J, Belosevic M (2012) Analysis of the immune response in infections of the goldfish (*Carassius auratus* L.) with *Mycobacterium marinum*. Dev Comp Immunol. 38:456–465.

Hoffmann C, Leis A, Niederweis M, Plitzko JM, Engelhardt H (2008) Disclosure of the mycobacterial outer membrane: Cryo-electron tomography and vitreous sections reveal the lipid bilayer structure. Proc Natl Acad Sci USA. 105:3963–3967.

Hoshino K, Takeuchi O, Kawai T, Sanjo H, Ogawa T, Takeda Y, Takeda K, Akira S (1999) Cutting edge: Toll-like receptor 4 (TLR4)-deficient mice are hyporesponsive to lipopolysaccharide: evidence for TLR4 as the Lps gene product. J Immunol. 162:3749–3752.

Hotter GS, Wards BJ, Mouat P, Besra GS, Gomes J, Singh M, Bassett S, Kawakami P, Wheeler PR, de Lisle GW, Collins DM (2005) Transposon mutagenesis of Mb0100 at the ppe1-nrp locus in Mycobacterium bovis disrupts phthiocerol dimycocerosate (PDIM) and glycosylphenol-PDIM biosynthesis, producing an avirulent strain with vaccine properties at least equal to those of *M. bovis* BCG. J Bacteriol. 187:2267–2277.

Hovav A-H, Davidovitch L, Nussbaum G, Mullerad J, Fishman Y, Bercovier H (2004) Mitogenicity of the recombinant mycobacterial 27-kilodalton lipoprotein is not connected to its antiprotective effect. Infect Immun. 72:3383–3390.

Hovav A-H, Mullerad J, Davidovitch L, Fishman Y, Bigi F, Cataldi A, Bercovier H (2003) The *Mycobacterium tuberculosis* recombinant 27-kilodalton lipoprotein induces a strong Th1-type immune response deleterious to protection. Infect Immun. 71:3146–3154.

Hovav A-H, Mullerad J, Maly A, Davidovitch L, Fishman Y, Bercovier H (2006) Aggravated infection in mice co-administered with *Mycobacterium tuberculosis* and the 27 kDa lipoprotein. Microbes Infect. 8:1750–1757.

Hsieh CS, Macatonia SE, Tripp CS, Wolf SF, O'Garra A, Murphy KM (1993) Development of Th1 $CD4^+$ T cells through IL-12 produced by Listeria-induced macrophages. Science 260:547–549.

Huebner RE, Schein MF, Bass JB (1993) The tuberculin skin test. Clin Infect Dis. 17:968–975.

Hunter RL (2011) Pathology of post primary tuberculosis of the lung: An illustrated critical review. Tuberculosis 91:497–509.

Hunter RL, Jagannath C, Actor JK (2007) Pathology of postprimary tuberculosis in humans and mice: contradiction of long-held beliefs. Tuberculosis 87:267–278.

Hutagalung AH, Novick PJ (2011) Role of Rab GTPases in membrane traffic and cell physiology. Physiol Rev. 91:119–149.

Hutchings MI, Palmer T, Harrington DJ, Sutcliffe IC (2009) Lipoprotein biogenesis in gram-positive bacteria: knowing when to hold “em, knowing when to fold ”em. Trends Microbiol. 17:13–21.

Ishikawa E, Ishikawa T, Morita YS, Toyonaga K, Yamada H, Takeuchi O, Kinoshita T, Akira S, Yoshikai Y, Yamasaki S (2009) Direct recognition of the mycobacterial glycolipid, trehalose dimycolate, by C-type lectin Mincle. J Exp Med. 206:2879–2888.

Jackson M, Raynaud C, Lanéelle MA, Guilhot C, Laurent-Winter C, Ensergueix D, Gicquel B, Daffé M (1999) Inactivation of the antigen 85C gene profoundly affects the mycolate content and alters the permeability of the *Mycobacterium tuberculosis* cell envelope. Mol Microbiol. 31:1573–1587.

Jasenosky LD, Scriba TJ, Hanekom WA, Goldfeld AE (2015) T cells and adaptive immunity to *Mycobacterium tuberculosis* in humans. Immunol Rev. 264:74–87.

Jayaraman P, Sada-Ovalle I, Nishimura T, Anderson AC, Kuchroo VK, Remold HG, Behar SM (2013) IL-1β promotes antimicrobial immunity in macrophages by regulating TNFR signaling and caspase-3 activation. J Immunol. 190:4196–4204.

Jin H-T, Jeong Y-H, Park H-J, Ha S-J (2011) Mechanism of T cell exhaustion in a chronic environment. BMB Reports 44:217–231.

Johansson U, Ivanyi J, Londei M (2001) Inhibition of IL-12 production in human dendritic cells matured in the presence of Bacillus Calmette-Guérin or lipoarabinomannan. Immunol Lett. 77:63–66.

Johnson PD, Stuart RL, Grayson ML, Olden D, Clancy A, Ravn P, Andersen P, Britton WJ, Rothel JS (1999) Tuberculin-purified protein derivative-, MPT64-, and ESAT-6-stimulated gamma interferon responses in medical students before and after *Mycobacterium bovis* BCG vaccination and in patients with tuberculosis. Clin Diagn Lab Immunol. 6:934–937.

Junqueira-Kipnis AP, Marques Neto LM, Kipnis A (2014) Role of fused *Mycobacterium tuberculosis* immunogens and adjuvants in modern tuberculosis vaccines. Front Immunol. 5:188.

Kagina BMN, Abel B, Scriba TJ, Hughes EJ, Keyser A, Soares A, Gamieldien H, Sidibana M, Hatherill M, Gelderbloem S, Mahomed H, Hawkridge A, Hussey G, Kaplan G, Hanekom WA (2010) Specific T cell frequency and cytokine expression profile do not correlate with protection against tuberculosis after Bacillus Calmette-Guérin vaccination of newborns. Am J Respir Crit Care Med. 182:1073–1079.

Kamerbeek J, Schouls L, Kolk A, van Agterveld M, van Soolingen D, Kuijper S, Bunschoten A, Molhuizen H, Shaw R, Goyal M, van Embden J (1997) Simultaneous detection and strain differentiation of *Mycobacterium tuberculosis* for diagnosis and epidemiology. J Clin Microbiol. 35:907–914.

Kang YA, Lee HW, Yoon Il H, Cho B, Han SK, Shim Y-S, Yim J-J (2005) Discrepancy between the tuberculin skin test and the whole-blood Interferon γ assay for the diagnosis of latent Tuberculosis infection in an intermediate tuberculosis-burden country. JAMA 293:2756–2761.

Kano H, Doi T, Fujita Y, Takimoto H, Yano I, Kumazawa Y (2005) Serotype-specific modulation of human monocyte functions by glycopeptidolipid (GPL) isolated from *Mycobacterium avium* complex. Biol Pharm Bull. 28:335–339.

Kao FF, Mahmuda S, Pinto R, Triccas JA, West NP, Britton WJ (2012) The secreted lipoprotein, MPT83 of *Mycobacterium tuberculosis* is recognized during human tuberculosis and stimulates protective immunity in mice. PLoS ONE 7:e34991.

Karlson AG, Lessel EF (1970) *Mycobacterium bovis nom. nov.* Int J of Syst Bacteriol. 20:273–282.

Karonga Prevention Trial Group (1996) Randomised controlled trial of single BCG, repeated BCG, or combined BCG and killed *Mycobacterium leprae* vaccine for prevention of leprosy and tuberculosis in Malawi. The Lancet 348:17–24.

Kasai H, Ezaki T, Harayama S (2000) Differentiation of phylogenetically related slowly growing mycobacteria by their gyrB sequences. J Clin Microbiol. 38:301–308.

Kasmar AG, Van Rhijn I, Magalhaes KG, Young DC, Cheng T-Y, Turner MT, Schiefner A, Kalathur RC, Wilson IA, Bhati M, Gras S, Birkinshaw RW, Tan LL, Rossjohn J, Shires J, Jakobsen S, Altman JD, Moody DB (2013) Cutting edge: CD1a tetramers and dextramers identify human lipopeptide-specific T cells *ex vivo*. J Immunol. 191:4499–4503.

Kaveh DA, Bachy VS, Hewinson RG, Hogarth PJ (2011) Systemic BCG immunization induces persistent lung mucosal multifunctional CD4 TEM cells which expand following virulent mycobacterial challenge. PLoS ONE 6:e21566.

Kim M-J, Wainwright HC, Locketz M, Bekker L-G, Walther GB, Dittrich C, Visser A, Wang W, Hsu F-F, Wiehart U, Tsenova L, Kaplan G, Russell DG (2010) Caseation of human tuberculosis granulomas correlates with elevated host lipid metabolism. EMBO Mol Med. 2:258–274.

King HC, Murphy A, James P, Travis E, Porter D, Hung Y-J, Sawyer J, Cork J, Delahay RJ, Gaze W, Courtenay O, Wellington EM (2015) The variability and seasonality of the environmental reservoir of *Mycobacterium bovis* shed by wild European badgers. Sci Rep. 5:12318.

Kirschning CJ, Wesche H, Merrill Ayres T, Rothe M (1998) Human Toll-like receptor 2 confers responsiveness to bacterial lipopolysaccharide. J Exp Med. 188:2091–2097.

Kitaura H, Kinomoto M, Yamada T (1999) Ribosomal protein L7 included in tuberculin purified protein derivative (PPD) is a major heat-resistant protein inducing strong delayed-type hypersensitivity. Scand J Immunol. 50:580–587.

Kleinnijenhuis J, Joosten LAB, van de Veerdonk FL, Savage N, van Crevel R, Kullberg BJ, van der Ven A, Ottenhoff THM, Dinarello CA, van der Meer JWM, Netea MG (2009) Transcriptional and inflammasome-mediated pathways for the induction of IL-1β production by *Mycobacterium tuberculosis*. Eur J Immunol. 39:1914–1922.

Klencke PFH (1846) Ueber die Ansteckung und Verbreitung der Scrophelkrankheit bei Menschen durch den Genuß der Kuhmilch. Verlag von Christian Ernst Kollmann.

Koch R (1890) I. Weitere Mittheilungen über ein Heilmittel gegen Tuberculose. Dtsch Med Wochenschr. 16:1029–1032.

Koch R (1891a) Fortsetzung der Mittheilungen über ein Heilmittel gegen Tuberculose. Dtsch Med Wochenschr. 17:101–102.

Koch R (1891b) Weitere Mittheilung über das Tuberkulin. Dtsch Med Wochenschr. 17:1189–1192.

Koch R (1882) Die Ätiologie der Tuberkulose. Berliner klinische Wochenschrift 15:1–18.

Koch R (1897) Über neue Tuberkulinpräparate. Dtsch Med Wochenschr. 14:1–10.

Koch R (1891c) Über bakteriologische Forschung. In: Verhandlungen des X. Internationalen Medizinischen Kongresses, Berlin.

Korduláková J, Gilleron M, Mikusova K, Puzo G, Brennan PJ, Gicquel B, Jackson M (2002) Definition of the first mannosylation step in phosphatidylinositol mannoside synthesis. PimA is essential for growth of mycobacteria. J Biol Chem. 277:31335–31344.

Korf J, Stoltz A, Verschoor J, De Baetselier P, Grooten J (2005) The *Mycobacterium tuberculosis* cell wall component mycolic acid elicits pathogen-associated host innate immune responses. Eur J Immunol. 35:890–900.

Kotani S, Kitaura T, Hirano T (1959) Isolation and chemical composition of the cell walls of BCG. Biken Journal 2:129–141.

Kothavade RJ, Dhurat RS, Mishra SN, Kothavade UR (2013) Clinical and laboratory aspects of the diagnosis and management of cutaneous and subcutaneous infections caused by rapidly growing mycobacteria. Eur J Clin Microbiol Infect Dis. 32:161–188.

Kovjazin R, Volovitz I, Daon Y, Vider-Shalit T, Azran R, Tsaban L, Carmon L, Louzoun Y (2011) Signal peptides and trans-membrane regions are broadly immunogenic and have high $CD8^+$ T cell epitope densities: Implications for vaccine development. Mol Immunol. 48:1009–1018.

Kruh NA, Troudt J, Izzo A, Prenni J, Dobos KM (2010) Portrait of a pathogen: the *Mycobacterium tuberculosis* proteome *in vivo*. PLoS ONE 5:e13938.

Kuznetsova I, Shurygina AP, Wolf B, Wolschek M, Enzmann F, Sansyzbay A, Khairullin B, Sandybayev N, Stukova M, Kiselev O, Egorov A, Bergmann M (2014) Adaptive mutation in nuclear export protein allows stable transgene expression in a chimaeric influenza A virus vector. J Gen Virol. 95:337–349.

Kyei GB, Vergne I, Chua J, Roberts E, Harris J, Junutula JR, Deretic V (2006) Rab14 is critical for maintenance of *Mycobacterium tuberculosis* phagosome maturation arrest. EMBO J. 25:5250–5259.

la Rua-Domenech de R (2006) Human *Mycobacterium bovis* infection in the United Kingdom: Incidence, risks, control measures and review of the zoonotic aspects of bovine tuberculosis. Tuberculosis 86:77–109.

Ladeira I, Carvalho I, Correia A, Carvalho A, Duarte R (2014) BCGitis in children. Rev Port Pneumol. 20:172–173.

Laemmli UK (1970) Cleavage of structural proteins during the assembly of the head of bacteriophage T4. Nature 227:680–685.

Lagranderie MR, Balazuc AM, Deriaud E, Leclerc CD, Gheorghiu M (1996) Comparison of immune responses of mice immunized with five different *Mycobacterium bovis* BCG vaccine strains. Infect Immun. 64:1–9.

Lam MH-W, Law G-L, Lee C-S, Wong K-L (2015) Organic molecules for optical imaging. In: Long N, Wong W-T (eds) The chemistry of molecular imaging. Wiley.

Langley RJ, Renno T (2011) Superantigens. In: eLS. John Wiley & Sons, Ltd: Chichester.

Lathigra R, Zhang Y, Hill M, Garcia MJ, Jackett PS, Ivanyi J (1996) Lack of production of the 19 kDa glycolipoprotein in certain strains of *Mycobacterium tuberculosis*. Res Microbiol. 147:237–249.

Layre E, Collmann A, Bastian M, Mariotti S, Czaplicki J, Prandi J, Mori L, Stenger S, De Libero G, Puzo G, Gilleron M (2009) Mycolic acids constitute a scaffold for mycobacterial lipid antigens stimulating CD1-restricted T cells. Chemistry and Biology 16:82–92.

le Roex N, Cooper D, van Helden PD, Hoal EG, Jolles AE (2015) Disease control in wildlife: evaluating a test and cull programme for bovine tuberculosis in african buffalo. Transbound Emerg Dis. doi: 10.1111/tbed.12329.

Leal IS, Smedegård B, Andersen P, Appelberg R (2001) Failure to induce enhanced protection against tuberculosis by increasing T cell-dependent interferon-gamma generation. Immunology 104:157–161.

Lederer E, Adam A, Ciorbaru R, Petit JF, Wietzerbin J (1975) Cell walls of mycobacteria and related organisms; chemistry and immunostimulant properties. Mol Cell Biochem. 7:87–104.

Lee H-K, Lee J, Tobias PS (2002) Two lipoproteins extracted from *Escherichia coli* K-12 LCD25 lipopolysaccharide are the major components responsible for Toll-like receptor 2-mediated signaling. J Immunol. 168:4012–4017.

Lee JS, Krause R, Schreiber J, Mollenkopf H-J, Kowall J, Stein R, Jeon B-Y, Kwak J-Y, Song M-K, Patron JP, Jorg S, Roh K, Cho S-N, Kaufmann SHE (2008) Mutation in the transcriptional regulator PhoP contributes to avirulence of *Mycobacterium tuberculosis* H37Ra strain. Cell Host Microbe 3:97–103.

Lefèvre P, Braibant M, de Wit L, Kalai M, Röeper D, Grötzinger J, Delville JP, Peirs P, Ooms J, Huygen K, Content J (1997) Three different putative phosphate transport receptors are encoded by the *Mycobacterium tuberculosis* genome and are present at the surface of *Mycobacterium bovis* BCG. J Bacteriol. 179:2900–2906.

Lefèvre P, Denis O, De Wit L, Tanghe A, Vandenbussche P, Content J, Huygen K (2000) Cloning of the gene encoding a 22 kilodalton cell surface antigen of *Mycobacterium bovis* BCG and analysis of its potential for DNA vaccination against tuberculosis. Infect Immun. 68:1040–1047.

Lehmann KB, Neumann RO (1896) Atlas und Grundriss der Bakteriologie und Lehrbuch der speciellen bakteriologischen Diagnostik. J. F. Lehmanns Verlag.

Lehmann KB, Neumann RO (1907) Atlas Und Grundriss Der Bakteriologie Und Lehrbuch Der Speziellen Bakteriologischen Diagnostik. J. F. Lehmanns Verlag.

Lehrer RI, Ladra KM, Hake RB (1975) Nonoxidative fungicidal mechanisms of mammalian granulocytes: demonstration of components with candidacidal activity in human, rabbit, and guinea pig leukocytes. Infect Immun. 11:1226–1234.

Lenaerts AJ, Hoff D, Aly S, Ehlers S, Andries K, Cantarero L, Orme IM, Basaraba RJ (2007) Location of persisting mycobacteria in a guinea pig model of tuberculosis revealed by r207910. Antimicrob Agents Chemother 51:3338–3345.

Lepper A, Corner LA (1983) Naturally occurring mycobacterioses of animals. In: Ratledge C (ed) The biology of mycobacteria. Wiley-Blackwell.

Lesslie I, Herbert C, Burn K, MacClancy B, Donnelly W (1975) Comparison of the specificty of human and bovine tuberculin PPD for testing cattle. Republic of Ireland. Vet Rec. 96:332–334.

Leung AS, Tran V, Wu Z, Yu X, Alexander DC, Gao GF, Zhu B, Liu J (2008) Novel genome polymorphisms in BCG vaccine strains and impact on efficacy. BMC Genomics 9:413.

Lew JM, Kapopoulou A, Jones LM, Cole ST (2011) TubercuList – 10 years after. Tuberculosis 91:1–7.

Lewis KN, Liao R, Guinn KM, Hickey MJ, Smith S, Behr MA, Sherman DR (2003) Deletion of RD1 from *Mycobacterium tuberculosis* mimics Bacille Calmette-Guérin attenuation. J Infect Dis.187:117–123.

Li YP, Yu SL, Huang ZJ, Huang J, Pan J, Feng X, Zhang XG, Wang JH, Wang J (2015) An impaired inflammatory cytokine response to gram-negative LPS in human neonates is associated with the defective TLR-mediated signaling pathway. J Clin Immunol. 35:218–226.

Lin PL, Dietrich J, Tan E, Abalos RM, Burgos J, Bigbee C, Bigbee M, Milk L, Gideon HP, Rodgers M, Cochran C, Guinn KM, Sherman DR, Klein E, Janssen C, Flynn JL, Andersen P (2012) The multistage vaccine H56 boosts the effects of BCG to protect cynomolgus macaques against active tuberculosis and reactivation of latent *Mycobacterium tuberculosis* infection. J Clin Invest. 122:303–314.

Lindestam Arlehamn CS, Paul S, Mele F, Huang C, Greenbaum JA, Vita R, Sidney J, Peters B, Sallusto F, Sette A (2015) Immunological consequences of intragenus conservation of *Mycobacterium tuberculosis* T cell epitopes. Proc Natl Acad Sci USA. 112:e147–55.

Lipner EM, Gopi PG, Subramani R, Kolappan C, Sadacharam K, Kumaran P, Prevots DR, Narayanan PR, Nutman TB, Kumaraswami V (2006) Coincident filarial, intestinal helminth, and mycobacterial infection: helminths fail to influence tuberculin reactivity, but BCG influences hookworm prevalence. Am J Trop Med Hyg. 74:841–847.

Loeb L, Wright S (1927) Transplantation and individuality differentials in inbred families of guinea pigs. Am J Pathol. 3:251–283.

Lopez M, Sly LM, Luu Y, Young D, Cooper H, Reiner NE (2003) The 19 kDa *Mycobacterium tuberculosis* protein induces macrophage apoptosis through Toll-like receptor 2. J Immunol. 170:2409–2416.

Lorgat F, Keraan MM, Lukey PT, Ress SR (1992) Evidence for *in vivo* generation of cytotoxic T cells. PPD-stimulated lymphocytes from tuberculous pleural effusions demonstrate enhanced cytotoxicity with accelerated kinetics of induction. Am Rev Respir Dis. 145:418–423.

Lottspeich F, Engels JW (2012) Bioanalytik. Spektrum Akademischer Verlag

Luabeya AKK, Kagina BMN, Tameris MD, Geldenhuys H, Hoff ST, Shi Z, Kromann I, Hatherill M, Mahomed H, Hanekom WA, Andersen P, Scriba TJ, Group1 H-0TS, Schoeman E, Krohn C, Day CL, Africa H, Makhethe L, Smit E, Brown Y, Suliman S, Hughes EJ, Bang P, Snowden MA, McClain B, Hussey GD (2015) First-in-human trial of the post-exposure tuberculosis vaccine H56:IC31 in *Mycobacterium tuberculosis*-infected and non-infected healthy adults. Vaccine 33:4130–4140.

Luca S, Mihaescu T (2013) History of BCG vaccine. Maedica 8:53–58.

Luzio JP, Pryor PR, Bright NA (2007) Lysosomes: fusion and function. Nat Rev Mol Cell Biol. 8:622–632.

Ly LH, Russell MI, McMurray DN (2008) Cytokine profiles in primary and secondary pulmonary granulomas of guinea pigs with tuberculosis. Am J Respir Cell Mol Biol. 38:455–462.

Lyons AB (1999) Divided we stand: tracking cell proliferation with carboxyfluorescein diacetate succinimidyl ester. Immunol Cell Biol. 77:509–515.

Lyons AB, Parish CR (1994) Determination of lymphocyte division by flow cytometry. J Immunol Methods 171:131–137.

Magnus K, Guld J, Waaler H, Magnusson M (1956) Instability of the potency of tuberculin dilutions; a second report. Am Rev Tuberc. 74:297–303.

Mahairas GG, Sabo PJ, Hickey MJ, Singh DC, Stover CK (1996) Molecular analysis of genetic differences between *Mycobacterium bovis* BCG and virulent *M. bovis*. J Bacteriol. 178:1274–1282.

Malik ZA, Denning GM, Kusner DJ (2000) Inhibition of Ca^{2+} signaling by *Mycobacterium tuberculosis* is associated with reduced phagosome-lysosome fusion and Increased survival within human macrophages. J Exp Med. 191:287–302.

Malik ZA, Iyer SS, Kusner DJ (2001) *Mycobacterium tuberculosis* phagosomes exhibit altered calmodulin-dependent signal transduction: contribution to inhibition of phagosome-lysosome fusion and intracellular survival in human macrophages. J Immunol. 166:3392–3401.

Malik ZA, Thompson CR, Hashimi S, Porter B, Iyer SS, Kusner DJ (2003) Cutting edge: *Mycobacterium tuberculosis* blocks Ca^{2+} signaling and phagosome maturation in human macrophages via specific inhibition of sphingosine kinase. J Immunol. 170:2811–2815.

Manca C, Tsenova L, Barry CE, Bergtold A, Freeman S, Haslett PA, Musser JM, Freedman VH, Kaplan G (1999) *Mycobacterium tuberculosis* CDC1551 induces a more vigorous host response *in vivo* and *in vitro*, but is not more virulent than other clinical isolates. J Immunol. 162:6740–6746.

Mandal SM, Sharma S, Pinnaka AK, Kumari A, Korpole S (2013) Isolation and characterization of diverse antimicrobial lipopeptides produced by *Citrobacter* and *Enterobacter*. BMC Microbiol. 13:152.

Marin ND, París SC, Vélez VM, Rojas CA, Rojas M, García LF (2010) Regulatory T cell frequency and modulation of IFN-gamma and IL-17 in active and latent tuberculosis. Tuberculosis 90:252–261.

Mariotti S, Nisini R (2009) Generation of human T cell clones. In: De Libero G (ed) T cell protocols. Humana Press Inc.

Marmiesse M, Brodin P, Buchrieser C, Gutierrez C, Simoes N, Vincent V, Glaser P, Cole ST, Brosch R (2004) Macro-array and bioinformatic analyses reveal mycobacterial “core” genes, variation in the ESAT-6 gene family and new phylogenetic markers for the *Mycobacterium tuberculosis* complex. Microbiology 150:483–496.

Martin C, Williams A, Hernandezpando R, Cardona P, Gormley E, Bordat Y, Soto C, Clark S, Hatch G, Aguilar D (2006) The live *Mycobacterium tuberculosis phoP* mutant strain is more attenuated than BCG and confers protective immunity against tuberculosis in mice and guinea pigs. Vaccine 24:3408–3419.

Matsuo K, Yamaguchi R, Yamazaki A, Tasaka H, Yamada T (1988) Cloning and expression of the *Mycobacterium bovis* BCG gene for extracellular alpha antigen. J Bacteriol. 170:3847–3854.

Mattow J, Schaible UE, Schmidt F, Hagens K, Siejak F, Brestrich G, Haeselbarth G, Müller E-C, Jungblut PR, Kaufmann SHE (2003) Comparative proteome analysis of culture supernatant proteins from virulent *Mycobacterium tuberculosis* H37Rv and attenuated *M. bovis* BCG Copenhagen. Electrophoresis 24:3405–3420.

Målen H, Berven FS, Fladmark KE, Wiker HG (2007) Comprehensive analysis of exported proteins from *Mycobacterium tuberculosis* H37Rv. Proteomics 7:1702–1718.

Målen H, Pathak S, Søfteland T, de Souza GA, Wiker HG (2010) Definition of novel cell envelope associated proteins in Triton X-114 extracts of *Mycobacterium tuberculosis* H37Rv. BMC Microbiol. 10:132.

McIlroy S, Neill S, McCracken R (1986) Pulmonary lesions and *Mycobacterium bovis* excretion from the respiratory tract of tuberculin reacting cattle. Vet Rec. 118:718–721.

McKeand JB, Knox DP, Duncan JL, Kennedy MW (1994) Genetic control of the antibody repertoire against excretory/secretory products and acetylcholinesterases of *Dictyocaulus viviparus*. Parasite Immunol. 16:251–260.

McNeil M, Daffé M, Brennan PJ (1990) Evidence for the nature of the link between the arabinogalactan and peptidoglycan of mycobacterial cell walls. J Biol Chem. 265:18200–18206.

McNeil M, Daffé M, Brennan PJ (1991) Location of the mycolyl ester substituents in the cell walls of mycobacteria. J Biol Chem. 266:13217–13223.

McShane H, Pathan AA, Sander CR, Keating SM, Gilbert SC, Huygen K, Fletcher HA, Hill AVS (2004) Recombinant modified vaccinia virus Ankara expressing antigen 85A boosts BCG-primed and naturally acquired antimycobacterial immunity in humans. Nature Medicine 10:1240–1244.

Menin Á, Fleith R, Reck C, Marlow M, Fernandes P, Pilati C, Báfica A (2013) Asymptomatic cattle naturally infected with *Mycobacterium bovis* present exacerbated tissue pathology and bacterial dissemination. PLoS ONE 8:e53884.

Meraviglia S, Daker El S, Dieli F, Martini F, Martino A (2011) γδ T cells cross-link innate and adaptive immunity in *Mycobacterium tuberculosis* infection. Clin Dev Immunol. 2011:587315.

Michel AL, Müller B, van Helden PD (2010) *Mycobacterium bovis* at the animal-human interface: A problem, or not? Vet Microbiol. 140:371–381.

Milstien JB, Gibson JJ (1990) Quality control of BCG vaccine by WHO: a review of factors that may influence vaccine effectiveness and safety. Bull World Health Organ 68:93–108.

Miltenyi S, Müller W, Weichel W, Radbruch A (1990) High gradient magnetic cell separation with MACS. Cytometry 11:231–238.

Minnikin DE (1982) Lipids: complex lipids, their chemistry, biosynthesis and roles. In: Ratledge C, Stanford J (eds) The biology of the mycobacteria. Academic Press.

Mittrücker H-W, Steinhoff U, Köhler A, Krause M, Lazar D, Mex P, Miekley D, Kaufmann SHE (2007) Poor correlation between BCG vaccination-induced T cell responses and protection against tuberculosis. Proc Natl Acad Sci USA. 104:12434–12439.

Mogues T, Goodrich ME, Ryan L, LaCourse R, North RJ (2001) The relative importance of T cell subsets in immunity and immunopathology of airborne *Mycobacterium tuberculosis* infection in mice. J Exp Med. 193:271–280.

Mohagheghpour N, Gammon D, Kawamura LM, van Vollenhoven A, Benike CJ, Engleman EG (1998) CTL response to *Mycobacterium tuberculosis*: identification of an immunogenic epitope in the 19 kDa lipoprotein. J Immunol. 161:2400–2406.

Moliva JI, Turner J, Torrelles JB (2015) Prospects in *Mycobacterium bovis* Bacille Calmette et Guérin (BCG) vaccine diversity and delivery: Why does BCG fail to protect against tuberculosis? Vaccine 33:5035–5041.

Moody DB, Young DC, Cheng T-Y, Rosat J-P, Roura-Mir C, O'Connor PB, Zajonc DM, Walz A, Miller MJ, Levery SB, Wilson IA, Costello CE, Brenner MB (2004) T cell activation by lipopeptide antigens. Science 303:527–531.

Moore VA (1913) Bovine tuberculosis and its control. Carpenter.

Moradi J, Mosavari N, Ebrahimi M, Arefpajohi R, Tebianian M (2015) Evaluation of *Mycobacterium tuberculosis* early secreted antigenic target 6 recombinant protein as a diagnostic marker in kkin test. Osong Public Health and Research Perspectives 6:34–38.

Mori T, Sakatani M, Yamagishi F, Takashima T, Kawabe Y, Nagao K, Shigeto E, Harada N, Mitarai S, Okada M, Suzuki K, Inoue Y, Tsuyuguchi K, Sasaki Y, Mazurek GH, Tsuyuguchi I (2004) Specific detection of tuberculosis infection: an interferon-gamma-based assay using new antigens. Am J Respir Crit Care Med. 170:59–64.

Morita YS, Patterson JH, Billman-Jacobe H, McConville MJ (2004) Biosynthesis of mycobacterial phosphatidylinositol mannosides. Biochem J. 378:589–597.

Murhead R, Burns K (1974) Tuberculosis in wild badgers in Gloucestershire: epidemiology. Vet Rec. 95:552–555.

Murphy KM (2011) Janeway's Immunobiology. Garland Science.

Murphy TL, Cleveland MG, Kulesza P, Magram J, Murphy KM (1995) Regulation of interleukin 12 p40 expression through an NF-kappa B half-site. Molecular and Cellular Biology 15:5258–5267.

Mutis T, Cornelisse YE, Ottenhoff TH (1993) Mycobacteria induce $CD4^+$ T cells that are cytotoxic and display Th1-like cytokine secretion profile: heterogeneity in cytotoxic activity and cytokine secretion levels. Eur J Immunol. 23:2189–2195.

Muzio M, Natoli G, Saccani S, Levrero M, Mantovani A (1998) The human toll signaling pathway: divergence of nuclear factor kappaB and JNK/SAPK activation upstream of tumor necrosis factor receptor-associated factor 6 (TRAF6). J Exp Med. 187:2097–2101.

Müller B, Dürr S, Alonso S, Hattendorf J, Laisse CJM, Parsons SDC, van Helden PD, Zinsstag J (2013) Zoonotic *Mycobacterium bovis*-induced tuberculosis in humans. Emerg Infect Dis. 19:899–908.

Nagai S, Wiker HG, Harboe M, Kinomoto M (1991) Isolation and partial characterization of major protein antigens in the culture fluid of *Mycobacterium tuberculosis*. Infect Immun. 59:372–382.

Nair AJ (2007) Animal-cell culture and application. In: Principles of biotechnology and genetic engineering. Laxmi Publisher.

Nakata T, Yasuda M, Fujita M, Kataoka H, Kiura K, Sano H, Shibata K (2006) CD14 directly binds to triacylated lipopeptides and facilitates recognition of the lipopeptides by the receptor complex of Toll-like receptors 2 and 1 without binding to the complex. Cell Microbiol. 8:1899–1909.

Nakayama H, Kurokawa K, Lee BL (2012) Lipoproteins in bacteria: structures and biosynthetic pathways. FEBS J. 279:4247–4268.

Naranjo V, Gortazar C, Vicente J, la Fuente de J (2008) Evidence of the role of European wild boar as a reservoir of *Mycobacterium tuberculosis* complex. Vet Microbiol. 127:1–9.

Naser SA, Sagramsingh SR, Naser AS, Thanigachalam S (2014) *Mycobacterium avium* subspecies *paratuberculosis* causes Crohn's disease in some inflammatory bowel disease patients. World J Gastroenterol. 20:7403–7415.

Nash DR, Douglass JE (1980) Anergy in active pulmonary tuberculosis. A comparison between positive and negative reactors and an evaluation of 5 TU and 250 TU skin test doses. Chest 77:32–37.

Natsuume-Sakai S, Motonishi K, Migita S (1977) Quantitative estimations of five classes of immunoglobulin in inbred mouse strains. Immunology 32:861–866.

Ndiaye BP, Thienemann F, Ota M, Landry BS, Camara M, Dièye S, Ndiaye Dieye T, Esmail H, Goliath R, Huygen K, January V, Ndiaye I, Oni T, Raine M, Romano M, Satti I, Sutton S, Thiam A, Wilkinson KA, Mboup S, Wilkinson RJ, McShane H (2015) Safety, immunogenicity, and efficacy of the candidate tuberculosis vaccine MVA85A in healthy adults infected with HIV-1: a randomised, placebo-controlled, phase 2 trial. The Lancet Respiratory 3:190–200.

Nell AS, D'lom E, Bouic P, Sabaté M, Bosser R, Picas J, Amat M, Churchyard G, Cardona P-J (2014) Safety, tolerability, and immunogenicity of the novel antituberculous vaccine RUTI: randomized, placebo-controlled phase II clinical trial in patients with latent tuberculosis infection. PLoS ONE 9:e89612.

Newport MJ, Huxley CM, Huston S (1996) A mutation in the interferon-γ receptor gene and susceptibility to mycobacterial infection. N Eng J Med 335:1941–1949.

Neyrolles O, Gould K, Gares MP, Brett S, Janssen R, O'Gaora P, Herrmann JL, Prevost MC, Perret E, Thole JE, Young D (2001) Lipoprotein access to MHC class I presentation during infection of murine macrophages with live mycobacteria. J Immunol. 166:447–457.

Neyrolles O, Guilhot C (2011) Recent advances in deciphering the contribution of *Mycobacterium tuberculosis* lipids to pathogenesis. Tuberculosis 91:187–195.

Nigou J, Zelle-Rieser C, Gilleron M, Thurnher M, Puzo G (2001) Mannosylated lipoarabinomannans inhibit IL-12 production by human dendritic cells: evidence for a negative signal delivered through the mannose receptor. J Immunol. 166:7477–7485.

Noss EH, Pai RK, Sellati TJ, Radolf JD, Belisle J, Golenbock DT, Boom WH, Harding CV (2001) Toll-like receptor 2-dependent inhibition of macrophage class II MHC expression and antigen processing by 19 kDa lipoprotein of *Mycobacterium tuberculosis*. J Immunol. 167:910–918.

Nugent G, Buddle BM, Knowles G (2015) Epidemiology and control of *Mycobacterium bovis* infection in brushtail possums (*Trichosurus vulpecula*), the primary wildlife host of bovine tuberculosis in New Zealand. N Z Vet J. 63:28–41.

Nunes-Alves C, Booty MG, Carpenter SM, Jayaraman P, Rothchild AC, Behar SM (2014) In search of a new paradigm for protective immunity to TB. Nat Rev Microbiol. 12:289–299.

O'Brien DJ, Fitzgerald SD, Lyon TJ, Butler KL, Fierke JS, Clarke KR, Schmitt SM, Cooley TM, Derry DE (2001) Tuberculous lesions in free-ranging white-tailed deer in Michigan. J Wildl Dis. 37:608–613.

O'Leary S, O'Sullivan MP, Keane J (2011) IL-10 blocks phagosome maturation in *Mycobacterium tuberculosis*-infected human macrophages. Am J Respir Cell Mol Biol. 45:172–180.

Oettinger T, Jørgensen M, Ladefoged A, Hasløv K, Andersen P (1999) Development of the *Mycobacterium bovis* BCG vaccine: review of the historical and biochemical evidence for a genealogical tree. Tuber Lung Dis. 79:243–250.

Ohara N, Kitaura H, Hotokezaka H, Nishiyama T, Wada N, Matsumoto S, Matsuo T, Naito M, Yamada T (1995) Characterization of the gene encoding the MPB51, one of the major secreted protein antigens of *Mycobacterium bovis* BCG, and identification of the secreted protein closely related to the fibronectin binding 85 complex. Scand J Immunol. 41:433–442.

Ohmen JD, Barnes PF, Grisso CL, Bloom BR, Modlin RL (1994) Evidence for a superantigen in human tuberculosis. Immunity 1:35–43.

Oppenheim JJ (2007) IL-2: more than a T cell growth factor. J Immunol. 179:1413–1414.

Ordway D, Henao-Tamayo M, Shanley C, Smith EE, Palanisamy G, Wang B, Basaraba RJ, Orme IM (2008) Influence of *Mycobacterium bovis* BCG vaccination on cellular immune response of guinea pigs challenged with *Mycobacterium tuberculosis*. Clin Vaccine Immunol. 15:1248–1258.

Ordway D, Palanisamy G, Henao-Tamayo M, Smith EE, Shanley C, Orme IM, Basaraba RJ (2007) The cellular immune response to *Mycobacterium tuberculosis* infection in the guinea pig. J Immunol. 179:2532–2541.

Orme IM (2014) A new unifying theory of the pathogenesis of tuberculosis. Tuberculosis 94:8–14.

Orme IM, Basaraba RJ (2014) The formation of the granuloma in tuberculosis infection. Semin Immunol. 26:601–609.

Ortalo-Magné A, Dupont MA, Lemassu A, Andersen AB, Gounon P, Daffé M (1995) Molecular composition of the outermost capsular material of the tubercle bacillus. Microbiology 141:1609–1620.

Ortalo-Magné A, Lemassu A, Lanéelle MA, Bardou F, Silve G, Gounon P, Marchal G, Daffé M (1996) Identification of the surface-exposed lipids on the cell envelopes of *Mycobacterium tuberculosis* and other mycobacterial species. J Bacteriol. 178:456–461.

Osborn TW (1983) Changes in BCG strains. Tubercle 64:1–13.

Ottenhoff TH, Ab BK, van Embden JD, Thole JE, Kiessling R (1988) The recombinant 65 kD heat shock protein of *Mycobacterium bovis* Bacillus Calmette-Guérin/*M. tuberculosis* is a target molecule for $CD4^+$ cytotoxic T lymphocytes that lyse human monocytes. J Exp Med. 168:1947–1952.

Ozinsky A, Underhill DM, Fontenot JD, Hajjar AM, Smith KD, Wilson CB, Schroeder L, Aderem A (2000) The repertoire for pattern recognition of pathogens by the innate immune system is defined by cooperation between Toll-like receptors. Proc Natl Acad Sci USA. 97:13766–13771.

Padilla-Carlin DJ, McMurray DN, Hickey AJ (2008) The guinea pig as a model of infectious diseases. Comp Med. 58:324–340.

Pagán AJ, Ramakrishnan L (2015) Immunity and immunopathology in the tuberculous granuloma. Cold Spring Harb Perspect Med. 5:a018499.

Pai RK, Convery M, Hamilton TA, Boom WH, Harding CV (2003) Inhibition of IFN-gamma-induced class II transactivator expression by a 19 kDa lipoprotein from *Mycobacterium tuberculosis*: a potential mechanism for immune evasion. J Immunol. 171:175–184.

Pailler J, Aucher W, Pires M, Buddelmeijer N (2012) Phosphatidylglycerol::prolipoprotein diacylglyceryl transferase (Lgt) of *Escherichia coli* has seven transmembrane segments, and its essential residues are embedded in the membrane. J Bacteriol. 194:2142–2151.

Pais TF, Silva RA, Smedegaard B, Appelberg R, Andersen P (1998) Analysis of T cells recruited during delayed-type hypersensitivity to purified protein derivative (PPD) versus challenge with tuberculosis infection. Immunology 95:69–75.

Palanisamy GS, DuTeau N, Eisenach KD, Cave DM, Theus SA, Kreiswirth BN, Basaraba RJ, Orme IM (2009) Clinical strains of *Mycobacterium tuberculosis* display a wide range of virulence in guinea pigs. Tuberculosis 89:203–209.

Palanisamy GS, Smith EE, Shanley CA, Ordway DJ, Orme IM, Basaraba RJ (2008) Disseminated disease severity as a measure of virulence of *Mycobacterium tuberculosis* in the guinea pig model. Tuberculosis 88:295–306.

Palmer MV, Thacker TC, Waters WR, Robbe-Austerman S (2014) Oral vaccination of white-tailed deer (*Odocoileus virginianus*) with *Mycobacterium bovis* Bacillus Calmette-Guérin (BCG). PLoS ONE 9:e97031.

Parasa VR, Rahman MJ, Ngyuen Hoang AT, Svensson M, Brighenti S, Lerm M (2014) Modeling *Mycobacterium tuberculosis* early granuloma formation in experimental human lung tissue. Dis Model Mech. 7:281–288.

Parish CR (1999) Fluorescent dyes for lymphocyte migration and proliferation studies. Immunol Cell Biol. 77:499–508.

Parra MC, Shaffer SA, Hajjar AM, Gallis BM, Hager A, Goodlett DR, Guina T, Miller S, Collins CM (2010) Identification, cloning, expression, and purification of *Francisella* lpp3: an immunogenic lipoprotein. Microbiol Res. 165:531–545.

Pasricha R, Saini NK, Rathor N, Pathak R, Sinha R, Varma-Basil M, Mishra K, Brahmachari V, Bose M (2014) The *Mycobacterium tuberculosis* recombinant LprN protein of *mce4* operon induces Th1 type response deleterious to protection in mice. Pathog Dis. 72:188–196.

Pathak SK, Basu S, Basu KK, Banerjee A, Pathak S, Bhattacharyya A, Kaisho T, Kundu M, Basu J (2007) Direct extracellular interaction between the early secreted antigen ESAT-6 of *Mycobacterium tuberculosis* and TLR2 inhibits TLR signaling in macrophages. Nat Immunol. 8:610–618.

Pecora ND, Gehring AJ, Canaday DH, Boom WH, Harding CV (2006) *Mycobacterium tuberculosis* LprA is a lipoprotein agonist of TLR2 that regulates innate immunity and APC function. J Immunol. 177:422–429.

Penn-Nicholson A, Geldenhuys H, Burny W, van der Most R, Day CL, Jongert E, Moris P, Hatherill M, Ofori-Anyinam O, Hanekom W, Team TVS, Bollaerts A, Demoitie M-A, Luabeya AKK, De Ruymaeker E, Tameris M, Lapierre D, Scriba TJ (2015) Safety and immunogenicity of candidate vaccine M72/AS01E in adolescents in a TB endemic setting. Vaccine 33:4025–4034.

Peyron P, Vaubourgeix J, Poquet Y, Levillain F, Botanch C, Bardou F, Daffé M, Emile J-F, Marchou B, Cardona P-J, de Chastellier C, Altare F (2008) Foamy macrophages from tuberculous patients' granulomas constitute a nutrient-rich reservoir for *M. tuberculosis* persistence. PLoS Pathog. 4:e1000204.

Philips JA (2008) Mycobacterial manipulation of vacuolar sorting. Cell Microbiol. 10:2408–2415.

Philips JA, Ernst JD (2012) Tuberculosis pathogenesis and immunity. Annu Rev Pathol. 7:353–384.

Pirquet von C (1907a) Die Allergieprobe zur Diagnose der Tuberkulose im Kindesalter. Wien Med Wochenschr. 28:1369–1374.

Pirquet von C (1907b) Der diagnostische Wert der kutanen Tuberkulinreaktion bei der Tuberkulose des Kindesalters auf Grund von 100 Sektionen. Wien Klin Wochenschr. 38:1123–1128.

Pitarque S, Herrmann J-L, Duteyrat J-L, Jackson M, Stewart GR, Lecointe F, Payre B, Schwartz O, Young DB, Marchal G, Lagrange PH, Puzo G, Gicquel B, Nigou J, Neyrolles O (2005) Deciphering the molecular bases of *Mycobacterium tuberculosis* binding to the lectin DC-SIGN reveals an underestimated complexity. Biochem J. 392:615–624.

Podell BK, Ackart DF, Kirk NM, Eck SP, Bell C, Basaraba RJ (2012) Non-diabetic hyperglycemia exacerbates disease severity in *Mycobacterium tuberculosis*-infected guinea pigs. PLoS ONE 7:e46824.

Pollock JM, Andersen P (1997a) Predominant recognition of the ESAT-6 protein in the first phase of interferon with *Mycobacterium bovis* in cattle. Infect Immun. 65:2587–2592.

Pollock JM, Andersen P (1997b) The potential of the ESAT-6 antigen secreted by virulent mycobacteria for specific diagnosis of tuberculosis. J Infect Dis. 175:1251–1254.

Porcelli S, Morita CT, Brenner MB (1992) CD1b restricts the response of human CD4-8-T lymphocytes to a microbial antigen. Nature 360:593–597.

Portaels F, Aguiar J, Debacker M, Guedenon A, Steunou C, Zinsou C, Meyers WM (2004) *Mycobacterium bovis* BCG vaccination as prophylaxis against *Mycobacterium ulcerans* osteomyelitis in Buruli ulcer disease. Infect Immun. 72:62–65.

Pourshafie MR, Sonnenfeld G, Barrow WW (1999) Immunological and ultrastructural disruptions of T lymphocytes following exposure to the glycopeptidolipid isolated from the *Mycobacterium avium* complex. Scand J Immunol. 49:405–410.

Poyntz HC, Stylianou E, Griffiths KL, Marsay L, Checkley AM, McShane H (2014) Non-tuberculous mycobacteria have diverse effects on BCG efficacy against *Mycobacterium tuberculosis*. Tuberculosis 94:226–237.

Prasad TSK, Verma R, Kumar S, Nirujogi RS, Sathe GJ, Madugundu AK, Sharma J, Puttamallesh VN, Ganjiwale A, Myneedu VP, Chatterjee A, Pandey A, Harsha HC, Narayana J (2013) Proteomic analysis of purified protein derivative of *Mycobacterium tuberculosis*. Clin Proteomics 10:8.

Puech V, Guilhot C, Perez E, Tropis M, Armitige LY, Gicquel B, Daffé M (2002) Evidence for a partial redundancy of the fibronectin-binding proteins for the transfer of mycoloyl residues onto the cell wall arabinogalactan termini of *Mycobacterium tuberculosis*. Mol Microbiol. 44:1109–1122.

Pym AS, Brodin P, Brosch R, Huerre M, Cole ST (2002) Loss of RD1 contributed to the attenuation of the live tuberculosis vaccines *Mycobacterium bovis* BCG and *Mycobacterium microti*. Mol Microbiol. 46:709–717.

Quah BJC, Warren HS, Parish CR (2007) Monitoring lymphocyte proliferation *in vitro* and *in vivo* with the intracellular fluorescent dye carboxyfluorescein diacetate succinimidyl ester. Nat Protoc. 2:2049–2056.

Ragas A, Roussel L, Puzo G, Rivière M (2007) The *Mycobacterium tuberculosis* cell-surface glycoprotein Apa as a potential adhesin to colonize target cells via the innate immune system pulmonary C-type lectin surfactant protein A. J Biol Chem. 282:5133–5142.

Ramakrishnan L (2012) Revisiting the role of the granuloma in tuberculosis. Nat Rev Immunol. 12:352–366.

Randall AE, Perez MA, Floyd S, Black GF, Crampin AC, Ngwira B, Pistoni WN, Mulawa D, Sichali L, Mwaungulu L, Bickle Q, Fine PEM (2002) Patterns of helminth infection and relationship to BCG vaccination in Karonga District, northern Malawi. Trans R Soc Trop Med Hyg. 96:29–33.

Rangel-Frausto MS, de Leon Rosales SP, Abaroa CM, Haslov K (2001) Tuberculosis and tuberculin quality: best intentions, misleading results. Infect Control Hosp Epidemiol. 22:481–484.

Rao V, Dhar N, Shakila H, Singh R, Khera A, Jain R, Naseema M, Paramasivan CN, Narayanan PR, Ramanathan VD, Tyagi AK (2005) Increased expression of *Mycobacterium tuberculosis* 19 kDa lipoprotein obliterates the protective efficacy of BCG by polarizing host Immune responses to the Th2 subtype. Scand J Immunol. 61:410–417.

Ratliff TL, Palmer JO, McGarr JA, Brown EJ (1987) Intravesical Bacillus Calmette-Guérin therapy for murine bladder tumors: initiation of the response by fibronectin-mediated attachment of Bacillus Calmette-Guérin. Cancer Res. 47:1762–1766.

Ravn P, Demissie A, Eguale T, Wondwosson H, Lein D, Amoudy HA, Mustafa AS, Jensen AK, Holm A, Rosenkrands I, Oftung F, Olobo J, Reyn von F, Andersen P (1999) Human T cell responses to the ESAT-6 antigen from *Mycobacterium tuberculosis*. J Infect Dis. 179:637–645.

Ravn P, Munk ME, Andersen AB, Lundgren B, Lundgren JD, Nielsen LN, Kok-Jensen A, Andersen P, Weldingh K (2005) Prospective evaluation of a whole-blood test using *Mycobacterium tuberculosis*-specific antigens ESAT-6 and CFP10 for diagnosis of active tuberculosis. Clin Diagn Lab Immunol. 12:491–496.

Reba SM, Li Q, Onwuzulike S, Ding X, Karim AF, Hernandez Y, Fulton SA, Harding CV, Lancioni CL, Nagy N, Rodriguez ME, Wearsch PA, Rojas RE (2014) TLR2 engagement on $CD4^+$ T cells enhances effector functions and protective responses to *Mycobacterium tuberculosis*. Eur J Immunol. 44:1410–1421.

Reddy TBK, Riley R, Wymore F, Montgomery P, DeCaprio D, Engels R, Gellesch M, Hubble J, Jen D, Jin H, Koehrsen M, Larson L, Mao M, Nitzberg M, Sisk P, Stolte C, Weiner B, White J, Zachariah ZK, Sherlock G, Galagan JE, Ball CA, Schoolnik GK (2009) TB database: an integrated platform for tuberculosis research. Nucleic Acids Res. 37:D499–508.

Reed MB, Domenech P, Manca C, Su H, Barczak AK, Kreiswirth BN, Kaplan G, Barry CE (2004) A glycolipid of hypervirulent tuberculosis strains that inhibits the innate immune response. Nature 431:84–87.

Rees AD, Faith A, Roman E, Ivanyi J, Wiesmuller KH, Moreno C (1993) The effect of lipoylation on CD4 T cell recognition of the 19,000 MW *Mycobacterium tuberculosis* antigen. Immunology 80:407–414.

Reiling N, Homolka S, Walter K, Brandenburg J, Niwinski L, Ernst M, Herzmann C, Lange C, Diel R, Ehlers S, Niemann S (2013) Clade-specific virulence patterns of *Mycobacterium tuberculosis* complex strains in human primary macrophages and aerogenically infected mice. mBio 4:e00250.

Reither K, Katsoulis L, Beattie T, Gardiner N, Lenz N, Said K, Mfinanga E, Pohl C, Fielding KL, Jeffery H, Kagina BM, Hughes EJ, Scriba TJ, Hanekom WA, Hoff ST, Bang P, Kromann I, Daubenberger C, Andersen P, Churchyard GJ (2014) Safety and immunogenicity of H1/IC31®, an adjuvanted TB subunit vaccine, in HIV-infected adults with $CD4^+$ lymphocyte counts greater than 350 cells/mm3: a phase II, multi-centre, double-blind, randomized, placebo-controlled trial. PLoS ONE 9:e114602.

Renart J, Reiser J, Stark GR (1979) Transfer of proteins from gels to diazobenzyloxymethyl-paper and detection with antisera: a method for studying antibody specificity and antigen structure. Proc Natl Acad Sci USA. 76:3116–3120.

Renshaw PS, Panagiotidou P, Whelan A, Gordon SV, Hewinson RG, Williamson RA, Carr MD (2002) Conclusive evidence that the major T cell antigens of the *Mycobacterium tuberculosis* complex ESAT-6 and CFP10 form a tight, 1:1 complex and characterization of the structural properties of ESAT-6, CFP10, and the ESAT-6*CFP10 complex. Implications for pathogenesis and virulence. J Biol Chem. 277:21598–21603.

Reyn von CF, Mtei L, Arbeit RD, Waddell R, Cole B, Mackenzie T, Matee M, Bakari M, Tvaroha S, Adams LV, Horsburgh CR, Pallangyo K (2010) Prevention of tuberculosis in Bacille Calmette–Guérin-primed, HIV-infected adults boosted with an inactivated whole-cell mycobacterial vaccine. AIDS 24:675–685.

Reyn von CF, Williams DE, Horsburgh CR, Jaeger AS, Marsh BJ, Hasløv K, Magnusson M (1998) Dual skin testing with *Mycobacterium avium* sensitin and purified protein derivative to discriminate pulmonary disease due to *M. avium* complex from pulmonary disease due to *Mycobacterium tuberculosis*. J Infect Dis 177:730–736.

Richardus JH, Oskam L (2015) Protecting people against leprosy: chemoprophylaxis and immunoprophylaxis. Clin Dermatol. 33:19–25.

Rindi L, Lari N, Garzelli C (1999) Search for genes potentially involved in *Mycobacterium tuberculosis* virulence by mRNA differential display. Biochem Biophys Res Commun. 258:94–101.

Roberts EA, Chua J, Kyei GB, Deretic V (2006) Higher order Rab programming in phagolysosome biogenesis. J Cell Biol. 174:923–929.

Robichon C, Vidal-Ingigliardi D, Pugsley AP (2005) Depletion of apolipoprotein N-acyltransferase causes mislocalization of outer membrane lipoproteins in *Escherichia coli*. J Biol Chem. 280:974–983.

Robinson JH, Case MC, Brooks CG (1992) Palmitic acid conjugation of a protein antigen enhances major histocompatibility complex class II-restricted presentation to T cells. Immunology 76:593–598.

Rodrigues LC, Diwan VK, Wheeler JG (1993) Protective effect of BCG against tuberculous meningitis and miliary tuberculosis: a meta-analysis. Int J Epidemiol. 22:1154–1158.

Rodwell TC, Kriek NP, Bengis RG, Whyte IJ, Viljoen PC, de Vos V, Boyce WM (2001) Prevalence of bovine tuberculosis in African buffalo at Kruger National Park. J Wildl Dis. 37:258–264.

Rohde KH, Veiga DFT, Caldwell S, Balázsi G, Russell DG (2012) Linking the transcriptional profiles and the physiological states of *Mycobacterium tuberculosis* during an extended intracellular infection. PLoS Pathog. 8:e1002769.

Roux A-L, Ray A, Pawlik A, Medjahed H, Etienne G, Rottman M, Catherinot E, Coppée J-Y, Chaoui K, Monsarrat B, Toubert A, Daffé M, Puzo G, Gaillard J-L, Brosch R, Dulphy N, Nigou J, Herrmann J-L (2011) Overexpression of proinflammatory TLR2-signalling lipoproteins in hypervirulent mycobacterial variants. Cell Microbiol. 13:692–704.

Russell WMS, Burch RL (1959) The principles of humane experimental technique. http://altweb.jhsph.edu/pubs/books/humane_exp/het-toc. Accessed 20 Aug 2015.

Sakamoto K (2012) The pathology of *Mycobacterium tuberculosis* infection. Vet Pathol. 49:423–439.

Sakthi S, Narayanan S (2013) The lpqS knockout mutant of *Mycobacterium tuberculosis* is attenuated in macrophages. Microbiol Res. 168:407–414.

Sakula A (1983) BCG: who were Calmette and Guérin? Thorax 38:806–812.

Sanchez A, Espinosa P, Esparza MA, Colon M, Bernal G, Mancilla R (2009) *Mycobacterium tuberculosis* 38 kDa lipoprotein is apoptogenic for human monocyte-derived macrophages. Scand J Immunol. 69:20–28.

Sander P, Rezwan M, Walker B, Rampini SK, Kroppenstedt RM, Ehlers S, Keller C, Keeble JR, Hagemeier M, Colston MJ, Springer B, Böttger EC (2004) Lipoprotein processing is required for virulence of *Mycobacterium tuberculosis*. Mol Microbiol. 52:1543–1552.

Sani M, Houben ENG, Geurtsen J, Pierson J, de Punder K, van Zon M, Wever B, Piersma SR, Jiménez CR, Daffé M, Appelmelk BJ, Bitter W, van der Wel N, Peters PJ (2010) Direct visualization by cryo-EM of the mycobacterial capsular layer: a labile structure containing ESX-1-secreted proteins. PLoS Pathog. 6:e1000794.

Santosuosso M, McCormick S, Zhang X, Zganiacz A, Xing Z (2006) Intranasal boosting with an adenovirus-vectored vaccine markedly enhances protection by parenteral *Mycobacterium bovis* BCG immunization against pulmonary tuberculosis. Infect Immun. 74:4634–4643.

Satti I, Meyer J, Harris SA, Thomas Z-RM, Griffiths K, Antrobus RD, BM RR, Lopez Ramon R, Smith M, Sheehan S, Bettinson H, McShane H (2014) Safety and immunogenicity of a candidate tuberculosis vaccine MVA85A delivered by aerosol in BCG-vaccinated healthy adults: a phase 1, double-blind, randomised controlled trial. Lancet Infect Dis. 14:939–946.

Saunders BM, Frank AA, Orme IM, Cooper AM (2000) Interleukin-6 induces early gamma Interferon production in the infected lung but is not required for generation of specific immunity to *Mycobacterium tuberculosis* infection. Infect Immun. 68:3322–3326.

Saunders BM, Frank AA, Orme IM, Cooper AM (2002) CD4 is required for the development of a protective granulomatous response to pulmonary tuberculosis. Cell Immunol. 216:65–72.

Saunders BM, Orme IM, Basaraba RJ (2008) Immunopathology of tuberculosis. In: Kaufmann SHE, Britton WJ (eds) Handbook of Tuberculosis. Wiley-VHC.

Sánchez A, Espinosa P, García T, Mancilla R (2012) The 19 kDa *Mycobacterium tuberculosis* lipoprotein (LpqH) induces macrophage apoptosis through extrinsic and intrinsic pathways: a role for the mitochondrial apoptosis-inducing factor. Clin Dev Immunol. 2012:950503.

Schaefer M, Reiling N, Fessler C, Stephani J, Taniuchi I, Hatam F, Yildirim AO, Fehrenbach H, Walter K, Ruland J, Wagner H, Ehlers S, Sparwasser T (2008) Decreased pathology and prolonged survival of human DC-SIGN transgenic mice during mycobacterial infection. J Immunol. 180:6836–6845.

Schaible UE, Winau F, Sieling PA, Fischer K, Collins HL, Hagens K, Modlin RL, Brinkmann V, Kaufmann SHE (2003) Apoptosis facilitates antigen presentation to T lymphocytes through MHC-I and CD1 in tuberculosis. Nature Medicine 9:1039–1046.

Schlesinger LS (1993) Macrophage phagocytosis of virulent but not attenuated strains of *Mycobacterium tuberculosis* is mediated by mannose receptors in addition to complement receptors. J Immunol. 150:2920–2930.

Schmidt-Traub H, Schulte M, Seidel-Morgenstern A (eds) (2012) Preparative Chromatography. John Wiley & Sons.

Schmiedel A, Gerloff W (1965) [Triple differentiation of mycobacteria in deep agar cultures]. Prax Pneumol. 19:528–536.

Schmitt SM, Fitzgerald SD, Cooley TM, Bruning-Fann CS, Sullivan L, Berry D, Carlson T, Minnis RB, Payeur JB, Sikarskie J (1997) Bovine tuberculosis in free-ranging white-tailed deer from Michigan. J Wildl Dis. 33:749–758.

Schoenen H, Bodendorfer B, Hitchens K, Manzanero S, Werninghaus K, Nimmerjahn F, Agger EM, Stenger S, Andersen P, Ruland J, Brown GD, Wells C, Lang R (2010) Cutting edge: Mincle is essential for recognition and adjuvanticity of the mycobacterial cord factor and its synthetic analog trehalose-dibehenate. J Immunol. 184:2756–2760.

Schorey JS, Sweet L (2008) The mycobacterial glycopeptidolipids: structure, function, and their role in pathogenesis. Glycobiology 18:832–841.

Schreiber HA, Harding JS, Hunt O, Altamirano CJ, Hulseberg PD, Stewart D, Fabry Z, Sandor M (2011) Inflammatory dendritic cells migrate in and out of transplanted chronic mycobacterial granulomas in mice. J Clin Invest. 121:3902–3913.

Schuck SD, Mueller H, Kunitz F, Neher A, Hoffmann H, Franken KLCM, Repsilber D, Ottenhoff THM, Kaufmann SHE, Jacobsen M (2009) Identification of T cell antigens specific for latent *Mycobacterium tuberculosis* infection. PLoS ONE 4:e5590.

Seibert FB (1934) The isolation and properties of the purified protein derivative of tuberculin. Am Rev Tuberc. 30:713–720.

Seibert FB, Glenn JT (1941) Tuberculin purified protein derivative preparation and analysis of a large quantity for standard. Am Rev Tuberc. 44:9-25.

Seid RC, Sadoff JC (1981) Preparation and characterization of detoxified lipopolysaccharide-protein conjugates. J Biol Chem. 256:7305–7310.

Senaratne RH, Mobasheri H, Papavinasasundaram KG, Jenner P, Lea EJ, Draper P (1998) Expression of a gene for a porin-like protein of the OmpA family from *Mycobacterium tuberculosis* H37Rv. J Bacteriol. 180:3541–3547.

Serra-Vidal MM, Latorre I, Franken KLCM, Díaz J, de Souza-Galvão ML, Casas I, Maldonado J, Milà C, Solsona J, Jimenez-Fuentes MÁ, Altet N, Lacoma A, Ruiz-Manzano J, Ausina V, Prat C, Ottenhoff THM, Domínguez J (2014) Immunogenicity of 60 novel latency-related antigens of *Mycobacterium tuberculosis*. Front Microbiol. 5:517.

Seshadri C, Turner MT, Lewinsohn DM, Moody DB, Van Rhijn I (2013) Lipoproteins are major targets of the polyclonal human T cell response to *Mycobacterium tuberculosis*. J Immunol. 190:278–284.

Shaler CR, Horvath C, Lai R, Xing Z (2012) Understanding delayed T cell priming, lung recruitment, and airway luminal T cell responses in host defense against pulmonary tuberculosis. Clin Dev Immunol. 2012:1–13.

Shaler CR, Horvath CN, Jeyanathan M, Xing Z (2013) Within the enemy's camp: contribution of the granuloma to the dissemination, persistence and transmission of *Mycobacterium tuberculosis*. Front Immunol. 4:1–8.

Shaler CR, Kugathasan K, McCormick S, Damjanovic D, Horvath C, Small CL, Jeyanathan M, Chen X, Yang PC, Xing Z (2011) Pulmonary mycobacterial granuloma. Am J Pathol. 178:1622–1634.

Shanley CA, Ireton GC, Baldwin SL, Coler RN, Reed SG, Basaraba RJ, Orme IM (2014) Therapeutic vaccination against relevant high virulence clinical isolates of *Mycobacterium tuberculosis*. Tuberculosis 94:140–147.

Sherman DR, Voskuil M, Schnappinger D, Liao R, Harrell MI, Schoolnik GK (2001) Regulation of the *Mycobacterium tuberculosis* hypoxic response gene encoding alpha-crystallin. Proc Natl Acad Sci USA. 98:7534–7539.

Shevach EM, Schwartz BD (1977) Overview of the structure and function of the major histocompatibility complex of the guinea pig. Fed Proc. 36:2260–2263.

Shrikrishna D, la Rua-Domenech de R, Smith NH, Colloff A, Coutts I (2009) Human and canine pulmonary *Mycobacterium bovis* infection in the same household: re-emergence of an old zoonotic threat? Thorax 64:89–91.

Sia JK, Georgieva M, Rengarajan J (2015) Innate immune defenses in human tuberculosis: an overview of the interactions between *Mycobacterium tuberculosis* and innate immune cells. J Immunol Res. 2015:747543.

Silva PE, Bigi F, Santangelo MP, Romano MI, Martin C, Cataldi A, Ainsa JA (2001) Characterization of P55, a multidrug efflux pump in *Mycobacterium bovis* and *Mycobacterium tuberculosis*. Antimicrob Agents Chemother. 45:800–804.

Simiele M, D'Avolio A, Baietto L, Siccardi M, Sciandra M, Agati S, Cusato J, Bonora S, Di Perri G (2011) Evaluation of the mean corpuscular volume of peripheral blood mononuclear cells of HIV patients by a coulter counter to determine intracellular drug concentrations. Antimicrob Agents Chemother. 55:2976–2978.

Simmons DP, Canaday DH, Liu Y, Li Q, Huang A, Boom WH, Harding CV (2010) *Mycobacterium tuberculosis* and TLR2 agonists inhibit induction of type I IFN and class I MHC antigen cross processing by TLR9. J Immunol. 185:2405–2415.

Sinha S, Arora S, Kosalai K, Namane A, Pym AS, Cole ST (2002) Proteome analysis of the plasma membrane of *Mycobacterium tuberculosis*. Comp Funct Genomics. 3:470–483.

Skeiky YA, Lodes MJ, Guderian JA, Mohamath R, Bement T, Alderson MR, Reed SG (1999) Cloning, expression, and immunological evaluation of two putative secreted serine protease antigens of *Mycobacterium tuberculosis*. Infect Immun. 67:3998–4007.

Skeiky YAW, Alderson MR, Ovendale PJ, Guderian JA, Brandt L, Dillon DC, Campos-Neto A, Lobet Y, Dalemans W, Orme IM, Reed SG (2004) Differential immune responses and protective efficacy induced by components of a tuberculosis polyprotein vaccine, Mtb72F, delivered as naked DNA or recombinant protein. J Immunol. 172:7618–7628.

Skjøt RL, Oettinger T, Rosenkrands I, Ravn P, Brock I, Jacobsen S, Andersen P (2000) Comparative evaluation of low molecular mass proteins from *Mycobacterium tuberculosis* identifies members of the ESAT-6 family as immunodominant T cell antigens. Infect Immun. 68:214–220.

Smaill F, Jeyanathan M, Smieja M, Medina MF, Thanthrige-Don N, Zganiacz A, Yin C, Heriazon A, Damjanovic D, Puri L, Hamid J, Xie F, Foley R, Bramson J, Gauldie J, Xing Z (2013) A human type 5 adenovirus-based tuberculosis vaccine induces robust T cell responses in humans despite preexisting anti-adenovirus immunity. Sci Transl Med. 5:205ra134.

Smith DW, Harding GE (1977) Animal model of human disease, pulmonary tuberculosis. Animal model: Experimental airborne tuberculosis in the guinea pig. Am J Pathol. 89:273–276.

Smith DW, McMurray DN, Wiegeshaus EH, Grover AA, Harding GE (1970) Host-parasite relationships in experimental airborne tuberculosis. IV. Early events in the course of infection in vaccinated and nonvaccinated guinea pigs. Am Rev Respir Dis. 102:937–949.

Smith J, Manoranjan J, Pan M, Bohsali A, Xu J, Liu J, McDonald KL, Szyk A, LaRonde-LeBlanc N, Gao LY (2008) Evidence for pore formation in host cell membranes by ESX-1-secreted ESAT-6 and its role in *Mycobacterium marinum* escape from the vacuole. Infect Immun. 76:5478–5487.

Smith KC, Starke JR (2004) Bacille Calmette-Guérin vaccine. In: Plotkin SA, Orenstein WA (eds) Vaccines, 4th edition. Elsevier.

Smith SM, Malin AS, Pauline T, Lukey, Atkinson SE, Content J, Huygen K, Dockrell HM (1999) Characterization of human *Mycobacterium bovis* Bacille Calmette-Guérin-reactive $CD8^+$ T cells. Infect Immun. 67:5223–5230.

Smith T (1898) A comparative study of bovine tubercle bacilli and of human bacilli from sputum. J Exp Med. 3:451–511.

Smyth TJP, Perfumo A, McClean S, Marchant R, Banat IM (2010) Isolation and analysis of lipopeptides and high molecular weight biosurfactants. In: Handbook of hydrocarbon and lipid microbiology. Springer.

Spaulding AR, Salgado-Pabón W, Kohler PL, Horswill AR, Leung DYM, Schlievert PM (2013) Staphylococcal and streptococcal superantigen exotoxins. Clin Microbiol Rev. 26:422–447.

Spohr C (2015) Etablierung einer 3R-Alternativmethode für die Chargenprüfung von bovinem Tuberkulin unter Berücksichtigung mykobakterieller Lipidantigene im Meerschweinchenmodell. Dissertation, Technische Universität Darmstadt, Germany.

Spohr C, Kaufmann E, Battenfeld S, Duchow K, Cussler K, Balks E, Bastian M (2015) A new lymphocyte proliferation assay for potency determination of bovine tuberculin PPDs. ALTEX 32:201-210.

Srivastava S, Ernst JD (2013) Cutting edge: direct recognition of infected cells by CD4 T cells is required for control of intracellular *Mycobacterium tuberculosis in vivo*. J Immunol. 191:1016–1020.

Stacey G (2004) Fundamental issues for cell-line banks in biotechnology and regulatory affairs. In: Fuller BJ, Lane N, Benson EE (eds) Life in the frozen state. CRC Press.

Stamm LM, Morisaki JH, Gao LY, Jeng RL, McDonald KL, Roth R, Takeshita S, Heuser J, Welch MD, Brown EJ (2003) *Mycobacterium marinum* escapes from phagosomes and is propelled by actin-based motility. J Exp Med. 198:1361–1368.

Stanford J, Stanford C, Grange J (2004) Immunotherapy with *Mycobacterium vaccae* in the treatment of tuberculosis. Front Biosci. 9:1701–1719.

Stegelmann F, Bastian M, Swoboda K, Bhat R, Kiessler V, Krensky AM, Roellinghoff M, Modlin RL, Stenger S (2005) Coordinate expression of CC chemokine ligand 5, granulysin, and perforin in $CD8^+$ T cells provides a host defense mechanism against *Mycobacterium tuberculosis*. J Immunol. 175:7474–7483.

Stein M-P, Feng Y, Cooper KL, Welford AM, Wandinger-Ness A (2003) Human VPS34 and p150 are Rab7 interacting partners. Traffic 4:754–771.

Steinberg TH (2009) Protein gel staining methods: an introduction and overview. In: Abelson JN, Simon MI, Pyle AM (eds) Methods in Enzymology, 1st edition. Elsevier.

Stenger S, Modlin RL (2002) Control of *Mycobacterium tuberculosis* through mammalian Toll-like receptors. Curr Opin Immunol. 14:452–457.

Stewart GR, Wilkinson KA, Newton SM, Sullivan SM, Neyrolles O, Wain JR, Patel J, Pool KL, Young DB, Wilkinson RJ (2005) Effect of deletion or overexpression of the 19 kilodalton lipoprotein Rv3763 on the innate response to *Mycobacterium tuberculosis*. Infect Immun. 73:6831–6837.

Steyn AJC, Joseph J, Bloom BR (2003) Interaction of the sensor module of *Mycobacterium tuberculosis* H37Rv KdpD with members of the Lpr family. Mol Microbiol. 47:1075–1089.

Stittelaar KJ, Hoogerhout P, Ovaa W, van Binnendijk RR, Poelen MC, Roholl P, van Els CA, Osterhaus AD, Wiertz EJ (2001) *In vitro* processing and presentation of a lipidated cytotoxic T cell epitope derived from measles virus fusion protein. Vaccine 20:249–261.

Stow JL, Murray RZ (2013) Intracellular trafficking and secretion of inflammatory cytokines. Cytokine Growth Factor Rev. 24:227–239.

Strugnell R, Zepp F, Cunningham A, Tantawichien T (2011) Vaccine antigens. Perspectives in Vaccinology 1:61–88.

Stukova MA, Sereinig S, Zabolotnyh NV, Ferko B, Kittel C, Romanova J, Vinogradova TI, Katinger H, Kiselev OI, Egorov A (2006) Vaccine potential of influenza vectors expressing *Mycobacterium tuberculosis* ESAT-6 protein. Tuberculosis 86:236–246.

Stylianou E, Griffiths KL, Poyntz HC, Harrington-Kandt R, Dicks MD, Stockdale L, Betts G, McShane H (2015) Improvement of BCG protective efficacy with a novel chimpanzee adenovirus and a modified vaccinia Ankara virus both expressing Ag85A. Vaccine 33:6800–6808.

Sulzenbacher G, Canaan S, Bordat Y, Neyrolles O, Stadthagen G, Zamboni VR, Rauzier J, Maurin D, Laval F, Daffé M, Cambillau C, Gicquel B, Bourne Y, Jackson M (2006) LppX is a lipoprotein required for the translocation of phthiocerol dimycocerosates to the surface of *Mycobacterium tuberculosis*. EMBO J. 25:1436–1444.

Supply P, Allix C, Lesjean S, Cardoso-Oelemann M, Rusch-Gerdes S, Willery E, Savine E, de Haas P, van Deutekom H, Roring S, Bifani P, Kurepina N, Kreiswirth B, Sola C, Rastogi N, Vatin V, Gutierrez MC, Fauville M, Niemann S, Skuce R, Kremer K, Locht C, van Soolingen D (2006) Proposal for standardization of optimized mycobacterial interspersed repetitive unit-variable-number tandem repeat typing of *Mycobacterium tuberculosis*. J Clin Microbiol. 44:4498–4510.

Supply P, Lesjean S, Savine E, Kremer K, van Soolingen D, Locht C (2001) Automated high-throughput genotyping for study of global epidemiology of *Mycobacterium tuberculosis* based on mycobacterial interspersed repetitive units. J Clin Microbiol. 39:3563–3571.

Sutcliffe IC, Harrington DJ (2004) Lipoproteins of *Mycobacterium tuberculosis*: an abundant and functionally diverse class of cell envelope components. FEMS Microbiol Rev. 28:645–659.

Sutcliffe IC, Harrington DJ, Hutchings MI (2012) A phylum level analysis reveals lipoprotein biosynthesis to be a fundamental property of bacteria. Protein Cell 3:163–170.

Sutcliffe IC, Russell RR (1995) Lipoproteins of gram-positive bacteria. J Bacteriol. 177:1123–1128.

Symmank H, Franke P, Saenger W, Bernhard F (2002) Modification of biologically active peptides: production of a novel lipohexapeptide after engineering of *Bacillus subtilis* surfactin synthetase. Protein Eng. 15:913–921.

Sørensen AL, Nagai S, Houen G, Andersen P, Andersen AB (1995) Purification and characterization of a low molecular mass T cell antigen secreted by *Mycobacterium tuberculosis*. Infect Immun. 63:1710–1717.

Tailleux L, Schwartz O, Herrmann J-L, Pivert E, Jackson M, Amara A, Legres L, Dreher D, Nicod LP, Gluckman JC, Lagrange PH, Gicquel B, Neyrolles O (2003) DC-SIGN is the major *Mycobacterium tuberculosis* receptor on human dendritic cells. J Exp Med. 197:121–127.

Takeda K, Akira S (2004) TLR signaling pathways. Semin Immunol. 16:3–9.

Takeda K, Takeuchi O, Akira S (2002) Recognition of lipopeptides by Toll-like receptors. J Endotoxin Res. 8:459–463.

Tameris M, Hokey DA, Nduba V, Sacarlal J, Laher F, Kiringa G, Gondo K, Lazarus EM, Gray GE, Nachman S, Mahomed H, Downing K, Abel B, Scriba TJ, McClain JB, Pau MG, Hendriks J, Dheenadhayalan V, Ishmukhamedov S, Luabeya AKK, Geldenhuys H, Shepherd B, Blatner G, Cardenas V, Walker R, Hanekom WA, Sadoff J, Douoguih M, Barker L, Hatherill M (2015) A double-blind, randomised, placebo-controlled, dose-finding trial of the novel tuberculosis vaccine AERAS-402, an adenovirus-vectored fusion protein, in healthy, BCG-vaccinated infants. Vaccine 33:2944–2954.

Tameris MD, Hatherill M, Landry BS, Scriba TJ, Snowden MA, Lockhart S, Shea JE, McClain JB, Hussey GD, Hanekom WA, Mahomed H, McShane H, the MVA85A 020 Trial Study Team (2013) Safety and efficacy of MVA85A, a new tuberculosis vaccine, in infants previously vaccinated with BCG: a randomised, placebo-controlled phase 2b trial. Lancet 381:1021–1028.

Tanne A, Ma B, Boudou F, Tailleux L, Botella H, Badell E, Levillain F, Taylor ME, Drickamer K, Nigou J, Dobos KM, Puzo G, Vestweber D, Wild MK, Marcinko M, Sobieszczuk P, Stewart L, Lebus D, Gicquel B, Neyrolles O (2009) A murine DC-SIGN homologue contributes to early host defense against *Mycobacterium tuberculosis*. J Exp Med. 206:2205–2220.

Taylor T (2013) Avoiding the problems associated with HPLC column overload. In: http://www.crawfordscientific.com/Chromatography-Technical-Tips-HPLC-Column-Overload.html. Accessed 20 Feb 2016.

Thakran S, Li H, Lavine CL, Miller MA, Bina JE, Bina XR, Re F (2008) Identification of *Francisella tularensis* lipoproteins that stimulate the Toll-like receptor (TLR) 2/TLR1 heterodimer. J Biol Chem. 283:3751–3760.

Theilacker C, Diederich A-K, Otto A, Sava IG, Wobser D, Bao Y, Hese K, Broszat M, Henneke P, Becher D, Huebner J (2015) *Enterococcus faecalis* glycolipids modulate lipoprotein content of the bacterial cell membrane and host immune response. PLoS ONE 10:e0132949.

Thoma-Uszynski S, Stenger S, Takeuchi O, Ochoa MT, Engele M, Sieling PA, Barnes PF, Röllinghoff M, Bölcskei PL, Wagner M, Akira S, Norgard MV, Belisle JT, Godowski PJ, Bloom BR, Modlin RL (2001) Induction of direct antimicrobial activity through mammalian Toll-like receptors. Science 291:1544–1547.

Thorel MF, Krichevsky M, Lévy-Frébault VV (1990) Numerical taxonomy of mycobactin-dependent mycobacteria, emended description of *Mycobacterium avium*, and description of *Mycobacterium avium* subsp. *avium* subsp. *nov.*, *Mycobacterium avium* subsp. *paratuberculosis* subsp. *nov.*, and *Mycobacterium avium* subsp. *silvaticum* subsp. *nov.* Int J of Syst Bacteriol. 40:254–260.

Tissot F, Zanetti G, Francioli P, Zellweger JP, Zysset F (2005) Influence of Bacille Calmette-Guérin vaccination on size of tuberculin skin test reaction: To what size? Clin Infect Dis. 40:211–217.

Torrado E, Cooper AM (2010) IL-17 and Th17 cells in tuberculosis. Cytokine Growth Factor Rev. 21:455–462.

Torres A, Juárez MD, Cervantes R, Espitia C (2001) Molecular analysis of *Mycobacterium tuberculosis* phosphate specific transport system in *Mycobacterium smegmatis*. Characterization of recombinant 38 kDa (PstS-1). Microbial Pathogenesis 30:289–297.

Towbin H, Staehelin T, Gordon J (1979) Electrophoretic transfer of proteins from polyacrylamide gels to nitrocellulose sheets: procedure and some applications. Proc Natl Acad Sci USA. 76:4350–4354.

Traub S, Aulock von S, Hartung T, Hermann C (2006) MDP and other muropeptides direct and synergistic effects on the immune system. J Endotoxin Res. 12:69–85.

Tree JA, Elmore MJ, Javed S, Williams A, Marsh PD (2006) Development of a guinea pig immune response-related microarray and its use to define the host response following *Mycobacterium bovis* BCG vaccination. Infect Immun. 74:1436–1441.

Trunz BB, Fine P, Dye C (2006) Effect of BCG vaccination on childhood tuberculous meningitis and miliary tuberculosis worldwide: a meta-analysis and assessment of cost-effectiveness. Lancet 367:1173–1180.

Tsai MC, Chakravarty S, Zhu G, Xu J, Tanaka K, Koch C, Tufariello J, Flynn J, Chan J (2006) Characterization of the tuberculous granuloma in murine and human lungs: cellular composition and relative tissue oxygen tension. Cell Microbiol. 8:218–232.

Tschumi A, Grau T, Albrecht D, Rezwan M, Antelmann H, Sander P (2012) Functional analyses of mycobacterial lipoprotein diacylglyceryl transferase and comparative secretome analysis of a mycobacterial lgt mutant. J Bacteriol. 194:3938–3949.

Tschumi A, Nai C, Auchli Y, Hunziker P, Gehrig P, Keller P, Grau T, Sander P (2009) Identification of apolipoprotein N-acyltransferase (Lnt) in Mycobacteria. J Biol Chem. 284:27146–27156.

Tuberculosis Research Centre ICMR (1999) Fifteen year follow up of trial of BCG vaccines in South India for tuberculosis prevention. Tuberculosis Research Centre (ICMR), Chennai. Indian J Med Res. 110:56–69.

Turner J, Dockrell HM (1996) Stimulation of human peripheral blood mononuclear cells with live *Mycobacterium bovis* BCG activates cytolytic CD8 T cells *in vitro*. Immunology 87:339–342.

Turner OC, Basaraba RJ, Orme IM (2003) Immunopathogenesis of pulmonary granulomas in the guinea pig after infection with *Mycobacterium tuberculosis*. Infect Immun. 71:864–871.

Ulrichs T, Kaufmann SH (2005) New insights into the function of granulomas in human tuberculosis. J Pathol. 208:261–269.

Ulrichs T, Moody DB, Grant E, Kaufmann SHE, Porcelli SA (2003) T cell responses to CD1-presented lipid antigens in humans with *Mycobacterium tuberculosis* infection. Infect Immun. 71:3076–3087.

Underhill DM, Ozinsky A, Smith KD, Aderem A (1999) Toll-like receptor-2 mediates mycobacteria-induced proinflammatory signaling in macrophages. Proc Natl Acad Sci USA. 96:14459–14463.

Urdahl KB (2014) Understanding and overcoming the barriers to T cell-mediated immunity against tuberculosis. Semin Immunol. 26:578–587.

Vaickus LJ, Bouchard J, Kim J, Natarajan S, Remick DG (2010) Inbred and outbred mice have equivalent variability in a cockroach allergen-induced model of asthma. Comp Med. 60:420–426.

van der Wel N, Hava D, Houben D, Fluitsma D, van Zon M, Pierson J, Brenner M, Peters PJ (2007) *M. tuberculosis* and *M. leprae* translocate from the phagolysosome to the cytosol in myeloid cells. Cell 129:1287–1298.

van Embden JD, Cave MD, Crawford JT, Dale JW, Eisenach KD, Gicquel B, Hermans P, Martin C, McAdam R, Shinnick TM (1993) Strain identification of *Mycobacterium tuberculosis* by DNA fingerprinting: recommendations for a standardized methodology. J Clin Microbiol. 31:406–409.

van Pinxteren LA, Ravn P, Agger EM, Pollock J, Andersen P (2000) Diagnosis of tuberculosis based on the two specific antigens ESAT-6 and CFP10. Clin Diagn Lab Immunol. 7:155–160.

van Rhijn I, Nguyen TKA, Michel A, Cooper D, Govaerts M, Cheng T-Y, van Eden W, Moody DB, Coetzer JAW, Rutten V, Koets AP (2009a) Low cross-reactivity of T cell responses against lipids from *Mycobacterium bovis* and *M. avium paratuberculosis* during natural infection. Eur J Immunol. 39:3031–3041.

van Rhijn I, Young DC, De Jong A, Vazquez J, Cheng T-Y, Talekar R, Barral DC, Barral D, León L, Brenner MB, Katz JT, Riese R, Ruprecht RM, O'Connor PB, Costello CE, Porcelli SA, Briken V, Moody DB (2009b) CD1c bypasses lysosomes to present a lipopeptide antigen with 12 amino acids. J Exp Med. 206:1409–1422.

van Rhijn I, Zajonc DM, Wilson IA, Moody DB (2005) T cell activation by lipopeptide antigens. Curr Opin Immunol. 17:222–229.

van Soolingen D, Hoogenboezem T, de Haas PE, Hermans PW, Koedam MA, Teppema KS, Brennan PJ, Besra GS, Portaels F, Top J, Schouls LM, van Embden JD (1997) A novel pathogenic taxon of the *Mycobacterium tuberculosis* complex, *Canetti*: characterization of an exceptional isolate from Africa. Int J of Syst Bacteriol. 47:1236–1245.

Vater J, Kablitz B, Wilde C, Franke P, Mehta N, Cameotra SS (2002) Matrix-assisted laser desorption ionization--time of flight mass spectrometry of lipopeptide biosurfactants in whole cells and culture filtrates of *Bacillus subtilis* C-1 isolated from petroleum sludge. Appl Environ Microbiol. 68:6210–6219.

Vekemans J, Amedei A, Ota MO, D'Elios MM, Goetghebuer T, Ismaili J, Newport MJ, Del Prete G, Goldman M, McAdam KP, Marchant A (2001) Neonatal Bacillus Calmette-Guérin vaccination induces adult-like IFN-gamma production by $CD4^+$ T lymphocytes. Eur J Immunol. 31:1531–1535.

Vergne I, Chua J, Deretic V (2003) Tuberculosis toxin blocking phagosome maturation inhibits a novel $Ca2^+$/calmodulin-PI3K hVPS34 cascade. J Exp Med. 198:653–659.

Vergne I, Fratti RA, Hill PJ, Chua J, Belisle J, Deretic V (2004) *Mycobacterium tuberculosis* phagosome maturation arrest: mycobacterial phosphatidylinositol analog phosphatidylinositol mannoside stimulates early endosomal fusion. Mol Biol Cell. 15:751–760.

Via LE, Lin PL, Ray SM, Carrillo J, Allen SS, Eum SY, Taylor K, Klein E, Manjunatha U, Gonzales J, Lee EG, Park SK, Raleigh JA, Cho SN, McMurray DN, Flynn JL, Barry CE (2008) Tuberculous granulomas are hypoxic in guinea pigs, rabbits, and nonhuman primates. Infect Immun. 76:2333–2340.

Vieira OV, Harrison RE, Scott CC, Stenmark H, Alexander D, Liu J, Gruenberg J, Schreiber AD, Grinstein S (2004) Acquisition of Hrs, an essential component of phagosomal maturation, is impaired by mycobacteria. Mol Cell Biol. 24:4593–4604.

Vilaplana C, Gil O, Cáceres N, Pinto S, Díaz J, Cardona P-J (2011) Prophylactic effect of a therapeutic vaccine against TB based on fragments of *Mycobacterium tuberculosis*. PLoS ONE 6:e20404.

Vogelzang A, Perdomo C, Zedler U, Kuhlmann S, Hurwitz R, Gengenbacher M, Kaufmann SHE (2014) Central memory $CD4^+$ T cells are responsible for the recombinant Bacillus Calmette-Guérin ΔureC::hly vaccine's superior protection against tuberculosis. J Infect Dis. 210:1928–1937.

Volkman HE, Clay H, Beery D, Chang JCW, Sherman DR, Ramakrishnan L (2004) Tuberculous granuloma formation is enhanced by a *Mycobacterium* virulence determinant. PloS Biol. 2:e367.

Vordermeier HM, Harris DP, Roman E, Lathigra R, Moreno C, Ivanyi J (1991) Identification of T cell stimulatory peptides from the 38 kDa protein of *Mycobacterium tuberculosis*. J Immunol. 147:1023–1029.

Walters SB, Dubnau E, Kolesnikova I, Laval F, Daffé M, Smith I (2006) The *Mycobacterium tuberculosis* PhoPR two-component system regulates genes essential for virulence and complex lipid biosynthesis. Mol Microbiol. 60:312–330.

Wang J, Thorson L, Stokes RW, Santosuosso M, Huygen K, Zganiacz A, Hitt M, Xing Z (2004) Single mucosal, but not parenteral, immunization with recombinant adenoviral-based vaccine provides potent protection from pulmonary tuberculosis. J Immunol. 173:6357–6365.

Wang L, Turner MO, Elwood RK, Schulzer M, FitzGerald JM (2002) A meta-analysis of the effect of Bacille Calmette-Guérin vaccination on tuberculin skin test measurements. Thorax 57:804–809.

Waters WR, Palmer MV (2015) *Mycobacterium bovis* infection of cattle and white-tailed deer: translational research of relevance to human tuberculosis. ILAR J. 56:26–43.

Waters WR, Whelan AO, Lyashchenko KP, Greenwald R, Palmer MV, Harris BN, Hewinson RG, Vordermeier HM (2010) Immune responses in cattle inoculated with *Mycobacterium bovis*, *Mycobacterium tuberculosis*, or *Mycobacterium kansasii*. Clin Vaccine Immunol. 17:247–252.

Wayne LG, Hayes LG (1996) An *in vitro* model for sequential study of shiftdown of *Mycobacterium tuberculosis* through two stages of nonreplicating persistence. Infect Immun. 64:2062–2069.

Wayne LG, Kubica GB (1986) Family *Mycobacteriaceae*. In: Holt JG, Sneath PH, Krieg NR (eds) Bergey's Manual of Systematic Bacteriology. Springer.

Weinrich Olsen A, van Pinxteren LA, Meng Okkels L, Birk Rasmussen P, Andersen P (2001) Protection of mice with a tuberculosis subunit vaccine based on a fusion protein of antigen 85B and ESAT-6. Infect Immun. 69:2773–2778.

Welin A, Lerm M (2012) Inside or outside the phagosome? The controversy of the intracellular localization of *Mycobacterium tuberculosis*. Tuberculosis 92:113–120.

Welin A, Winberg ME, Abdalla H, Särndahl E, Rasmusson B, Stendahl O, Lerm M (2008) Incorporation of *Mycobacterium tuberculosis* lipoarabinomannan into macrophage membrane rafts is a prerequisite for the phagosomal maturation block. Infect Immun. 76:2882–2887.

Welsh KJ, Risin SA, Actor JK, Hunter RL (2011) Immunopathology of postprimary tuberculosis: increased T regulatory cells and DEC-205-positive foamy macrophages in cavitary lesions. Clin Dev Immunol. 2011:307631.

Whitman W, Goodfellow M, Kämpfer P, Busse H-J, Trujillo M, Ludwig W, Suzuki K-I, Parte A (2012) Bergey's Manual of Systematic Bacteriology. Springer Science & Business Media, New York, NY.

WHO-UNICEF (2014) WHO-UNICEF, estimates of BCG coverage, 2014.

Wiegeshaus EH, McMurray DN, Grover AA, Harding GE, Smith DW (1970) Host-parasite relationships in experimental airborne tuberculosis: III. Relevance of microbial enumeration to acquired resistance in guinea pigs. Am Rev Resp Dis. 102:422–9.

Wiker HG, Harboe M (1992) The antigen 85 complex: a major secretion product of *Mycobacterium tuberculosis*. Microbiol Rev 56:648–661.

Wiker HG, Harboe M, Lea TE (1986) Purification and characterization of two protein antigens from the heterogeneous BCG85 complex in *Mycobacterium bovis* BCG. Int Arch Allergy Appl Immunol. 81:298–306.

Wiker HG, Sletten K, Nagai S, Harboe M (1990) Evidence for three separate genes encoding the proteins of the mycobacterial antigen 85 complex. Infect Immun. 58:272–274.

Wilkinson KA, Newton SM, Stewart GR, Martineau AR, Patel J, Sullivan SM, Herrmann J-L, Neyrolles O, Young DB, Wilkinson RJ (2009) Genetic determination of the effect of post-translational modification on the innate immune response to the 19 kDa lipoprotein of *Mycobacterium tuberculosis*. BMC Microbiol 9:93.

Williams A, Hall Y, Orme IM (2009) Evaluation of new vaccines for tuberculosis in the guinea pig model. Tuberculosis 89:389–397.

Wilson ME, Fineberg HV, Colditz GA (1995) Geographic Latitude and the Efficacy of Bacillus Calmette-Guerin Vaccine. Clin Infect Dis. 20:982–991.

Wilson RA, Maughan WN, Kremer L, Besra GS, Fütterer K (2004) The structure of *Mycobacterium tuberculosis* MPT51 (FbpC1) defines a new family of non-catalytic α/β hydrolases. J Mol Biol. 335:519–530.

Winau F, Weber S, Sad S, de Diego J, Hoops SL, Breiden B, Sandhoff K, Brinkmann V, Kaufmann SHE, Schaible UE (2006) Apoptotic vesicles crossprime CD8 T cells and protect against tuberculosis. Immunity 24:105–117.

Wolfe LM, Mahaffey SB, Kruh NA, Dobos KM (2010) Proteomic definition of the cell wall of *Mycobacterium tuberculosis*. J Proteome Res. 9:5816–5826.

World Health Organization (2015a) Global Tuberculosis Report 2015.

World Health Organization (2015b) Media centre. Tuberculosis, Fact sheet No. 104.

World Health Organization (2015c) Summary of WHO position papers – recommendations for routine immunization.

World Health Organization (2004) Weekly epidemiological record: relevé épidémiologique hebdomadaire.

Wright S, Eaton ON (1929) The persistence of differentiation among inbred families of guinea pigs. Technical Bulletin No. 103, United States Department of Agriculture, Washington, D.C.

Yang H, Kruh-Garcia NA, Dobos KM (2012) Purified protein derivatives of tuberculin – past, present, and future. FEMS Immunol Med Microbiol. 66:273–280.

Yang RB, Mark MR, Gray A, Huang A, Xie MH, Zhang M, Goddard A, Wood WI, Gurney AL, Godowski PJ (1998) Toll-like receptor 2 mediates lipopolysaccharide-induced cellular signalling. Nature 395:284–288.

Yang X-Y, Chen Q-F, Cui X-H, Yu Y, Li Y-P (2010) *Mycobacterium vaccae* vaccine to prevent tuberculosis in high risk people: A meta-analysis. J Infect 60:320–330.

Yeremeev VV, Stewart GR, Neyrolles O, Skrabal K, Avdienko VG, Apt AS, Young DB (2000) Deletion of the 19 kDa antigen does not alter the protective efficacy of BCG. Tuber Lung Dis. 80:243–247.

Yoneda M, Fukui Y (1965) Isolation, purification, and characterization of extracellular antigens of *Mycobacterium tuberculosis*. Am Rev Respir Dis. 92:9–18.

Yuan Y, Zhu Y, Crane DD, Barry CE (1998) The effect of oxygenated mycolic acid composition on cell wall function and macrophage growth in *Mycobacterium tuberculosis*. Mol Microbiol 29:1449–1458.

Zeya HI, Spitznagel JK (1966) Cationic proteins of polymorphonuclear leukocyte lysosomes. I. Resolution of antibacterial and enzymatic activities. J Bacteriol. 91:750–754.

Zhang H, Ouyang H, Wang D, Shi J, Ouyang C, Chen H, Xiao S, Fang L (2015) *Mycobacterium tuberculosis* Rv2185c contributes to nuclear factor-κB activation. Mol Immunol. 66:147–153.

Zhang SM, Wang YX, Meng LQ, Li J, Zhao XY, Cao X, Chen XL, Wang AX, Li JF (2012) Isolation and characterization of antifungal lipopeptides produced by endophytic *Bacillus amyloliquefaciens* TF28. African Journal of Microbiology Research 6:1747–1755.

Zhu X, Venkataprasad N, Ivanyi J, Vordermeier HM (1997) Vaccination with recombinant vaccinia viruses protects mice against *Mycobacterium tuberculosis* infection. Immunology 92:6–9.

Zopf W (1883) Die Spaltpilze. Trewendt.

Zuber B, Chami M, Houssin C, Dubochet J, Griffiths G, Daffé M (2008) Direct visualization of the outer membrane of mycobacteria and corynebacteria in their native state. J Bacteriol. 190:5672–5680.

Zueckert WR (2014) Secretion of bacterial lipoproteins: through the cytoplasmic membrane, the periplasm and beyond. BBA – Molecular Cell Research 1843:1509–1516.

9 Annex

Annex 1 Defined proteins in Purified Protein Derivatives

Table A1.1 Defined proteins in *M. tuberculosis* PPD-S2 and -CT86.

Only proteins which have previously been described as T cell antigens (according to Cho *et al.* (2012)) are displayed. The fifth column indicates whether they have additionally been found in UK or Brazilian *M. bovis* PPD. Data originate from Borsuk *et al.* (2009), Cho *et al.* (2012), and Prasad *et al.* (2013). Most abundant protein representatives in standard *M. tuberculosis* PPD-S2 are indicated in red. The asterisks mark genes which are deleted in the vaccine strain *M. bovis* BCG.

Protein Accession Number	Synonym	MW [kDa]	Functional classification	Present in UK or BR *M. bovis* PPD?	Present in *M. tuberculosis* PPD-S2 and -CT68?
Rv0009	PpiA	19.2	information pathways	–	Yes
Rv0054	Ssb	17.3	information pathways	Yes	Yes
Rv0440	GroEL2	56.7	virulence, detoxification, adaptation	Yes	Yes
Rv0475	HbhA	21.5	cell wall and cell processes	Yes	Yes
Rv0577	TB27.3	27.3	conserved hypotheticals	Yes	Yes
Rv0667	RpoB	129.2	information pathways	–	Yes
Rv0685	Tuf	43.6	information pathways	Yes	Yes
Rv0733	Adk	20.1	intermediary metabolism and respiration	Yes	Yes
Rv0831c	Hypothetical protein	30.2	conserved hypotheticals	Yes	Yes
Rv0952	SucD	31.2	intermediary metabolism and respiration	–	Yes
Rv1211	Hypothetical protein	7.8	conserved hypotheticals	–	Yes
Rv1352	Hypothetical protein	12.8	conserved hypotheticals	Yes	Yes

The table continues on the next page.

Table A1.1 (continued)

Protein Accession Number	Synonym	MW [kDa]	Functional classification	Present in UK or BR *M. bovis* PPD?	Present in *M. tuberculosis* PPD-S2 and -CT68?
Rv1626	Probable transcriptional regulator	22.7	regulatory proteins	–	Yes
Rv1827	CFP17	17.2	conserved hypotheticals	Yes	Yes
Rv1908c	KatG	80.6	virulence, detoxification, adaptation	–	Yes
Rv1926c	Mpt63	16.5	cell wall and cell processes	Yes	Yes
Rv1984c	CFP21	21.8	cell wall and cell processes	Yes	Yes
Rv2031c	HspX	16.2	virulence, detoxification, adaptation	Yes	Yes
Rv2220	GlnA1	53.5	intermediary metabolism and respiration	Yes	Yes
Rv2346c	EsxO	9.9	cell wall and cell processes	–	Yes
Rv2376c	CFP2	16.6	cell wall and cell processes	Yes	Yes
Rv2461c	ClpP	21.7	intermediary metabolism and respiration	–	Yes
Rv2626c	Hypothetical protein	15.5	conserved hypotheticals	Yes	Yes
Rv2780	Ald	38.7	intermediary metabolism and respiration	–	Yes
Rv2878c	Mpt53	18.4	cell wall and cell processes	Yes	Yes
Rv2945c	LppX	24.1	cell wall and cell processes	Yes	Yes
Rv3029c	FixA	28.1	intermediary metabolism and respiration	–	Yes
Rv3763	LpqH	15.1	cell wall and cell processes	–	Yes

The table continues on the next page.

Table A1.1 (continued)

Protein Accession Number	Synonym	MW [kDa]	Functional classification	Present in UK or BR *M. bovis* PPD?	Present in *M. tuberculosis* PPD-S2 and -CT68?
Rv3841	BfrB	20.4	intermediary metabolism and respiration	Yes	Yes
Rv3874 *	CFP10	10.8	cell wall and cell processes	Yes	Yes
Rv3875 *	ESAT-6	9.9	cell wall and cell processes	Yes	Yes

Annex 2 Multiple cardiocenteses in guinea pigs

In the context of this project, the competent authority (Regierungspraesidium Darmstadt) prompted us to assess whether multiple cardiocenteses cause distress to guinea pigs.

Study design

Twenty-five guinea pigs were involved in this pilot study. Five guinea pigs were sensitized with iAN5 and 15 with BCG. The 5 guinea pigs of the control group did not receive sensitization, neither cardiocenteses, only anesthesias. The animals, the sensitization procedures and the cardiocentesis are described in sections 3.5.1, 3.6.2, and 3.6.3. Blood samples were collected 6 times in 4-week intervals. A clinical examination and scoring of each animal was performed by a veterinarian before anesthesia at days of cardiocentesis and one day as well as one week after cardiocentesis. The scoring categories have been approved by the competent authority (Regierungspraesidium Darmstadt) and were investigated in the following order:

	Score
Appearance:	
– Smooth and shiny fur; grooming; shining eyes	0
– Dull coat; reduced or restricted grooming	1
– Partially shaggy, slightly ruffled coat; eye or nasal discharge; sunken eyes; clotted orifices	2
– Completely shaggy, dull coat; abnormal body position; bent back; closed eyes; cyanosis	3
Behavior:	
– Attentive; active; social interactions; normal movement; curious	0
– Reduced reactions; reduced movement; reduced or excessive activity	1
– Gathering and partial isolation from the group; reduced movement; pain while walking	2
– Apathetic; no reaction or aggression while handling; movement severely restricted; isolation; shuffling gait	3
Respiration:	
– Even, slow and regular	0
– Slightly deeper respiration	1
– Clearly deeper respiration	2
– Cyanotic mucosa; gasping	3
Auscultation of the heart:	
– Even, detached heart sounds	0
– Slight heart murmur	1
– Arrhythmic heart beats; clear heart murmur	2
– Abnormal frequency; strong heart murmur	3
Body weight:	
– Slightly increasing/constant	0
– Decrease since the beginning of the experiment: < 10 %	1
– Decrease since the beginning of the experiment: > 10 %, but < 20 %	2
– Decrease since the beginning of the experiment: ≥ 20 %	3

If clinical signs were determined to fall between two score values, they were classified as 0.5.

For each day and for each animal, total scores were calculated by addition of the single scores. The **total scores** could range from 0 to 15 with **0 – 2** = “no harm, normal”, **3 – 4** = “minor burden”, **5 – 7** = “moderate burden, requiring additional support, e.g., fluids, pain relief medication, and an increased control measurement frequency of 4 – 7 follow-up examinations in ≤ 24 hours”, **> 8** = “high burden, implicating direct termination of the trial for the individual animal by euthanasia”. A score of 3 for a single parameter would have directly terminated the trial for this animal as well.

One week after the 6th cardiocentesis and after clinical examination, all guinea pigs were anesthetized and sacrificed with CO_2. Directly after euthanasia, a necropsy was performed. Particular attention was paid to the thorax and the heart as well as signs of circulation insufficiency.

Heart samples of each guinea pig and in two cases kidney samples were further examined in histology. Therefore, samples of each animal with special regard to the cardiac apex and the valves were stained with Hematoxylin-Eosin. In suspicious cases, additional slides were stained with Trichrome-Masson for detection of fibrinous areas. The stainings were kindly performed by Marion Wingerter, PEI. Histological slides were examined by light microscopy.

Results

General tolerance and risk: Six cardiocenteses per animal with 20 guinea pigs involved in the test group were planned. During the course of the project, two guinea pigs died during anesthesia. #4 died after the third cardiocentesis without evidence for direct impact of the cardiocentesis in the necropsy. The putative cause of death was intolerance to the anesthesia. #19 died after the fifth cardiocentesis. The necropsy revealed an iatrogenic cardiac tamponade. Together with the fact that 18 of 20 test animals survived all 6 cardiocenteses, this implicated a total death risk of 10 % for each animal during the 6-month procedure. All 5 control animals survived the 6 anesthesias.

Clinical examination: The change in body weight revealed no significant differences between the test and the control group. In both groups there was a slight decrease in body weight one day after anesthesia. This decrease was always less than 10 % of the initial body weight (body weight score 0). In all cases the decrease could be reestablished and even exceeded within one week. At the beginning of the study, the average weight within the test group was 720 g and within the control group 780 g. At the end of the study, the average weight within the test group was 1003 g and within the control group 957 g (**Figure A2.1**).

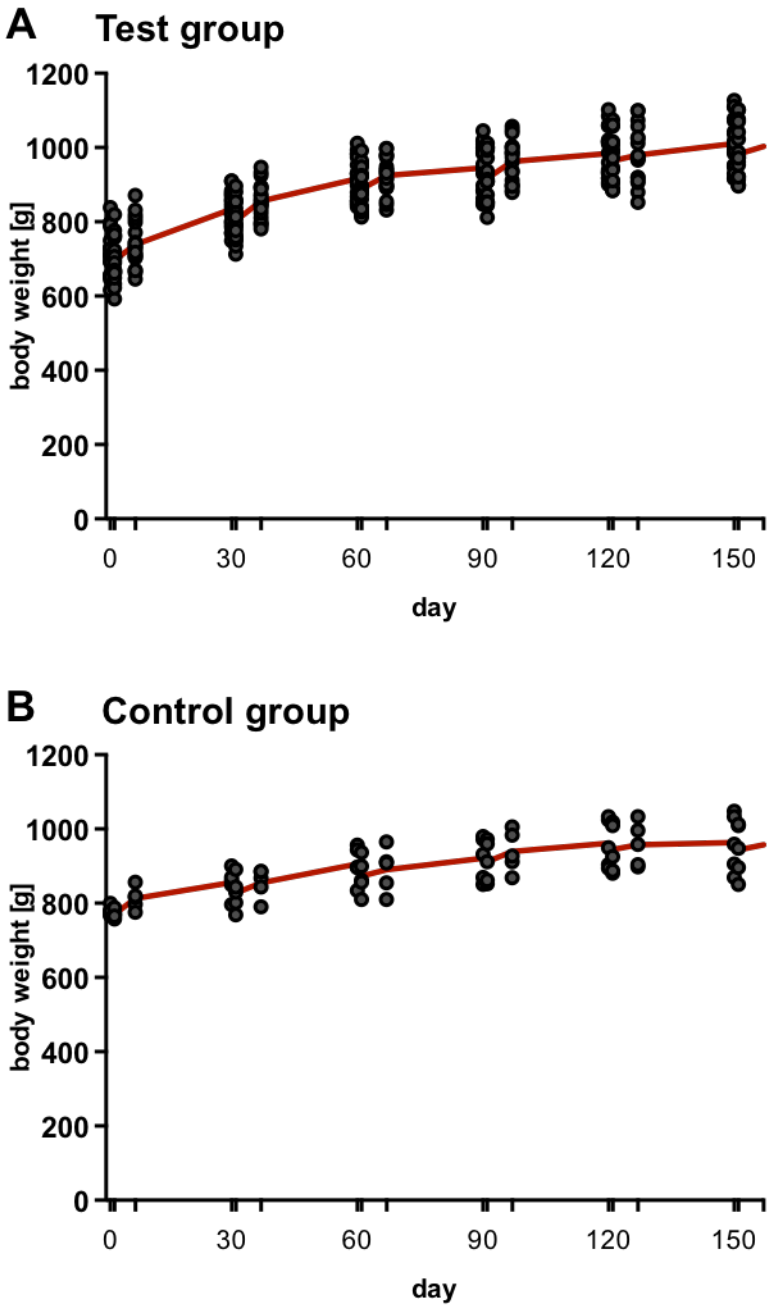

Figure A2.1 Change in body weight.

The x-axis displays the time with indication of the examination days x, x + 1, x + 7. The y-axis displays the body weight in grams. Each dot represents the weight of one guinea pig at the indicated day. The red line indicates the arithmetic mean over all animals. **A.** Test group; **B.** Control group.

By auscultation of the heart, 5 of 20 guinea pigs were diagnosed with a temporary, slight heart murmur (auscultation score 0.5 or 1) (**Table A2.1**). A clear heart murmur (auscultation score 2) was observed in guinea pig #10 for the first time before the 4th cardiocentesis. In no case was there coinciding cardio-respiratory symptoms such as circulation depression, arrhythmia, reduced capillary refill, enhanced respiration or reduced behavior and the affected animals tolerated the anesthesias as well as the non-affected ones. All guinea pigs

showing heart murmurs at any time point survived until euthanasia. However, none of the 5 control animals had heart murmurs.

Table A2.1 Auscultation scores of the test group.

Day	Auscultation score																			
	Guinea pig #																			
	1	2	3	4	5	6	7	8	9	10	11	12	13	14	15	16	17	18	19	20
0	0	0	0	0	0	0	0	0	0	0	0	0	0	0	0	0	0	0	0	0
1	0	0	0	0	0	0	0	0	0	0	0	1	0		0	0	1	0	0	0
7	0	0	0	0	0	0	0	0	0	0	0	1	0	0	0	0	1	0	0	0
30	0	0	0	0	0	0	0	0	0	0	0	0	0	0	0	0	1	0	0	0
31	0	0	0	0	0	0	0	0	0	0	0	0.5	0	0	0	0	1	0	0	0
37	0	0	0	0	0	0	0	0	0	0	0	0.5	0	0	0	0	1	0	0	0
60	0	0	0	0	0	0	0	0	0	0	0	0.5	0	0	0	0	1	0	0	0
61	0	0	0		0	0	0	0	0	0	0	0.5	0	0	0	0	1	0	0	0
67	0	0	0		0	0	0	0	0	0	0	0	0	0	0	0	0.5	0	0	0
90	0	0	0		0	0	0	0	0	2	0	0	0	0	0.5	0	1	0	0	0
91	0	0	0		0	0	0	0	0	2	0	0	0	0	1	0	1	0	0	0
97	0	0	0		0	0	0	0	0	2	0	0	0	0	0.5	0	1	0	0	0
120	0	0	0		0	0	0	0	0	1	0	0	0	0	0.5	0	1	0	0	0
121	0	0	0		0	0	0	0	0	1	0	0	0	0	0.5	0	1	0		0
127	0	0	0		0	0	0	0	0	1	0	0	0	0	1	0	1	0		1
150	0	0	0		0	0	0	0	0	1	0	0	0	0	0	0	1	0		0
151	0	0	0		0	0	0	0	0	1	0	0	0	0	0.5	0	1	0		0
157	0	0	0		0	0	0	0	0	1	0	0	0	0	1	0	1	0		0

No differences in the appearance between test and control group could be observed. Two guinea pigs in the test group showed low-grade apathy once at independent time points (behavior score 1), one at day 61 and one at day 97. Two other guinea pigs showed low-grade increased respiration frequency once at independent time points (respiration score 1), one at day 61 and the other one at day 67.

All single parameter scores were added for each guinea pig at each time point to determine daily total scores. The overall analysis of these total scores of the test group demonstrated that at no time point was a total score higher than 2 of 15 achieved (**Figure A2.2**). The total scores of the control group were constantly 0.

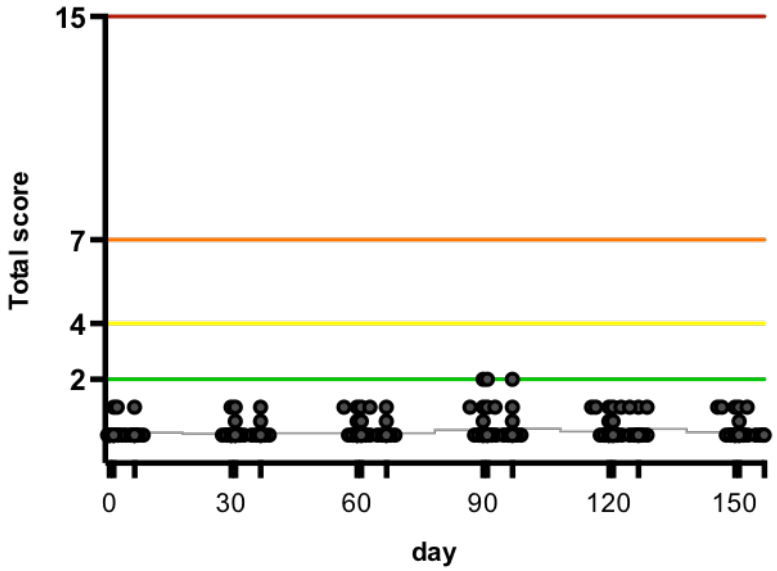

Figure A2.2 Total scores of the test group.

The x-axis displays the time with indication of the examination days x, x + 1, x + 7. The y-axis represents the range of the total scores with its classification 0 – 2 = normal, 3 – 4 = minor burden, 5 – 7 = moderate burden, and > 8 = high burden. The total score is the addition of the single scores in appearance, behavior, respiration, auscultation and body weight with a range of 0 – 3 in each category. Each dot represents the total score of one animal on the indicated examination day.

Necropsy: One week after the last cardiocentesis, a necropsy with special regard to alterations in the thorax and especially the heart was performed after euthanasia by CO_2-inhalation during Ketamin-Xylazin-anesthesia. Only minor findings were observed. In some animals there was a small, brownish spot the size of a pinhead at the cardiac apex which could be a hematoma from the last cardiocentesis one week before. However, it could be demonstrated in the sliced samples that this spot did not reach into the muscle. There was no further pathological evidence for inflammation, scars or valve defects, which could have been expected after multiple cardiocenteses. The epicard was always shiny without detachment. All findings are summarized in **Table A2.2**.

Table A2.2 Necropsy results.

Necropsy findings	Number of affected test animals (n = 18)	Number of affected control animals (n = 5)
Small hematoma in cardiac apex; if examined, no intramuscular traction	10	0
Adiposity	9	5
Slightly round heart	0	1
Low-grade puckered kidney surface, low-grade smaller kidney, capsule easy to peel off	1	0

Histopathology: In some guinea pigs HE staining of the heart muscle revealed low-grade, focal infiltration of the myocard with lymphocytes or rodent-specific pseudoeosinophilic granulocytes that could in few cases be localized in the valves area. Subepicardial infiltration with granulocytes and lymphocytes was present in one control animal. A multifocal, but local, and low-grade fibrosis of the heart muscle that was confirmed by Trichrome-Masson-staining was found in one guinea pig of the test group. In no examined case was there evidence for stitch channels with lymphocyte infiltration or fibrosis. All histological findings are summarized in **Table A2.3.**

Table A2.3 Histopathology results.

Histological findings	Number of affected test animals (n = 18)	Number of affected control animals (n = 5)
Low-grade diffuse myocarditis with a low generalized infiltration of the myocard with granulocytes	1	0
Low-grade localized infiltration of the myocard with pseudoeosinophilic granulocytes and lymphocytes, not associated with the cardiac apex	2	0
Low-grade localized fatty atrophy in the myocard, not associated with the cardiac apex	2	1
Small subepicardial infiltration with pseudoeosinophilic granulocytes and lymphocytes	0	1
Middle-grade localized fatty atrophy at the cardiac apex and around the valves and low- to middle-grade myocarditis with multifocal infiltrations with lymphocytes and pseudoeosinophilic granulocytes in the valves area, subacute to chronically	1	0
Low-grade localized fibroid infiltration of the myocard (Trichrome-Masson-staining), low-grade fatty atrophy and low-grade multifocal infiltration with lymphocytes in the valves area	1	0
Low-grade sclerosis of the kidney, chronically	2	0

Concluding remarks

Cardiocentesis is a suitable technique to obtain the amount of guinea pig blood which was required for our studies. Guidelines for the use of laboratory animals do not recommend to perform non-terminal cardiocenteses. However, there is not much information on their impact on the animals. The systematically achieved results of this pilot study confirmed that there is a certain risk that cardiocenteses may lead to cardiac tamponade, but the impact of the repeated sampling remains unclear. However, the guinea pigs showed no weight loss, had a healthy appearance and exhibited a normal behavior. While we were unable to attribute significant distress to repeated cardiocenteses, it substantially helped to reduce the number of animals and was a prerequisite to do time-course experiments.

Annex 3 Media, buffers, chemicals, consumables and other material, antibodies

Table A3.1 List of media.

Name	Ingredients or supplier
BBL™ Herrold's Egg Yolk Agar Slant with mycobactin J and ANV (amphotericin B, nalidixic acid, vanco-mycin)	Co. Becton, Dickinson and Company, Sparks, MD, USA
DMEM with ultraglutamine, 4.5 g/l glucose, 500 mL	Co. Lonza Biosciences, Amboise, France
Middlebrook 7H11 agar modified with mycobactin J	0.9 l/l (v/v) ultrapure water; 21 g/l (w/v) Middlebrook 7H11 mycobacteria agar (Difco); 5 ml/l (v/v) glycerin (Merck); 2 mg/l (w/v) mycobactin J (Allied Monitor); 100 ml/l (v/v) Middlebrook OADC enrichment
Middlebrook 7H9 medium with glycerin	0.9 l/l (v/v) ultrapure water; 4.7 g/l (w/v) Middlebrook 7H9 broth (Difco); 2 ml/l (v/v) glycerin; 100 ml/l (v/v) Middlebrook OADC enrichment
Modified Watson-Reid medium with ammonium citrate, mycobactin J and pyruvate, pH 6.0	Ultrapure water; 5 g/l (w/v) L-asparagine monohydrate (MW 150.13); 10 g/l (w/v) d-glucose (H_2O-free, MW 180.16); 4.1 g/l (w/v) sodium pyruvate (MW 110.04); 60 g/l (w/v) glycerin (H_2O-free, MW 92.09); 2 g/l (w/v) di-ammonium-hydrogen-citrate (MW 226.18); 0.075 g/l (w/v) ammonium-ferric (III)-citrate (CAS 1185-57-5); 2 g/l (w/v) KH_2PO_4 (MW 136.086); 2 g/l (w/v) NaCl (MW 58.44); 1 g/l (w/v) $MgSO_4$ x $7H_2O$ (MW 246.47); 0.01 g/l (w/v) $ZnSO_4$ x $7H_2O$ (MW 287.56); 0.02 g/l (w/v) $CaCl_2$ x $2H_2O$ (MW 147.01); 0.002 g/l (w/v) $CoCl_2$ x $6H_2O$ (MW 237.93); 2 mg/l (w/v) mycobactin J; pH 6.0 with 1 N NaOH or 1 N HCl
SF-IMDM (Serum-free-Iscove's Modified Dulbecco's Medium)	Ultrapure water; 1 packaging unit / 10 L medium 1 x IMDM powder Biochrom TX 046-10; 3.024 g/l (w/v) $NaHCO_3$ (Merck); 10 ml/l (v/v) penicillin-streptomycin (Gibco); 10 ml/l (v/v) MEM non-essential amino acid (100x, Gibco); 1 ml/l (v/v) insulin from pork (acid solution, 5 mg/ml in PBS); 0.5 ml/l (v/v) 2-mercapto-ethanol (0.1 M, Fluka); 3 ml/l (v/v) Primatone RL (10 % w/v, Quest); 20 ml/l (v/v) glutamine solution (0.2 M, Sigma); pH 7.0 with 1 N NaOH

Table A3.2 List of buffers.

Name	Ingredients
10 x Laemmli buffer, pH 8.3	Ultrapure water; 30 g/l (w/v) Tris; 150 g/l (w/v) glycerin; 10 g/l (w/v) SDS; pH 8.3
2 x non-reducing loading buffer	170 ml/l (v/v) upper buffer; 200 ml/l (v/v) glycerin; 450 ml/l (v/v) 10 % SDS; 100 ml/l (v/v) β-mercaptoethanol, 80 ml/l (v/v) bromophenol blue
4 x lower buffer	Ultrapure water; 1.5 M Tris/HCl; 0.4 % (w/v) SDS; pH 8.8
AEC buffer	10 ml substrate buffer; 600 µl AEC solution (1 AEC tablet dissolved in 3 ml DMF); 5 µl 30 % H_2O_2 immediately prior to use

The table continues on the next page.

Table A3.2 (continued)

Name	Ingredients
Anode solution 1	Ultrapure water; 0.3 M Tris/HCl; 20 % (v/v) methanol; pH 10.4
Anode solution 2	Ultrapure water; 0.025 M Tris/HCl; 20 % (v/v) methanol; pH 10.4
Blocking buffer	PBS + 0.0 % Tween 20; 2 % (w/v) skim milk powder
Cathode Solution	Ultrapure water; 0.04 M e-amino-n-capronic acid; 10 % (v/v) methanol; pH 7.6
Erythrolysis buffer	Ultrapure water, 8.29 g/l (w/v) NH_4Cl (0.15 M); 1 g/l (w/v) $KHCO_2$ (10 mm); 37 mg/l (w/v) EDTA (0.1 mM)
MACS buffer	PBS; 1 % (v/v) FCS; 2 nM EDTA
PBS (phosphate-buffered saline) without calcium and magnesium, pH 7.1	Ultrapure water; 8 g/l (w/v) NaCl, 0.2 g/l (w/v) KCl, 0.2 g/l (w/v) KH_2PO_4; 1.15 g/l (w/v) Na_2HPO_4; pH 7.1 with HCl
PBS without calcium and magnesium, pH 7.1 + 0.05 % Tween 20	PBS; 0.5 ml/l (v/v) Tween 20
Sodium chloride 0.85 %	Ultrapure water; 8.5 g/l sodium chloride
Sodium citrate	Ultrapure water; 0.1 M trisodium-citrate-dihydrate (294.1 M/L)
Substrate buffer	Ultrapure water; 0.05 M sodium acetate, pH 5.0
TMB substrate	9 ml *aqua destillata*; 1 ml sodium acetate (1.1 M, pH 5.5); 167 µl TMB stock solution (1 ml ethanol; 6 mg (w/v) TMB); 2 µl 30 % H_2O_2
Upper buffer	Ultrapure water; 0.5 M Tris/HCl; 0.4 % (w/v) SDS; pH 6.8

Table A3.3 List of chemicals.

Name	Supplier
3-Amino-9-ethylcarbazole (AEC)	Sigma-Aldrich, St. Louis, MO, USA
3,3',5,5'-Tetramethylbenzidine (TMF)	Sigma-Aldrich, St. Louis, MO, USA
Acetonitrile C_2H_3N Chromasolv® Plus	Sigma-Aldrich, St. Louis, MO, USA
Acrylamide/Bis Solution (30 % w/v), 2.6 % C	Serva, Heidelberg, Germany
CFSE 50 mm in DMSO	Enzo Life Sciences (former Alexis biochemicals), Loerrach, Germany
Chloroform $CHCl_3$ Chromasolv® Plus	Sigma-Aldrich, St. Louis, MO, USA
Cyclohexane C_6H_{12} Chromasolv® Plus	Sigma-Aldrich, St. Louis, MO, USA
Dimethyl-Sulphoxide (DMSO) Hybri-Max®	Sigma-Aldrich, St. Louis, MO, USA
Ethanol 96%	Solvent and media supply unit, Paul-Ehrlich-Institut, Langen, Germany
Ethanol C_2H_6O Emsure®	Merck KGaA, Darmstadt, Germany
H_2SO_4, 1M	Merck KGaA, Darmstadt, Germany
Hydrochloric acid HCl Emsure® 32 %	Merck KGaA, Darmstadt, Germany
Hydrogen peroxide H_2O_2 Perhydrol® 30 %	Merck KGaA, Darmstadt, Germany

The table continues on the next page.

Table A3.3 (continued)

Name	Supplier
Methanol	Solvent and media supply unit, Paul-Ehrlich-Institut, Langen, Germany
Methanol CH_4O Emplura®	Merck KGaA, Darmstadt, Germany
N,N-Dimethylformamide (DMF)	Sigma-Aldrich, St. Louis, MO, USA
N,N,N';N'-Tetramethyl-ethylenediamine (TEMED)	Serva, Heidelberg, Germany
QUANTI-Blue™	InvivoGen, Toulouse, France
Roti®-Blue	Carl Roth GmbH + Co. KG, Karlsruhe, Germany
Sodium hydroxide NaOH Titripur®	Merck KGaA, Darmstadt, Germany
Trifluoroacetic acid, 13N (TFA)	Sigma-Aldrich, St. Louis, MO, USA
Trisodiumcitrate-dihydrate 0.1 M (294.1 M/L)	Carl Roth GmbH + Co. KG, Karlsruhe, Germany
Trypan Blue solution 0.4 %	Sigma-Aldrich, St. Louis, MO, USA
Ultrapure water	Solvent and media supply unit, Paul-Ehrlich-Institut, Langen, Germany

Table A3.4 List of consumables.

Name	Supplier
24-well microtiter plates Falcon® Multiwell™ Primaria™	Becton Dickinson, Franklin Lakes, NJ, USA
384-well microtiter plates Nunc Nunclon™ Delta Surface	Thermo Fisher Scientific Inc., Whaltham, MA, USA
500 ml Nalgene® Rapid-Flow Bottle Top Filter 0.2 µl SFCA membrane, 75 mm diameter, 45 mm neck	Thermo Electron LED GmBH, Eindhout, Belgium
6-well microtiter plates collagen I cellware Biocoat® Cell Environments™	Becton Dickinson, Bedford, MA, USA
96-well deep well plates	Brand, Wertheim, Germany
96-well microtiter plate flat bottom cert. Maxisorp Nunc-Immuno plate	Thermo Fisher Scientific Inc., Whaltham, MA, USA
96-well microtiter plates polystyrene flat bottom Nunc Microwell	Thermo Fisher Scientific, Roskilde, Denmark
96-well microtiter plates round bottom Nunclon™ Delta Surface	Thermo Fisher Scientific, Roskilde, Denmark
Brown glass tubes, Kurzgewindeflaschen ND9, 1.5 ml, 32 x 11.6 mm, Braunglas, weite Öffnung, Beschr. Feld, VE 100	Thermo Fisher Scientific, Division Fisherbrand, Schwerte, Germany
Bulk packing material for preparative HPLC columns, SepTech™ C18 reversed phase media: ST150 10-C18 reversed phase bulk media, end capped; 150 Å; 10 µm; 100 g	Agilent Technologies, Inc., Santa Clara, CA, USA

The table continues on the next page.

Table A3.4 (continued)

Name	Supplier
C4 reversed phase silica column Interchim, Puriflash PT 15 UM 6G Flash Colu	Interchim, Montluçon, France
Cellstar® Polypropylene tubes, 15 ml, 50 ml	Greiner Bio-one, Frickenhausen, Germany
Cover slides 24 x 60 mm	Menzel GmbH & Co KG, Braunschweig, Germany
Cryogenic vials Cryoware™ 4.5 ml	Nalgene® Nunc International, Rochester, NY, USA
Cryogenic Vials Nalgene® Cryoware 1.8 ml	Thermo Fisher Scientific, Rochester, NY, USA
Diagnostic slides	Menzel GmbH & Co KG, Braunschweig, Germany
FACS-Tubes, 5 ml	Greiner Bio-one, Frickenhausen, Germany
Gel Blotting Papers Whatman®	GE Healthcare Life Sciences, Freiburg, Germany
Gloves Manufix® Sensitive latex M	B. Braun, Melsungen, Germany
Gloves TouchNTuff® nitrile M	Ansell Healthcare LLC, Iselin, NJ, USA
MACS® Separation Columns MS	Miltenyi Biotec GmbH, Bergisch Gladbach, Germany
Maxisorp Nunc-Immuno plate Flat bottomed 96-well	Thermo Fisher Scientific, Roskilde, Denmark
Needles 100 Sterican 21 G, 26 G	B. Braun, Melsungen, Germany
Needles Neolus 22G	Terumo, Tokyo, Japan
Nitrocellulose Whatman™ Protran BA85	GE Healthcare Life Sciences, Freiburg, Germany
Parafilm® M American National Can™	Bemis, Oshkosh, WI, USA
Pasteur pipets Volac 230 mm	Poulten & Graf GmbH, Wertheim, Germany
PCR-Tubes Rotilabo®-PCR-Reaktionsgefaesse 0,2 ml Standard, PP	Carl Roth GmbH + Co. KG, Karlsruhe, Germany
pH-Fix test strips 0-14	Carl Roth GmbH + Co. KG, Karlsruhe, Germany
Pipet tips ep T.I.P.S® Standard 0.5 – 20 µl, 2 – 200 µl, 50 – 1,000 µl, 500 – 2,500 µl	Eppendorf AG, Hamburg, Germany
Plastic pipets Cellstar® 2 ml, 10 ml, 25 ml	Greiner Bio-one, Frickenhausen, Germany
Reaction tubes 3810X 1.5 ml	Eppendorf AG, Hamburg, Germany
Reaction tubes safe-lock tubes 2 ml	Eppendorf AG, Hamburg, Germany
Scalpels, surgical, disposable	B. Braun, Aesculap Division, Melsungen, Germany
Serum tubes Vacuette®	Greiner Bio-one, Frickenhausen, Germany
Short threaded screw-cap (chloroform-proof)	Thermo Fisher Scientific, Division Fisherbrand, Schwerte, Germany
Silica gel in TLC plates L x W 5 cm x 10 cm, with fluorescent indicator 254 nm	Sigma-Aldrich (former Fluka Analytical), St. Gallen, Switzerland
Spectra Por dialysis membrane, MWCO 1,000, flat width 38mm, diameter 24 mm, vol/length 4.6 ml/cm, wet in 0.1 % sodium acid	Spectrum Laboratories, Inc., Rancho Dominguez, CA, USA
Sterile filter Minisart® 0.2 µm	Sartorius AG, Goettingen, Germany
Syringe Omnifix® Luer Solo 1 ml, 5 ml, 10 ml	B. Braun AG, Melsungen, Germany
Syringe stopper Luer top	Henry Schein®, Melville, NY,USA

The table continues on the next page.

Table A3.4 (continued)

Name	Supplier
Tissue Culture Roller Bottle Falcon®	Becton-Dickinson, Franklin Lakes, NJ, USA
vwr® disposable Pasteur Pipets, glass, short tip, 9´	vwr International, Radnor, PA, USA
White glass tubes with screw-caps	I.C.S., Lapeyrousse Fossat, France

Table A3.5 List of other material.

Name	Supplier
Bovine serum albumin (BSA), heat shock fraction, pH 7, ≥98 %	Sigma-Aldrich, St. Louis, MO, USA
EZ-Link® Sulfo-NHS-LC-Biotin	Thermo Fisher Scientific, Rochester, NY, USA
Fetal Bovine Serum, sterile filtered (FCS)	Sigma-Aldrich, St. Louis, MO, USA
Ficoll-Paque™ Plus, density 1.077	GE Healthcare, Uppsala, Sweden
gp IL-2 soup III.1 PEI 2012	Veterinary immunobiology group, Paul-Ehrlich-Institut, Langen, Germany
Guinea pig TNFα Standard 5 mg/ml	Kingfisher Biotech, Inc., Saint Paul, MN, USA
Invitrogen SilverQuest™ Silver Staining Kit	Life Technologies GmbH, Darmstadt, Germany
Ketamin 10 %	Wirtschaftsgenossenschaft deutscher Tieraerzte (WDT) eG, Garbsen, Germany
Light mineral oil, paraffin	Merck KGaA, Darmstadt, Germany
Mycobactin J	Allied Monitor, Inc., Fayette, MO, USA
OADC BBL™ Middlebrook Enrichment	Becton Dickinson, Franklin Lakes, NJ, USA
PageRuler™ Plus	Thermo Fisher Scientific, Rochester, NY, USA
Pam_3CSK4	Cayla-InvivoGen, Toulouse, France
Penicillin-streptomycin solution (5,000:5,000)	Lonza Biosciences, Amboise, France
PHA (Phytohaemagglutinin)	Thermo Fisher Scientific, Division Oxoid Limited, Hampshire, UK
Proteinase K from *Engyodontium album* (formerly *Tritirachium album*)	Sigma-Aldrich, St. Louis, MO, USA
Pronase E von *Streptomyces griseus*	Sigma-Aldrich, St. Louis, MO, USA
Recombinant *M. tuberculosis* Antigen 85A	Lionex GmbH, Braunschweig, Germany
Rompun 2 % (xylazine hydrochloride)	Bayer Healthcare AG, Animal Health Division, Leverkusen, Germany
Skin disinfectant Safe Sept	Henry Schein Medical GmbH, Berlin, Germany
Streptavidin MicroBeads	Miltenyi Biotec GmbH, Bergisch Gladbach, Germany
Thilo-Tears® Gel	Alcon Pharma GmbH, Freiburg im Breisgau, Germany

Table A3.6 List of antibodies and streptavidin.

Name	Supplier
Anti-guinea pig $CD8^{biotin}$ B607	Kindly provided by Dr. Hubert Schaefer, Robert-Koch-Institut Berlin, Germany Purified at veterinary immunobiology group, Paul-Ehrlich-Institut, Langen, Germany
Capture antibody anti-guinea pig TNFα, PAb PB0446GP-100	Kingfisher Biotech, Inc., Saint Paul, MN, USA
Detection antibody anti-guinea pig^{biotin} TNFα, PAb PBB0452GP-050	Kingfisher Biotech, Inc., Saint Paul, MN, USA
Isotype control mouse IgG1 [MOPC-21] (Biotin) kappa (ab18434)	Abcam, Cambridge, MA, USA
Isotype control-APC, mouse IgG1 kappa	BD, Pharmingen, Germany
Isotype control-PE, mouse IgG1 kappa (MOPC-21)	BD, Pharmingen, Germany
Murine anti-guinea pig $CD4^{PE}$, MCA749PE	Bio-Rad AbD Serotec GmbH, Puchheim, Germany
Murine anti-guinea pig T $cell^{APC}$, MCA751APC	Bio-Rad AbD Serotec GmbH, Puchheim, Germany
$Streptavidin^{HRP}$ (horseradish peroxidase conjugated)	Dianova GmbH, Hamburg, Germany
$Streptavidin^{PE\text{-}Cy5.5}$ SA1018	Life Technologies GmbH, Darmstadt, Germany

Annex 4 Instruments and devices

Table A4.1 List of instruments.

Name	Supplier
Beaker glasses Duran	Schott AG, Mainz, Germany
Cell counter Neubauer Improved, 0.1 mm depth, 0.0025 mm^2	Laboroptik, Friedrichsdorf, Germany
Erlenmeyer flasks	Schott AG, Mainz, Germany
Forceps	B. Braun, Aesculap Division, Melsungen, Germany
Glass bottles with blue cap Duran	Schott AG, Mainz, Germany
Glass pipets 1ml, 5 ml, 10 ml, 20 ml, 25 ml	Brand GmbH + Co KG, Wertheim, Germany
Glass tubes round bottom, red cap Schott GL25 and GL45	Schott AG, Mainz, Germany
Glass tubes with screw-cap 30 ml	Gerresheimer, Division Kimble Chase Life Science and Research Products LLC, Vineland, NJ, USA
Plastic tubes with screw-cap 30 ml Nalgene®	Thermo Fisher Scientific, Rochester, NY, USA
Plastic tubes with screw-cap 300 ml Nalgene®	Thermo Fisher Scientific, Rochester, NY, USA
Spray diffusers, brown glass	Carl Roth GmbH + Co. KG, Karlsruhe, Germany
Thermometer Geratherm® color	Geratherm Medical AG, Geschwenda, Germany

Table A4.2 List of mechanical devices.

Name	Supplier
-85 °C Ultra low freezer New Brunswick Scientific	Eppendorf AG, Hamburg, Germany
Bioblock heater	Fisher Scientific SAS, Illkirch, France
Biological Hood SterilGARD Hood Class II Type A/B3	Baker and Baker Ruskinn, Sanford, ME, USA
Blotting device Semi-Phor™	Hoefer Scientific Instruments, San Francisco, CA, USA
Centrifuge CR412	Thermo Fisher Scientific, Division Thermo Electron (former Jouan), Waltham, MA, USA
Centrifuge Cryofuge 8500	Heraeus Sepatech, Hanau, Germany
Centrifuge Varifuge RF	Heraeus Sepatech, Hanau, Germany
Chemical fume hood Model 3650	Labcaire Systems Ltd, Clevedon, UK
Circulator Bath RCB 500	Hoefer, Inc., Holliston, MA, USA
CO supply DruVa	GCE, Fulda, Germany
Diaphragm vacuum pump	Vacuumbrand GmbH + CO KG, Wertheim, Germany
Electrophoresis device Mini-Protean® Tetra Cell	BioRad, Hercules, CA, USA

The table continues on the next page.

Table A4.2 (continued)

Name	Supplier
Electrophoresis Low voltage power supply Model P25 T	Biometra GmbH, Goettingen, Germany
ELISA-Reader Sunrise™	Tecan Group Ltd., Maennedorf, Switzerland
FACS Accuri C6, Program: BD Accuri C6 Analysis	Becton Dickinson, Franklin Lakes, NJ, USA
FACS LSR II, Program: BD FACSDiva™ software	Becton Dickinson, Franklin Lakes, NJ, USA
FlowJo Single Cell Analysis Software with FlowJo Dongle	FlowJo, LLC, Ashland, OR, USA
Fluorescence microscope Axiovert 405M with AXIO Observer Z1 HXP 120 C	Carl Zeiss AG, Oberkochen, Germany
Fridges 4 °C and freezers –20 °C	Liebherr GmbH, Biberach an der Riss, Germany
Heto vacuum centrifuge	Oy Halton Group Ltd., Helsinki, Finland
High-speed centrifuge Avanti® J-26 XPI	Beckman Coulter™, Krefeld, Germany
HPLC system	Knauer Wissenschaftliche Geraete GmbH, Berlin, Germany
Ice machine	Co. Ziegra-Eismaschinen GmbH, Isernhagen, Germany
Incubator HERAcell 150 i	Thermo Fisher Scientific, Rochester, NY, USA
Incubator Typ B 6200	Heraeus Instruments, Hanau, Germany
Incubator Typ BB 6220	Heraeus Instruments, Hanau, Germany
Interchim Puriflash 430, Program: Interchim Soft V5.0f09	Interchim, Montluçon, France
Magnetic stirrer	Thermo Fisher Scientific, Division Fisherbrand, Schwerte, Germany
Magnetic stirrer and heater MR 3002	Heidolph Instruments GmbH & Co. KG, Schwabach, Germany
Microplate Spectrophotometer µQuant™	BioTek Instruments, Inc., Winooski, VT, USA
Microscope Axio Vision	Carl Zeiss AG, Oberkochen, Germany
Microscope Axiovert 405 M	Carl Zeiss AG, Oberkochen, Germany
Milli-Q® Gradient	Merck KGaA, Division Merck Millipore, Darmstadt, Germany
Mini Protean N™ gel electrophoresis chamber	BioRad, Hercules,CA, USA
Multichannel automatic pipet 20-300µl	Eppendorf AG, Hamburg, Germany
Multichannel automatic pipet 50-1200µl	Eppendorf AG, Hamburg, Germany
Multichannel pipet Research plus 10 – 100 µl	Eppendorf AG, Hamburg, Germany
NanoPhotometer	Implen, Inc., Westlake Village, CA, USA
NeoLab-Rotator 2-1175	NeoLab, Heidelberg, Germany
Photometer CLARIOstar	BMG Labtech GmbH, Ortenberg, Germany
Pipet boy accu-jet® pro	Brand GmbH + Co KG, Wertheim, Germany

The table continues on the next page.

Table A4.2 (continued)

Name	Supplier
Pipets Reference 0.5 – 10 µl, 10 – 100 µl, 100 – 1,000 µl, 500 – 2,500 µl	Eppendorf AG, Hamburg, Germany
Radiation Anlage Gamma-irradiation Cäsium-137	STS Steuerungstechnik – Strahlenschutz GmbH, Braunschweig, Germany
Rotary slide vacuum pumps type RE2 and MD40	Vacuumbrand GmbH + CO KG, Wertheim, Germany
Rotavap Laborota 4000 with heating bath	Heidolph Instruments GmbH & Co. KG, Schwabach, Germany
Rotavapor® and heating bath B-490	Buechi Labortechnik AG, Flawil, Switzerland
Scale	Ohaus, Parsippany, NJ, USA
Scanner CanoScan LiDE 200, Program: Windows-Scan	Canon Deutschland GmbH, Krefeld, Germany
Shaker Biometra® WT 12	Biometra GmbH, Goettingen, Germany
SpeedVac® Savant Plus SC110A	Thermo Fisher Scientific, Rochester, NY, USA
Table centrifuge Biofuge 13	Thermo Fisher Scientific, Rochester, NY, USA
Thermocycler vapo.protect	Eppendorf AG, Hamburg, Germany
Thermomixer 5437	Eppendorf AG, Hamburg, Germany
Ultracentrifuge OptimaTM L-80 XP	Beckman Coulter™, Krefeld, Germany
Ultrasonic probe	Bandelin electronic GmbH & Co. KG, Berlin, Germany
Ultrasound water bath Laboson 200	Bender & Hobein GmbH, Ismaning, Germany
UV-Chamber G-Box, Program: GeneSnap, version 7.08	SynGene, Cambridge, UK
Vacuum pump model Rv8	Edwards France SAS, Gennevilliers, France
Vacuum pump type Duo 1.5 A	Pfeiffer Vacuum GmbH, Asslar, Germany
Vortex bioblock scientific Heidolph top mix 94323	Heidolph Instruments GmbH & Co. KG, Schwabach, Germany
Vortex Reax 2000	Heidolph Instruments GmbH & Co. KG, Schwabach, Germany
Waterbath GFL 1083	GFL Gesellschaft fuer Labortechnik GmbH, Burgwedel, Germany

Annex 5 N-terminal amino acid sequences of *M. tuberculosis* lipoproteins

Table A5.1 N-terminal amino acid sequences of *M. tuberculosis* lipoproteins.

Sources: TB Database (http://genome.tbdb.org/annotation/ genome/tbdb/FeatureSearch.html) (Reddy *et al.* 2009; Galagan *et al.* 2010) and tubercuList (http://tuberculist.epfl.ch) (Lew *et al.* 2011).
The sequences of interest were kindly defined and provided by Dr. Max Bastian.
"**C**" indicates a classical pattern for the cleavage of the signal peptide from the lipoprotein. "C" indicates a non-classical pattern, while "C" marks an alternative N-terminus.

Lipoprotein			Synthetic peptide		
Protein Accession Number	**Name**	**Description**	**Name**	**AA positions**	**AA sequence**
Rv3666c	DppA	probable periplasmic dipeptide-binding lpp.	**DppA**	MP 1-15	**C**GGGVLSPDVV LVNG
Rv1677	DsbF	probable conserved lpp.	**DsbF**	MP 1-15	**C**GSQPKSQPAV APTG
Rv3044	FecB	probable FEIII-dicitrate binding periplasmic lpp.	**FecB**	MP 1-15	**C**GSDQPAHKAS QSMI
Rv0411c	GlnH	glutamine-binding protein	**GlnH**	MP 1-15	**C**GHSETLGVEAT PTL
Rv1911c	LppC	probable lpp.	**LppC**	MP 1-15	**C**GGGGGDSRET PPYV
Rv1899c	LppD	possible lpp.	**LppD**	MP 1-15	**C**AAHPALAGLTA GAR
Rv1881c	LppE	possible conserved lpp.	**LppE**	MP 1-15	**C**GQAQTVPRKA ARLT
Rv1921c	LppF	probable conserved lpp.	**LppF**	MP 1-15	**C**SAHQPPTPAS GCRQ
Rv3576	LppH	possible conserved lpp.	**LppH**	MP 1-15	**C**TNVVDGTAVA ADKS
RV2046	LppI	probable lpp.	**LppI**	MP 1-15	**C**SREVGGDVGQ SQTI
Rv2080	LppJ	lpp.	**LppJ**	MP 1-15	**C**ALVMHKPHSA GSSN
Rv2116	LppK	conserved lpp	**LppK**	MP 1-15	**C**SHPEFKRSSPP APS
Rv2138	LppL	probable conserved lpp.	**LppL**	MP 1-15	**C**SSNPLANFAPG YPP
Rv2171	LppM	probable conserved lpp.	**LppM**	MP 1-15	**C**LRVRASITISPD DL
Rv2270	LppN	probable lpp.	**LppN**	MP 1-15	**C**SSNGARGGIAS TNM

The table continues on the next page.

Table A5.1 (continued)

Lipoprotein			Synthetic peptide		
Protein Accession Number	**Name**	**Description**	**Name**	**AA positions**	**AA sequence**
Rv2290	LppO	probable conserved lpp.	**LppO**	MP 1-15	**C**SAHSGPGSPPSAPS
Rv2330c	LppP	probable lpp.	**LppP**	MP 1-15	**C**AWKPPTTRPSPPNT
Rv2403c	LppR	probable conserved lpp.	**LppR**	MP 1-15	**C**TTTTTGKAGLAPNA
Rv2518c	LppS	probable conserved lpp.	**LppS**	MP 1-15	**C**GSGRGPAPIKVIAD
Rv1799	LppT	probable lpp.	**LppT**	MP 1-15	CLAEGPPLGRNPQGA
Rv2784c	LppU	probable lpp.	**LppU**	MP 1-15	**C**SSATNVAELKVGDC
Rv2796c	LppV	probable conserved lpp.	**LppV**	MP 1-15	**C**GPSGHGTRAGEEGP
Rv2905	LppW	probable conserved alanine rich lpp.	**LppW**	MP 1-15	**C**EARVEAEAYSAADR
Rv2945c	LppX	probable conserved lpp.	**LppX-1**	SP 1-15	MNDGKRAVTSAVLVV
			LppX-2	SP 11-25	AVLVVLGACLALWLS
			LppX-3	MP 1-15	**C**SSPKPDAEEQGVPV
Rv2999	LppY	probable conserved lpp.	**LppY**	MP 1-15	**C**SSGSKGGAGSGHAG
Rv3006	LppZ	probable conserved lpp.	**LppZ**	MP 1-15	**C**ARFNDAQSQPFTTE
Rv3016	LpqA	probable lpp.	**LpqA**	MP 1-15	**C**TRVVGGTASATFGG
Rv3244c	LpqB	probable conserved lpp.	**LpqB**	MP 1-15	**C**ASVPSTSAPQAIGT
Rv3298c	LpqC	possible esterase lpp.	**LpqC**	MP 1-15	**C**GGDQLLARHASSVA
Rv3390	LpqD	probable conserved lpp.	**LpqD**	MP 1-15	**C**GGPTQPRSITLTFI
Rv3584	LpqE	possible conserved lpp.	**LpqE**	MP 1-15	**C**GAGQISQTANQKPA

The table continues on the next page.

Table A5.1 (continued)

Lipoprotein			Synthetic peptide		
Protein Accession Number	**Name**	**Description**	**Name**	**AA positions**	**AA sequence**
Rv3593	LpqF	probable conserved lpp.	**LpqF**	MP 1-15	**C**SSAPTPSANAA NHG
Rv3623	LpqG	probable conserved lpp.	**LpqG**	MP 1-15	**C**DSHNSGSLGA DPRQ
Rv3763	LpqH	19 kDa lpp. antigen precursor	**LpqH-1**	SP 1-15	MKRGLTVAVAG AAIL
			LpqH-2	SP 11-25	GAAILVAGLSG**C** SSN
			LpqH-3	MP 1-15	**C**SSNKSTTGSG ETTT
Rv0237	LpqI	probable conserved lpp.	**LpqI**	MP 1-15	**C**SHGGTPTGSS TTSG
Rv0344c	LpqJ	probable lpp.	**LpqJ**	MP 1-15	**C**NTTIDGRPVAS PGS
Rv0399c	LpqK	possible conserved lpp.	**LpqK**	MP 1-15	**C**APPRTGPASS PTNN
Rv0418	LpqL	probable Lpp. amino peptidase	**LpqL**	MP 1-15	**C**IRWSTQSRPVV NGP
Rv0419	LpqM	possible lpp. Peptidase	**LpqM**	MP 1-15	**C**LAAVVVIAGCT TVV
Rv0583c	LpqN	probable conserved lpp.	**LpqN**	MP 1-15	**C**SFNIKTDSAPT TSP
Rv0604	LpqO	probable conserved lpp.	**LpqO**	MP 1-15	**C**AGSDDKGEPD DGGD
Rv0671	LpqP	possible conserved lpp.	**LpqP**	MP 1-15	**C**SGGTRLAAGF GNGN
Rv0835	LpqQ	possible lpp.	**LpqQ**	MP 1-15	**C**SFQATSTQPST APP
Rv0838	LpqR	probable conserved lpp.	**LpqR**	MP 1-15	**C**ACDRVSAGRW SESP
Rv0847	LpqS	probable lpp.	**LpqS**	MP 1-15	**C**WLPQLHRHVA HPNH
Rv1016c	LpqT	probable conserved lpp.	**LpqT**	MP 1-15	**C**GPKSPDFQSIL STS
Rv1022	LpqU	probable conserved lpp.	**LpqU**	MP 1-15	**C**TWQLSLFITDG VPP
Rv1064c	LpqV	possible lpp.	**LpqV**	MP 1-15	**C**SRGGSSKAGR SSSV

The table continues on the next page.

Table A5.1 (continued)

Lipoprotein			Synthetic peptide		
Protein Accession Number	**Name**	**Description**	**Name**	**AA positions**	**AA sequence**
Rv1166	LpqW	probable conserved lpp.	**LpqW**	MP 1-15	**C**TVSPPPAPQSTDTP
Rv1228	LpqX	probable lpp.	**LpqX**	MP 1-15	**C**SRPGTEEPDCPTKI
Rv1235	LpqY	probable sugar-binding lpp.	**LpqY**	MP 1-15	**C**GADSQGLVVSFYTP
Rv1244	LpqZ	probable lpp.	**LpqZ**	MP 1-15	**C**SADTGDRHPELVVG
Rv1270c	LprA	possible lpp.	**LprA-1**	SP 1-15	MKHPPCSVVAAATAI
			LprA-2	SP 11-25	AATAILAVVLAIGG**C**
			LprA-3	MP 1-15	**C**STEGDAGKASDTAA
Rv1274	LprB	possible lpp.	**LprB**	MP 1-15	**C**SDSGDNKPGATIPS
Rv1275	LprC	possible lpp.	**LprC**	MP 1-15	**C**TKSISGTAVKAGGA
Rv1343c	LprD	probable conserved lpp.	**LprD**	MP 1-15	**C**GCLALGWWQWTRFQ
Rv1252c	LprE	probable lpp.	**LprE**	MP 1-15	**C**GSGDSTVAKTPEAT
Rv1368	LprF	probable conserved lpp.	**LprF-1**	SP 1-15	MNGLISQACGSHRPR
			LprF-2	SP 11-25	SHRPRRPSSLGAVAI
			LprF-3	MP 1-15	**C**GKKPTTASSPSPGS
Rv1411c	LprG	conserved lpp.	**LprG-1**	SP 1-15	MRTPRRHCRRIAVLA
			LprG-2	SP 11-25	IAVLAAVSIAATVVA
			LprG-3	MP 1-15	**C**SSGSKPSGGPLPDA
Rv1418	LprH	probable lpp.	**LprH**	MP 1-15	**C**TESVAGRAMRATDR
Rv1541c	LprI	possible lpp.	**LprI**	MP 1-15	**C**AANPPANTTSPTAG

The table continues on the next page.

Table A5.1 (continued)

Lipoprotein			Synthetic peptide		
Protein Accession Number	**Name**	**Description**	**Name**	**AA positions**	**AA sequence**
Rv1690	LprJ	probable lpp.	**LprJ**	MP 1-15	**C**AAPIQADMMG NAFL
Rv0173	LprK	mce-family protein, possible mce-family lpp. mce1E	**LprK**	MP 1-15	**C**GWRGISNVAIP GGP
Rv0593	LprL	mce-family protein, possible mce-family lpp. mce2E	**LprL**	MP 1-15	**C**GVSAGHRGSV FLLA
Rv1970	LprM	mce-family protein, possible mce-family lpp. mce3E	**LprM**	MP 1-15	**C**GWRGLNSLPL PGTQ
Rv3495c	LprN	mce-family protein, possible mce-family lpp. mce4E	**LprN**	MP 1-15	**C**QFGGLNSLPLP GTA
Rv0179c	LprO	possible lpp.	**LprO**	MP 1-15	**C**YAALAV**C**AALA CTT
Rv0962c	LprP	possible lpp.	**LprP**	MP 1-15	**C**IKPNTFDPYAN PGR
Rv1857	ModA	probable molybdate-binding lpp.	**ModA**	MP 1-15	CGSNSPASSPA GPTQ
Rv2873	MPT83	cell surface lpp.	**MPT83-1**	SP 1-15	MINVQAKPAAAA SLA
			MPT83-2	SP 11-25	AASLAAIAIAFLA G**C**
			MPT83-3	MP 1-15	**C**SSTKPVSQDTS PKP
Rv3759c	ProX	possible osmoprotectant (glycine betaine/carnitine/ choline/L-proline) binding lipoprotein	**ProX**	MP 1-15	**C**LVASCANADPL GSA
Rv0934	PstS1	periplasmic phosphate-binding lpp.	**PstS1-1**	SP 1-15	MKIRLHTLLAVLT AA
			PstS1-2	SP 11-25	VLTAAPLLLAAA G**C**G
			PstS1-3	MP 1-15	**C**GSKPPSGSPE TGAG

The table continues on the next page.

Table A5.1 (continued)

Lipoprotein			Synthetic peptide		
Protein Accession Number	**Name**	**Description**	**Name**	**AA positions**	**AA sequence**
Rv0932c	PstS2	periplasmic phosphate-binding lpp.	**PstS2-1**	SP 1-15	MKFARSGAAVSLLAA
			PstS2-2	SP 11-25	SLLAAGTLVLTA**C**GG
			PstS2-3	MP 1-15	**C**GGGTNSSSSGAGGT
Rv0928	PstS3	periplasmic phosphate-binding lpp.	**PstS3-1**	SP 1-15	MKLNRFGAAVGVLAA
			PstS3-2	SP 11-25	GVLAAGALVLSA**C**GN
			PstS3-3	MP 1-15	**C**GNDDNVTGGGATTG
Rv0265c	PitIp	probable periplasmic iron-transport lpp.	**PitIp**	MP 1-15	**C**SSPKPPPGTPGGAA
Rv2864c	PbIp	probable penicillin-binding lpp.	**PbIp**	MP 1-15	**C**TPRPQGPGPAAEKF
Rv2041c	SbIp	probable sugar-binding lpp.	**SbIp**	MP 1-15	CAADDDDALTFFFAA
Rv2833c	UgpB	probable Sn-glycerol-3-phosphate-binding lpp.	**UgpB**	MP 1-15	**C**AGMGGGGSVKSGSG

Abbreviations: AA = amino acid; **lpp.** = lipoprotein; **MP** = mature protein; **SP** = signal peptide

Annex 6 Numbers of Dunkin-Hartley guinea pigs used in the present study

Table A6.1 Numbers of Dunkin-Hartley guinea pigs used in the present study.

Sensitization strategy	Day of blood sample collection	Group name	Number of animals in the group = number of datasets obtained	Data displayed in the following figures of the thesis showing results of the *ex vivo* lymphocyte proliferation assay
BCG	d0	A	5	5 in Fig. 4.1B 5 in Fig. 4.4B
		B	5	3 in Fig. 4.7B
		C	5	4 in Fig. 4.7B
		D	10	–
		E	5	5 in Fig. 4.1B 5 in Fig. 4.4B 4 in Fig. 4.7B
	d30	A	5	5 in Fig. 4.1B 5 in Fig. 4.4B 5 in Fig. 4.5B and in Fig. 4.14B 5 in Fig. 4.11C 5 in Fig. 4.11D
		B	5	5 in Fig. 4.5B and in Fig. 4.14B 5 in Fig. 4.6B 3 in Fig. 4.7B 5 in Fig. 4.9
		C	5	3 in Fig. 4.5B and in Fig. 4.14B 3 in Fig. 4.6B 4 in Fig. 4.7B 3 in Fig. 4.9
		D	9	–
		E	5	5 in Fig. 4.1B 5 in Fig. 4.4B 5 in Fig. 4.5B and in Fig. 4.14B 5 in Fig. 4.6A 4 in Fig. 4.7B
		F	5	–
		G	5	3 in Fig. 4.5B and in Fig. 4.14B
		H	10	8 in Fig. 4.3B 9 in Fig. 4.5B and in Fig. 4.14B 8 in Fig. 4.8 9 in Fig. 4.9 8 in Fig. 4.11C 7 in Fig. 4.11D 8 in Fig. 4.12C 8 in Fig. 4.12D 8 in Fig. 4.25

The table continues on the next page.

Table A6.1 (continued)

Sensitization strategy	Day of blood sample collection	Group name	Number of animals in the group = number of datasets obtained	Data displayed in the following figures of the thesis showing results of the *ex vivo* lymphocyte proliferation assay
BCG (continued)	d30 (continued)	I	10	8 in Fig. 4.3B 9 in Fig. 4.5B and in Fig. 4.14B 7 in Fig. 4.8 9 in Fig. 4.9 9 in Fig. 4.10 7 in Fig. 4.11C 9 in Fig. 4.11D 9 in Fig. 4.12C 8 in Fig. 4.12D 9 in Fig. 4.25
		J	9	6 in Fig. 4.5B and in Fig. 4.14B 6 in Fig. 4.8 5 in Fig. 4.10 5 in Fig. 4.26A 6 in Fig. 4.26B
		K	5	5 in Fig. 4.33 5 in Fig. 4.34 5 in Fig. 4.35
	d60	A	4	–
		B	5	3 in Fig. 4.7B
		C	5	4 in Fig. 4.7B
		E	5	4 in Fig. 4.7B
		F	5	–
		G	5	–
		L	3	–
	d90	B	4	3 in Fig. 4.7B
		C	5	4 in Fig. 4.7B
		E	5	4 in Fig. 4.7B
		F	5	–
		G	5	–
		M	7	–
	d120	B	4	3 in Fig. 4.7B
		C	5	4 in Fig. 4.7B
		E	5	4 in Fig. 4.7B
	d150	B	4	3 in Fig. 4.7B
		C	5	4 in Fig. 4.7B
		E	4	4 in Fig. 4.7B

The table continues on the next page.

Table A6.1 (continued)

Sensitization strategy	Day of blood sample collection	Group name	Number of animals in the group = number of datasets obtained	Data displayed in the following figures of the thesis showing results of the *ex vivo* lymphocyte proliferation assay
iAN5	d0	N	5	4 in Fig. 4.1A 3 in Fig. 4.4A
		O	5	5 in Fig. 4.1A 5 in Fig. 4.4A 5 in Fig. 4.7A
	d30	N	4	4 in Fig. 4.1A 3 in Fig. 4.4A
		O	5	5 in Fig. 4.1A 5 in Fig. 4.4A
	d60	N	4	3 in Fig. 4.5A and in Fig. 4.14A
		O	5	5 in Fig. 4.5A and in Fig. 4.14A 5 in Fig. 4.7A
		P	3	3 in Fig. 4.12A 3 in Fig. 4.12B
		Q	7	5 in Fig. 4.5A and in Fig. 4.14A 5 in Fig. 4.11A 5 in Fig. 4.11B 5 in Fig. 4.12A 4 in Fig. 4.12B 5 in Fig. 4.13A 5 in Fig. 4.13B 5 in Fig. 4.27
		R	11	6 in Fig. 4.3A 9 in Fig. 4.5A and in Fig. 4.14A 5 in Fig. 4.11A 6 in Fig. 4.11B 3 in Fig. 4.12A 3 in Fig. 4.12B 6 in Fig. 4.13A 5 in Fig. 4.13B
		S	10	3 in Fig. 4.3A 9 in Fig. 4.5A and in Fig. 4.14A 9 in Fig. 4.11A 9 in Fig. 4.11B 9 in Fig. 4.12A 9 in Fig. 4.12B 6 in Fig. 4.13A 4 in Fig. 4.13B
		T	9	4 in Fig. 4.3A 4 in Fig. 4.5A and in Fig. 4.14A
		U	2	2 in Fig. 4.31
	d90	O	5	5 in Fig. 4.7A
	d120	O	5	5 in Fig. 4.7A
	d150	O	5	5 in Fig. 4.7A

10 Abbreviations

~	approximately
°C	degree Celsius
AA	amino acids
ABC	ATP-binding cassette
AcN	acetonitrile
AEC	3-amino-9-ethylcarbazole
AIDS	acquired immune deficiency syndrome
AM	alveolar macrophage
AP-1	activator protein 1
APC	antigen-presenting cell
APC (dye)	allophycocyanine
Ara	arabinan
ATCC	American Type Culture Collection
ATP	adenosine triphosphate
BCG	Bacille Calmette-Guérin
BEI Resources	Biodefense and Emerging Infectious research Resources repository
BSA	bovine serum albumin
C/EBP	CCAAT enhancer-binding proteins
Ca	calcium
CaM	calmodulin
CaMKII	CaM-dependent protein kinase II
CD	cluster of differentiation
CFP	culture filtrate protein
CFSE	carboxy-fluorescein-succinimidyl-ester
CFU	colony forming unit
CLIP	class II-associated invariant-chain peptide
CME	chloroform-methanol extract
CR	complement receptor
CSU	Colorado State University, CO, USA
Cy	cyanine
d	day
Da	dalton
DAG	diacylglycerol
DAT	di-acyltrehaloses
DC	dendritic cell
DC-SIGN	dendritic cell-specific intercellular adhesion molecule-3 grabbing non-integrin
DMEM	Dulbecco's modified Eagle medium
DNA	deoxyribonucleic acid
DR	direct repeat
DU	duplication
E. coli	*Escherichia coli*
e.g.	for example
EEA1	early endosome autoantigen 1
ELISA	enzyme-linked immunosorbent assay
ER	endoplasmic reticulum
ESAT	Early secretory antigen
FACS	fluorescence-activated cell sorting
FcR	Fc receptor
FCS	fetal calf serum
FSC	forward scatter
g	gram
G	Gauge
GAS	glycerol-alanine-salts medium
GILT	IFN-γ-induced lysosomal thiol reductase
GMM	glucose monomycolate
gpIL-2	guinea pig Interleukin-2
GPL	glycopeptidolipid
h	hour

HIV	human immunodeficiency virus
HPLC	High-performance liquid chromatography
Hsp	heat shock protein
i.e.	that is (Latin: *id est*)
i.m.	intramuscular
IFN-γ	interferon-gamma
Ig	immunoglobulin
Ii	MHC class II-associated invariant chain
IKK	IκB kinase kinase
IL	Interleukin
IP_3	inositol 1,4,5-triphosphate
IPBS	Institut de Pharmacologie et de Biologie Structurale, Toulouse, France
IRAK	IL-1 receptor-associated kinase
IS	Insertion sequence
ITAM	immunoreceptor tyrosine-based activation motifs
ITS	internal transcribed spacer
JLU	Justus Liebig University, Giessen, Germany
k	thousand
kDa	kilodalton
L	liter
LAM	lipoarabinomannan
LC-MS/MS	liquid chromatography – tandem mass spectrometry
LM	lipomannan
LOS	lipooligosaccharides
lpp.	lipoprotein
LppEL	lipopeptide-enriched subfraction (French: lipopeptides de l'extrait lipidique)
LPS	lipopolysaccharides
LTBI	latent tuberculosis infection
M.	*Mycobacterium*
MAA	*Mycobacterium avium* ssp. *avium*
ManLAM	mannosylated lipoarabinomannan
MAP	*Mycobacterium avium* ssp. *paratuberculosis*
MB	Middlebrook medium
MDM	monocyte-derived macrophage
MDP	muramyl dipeptide
mg	milligram
MHC	major histocompatibility complex
min	minute
MIRU	mycobacterial interspersed repetitive units
ml	milliliter
MMP	matrix metalloproteinase
MP	mature protein
MR	mannose receptor
MRL	Mycobacteria Research Laboratories, Fort Collins, CO, USA
ms	milliseconds
MTC	*Mycobacterium tuberculosis* complex
MW	molecular weight
mWR	modified Watson-Reid medium
n	number of independent experiments
N	Normal
n.t.	not tested
NaCl	sodium chloride
NF-κB	nuclear factor kappa beta
NFAT	nuclear factor of activated T cells
NIAID	National Institute of Allergy and Infectious Diseases, USA
NIBSC	National Institute for Biological Standards and Control, UK
NIH	National Institutes of Health, USA
NK T cells	natural killer T cell
NO	nitric oxide
NOS2	nitric oxide synthetase 2
NPC	normal phase chromatography
ns	not significant

NTM	non-tuberculous mycobacteria
OD	optical density
OT	Koch's Old Tuberculin
PAMP	pathogen-associated molecular pattern
PAT	poly-acyltrehalose
PBMC	peripheral blood mononuclear cell
PBS	phosphate buffered saline
PCR	polymerase chain reaction
PDIM	phtiocerol dimycocerosates
PE	phycoerythrin
PEI	Paul-Ehrlich-Institut, Langen, Germany
PGL	phenolic glycolipid
Pi_3P	phosphatidylinositol 3-phosphate
PILAM	phospho-inositol-capped lipoarabinomannan
PIM	phosphytidyl-*myo*-inositol mannosides
PIP_2	phosphatidylinositol 4,5-bisphosphate
PIP_3	phosphatidylinositol 3,4,5-trisphosphate
PLC-γ	phospholipase C-gamma
PPD	Purified Protein Derivative
PPD-CT68	Connaught Tuberculin 68
PPD-RT23	Danish standard PPD
PPD-S2	US standard PPD
r	correlation coefficient
RCB	Research Center Borstel, Germany
RD	region of difference
ref.	reference
RFLP	restriction fragment length polymorphism
RKI	Robert-Koch-Institut, Berlin, Germany
RNA	ribonucleic acid
RPC	reversed phase chromatography
rRNA	ribosomal ribonucleic acid
RT	room temperature
S. Typhi	*Salmonella enterica* ssp. *enterica* serovar Typhi
s.c.	subcutaneous
SAv	streptavidin
SDS-PAGE	sodium dodecyl sulfate polyacrylamide gel electrophoresis
sec	second
SF-IMDM	serum-free Iscov's modified Dulbecco's medium
SL	sulfatides
SP	signal peptide
SSC	side scatter
ssp.	subspecies
STAT protein	signal transducers and activators of transcription protein
TAB	TGF-β-activated kinase binding protein
TAK1	TGF-β-activated kinase 1
TAP	transporter associated with antigen processing
TAT	tri-acyltrehaloses
TB	tuberculosis
TCR	T cell receptor
TDM	6,6'-dimycoloyl-a-D-trehalose, cord factor
TFA	trifluoroacetic acid
Th cell	T helper cell
TLC	thin layer chromatography
TLR	Toll-like receptor
TMM	trehalose monomycolate
TNF	tumor necrosis factor
TRAF	TNF receptor-associated factor
T_{reg} cell	regulatory T cell
TST	tuberculin skin test
UK	United Kingdom
USA	United States of America
v	volume

VNTR	variable numbers tandem repeats
w	weight
WHO_{av}	WHO International Standards for Purified Protein Derivatives *M. avium* ssp. *avium*
WHO_{bov}	WHO International Standards for Purified Protein Derivatives *M. bovis*
WHO_{hum}	WHO International Standards for Purified Protein Derivatives *M. tuberculosis*
x *g*	gravitational acceleration
ZAP	zeta chain-associated protein kinase 70
µg	microgram
µl	microliter

11 List of figures

12 List of tables

13 Acknowledgements

It is my pleasure to thank my supervisors, colleagues, family and friends who supported my research and thesis during these past years.

I would like to express my deep gratitude to my supervisor Dr. Max Bastian for permitting me to work on his cherished project, for his guidance throughout this time, for many inspiring discussions and for always keeping his positive and understanding attitude. His support during this project is greatly appreciated as well as the many possibilities to present my data on conferences. I sincerely thank him for encouraging me to move into the scientific community. The past years working on this project undoubtedly led to personal growth and shaped my scientific interest.

I am equally grateful to my supervisor Prof. Dr. Rolf Bauerfeind for the experienced support and guidance that he provided during this thesis project and beyond it in several research proposals. I always felt understood and that we were working towards the best solutions. In particular, his useful critiques through excellent questions taught me to provide exact answers and to focus on the real matter at hand. I appreciate his profound interest in my project and his valuable advice which will surely also prove helpful during my future endeavors in the field of science.

I sincerely thank Dr. Martine Gilleron not only for providing me with the most important reagents used in this study, namely CME_{H37Rv}, CME_{BCG} and LppEL, but also for enabling my one-month scientific stay at the IPBS Toulouse. I gained a lot of valuable scientific knowledge during this time which greatly advanced the project and which will surely be helpful in the future as well. In this regard I would also like to thank Dr. Diane Cala-de Paepe for generating the valuable LppEL and Dr. Jacques Prandi for his support in the chromatography unit.

I would like to express my sincerest gratitude to the German Ministry of Education and Research and to the German National Academic Foundation for kindly providing the funding for this project and for me.

I am very thankful for the scientific advice of my additional thesis committee members which contributed significantly to the successful completion of the project: Prof. Dr. Stefan Vieths, PD Dr. Ger van Zandbergen, Dr. Veronika von Messling, and Dr. Holger Loessner. In particular, I would like to sincerely thank Dr. von Messling not only for her very experienced scientific guidance, but especially for her continuous support. I would like to offer my special thanks to Prof. Dr. Vieths for his valuable and constructive suggestions and his personal contribution in the realization thereof by generously offering access to the facilities and the knowledge of his division. I would like to express my appreciation to Dr. Detlef Bartel and especially Dr. Frank Fuehrer and Christine Cigan for their great support in this regard. My thanks go to Dr. Loessner for provision of bacterial strains for control purposes.

I owe my deepest gratitude to Friederike Mohs and Anna Geissler for their much appreciated support during the long days of animal experiments and for their friendship.

I wish to acknowledge all the people who took such good care of the animals every single day. I am particularly grateful for their excellent support with the inbred guinea pig breeding. In particular I would like to thank Alexandra Janovich, Beata Bahlo, Kyriakos Papadopulos, Ewald Euteneier, Juergen Engelmann, and Regina Horvath. I would like to thank the veterinarians of the animal facility, Dr. Roland Plesker, Dr. Cheick Coulibaly, Dr. Edgar Holznagel and Dr. Claudia Hergenhan for their great support. In particular, I thank Dr. Plesker for very interesting pathology and histology rounds and Dr.

Coulibaly for inspiring discussions on tuberculosis. I would like to highlight the importance of the animals for this project. It is our responsibility to always remember the value of the data they provided.

I would like to offer my special thanks to the colleagues of the Research Center Borstel, namely Prof. Dr. Stefan Niemann, PD Dr. Norbert Reiling, Dr. Susanne Homolka and Lisa Niwinski for the good collaboration and for providing me with clinical *M. tuberculosis* strains. I would further like to thank Dr. Reiling for the inspiring discussions and his very useful advice.

My gratitude goes to Dr. Thomas Holzhauser and Stefanie Randow for synthesizing many *M. tuberculosis* peptides. I thank Dr. Hubert Schaefer from RKI Berlin for guinea pig-specific reagents and Dr. Schaefer and Dr. Mechthild Ladwig from the German Federal Institute for Risk Assessment for the generous provision of rare inbred strain 2 guinea pigs. In this line, I would like to express my gratitude to Dr. Joerg Kirberg for his valuable advice on inbred breeding and bacterial cultures. My thanks go to Dr. Sven Flindt for his tips concerning the FACS and for graciously allowing me the use of two additional magnetic devices, without which some long days in the lab would have been even longer. I thank Dr. Elisabeth Balks for providing me with much information on tuberculin as well as interesting discussions on papers. I would further like to thank Dr. Karin Duchow, Dr. Beate Kraemer, Dr. Ingun Lemke, Dr. Klaus Cussler, Dr. Andreas Hoffmann, and Rolf Beckmann for their great collegiality and support during the past years. My appreciation goes to all technicians of the division of veterinary medicine for their enthusiasm to provide advice and tools whenever needed, in particular I would like to name Heidi, Ursel, Conny, Franzi, and Annett – the one to ask when searching for something really exceptional. I sincerely thank Dr. Kay-Martin Hanschmann and Jan-Hendrik Troesemeier for their prompt assistance with all statistical questions, sometimes late in the night. I thank Dr. Walter Matheis for provision of the BCG Pasteur strain and helpful information on the Koch's Old Tuberculin standard, Marion Wingerter for preparing the histological slides, Dr. Peter Schaufuss from WDT Serumwerk Memsen for providing bacterial wet masses, my former internship colleague Dr. Mathias Weigold for his valuable tips on growing MAA and MAP and Sabine Kinzer for preparing the media.

Thorsten Friedel deserves many thanks for our motivational discussions during these past years and for sharing his vast knowledge on advantageous approaches in many IT programs. My gratitude goes to Dr. Tobias Abel for his valuable tips on writing. I am thankful for the company of my office and lab colleagues during all the hours of data analysis, poster preparation, and appreciated distracting conversations: Rahel, Christina, Sibylle, Emina, Lena, Yvonne, Lisa, Rebecca, Karen, Theresa, Bevan, Sarah, Richard, Ramona and especially Elise. I would also like to thank Paul, who spent his DAAD RISE internship in our group, for our open dialogue on motivation and beyond, which taught me a lot about expectations. My gratitude also extends to my colleagues from IPBS Toulouse: first of all to Sophie for teaching me many methods in an incredibly short period of time, Landry, Sandro, Alexiane, Emeline and last but not least Mouin for his very much appreciated companionship in Toulouse.

I would like to thank all colleagues and friends in- and outside the PEI for their contributions to making the past years such a valuable time that I will definitely miss.

My deepest gratitude goes to my dear friend Eranée Stewart for her valuable support by proofreading my thesis and for getting through these long weeks with me. I sincerely thank my sister Lisa for her prompt answers to my "easy" questions on the formatting of graphics.

I would like to thank my family as well as Alexander's for their continuous support and understanding. I am eternally grateful to my parents for teaching me confidence and perseverance and for their constant encouragement and support which surely pushed me beyond my comfort zone from time to time – the place to be to achieve one's goals.

Last but not least, my heartfelt thanks are more than deserved by Alexander for his incredible and endless patience, motivation and unwavering support during every good and tough time and for not questioning my dedication to the project for one single day.

Thank you.

14 Erklärung

"Ich erkläre: Ich habe die vorgelegte Dissertation selbständig und ohne unerlaubte fremde Hilfe und nur mit den Hilfen angefertigt, die ich in der Dissertation angegeben habe. Alle Textstellen, die wörtlich oder sinngemäß aus veröffentlichten oder nicht veröffentlichten Schriften entnommen sind, und alle Angaben, die auf mündlichen Auskünften beruhen, sind als solche kenntlich gemacht. Bei den von mir durchgeführten und in der Dissertation erwähnten Untersuchungen habe ich die Grundsätze guter wissenschaftlicher Praxis, wie sie in der "Satzung der Justus-Liebig-Universität Gießen zur Sicherung guter wissenschaftlicher Praxis" niedergelegt sind, eingehalten."

Eva Kaufmann

édition scientifique
VVB LAUFERSWEILER VERLAG

VVB LAUFERSWEILER VERLAG
STAUFENBERGRING 15
D-35396 GIESSEN

Tel: 0641-5599888 Fax: -5599890
redaktion@doktorverlag.de
www.doktorverlag.de

ISBN: 978-3-8359-6442-6

Cover photos: left: © Dr_Kateryna @ fotolia.de
right: © luismmolina @ iStockPhoto.com